

Therapeutic targeting of autophagy in gastric cancer

**Thesis submitted for the degree of
Doctor of Philosophy (Science)
in
Life Science and Bio-technology**

By

UZMA KHAN

(Index No.: 54/20/Life Sc./27)

**Department of Life Science and Bio-technology
Jadavpur University
Kolkata, India**

2023

ABSTRACT

Title of the Thesis: Therapeutic targeting of autophagy in gastric cancer.

Index No.: 54/20/Life Sc./27

Helicobacter pylori is a well-established inhabitant of the human stomach, and a major risk factor for the progression of gastritis, peptic ulcers, and even gastric cancer. *H. pylori* can be transmitted through contaminated food and water. In response to infection, host cells often stimulate autophagy as a protective mechanism to maintain cellular homeostasis. However, *H. pylori* has evolved strategies to subvert the host's autophagic machinery to persist within the epithelial cells of the stomach. Mechanisms by which *H. pylori* accomplishes its survival are still being investigated, but it often involves a complex interplay between bacterial effector and host cell proteins. High Mobility Group Box 1 (HMGB1) a nuclear host protein serves as a key regulator of autophagy and exhibits increased expression levels in several diseases and various types of cancer including gastric cancer. However, the role of HMGB1 in autophagy during *H. pylori* infection has not been explored to date. Hence, HMGB1 is targeted as a therapeutic candidate for the treatment of gastric disorders.

Human gastric cancer cell line (AGS) were infected with *H. pylori* strains SS1 and 26695. Western blot was used to examine autophagy protein expression. Autophagy and lysosomal activities were observed by fluorescence assays. Glycyrrhizin was used to inhibit HMGB1, and an *in vivo* mouse model of *H. pylori* infection was established to study the effect of glycyrrhizin treatment. Co-immunoprecipitation assays were performed in AGS and RAW 264.7 cells to study autophagy modulation by *H. pylori*.

We demonstrated that *H. pylori* infection modulates autophagy pathway and concomitantly increases the expression of HMGB1 in gastric cancer cells and macrophage cells. Autophagy modulation by *H. pylori* leads to its intracellular growth within the defective autophagosomes. To unravel HMGB1's role during autophagic dysregulation, we inhibited HMGB1 expression using glycyrrhizin, a known inhibitor of HMGB1. Inhibition of HMGB1 results in increase of autophagic flux which in turn, effectively reduces intracellular *H. pylori* burden, even in the case of antibiotic-resistant strains. Elevated autophagic response by glycyrrhizin was validated by using lysosomal inhibitors, chloroquine, and bafilomycin.

To gain deeper insights into the mechanisms underlying bacterial clearance, for the first time we reported that inhibition of HMGB1 by glycyrrhizin rescued the gastric cancer cells from lysosomal membrane permeabilization induced by *H. pylori* infection. Following that, glycyrrhizin treatment restored the lysosomal membrane integrity. The restored lysosomal function increases autolysosome formation and inhibits intracellular *H. pylori* growth. Additionally, glycyrrhizin treatment inhibited inflammation and repaired gastric tissue damages in mice. Interestingly we also found that increased HMGB1 during *H. pylori* infection interacts with multiple autophagy proteins, (including Beclin1, UVRAG, and WIPI2) that might modulate the autophagy mechanism.

Therefore, our study provides clear evidence that inhibiting HMGB1 restored lysosomal activity, thus mitigating the impact of *H. pylori* infection. It also demonstrated the potential of glycyrrhizin as an antibacterial agent to address the problem of antimicrobial resistance.



icmr
INDIAN COUNCIL OF
MEDICAL RESEARCH

NICED
NATIONAL INSTITUTE OF
CHOLERA AND ENTERIC DISEASES

आई. सी. एम. आर. - राष्ट्रीय कॉलरा और आंत्र रोग संस्थान
ICMR - NATIONAL INSTITUTE OF CHOLERA AND ENTERIC DISEASES
स्वास्थ्य अनुसंधान विभाग, स्वास्थ्य और परिवार कल्याण मंत्रालय, भारत सरकार
Department of Health Research, Ministry of Health and Family Welfare, Govt. of India

WHO COLLABORATING CENTRE FOR RESEARCH AND TRAINING ON DIARRHOEAL DISEASES

CERTIFICATE FROM THE SUPERVISOR

This is to certify that the thesis entitled “Therapeutic targeting of autophagy in gastric cancer” Submitted by ~~Sh~~/Smt Uzma Khan who got his/her name registered on 09/11/2019 for the award of Ph.D. (Science) degree of Jadavpur University, is absolutely based upon her own work under the supervision of Dr. SUSHMITA BHATTACHARYA and that neither this thesis nor any part of this has been submitted for either any degree/diploma or any other academic award anywhere before.

Sushmita Bhattacharya

(Signature of the supervisor date with official seal)

Dr. Sushmita Bhattacharya
Scientist - C
Biochemistry Division
ICMR National Institute of Cholera
and Enteric Diseases
Beliaghata, Kolkata-700010

पी-३३, सी.आई.टी. रोड, स्किम - १०एम, बेलियाघाटा, कोलकाता - ७०००१०, भारत

P-33, C.I.T. Road, Scheme - XM, Beliaghata, Kolkata - 700010, India

निदेशक / Director : 91-33-2363 3373, 2370 1176, पि.बि.एस / PBX : 91-33-2353 7469 / 7470, 2370 5533 / 4478 / 0448

फैक्स / Fax : 91-33-2363 2398, 2370-5066, वेब / Website : www.niced.org.in

To...
Nasreen Fatima
Maa
&
Nisar Ulla Khan
Papa

For being my first teacher and for supporting and encouraging me to believe
in myself

ACKNOWLEDGEMENT

In presenting this thesis, it is essential to extend my heartfelt gratitude not only to my own efforts but also to the exceptional individuals who have played an indispensable role in its realization. Their selfless contributions, ceaseless support, encouragement, and astute guidance have been instrumental in shaping the trajectory of this research endeavor. The investment of their time, affection, and commitment has left an indelible mark on the outcome of this work, and for this, I am profoundly thankful.

I am immensely grateful for the unwavering support and guidance provided by my guide, **Dr. Sushmita Bhattacharya**, without whom completing this work would not have been possible. She has been a great teacher who inspires hope, ignites the imagination, and imprints a love for science and research. Her meticulousness to the details and diligence has taught me that the little steps are the secret to mounting greater heights. Over the past five years, this journey has been quite a roller-coaster ride.

I am grateful to **Dr. Shanta Dutta**, the director of ICMR-NICED for providing me the workplace.

I express my sincere thanks to **Dr. Asish K. Mukhopadhyay**, Scientists of ICMR- NICED for providing us with the *Helicobacter pylori* culture, cell lines and all the support whenever we needed.

I am grateful to **Dr. Nabendu Shekhar Chatterjee, Dr. Santasabuj Das, Dr. Amit Pal and Dr. Mamta Chawla Sarkar**, Scientists of ICMR- NICED for helping me with their critical reviews as well providing, cell lines, reagents, and chemicals. I would like to thank **Department of life science and biotechnology, Jadavpur University**. All my teachers from my post-graduation days, graduation days as well as school days – thank you, for

providing academic co-operation and helping me to grow. To the **non-teaching staffs** and **office staffs** that have provided technical help of all sorts, thank you for every help. For financial assistance I remain ever grateful. Here I would like to thank **Council of Scientific and Industrial Research, Government of India** for my fellowship and **Department of Biotechnology, Government of India** for funding the project.

I would like to convey my profound and heartfelt gratitude to my beloved parents, **Nasreen Fatima and Nisar Ulla Khan**, who not only allowed me to dream but also nurtured those dreams with their boundless love, unwavering guidance, selfless sacrifices and support. They have been my pillar of strength throughout the myriad ups and downs. My journey toward achieving my goals would not have been possible without their constant belief in me, and their sacrifices provided me with the opportunity to concentrate on my studies and pursue my aspirations with confidence. Throughout this journey, they have remained my most ardent cheerleaders, extending both emotional and financial support whenever I needed it.

I am also deeply indebted to my bhaiya, **Akhilesh Singh**, who has been an enduring presence in my pursuit of these dreams. His unwavering encouragement has boosted me to overcome obstacles, strive for excellence, and believe in myself. His support has not only been instrumental in my accomplishments but has also instilled in me the importance of determination and resilience.

I am really grateful to my seniors particularly **Dr. Bipul Chandra Karmakar**, for his continual assistance and support during the execution of my experiments without whom I would not been able to complete this journey of five years. I am immensely grateful to my other seniors **Dr. Sangita Paul, Dr. Suman Das, Dr. Debjyoti Bhakat, Dr. Kalyani Saha, Dr. Deotima Sarkar, Dr. Priyanka Basak**, for their help in learning the methodologies and techniques. I learnt a lot from my juniors, **Mr. Indranil Mondal, Ms. Priyanka Maitra, Ms. Sushmita Kundu, Mr. Sourin Alu, Mr. Abhishek Singh** and really thankful for their help

in execution of my experiments. I am extremely thankful to **Animesh Gope** for his invaluable assistance during the confocal microscopy.

To all those of you I could not mention here, thank you too, every big and small role played has helped me to achieve the dream of a PhD degree together.

Date: 17/11/2023

Uzma Khan

(Uzma Khan)

CONTENTS

			Page No.
Section 1		INTRODUCTION	1-2
Section 2		REVIEW OF LITERATURE	3-49
Section 3		MATERIALS AND METHODS	50-69
Section 4		AIMS AND OBJECTIVES	70-71
Section 5		RESULTS	72-143
Objective I	Chapter 1	<i>H. pylori infection augments HMGB1 expression and modulates autophagy in gastric epithelial cells</i>	77-89
	1.1	<i>H. pylori- infection activates HMGB1 expression in gastric epithelial cells</i>	77-80
	1.1.1	<i>HMGB1 expression at different MOI of H. pylori 26695-infection in AGS cells</i>	77 -78
	1.1.2	<i>HMGB1 expression at different time points of H. pylori SS1- infection in AGS cells</i>	78-79
	1.1.3	<i>Subcellular location of HMGB1 by H. pylori SS1- infection in AGS cells</i>	79-80
	1.2	<i>H. pylori- infection modulates autophagy in gastric epithelial cells</i>	80-85
	1.2.1	<i>H. pylori 26695- modifies autophagy in AGS cells</i>	80-83
	1.2.2	<i>H. pylori SS1- regulates autophagy in AGS cells</i>	83-85
	1.3	<i>HMGB1 expression and autophagy regulation by H. pylori- infection in HGC-27 cells</i>	85-86
	1.4	<i>H. pylori- infection induces HMGB1 expression and modifies autophagy in RAW 264.7 cells</i>	87-89
	Chapter 2	<i>Autolysosomal degradation function was compromised due to H. pylori infection</i>	90-100
	2.1	<i>Downregulation of late autophagy marker protein expression</i>	93-94
	2.2	<i>H. pylori infection down-regulates autophagic flux</i>	94-97
	2.2.1	<i>Autophagic flux downregulation</i>	94-95
	2.2.2	<i>Visualization of autophagic flux downregulation using confocal microscopy</i>	96-97
	2.3	<i>H. pylori survive and replicate in AGS cells</i>	97-98

		Page No.
	2.4	<i>H. pylori</i> exploites autophagosomes as a survival niche in human stomachs
	Chapter 3	<i>Inhibiting HMGB1 induces autolysosomal degradation function in gastric cells.</i>
	3.1	Glycyrrhizin induces autophagy in gastric adenocarcinoma cells
	3.1.1	Induction of autophagic marker protein expression by western blot analysis
	3.1.2	Induction of autophagy by confocal microscopy
	3.2	Activation of autophagy in <i>H. pylori</i> -infected gastric adenocarcinoma cells
	3.2.1	Induction of autophagic protein expression by western blot analysis
	3.2.2	Enhancement of autophagy due to drug treatment
	3.3	Glycyrrhizin stimulates autophagy flux in <i>H. pylori</i> -infected gastric adenocarcinoma cells
	3.3.1	Regulation of autophagic flux by glycyrrhizin
	3.3.2	Visualization of fusion of autophagosomes and lysosomes using immunofluorescence
	3.3.3	Visualization of the formation of autophagosomes and autolysosomes
	3.4	Anti- <i>H. pylori</i> action of glycyrrhizin by induced Autophagy
	3.4.1	Determining the effect of glycyrrhizin on intracellular <i>H. pylori</i>
	3.4.2	Determining the effect of glycyrrhizin on a resistant strain of <i>H. pylori</i> [OT-14 (3)]
	3.5	Activation of autophagy pathway by glycyrrhizin is mediated through HMGB1 suppression
	3.6	Effect of glycyrrhizin on autophagic induction while using lysosomal inhibitors
	3.7	Analysis of the effects of different doses of glycyrrhizin on AGS cell viability
	3.8	Analysis of glycyrrhizin on <i>Helicobacter pylori</i> viability
	3.9	Determination of MIC of glycyrrhizin in BHIA plate

			Page No.
Objective II	Chapter 4	<i>Unraveling the mechanism to interlink autophagic targets with inflammation during <i>H. pylori</i> infection.</i>	118-127
	4.1	<i>Glycyrrhizin restores lysosomal pH during <i>H. pylori</i>-infection</i>	<i>121-123</i>
	4.1.1	<i>Evaluation of Lysosomal pH using Acridine orange</i>	<i>121</i>
	4.1.2	<i>Evaluation of Lysosomal pH using LysoTracker Red (LTR)</i>	<i>122-123</i>
	4.2	<i>Glycyrrhizin promotes lysosomal degradation function by reducing lysosomal membrane permeabilization (LMP)</i>	<i>124-126</i>
	4.2.1	<i>Determination of LMP using double immunofluorescence (Galectin3 & LAMP1)</i>	<i>124-125</i>
	4.2.2	<i>Determination of LMP using Alexa Fluor labelled dextran molecules</i>	<i>125-126</i>
	4.3	<i>Glycyrrhizin suppresses reactive oxygen species (ROS) and inflammation in <i>H. pylori</i> infected gastric cells</i>	<i>126-127</i>
	Chapter 5	<i>Glycyrrhizin alleviates <i>H. pylori</i> infection in in vivo mice model</i>	128-133
	5.1	<i>Glycyrrhizin induces autophagy in an in vivo mice model</i>	<i>130</i>
	5.2	<i>Glycyrrhizin reduces the inflammatory cytokine levels during <i>H. pylori</i> infection</i>	<i>131-132</i>
	5.3	<i>Glycyrrhizin effectively reduces inflammation in gastric tissues</i>	<i>132-133</i>
Objective III	Chapter 6	<i>Dissecting the role of novel signature autophagic targets due to HMGB1 activation</i>	134-143
	6.1	<i>Determination of autophagic targets of HMGB1 using Co- Immunoprecipitation</i>	<i>137-139</i>
	6.1.1	<i>Western blotting</i>	<i>137-138</i>
	6.1.2	<i>Determining interaction of HMGB1 with Beclin1 by immunofluorescence</i>	<i>138-139</i>
	6.2	<i>Interaction studies of HMGB1 and Beclin1 in overexpressed HMGB1 cells</i>	<i>139-141</i>
	6.2.1	<i>Western blotting</i>	<i>139-140</i>
	6.2.2	<i>Confocal microscopy</i>	<i>140-141</i>

			<i>Page No.</i>
	6.3	<i>Autophagic targets interacting with HMGB1 in macrophages</i>	<i>141-142</i>
	6.4	<i>Unraveling the Mechanism Regulated by HMGB1</i>	<i>142-143</i>
<i>Section 6</i>		<i>DISCUSSION</i>	<i>144-152</i>
<i>Section 7</i>		<i>CONCLUSION</i>	<i>153-155</i>
<i>Section 8</i>		<i>REFFERENCES</i>	<i>156-185</i>
<i>Section 9</i>		<i>ABBREVIATION</i>	<i>186-188</i>
<i>Section 10</i>		<i>PUBLICATIONS AND CONFERENCES</i>	<i>189-190</i>

Section 1

INTRODUCTION

Helicobacter pylori a Gram-negative microaerophilic bacterium, is known to inhabit the stomachs of nearly half the global population. Infection usually develops in childhood and causes a chronic, progressive stomach inflammation that leads to clinical problems in 1-10% of infected people (Khatoon et al., 2016; Li et al., 2017). This resilience in colonization can be recognized as contributing factors to the global concern of antibiotic resistance in *H. pylori*. Consequently, the World Health Organization (WHO) has added *H. pylori* in its high-priority pathogens. *H. pylori* infection reprograms host cellular pathways, including autophagy (Chmiela et al., 2017). Autophagy is a crucial pathway involved in the recognition and sequestration of intracellular bacteria to facilitate their elimination (Yang et al., 2016; Raju et al., 2012). *H. pylori* have evolved strategies to restrain and manipulate autophagy for their survival. *H. pylori* downregulates autophagic flux and employs non-degradative autophagosomes for its intracellular survival and replication in the stomach's gastric epithelial cells (Yang et al., 2018; Tang et al., 2012).

A recent study has demonstrated an augmentation of High Mobility Group Box 1 (HMGB1) in gastric cells during *H. pylori* infection (Lin et al., 2016). HMGB1 is involved in the regulation of autophagy acting as both an anti-autophagic or a pro-autophagic factor based on the specific cellular conditions. Nevertheless, the function of HMGB1-mediated autophagy in *H. pylori* infection remains elusive. In our study, we focussed our attention on determining HMGB1-mediated specific targets in the autophagic regulatory network. Hence, we targeted to investigate the role of HMGB1 in autophagy and uncover the underlying mechanism involved with infection and henceforth we therapeutically exploited HMGB1 for inhibiting *H. pylori* infection.

Section 2

REVIEW OF LITERATURE

2.1 Discovery of *Helicobacter pylori*

The discovery of *Helicobacter pylori* (*H. pylori*) is a long fascinating story, with many twists and turns. Previously, peptic ulcer disease played havoc with people's lives and had been plaguing the community for years. Throughout most of the twentieth century, conventional thinking held that peptic ulcer illness was caused by stress, spicy foods, and gastric juice corroding susceptible mucosa. The no acid- no ulcer ruled the day, and neutralization of stomach acid was the basis of management. This enigmatic illness had puzzled doctors and scientists alike, with no clear understanding of its cause or cure.

In the early 1980s, Barry J Marshall, an Australian physician, and J Robin Warren, a pathologist, were working at the Royal Perth Hospital in Western Australia. They were determined to unravel this medical puzzle, started collecting samples from the afflicted patients. The initial cultures from approximately 30 patients yielded negative results. However, due to an unexpected circumstance, one culture was mistakably incubated for an extended period of 5 days over an Easter holiday. To their astonishment, the first colonies from the culture were finally observed in the year 1982. They discovered the presence of a previously unidentified spiral-shaped bacterium in the stomach lining of many of these patients. This bacterium was named *Helicobacter pylori* (*H. pylori*) due to its helical or spiral shape. This was the breakthrough in understanding the real cause of peptic ulcers by the revolutionary research of two Australians, Barry Marshall and Robin Warren (**Marshall and Warren, 1984; Warren et al., 1983**).

Marshall and Warren hypothesized that *H. pylori* might play a role in causing gastritis and ulcers. Their findings challenged the prevailing medical belief that no bacteria could survive in the highly acidic environment of the stomach. After failing to create an animal model, Marshall became determined and ingested a culture of *H. pylori* himself to prove their hypothesis that *H. pylori* causes gastritis. This act of self-experimentation led to the

development of gastritis and also confirmed the link between *H. pylori* and gastric diseases. Marshall later cured the infection with antibiotics and fulfilled Koch's postulates, initiating the research of *H. pylori* as a pathogen (**Marshall et al., 1985**). In 1892, **Bizzozero**, an Italian pathologist first discovered spiral creatures in the stomachs of dogs. However, it was first reported in the human gastric cancerous patient in 1906 by **Krienitz**. Later in 1994, *H. pylori* was termed as a type I carcinogen, as it is considered the most common agent of infection associated with cancer (**Parkin et al., 2002**). Owing to the discovery of this bacterium, Marshall and Warren were awarded the Nobel Prize in 2005.

The discovery of *H. pylori* revolutionized the understanding and treatment of peptic ulcers and gastritis. It led to the development of antibiotics as a standard treatment for these conditions, effectively curing many patients and significantly reducing the need for surgical interventions. Marshall and Warren's persistence and ground-breaking research had a profound impact on the field of medicine and have saved countless lives by providing a more accurate understanding of the causes of gastric diseases.



Figure1. Discovery of *Helicobacter pylori* by Warren and Marshall (Source: doi.org/10.1002/cmdc.200600121)

2.2 Advancement of *H. pylori* infection on human health

By 1984, it was already established that *H. pylori* infection was strongly associated with the presence of inflammation in the gastric mucosa, specifically **chronic superficial gastritis**, and notably with polymorphonuclear cell infiltration, indicative of chronic active gastritis. However, several years before an etiologic role was conclusively established (Blaser 1990) that *H. pylori* persists for life, unless eradicated by antimicrobial therapy (Blaser 1992 and Blaser 1997). A significant study in 1991, unveiled the associations between *H. pylori* infection and **gastric cancer** development. In 1994, the International Agency for Research on Cancer (IARC), a branch of the World Health Organization (WHO), officially recognized *H. pylori* as a human carcinogen. *H. pylori* infection has also been linked to the development of gastric non-Hodgkin's lymphomas and another lymphoproliferative disorder known as **gastric mucosa-associated lymphoid tissue (MALT) lymphoma**, often referred to as **MALToma**. Remarkably, the treatment of patients with gastric MALToma using antibiotics frequently results in tumor regression. However, owing to the increasing antibiotic resistance of *H. pylori*, WHO has classified *H. pylori* into high priority pathogen list (Myran and Zarbock 2018). Henceforth, *H. pylori*, is now linked to numerous critical gastrointestinal diseases.

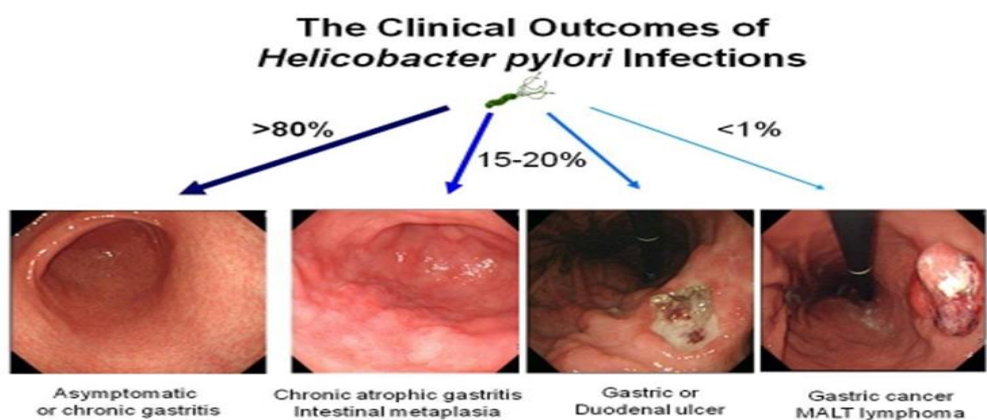


Figure2. Various clinical outcomes of *H. pylori* infection: Chronic gastritis, Intestinal metaplasia, Gastric or duodenal ulcer, Gastric Cancer (Source: www.promedendoscopyclinic.com/)

***Helicobacter* genus**

The isolated organism by Warren and Marshall exhibited several similarities to *Campylobacter*, including its curved morphology, ability to thrive on rich media under microaerophilic conditions, inability to ferment glucose, and a G + C content of 34%. Initially, it was designated as "pyloric *Campylobacter*" (pylorus, from the Greek word meaning "gatekeeper" or "one who looks both ways") and officially recognized as *Campylobacter pyloridis* in 1985 (**Anonymous, 1985**). However, it was subsequently corrected to *pylori* in 1987, as *pyloridis* was found to be an inaccurate Latin term. In 1989, as it became evident that *H. pylori* did not belong to the *Campylobacter* genus, the genus name underwent a change to *Helicobacter*, reflecting its distinctive functional and enzymatic characteristics (**Goodwin et al., 1990**). Subsequent electron micrographs revealed the presence of multiple sheathed unipolar flagella in the bacterium, distinguishing it from the single bipolar unsheathed flagellum typically found in *Campylobacter* spp (**Goodwin et al., 1985**). Furthermore, significant differences in fatty acids and major protein bands compared to *Campylobacter* species were noted (**Goodwin et al., 1985**).

Based on 16S rRNA gene sequencing, it was officially renamed *Helicobacter pylori* (*H. pylori*) in 1989, marking the discovery of the new *Helicobacter* genus (**Goodwin et al., 1989**). The name "Helicobacter" was derived from the helical shape of the bacterium, while "pylori" was chosen due to its frequent isolation from the pylorus of the stomach (**Goodwin et al., 1989**). *H. pylori* were classified as 'S-type' based on their amino acid compositions derived from the complete genome, a classification independent of gram staining (**Sorimachi et al., 2004**).

Table1.
Scientific Classification
Kingdom: Bacteria
Phylum: Proteobacteria
Class: Epsilon Proteobacteria
Order: Campylobacterales
Family: Helicobacteraceae
Genus: <i>Helicobacter</i>
Species: <i>pylori</i>
Binomial name
<i>Helicobacter pylori</i>
(Marshall et al., 1985, Goodwin et al., 1989)

2.4 Epidemiology of *H. pylori* infection

Once individuals acquire an *H. pylori* infection, the pathogen typically persists throughout their lifetime (Suerbaum and Michetti 2002). Nevertheless, spontaneous clearance is possible, as reported in a 2002 study where 9 out of 58 children (15.5%) cleared the infection during a 20-year follow-up period (Malaty et al., 2002). Clearance is more common in patients with advanced atrophic gastritis (Gao et al., 2009). The global prevalence of *H. pylori* infection in adults has declined from 50-55% to 43% between 2014 and 2020, likely due to improvements in socioeconomic status, living standards, hygiene conditions, and the increased use of antibiotics, including eradication therapies (Hooi et al., 2017; Parsonnet et al., 1991). A 2002 study showed that the incidence rate of new infections in younger age groups was 1.4% per year, with the highest rates in children aged 4-5 years (Malaty et al., 2002). Between 2014 and 2020, the prevalence of infection in both children and adults was

higher in low- and middle-income countries (including regions such as Africa, the Eastern Mediterranean, Russia, Middle America, and South America) than in high-income countries, urban developed regions. The global prevalence of infection in children remained relatively high at 34% during this period (**Liou et al., 2020; Yuan et al., 2022**). The higher prevalence observed in older individuals compared to children can be attributed to the fact that the vast majority (90%) of *H. pylori* infections are acquired during childhood and persist throughout one's life, rather than indicating a higher risk of infection at an older age.

Genetic and environmental factors, such as food sharing and housing habits, contribute in susceptibility to *H. pylori* infection (**Yuan et al., 2022**). For example, in the Sumatra islands of Indonesia, the prevalence of *H. pylori* infection is very low in the Malay and Java populations, but is high in Batak populations (**Syam et al., 2021**). This suggests that genetic factors may play a role. Gene and genome-wide association studies have identified that polymorphisms in IL-1B, Toll-like receptor 1 (TLR1) locus, and the FCGR2A locus are associated with *H. pylori* seroprevalence (**Liou et al., 2007; Mayerle et al., 2013**). However, a 2022 study has raised doubts on the role of TLR1/6/10 locus in *H. pylori* seroprevalence (**Lam et al., 2022**), and henceforth further studies are needed.

H. pylori is transmitted primarily through the fecal-oral and oral-oral routes, but contaminated water may also be a source of infection in developing countries (**Stefano et al., 2018; Brown et al., 2000 and Fox et al., 1985**). The bacteria can be cultivated from the vomitus, stool, and saliva of infected individuals, indicating that it can be transmitted through all of these body fluids (**Parsonnet et al., 1999**). However, more research is needed to determine the relative importance of each transmission pathway.

H. pylori is commonly transmitted within families, especially from mothers and siblings, in developing countries (**Weyermann et al., 2009**). Genotyping studies have shown that the same strain of *H. pylori* is found in 56% of mother-child pairs and 0% of father-child pairs

(Kivi et al., 2003). This is because *H. pylori* has genomic diversity, which makes it possible to track the spread of the bacteria between individuals. Newer molecular typing methods, such as seven-gene multilocus sequence typing (Schwarz et al., 2008) and whole-genome sequence analysis (Didelot et al., 2013) have allowed researchers to reconstruct the spread of *H. pylori* in families and have the potential to answer many unanswered questions about *H. pylori* epidemiology.

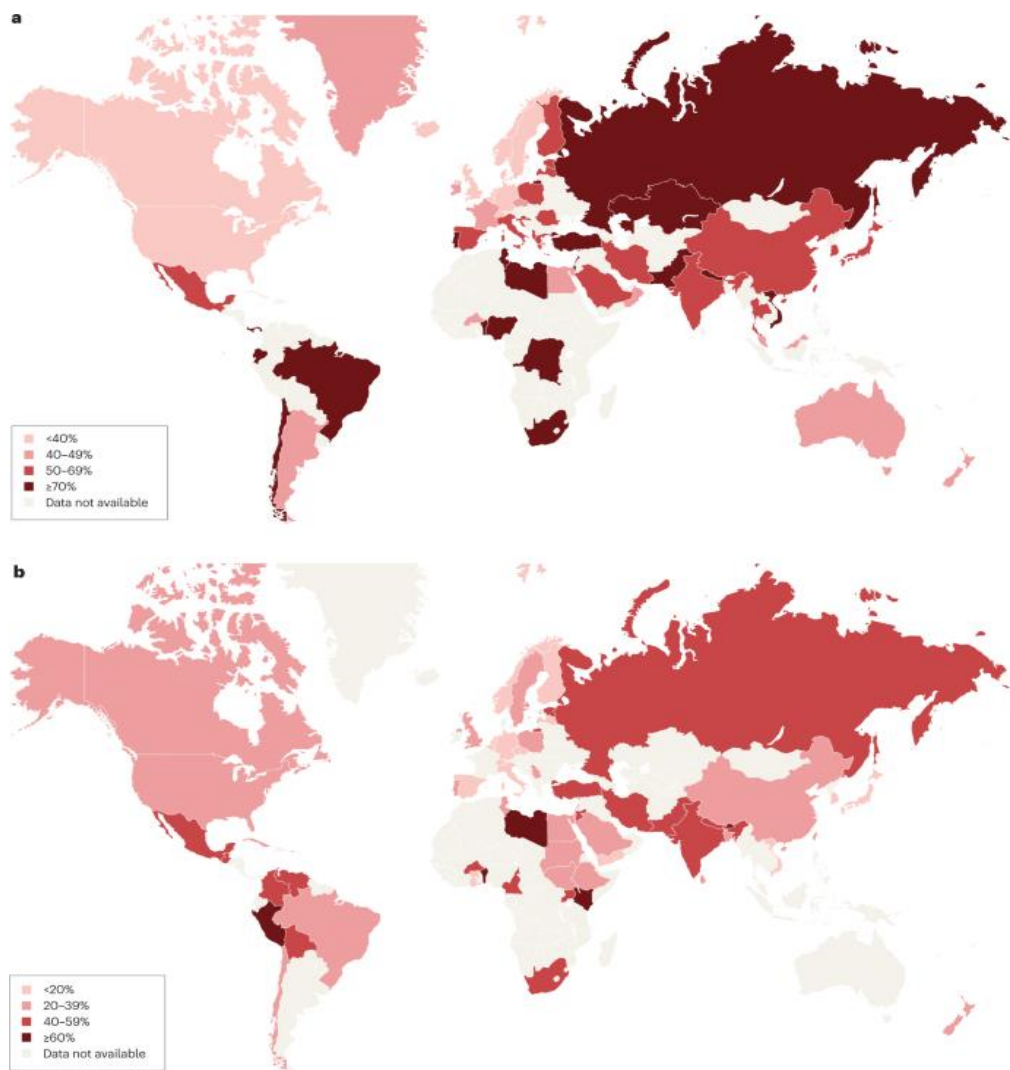


Figure3. Map shows the prevalence of *H. pylori* infection in both adults and children. (A) Global map shows the prevalence of *H. pylori* infection in adults from the period 1970 to 2016 in several regions, including Africa, Eastern Mediterranean regions, Russia, Middle America, Asia and South America. (B) Global map shows the prevalence of *H. pylori* infection in children and adolescents under 20 years old from the years 2000 to 2021 in Russia, Western Pacific regions, and European regions. (Source:doi.org/10.1038/s41572-023-00431-8)

2.5 Microbial Characteristics

2.5.1 Morphology

Helicobacter pylori a Gram-negative, helical-shaped, microaerophilic bacterium survives in the close proximity of the stomach lining (**Buck et al., 1990**). Its helical structure (from which the genus name, *Helicobacter*, derives) is assumed to have evolved in order to pierce the stomach mucoid lining and therefore establish infection (**Yamaoka et al., 2008**) and (**Brown et al., 2000**). This bacterium has a diameter of 0.5 μ m and a length of roughly 3 μ m (**Goodwin et al., 1993**). Gram stain, Giemsa stain, haematoxylin-eosin stain, Warthin-Starry silver stain, acridine orange stain, and phase-contrast microscopy are used to identify *H. pylori* in tissue (**Stark et al., 1999**). It can change from spiral to a potentially viable but non-culturable coccoid form, (**Chan et al., 1994**) and it can also produce biofilms (**Stark et al., 1999**).



Figure4. Electron Microscopic image of *H. pylori* (Source:<https://www.otsuka.co.jp>)

2.5.2 Growth requirements

Microaerophilic condition is critical for *H. pylori*, with optimal growth at O₂ levels of 2 to 5% and additional requirements of 5 to 10% CO₂ and extreme humidity. Although H₂ is not required for growth, it is not harmful. For *H. pylori* cultivation, many laboratories use typical microaerobic conditions of 85% N₂, 10% CO₂, and 5% O₂ (**Andersen et al., 1988**;

Andersen et al., 1992; Andersen et al., 1987; Andersen et al., 199; Jiang et al., 1987; Nederskov-Sørensen et al., 1988; Nichols et al., 1991). The optimal temperature for growth is between 34° and 40° Celsius. The bacterium can survive in pH conditions as low as 4, however it can only thrive in a rather narrow pH range of 5.5 to 8.0, with neutral pH being the best.

H. pylori, a fastidious microorganism has specific growth requirements. Media typically contains supplementation with several components such as whole blood, heme, serum, charcoal, corn starch, or egg yolk emulsion (Hachem et al., 1995; Henriksen et al., 1995). These additives have multifaceted role beyond providing essential nutrients; they also play a vital role in detoxifying the medium and safeguarding the organisms against the potential harmful effects of long-chain fatty acids, as indicated by (Hazell et al., 1990). For primary isolation and also routine culture, selective antibiotics are used such as vancomycin, trimethoprim, polymyxin B and nalidixic acid.

2.5.3 Respiration and Metabolism

H. pylori does not utilize carbohydrates for either fermentation or oxidation (Goodwin et al., 1993). Notably, *H. pylori* exhibit glucose kinase activity and display enzyme activity consistent with the pentose phosphate pathway (Mendz et al., 1991). Moreover, *H. pylori* possess specific D-glucose transporters, and certain features of its glucose transport system appear to be distinctively unique (Mendz et al., 1995).

H. pylori exhibits urea cycle activity, serving as an effective mechanism for expelling excess nitrogen from bacterial cells (Mendz et al., 1996). Additionally, the presence of the Entner-Doudoroff pathway has been confirmed in *H. pylori* (Mendz et al., 1994). Fumarate reductase plays a vital role in the metabolism of *H. pylori*, while the bacterium is also capable of metabolizing amino acids (Mendz et al., 1995a). Furthermore, cytochromes involved in the termination of the respiratory chain in *H. pylori* have been well-characterized (Mendz et al., 1995a).

2.54 Cell envelope and LPS

The cell wall of *H. pylori* is a complex structure and it is essential for its survival in the harsh acidic environment of the stomach. It is composed of three main layers: the inner membrane, the peptidoglycan layer, and the outer membrane. **The inner membrane** is a phospholipid bilayer that forms a barrier between the cytoplasm and the periplasm. It contains a variety of proteins that are involved in essential cellular processes, such as transport, metabolism, and cell signalling. **Peptidoglycan layer** is a polymer of N-acetylglucosamine (GlcNAc) and N-acetylmuramic acid (MurNAc), which is covalently cross-linked to form a strong and flexible mesh that gives *H. pylori* its characteristic spiral shape and protects it from osmotic pressure (Typas et al., 2012; Taylor et al., 2020). **The outer membrane** is an asymmetric phospholipid bilayer that contains a variety of proteins, including lipoproteins, porins, and adhesins. Lipoproteins are involved in anchoring the outer membrane to the peptidoglycan layer. Porins are channels that allow the passage of small molecules into and out of the cell. Adhesins are proteins that allow *H. pylori* for attachment to host cells. Interestingly, the phospholipid component within the *H. pylori* outer membrane contains cholesterol glucosides, a feature exceedingly uncommon among bacterial species (Bukholm et al., 1997; Haque et al., 1996; Tannaes et al., 2005).

The cell envelope of *H. pylori* has distinctive features such as high concentration of lipopolysaccharide (LPS) that distinguish it from other gram-negative bacteria (Moran et al., 2002). LPS comprises three distinct domains outer membrane's lipid A, which varies in its acylation and phosphorylation levels; the core oligosaccharide, consisting of inner and outer components linked to lipid A by 3-deoxy-d-manno-octulosonic acid (Kdo); and the O-antigen or O-specific polysaccharide, with the latter two regions exposed to the aqueous environment (Caroff et al., 2019). A notable characteristic of the O-chain in the LPS of many *H. pylori* strains is the expression of Lewis (Le) antigens, which mimic those expressed by the gastric epithelium (Monteiro et al., 2001). This mimicry serves as a camouflage that aids the

bacteria in evading the host's immune responses and may also trigger autoimmune disorders, thereby contributing to the infection's severity and chronicity (Moran et al., 2001).

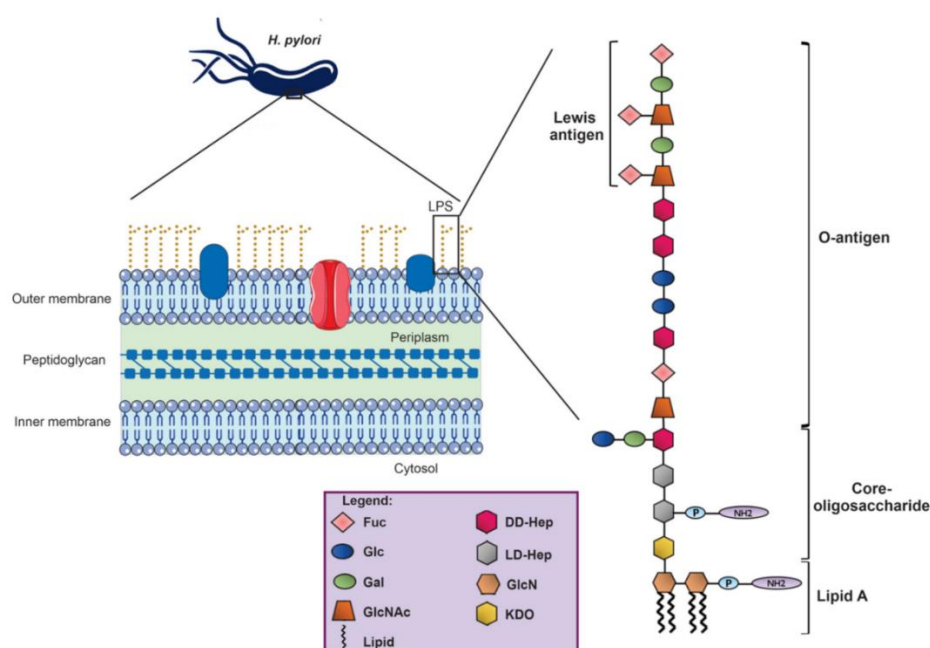


Figure5. LPS structure of *H. pylori*. (Source: doi.org/10.3390/ijms23073531)

2.6 *H. pylori* associated diseases

Infection with *H. pylori* is a major cause for the development of gastritis, duodenal ulcers, and gastric cancer. Investigators Warren and Marshall demonstrated that acute *H. pylori* infection occurs due to ingestion of a culture of the bacterium (Marshall et al., 1985; Morris et al., 1987). **Chronic active gastritis** is characterized by non-atrophic and superficial inflammation of the stomach mucosal lining. This histological form of *H. pylori* gastritis is typically asymptomatic but may be associated to **peptic ulcer disease (PUD)** and common complications like **chronic atrophic gastritis**, gastric adenocarcinoma, and gastric lymphoma.

The term PUD is used to refer ulcerations in the stomach, duodenum, or any other part of the gastrointestinal tract exposed to sufficient concentrations and durations of acid and pepsin. Prevalence of the PUD in individual's lifetime with *H. pylori* infection is estimated to be approximately 10% (Malfertheiner et al., 2009; Kuipers et al., 1995; Lanas et al., 2017).

In a prospective investigation, people infected with *cagA*-positive *H. pylori* strains had an 18.4-fold and 2.9-fold greater lifetime risk of developing duodenal and stomach ulcers (Schottker, et al., 2012).

In some individuals, chronic superficial *H. pylori* gastritis can evolve over time into atrophic gastritis with an annual ranging from 1% to 3% (Villako et al., 1991; Kuipers et al., 1995; Ihamaki et al., 1985). As the degree of atrophy advances, the presence of an active *H. pylori* infection tends to decrease. This decline is likely linked to the transformation of the stomach lining, transitioning from the *H. pylori*-friendly normal superficial epithelial cells to **intestinal metaplasia**, where *H. pylori* are rarely found. Furthermore, **hypochlorhydria** stomach acid production can create an inhospitable environment for the organism. In the absence of sufficient acid, other microorganisms can

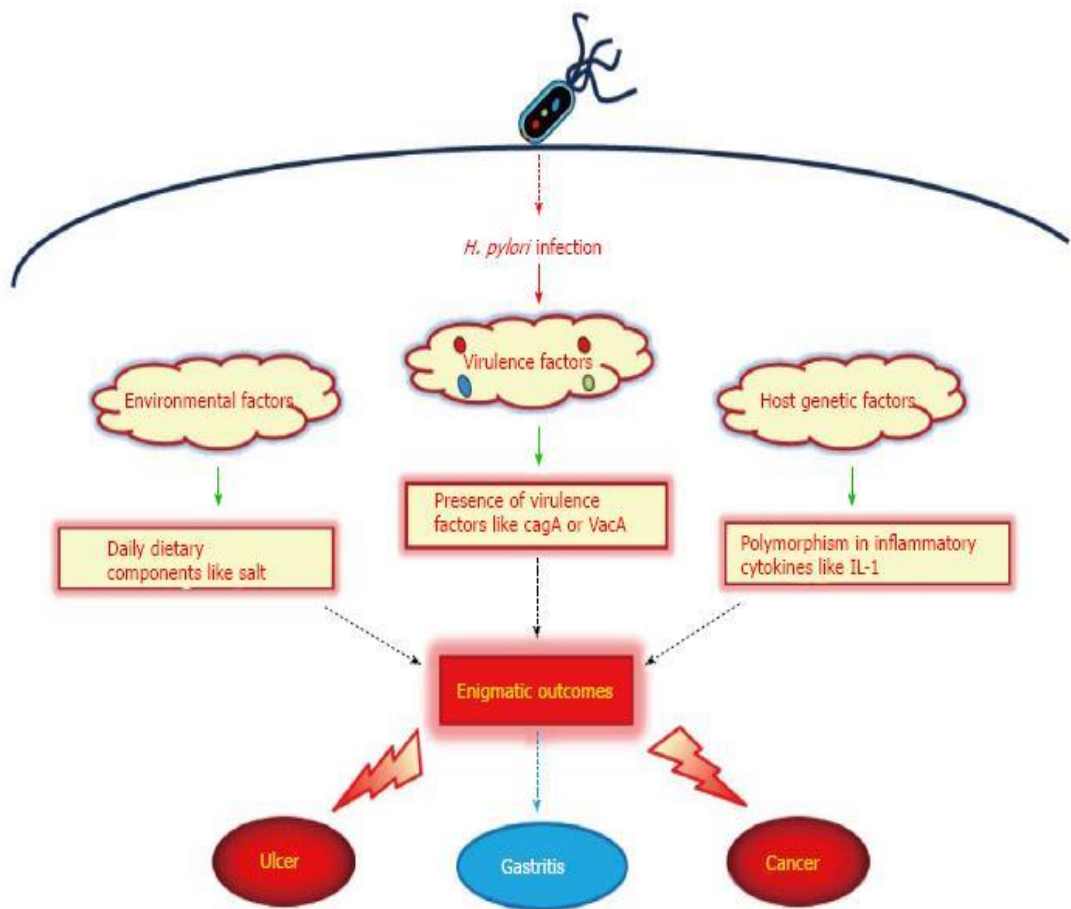


Figure6. *Helicobacter pylori* association involves a complex interplay of factors, including (1) bacterial virulence factors, (2) host genetic factors, and (3) environmental factors. (Source: doi: 10.4251/wjgo.v8.i4.341)

thrive in the stomach, leading to competition for resources. The process through which gastric mucosal damage advances from superficial gastritis to atrophy remains unclear and is likely influenced by multiple factors. The interplay among host genetics, immune response, bacterial virulence expression, dietary factors, micronutrient availability, and the structure of microbiome collectively shape disease outcomes. It is likely that dietary modifications designed to manipulate the microbiota in *H. pylori* carriers could be harnessed to mitigate disease risk and enhance gastric health. Nevertheless, our comprehension of the intricate connections among these variables remains limited. Ethnicity and environmental factors may play a significant role, as evidenced by the considerable variation in the proportion of infected population in different geographic regions.

People with *H. pylori* infection have 1-5% lifetime risk of developing stomach cancer **(Suerbaum & Michetti et al., 2002; Liou et al., 2020; Fann et al., 2018)**. Gastric cancer is the cumulative outcome of long-term gastric mucosal infection and chronic inflammation. A key mechanism implicated in *H. pylori*-induced gastric carcinogenesis seems to be initiation of chronic inflammation, which in turn leads to amplified oxidative stress followed by formation of oxygen-free radicals capable of causing DNA damage. Additionally, it triggers increased cytokine production, leading to enhanced cell turnover and impaired DNA repair mechanisms **(Ernst et al., 1999)**. Approximately 90% of instances of gastric cancer can be linked to *H. pylori* infection **(Moss et al., 2017)**. A total of 812,000 cases of gastric cancer, including non-Hodgkin lymphoma of the gastrointestinal region, were reported in 2018, making *H. pylori* the most common bacterium known to cause cancer **(de Martel et al., 2020)**. There are considerable regional differences in the incidence and mortality of gastric cancer, with Asia and Eastern Europe having the highest rates. Some groups are more likely to develop stomach cancer after *H. pylori* infection, depending on the genetic factors, environmental circumstances, and dietary preferences, such as higher use of salted or pickled

foods in East Asian populations. Additionally, traditional groups in the USA, notably Asian Americans (Kumar et al., 2020) and indigenous communities around the world (Arnold et al., 2014) have significantly higher rates of stomach cancer. Smoking and the amount of salt consumption are lifestyle and dietary factors that contribute to the development of gastric cancer, however *H. pylori* infection is the most important component in determining these other factors (Gonzalez et al., 2010; Venneman et al., 2018).

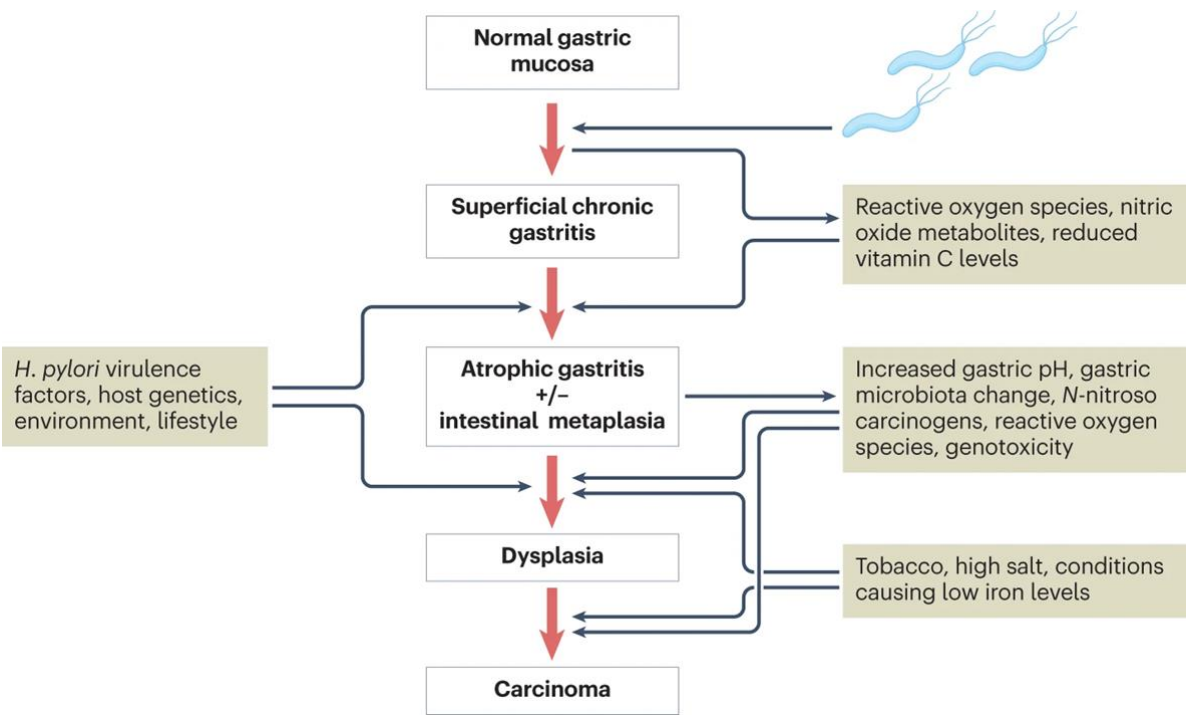


Figure7. Elucidating the Pathogenesis of Gastric Adenocarcinoma Induced by *H. pylori*
(Source: doi.org/10.1038/s41572-023-00431-8)

2.7 Genome of *H. pylori*

In 1997, *H. pylori* 26695 was the first strain to be sequenced (Tomb et al., 1997). It was isolated from a chronic gastritis patient in England. The circular chromosome of strain 26695 contains 1667867 base pairs and an average GC content of roughly 39%. In the initial annotation 1,590 open reading frames were potentially identified as protein-coding genes, alongside RNA coding genes including two copies each of 16SrRNA and 23SrRNA genes, as well as 36tRNA genes (Tomb et al., 1997). The *H. pylori* genome encodes fewer global

regulatory proteins when compared to established models like *E. coli*. In a departure from typical gram-negative bacteria, several key regulatory proteins found in others were conspicuously absent in *H. pylori*. Instead, this genome revealed the presence of four genes with perfect helix-turn-helix motifs, a hallmark characteristic of DNA-binding proteins (Tomb et al., 1997).

Notably, the bacterium did harbour homologues for four histidine kinases and six response regulators involved in two-component systems, enabling it to respond to various environmental cues and challenges (Beier et al., 2000). Nevertheless, *H. pylori* appeared to lack sigma factors associated with stress regulation, as indicated by Alm et al., in 1999. This deficiency might signify that *H. pylori's* lifestyle exposes it to a more limited array of environmental conditions compared to other organisms, thus shaping its distinct regulatory protein profile.

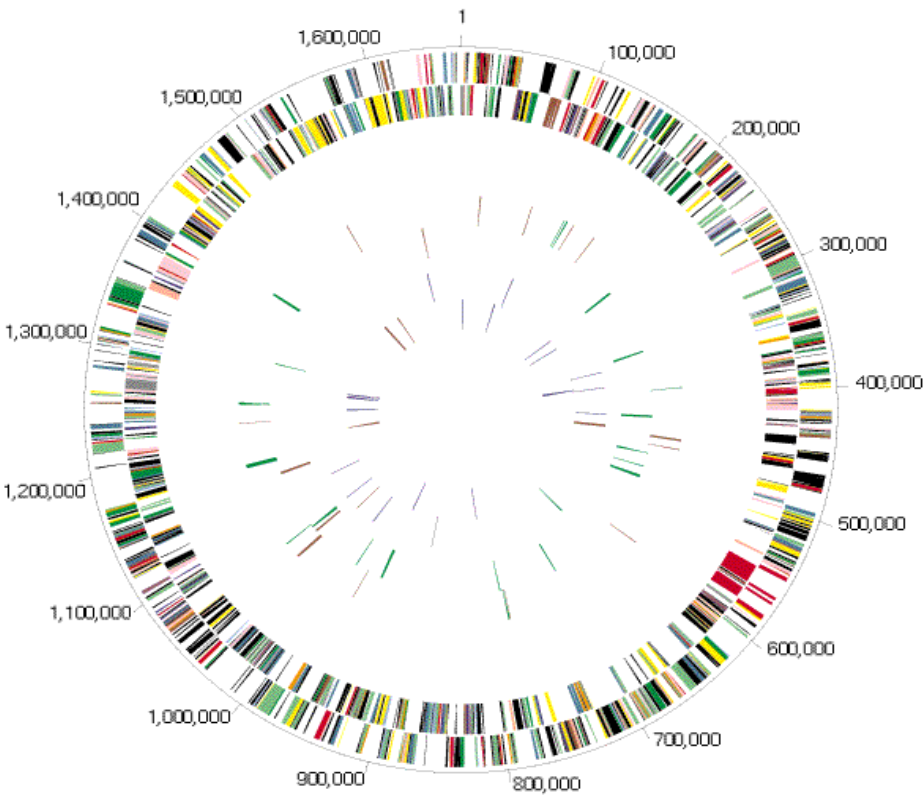


Figure8. Circular representation of the *H. pylori* 26695 chromosome (Source: DOI: 10.1038/38792

2.8 Genetic plasticity in *H. pylori*

H. pylori, is known for its unparalleled genetic diversity, a characteristic that sets it apart from many other bacterial pathogens (Covacci et al., 1998; Logan et al., 1996). These bacteria have a unique ability to colonize in the protective mucus lining of the stomach and adapt in the acidic hostile environment of the gastric mucosa. This often leads to gastritis, which tends to be mostly asymptomatic (Watari et al., 2014). The chronic inflammatory character of the infection, bacterium's elevated mutation and recombination rates contribute to the diverse bacterial population, referred to as a quasispecies, within the gastric mucosa of infected individuals. Notably, bacteria colonize the antrum and corpus regions of the stomach and encounter varying levels of acidity, inflammatory factors, and have diverse accessibility to protective glands and mucus. This diversity in environmental conditions within the stomach may serve as a driving force for bacterial diversification over time (Jorgensen et al., 1996). Comprehensive genetic analyses, often from single colony isolates from individual patients, both at global and regional level, have greatly contributed to the identification of specific genotypes associated with varying disease types and their respective severity levels (Cortes et al., 2010; Kojima et al., 2016; Vale et al., 2015). For example, a recent genome-wide association study (GWAS), pinpointed specific single nucleotide polymorphisms (SNPs) and genes within *H. pylori* genomes that can serve as valuable tools for evaluating the risk of developing gastric cancer among infected individuals (Berthenet et al., 2018). The extensive genetic diversity observed in *H. pylori* has significant implications in treatment procedure for development of vaccines. Nevertheless, the precise attributes of *H. pylori* diversity within infected individuals remain an area of ongoing investigation and have not been comprehensively elucidated.

2.9 Adaptation Strategies of *Helicobacter pylori*

2.9.1 Helical shape

The helical configuration enables a corkscrew-like mechanistic movement, aiding in the efficient penetration of the epithelium. Significantly, a set of genes responsible for shaping the bacterium's morphology, namely Ccrp58, Ccrp89, Ccrp1142, and Ccrp1143, has emerged as key players (**Martínez et al., 2016**).

2.9.2 Motility

Flagella are essential for *H. pylori* to colonize and persist in the human gut. The propulsive action of flagella helps *H. pylori* to reach its preferred niche into the host epithelial mucosa. In addition to the crucial flagellar filamentous proteins, FlaA and FlaB, there are over 40 other proteins intricately involved in the biosynthesis and functionality of the flagellum (**Gu et al., 2017**).

2.9.3 Chemotaxis

H. pylori has evolved chemotaxis, a mechanism that allows it to sense and respond to changes in pH, to colonize and persist in the narrow niche on the surface of epithelial cells in the stomach. Chemotaxis is essential for *H. pylori* to evade the harsh acidic environment of the stomach lumen and establish infection (**Terry et al., 2005**). Key proteins such as CheA, CheW, CheY, and ChePep play important roles in governing the bacterium's chemotactic properties (**Howitt et al., 2011**).

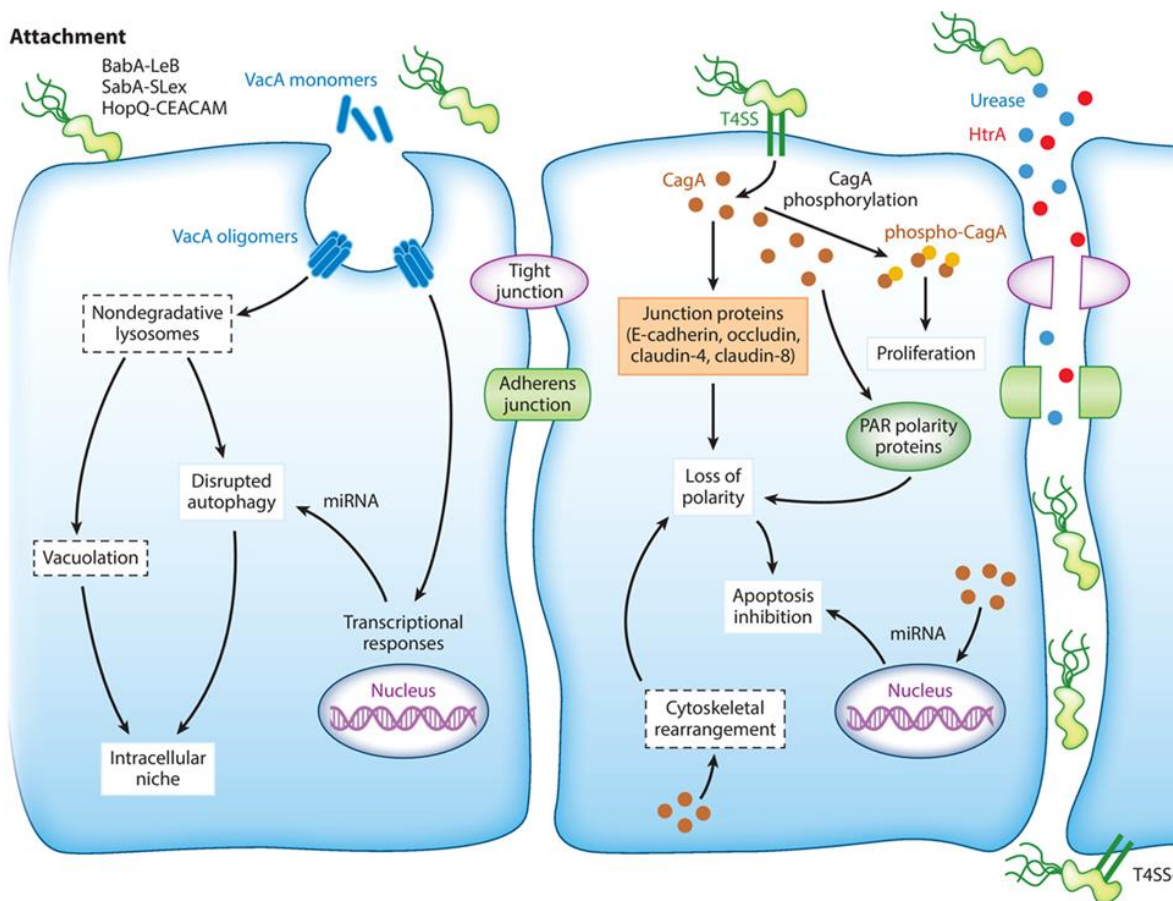


Figure9. Mechanism of *H. pylori* colonization into the Gastric Epithelial Cells. (Source: doi.org/10.1146/annurev-physiol-061121-035930)

2.9.4 Urease

Acid resistance is the most crucial phenomena to survive in the gastric niche. Urease primarily hydrolyzes urea to bicarbonate and ammonia. This results in a net increase in the pH of the surrounding acidic microenvironment which enables intracellular homeostasis of *H. pylori* and permits successful bacterial colonization of the stomach. More than 300 genes regulate acid resistance (Wen et al., 2002 and McGowan et al., 2002) and one of these genes encodes an enzyme urease. Urease gene cluster consist of the catalytic subunits (ureA/B), an acid-gated urea channel (ureI), and associated assembly proteins (ureC, ureD, ureI, ureE, ureF, ureG, and ureH) (Mobley et a., 1995). Translation of these genes takes place in the presence of nickel (Ni), ultimately giving rise to a nickel-dependent urease.

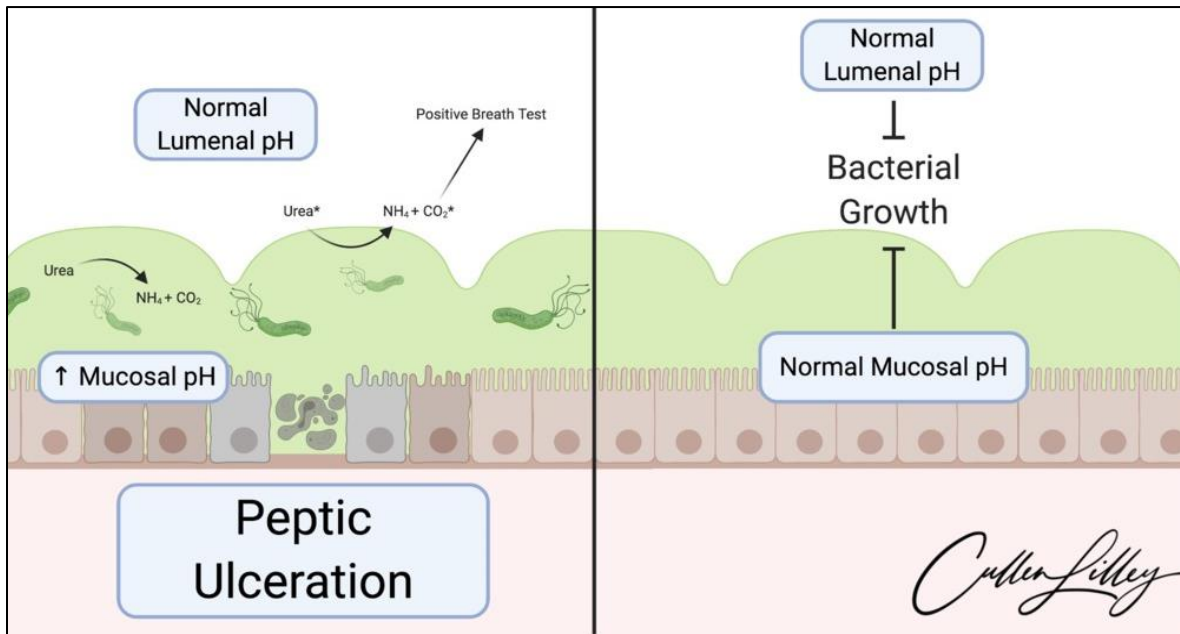


Figure10. *H. pylori* invading Gastric Epithelial Cells. (Source: <https://www.patholective.com/micromedex/pathogens-surviving-the-stomach>)

2.9.5 Adhesions to cellular surface receptors

The expression of adhesion molecules is a crucial phenomenon for the long-term persistence of *H. pylori* within the host. The interaction of bacterial adhesions with cellular receptors prevents *H. pylori* from being forced out of the stomach when it colonises the gastric epithelial layer and then bacteria acquire metabolic substrates and nutrients to grow and further releases toxins to damage the host cells. Several known adhesions such as blood-antigen binding protein A (BabA), sialic acid-binding adhesion (SabA) (Ilver et al., 1998) and (Mahdavi et al., 2002) neutrophil-activating protein (NAP) (Teneberg et al., 1997), heat shock protein 60 (Hsp60) (Yamaguchi et al., 1997), adherence-associated proteins (AlpA and AlpB) (Odenbreit et al. 1999) are the well-characterized adhesions studied so far.

2.9.6 Toxin and host tissue damage

The high pathogenicity of *H. pylori* is primarily attributed to an array of virulence factors, including vacuolating cytotoxin A (VacA), cytotoxin-associated gene A (CagA), gamma-

glutamyltranspeptidase (HpGGT), HP0175, high temperature requirement A (HtrA). Among these, VacA and CagA stand out as the most common virulence factors, involved in promoting the development of gastric cancer.

Vacuolating cytotoxin A (VacA)

VacA is an important virulence factor named after its capability to induce the formation of substantial vacuoles within targeted host cells. VacA is produced as a 140 kDa pre- protoxin and then secreted by the type IV autotransporter system into an 88 kDa monomer of mature toxin which consists of two fragments: N terminal p33 domain and p55 domain at the C-terminus. Pore-forming activity is carried out by p33 domain and binding with the host cell receptor is carried out by p55 domain (**Chambers et al., 2013**). Notably, VacA create pores for chloride-selective membrane channels, a property of utmost importance for instigating various cytotoxic effects within affected cells. This process leads to water influx, resulting in vesicle swelling and the formation of vacuoles, particularly in the presence of weak bases like ammonium chloride (**Szabo et al., 1999; Morbiato et al., 2001**). In the absence of weak bases, VacA does not induce cell vacuolation, but it does produce observable changes in late endocytic compartments. These alterations are the inhibition of intracellular degradation of epidermal growth factor, inhibition of procathepsin D maturation (**Satin et al., 1997**), the clustering of late endocytic compartments (**Li et al., 2004**), and the inhibition of antigen presentation (**Molinari et al., 1998**).

VacA has a range of effects on gastric epithelial cells, including the initiation of apoptotic cell death through mitochondrial membrane damage, or the triggering of necrosis (**Kim et al., 2012**). Additionally, it can induce autophagy and inhibit the proliferation of T cells and B cells (**Altobelli et al., 2019**). It also affects other immune cells. Collectively, these actions serve to down-regulate immune responses to *H. pylori* infection and raise host tolerance toward the organism.

Several reports indicate that VacA elevates the level of reactive oxygen species (ROS) and stimulates the production of proinflammatory cytokines in gastric epithelial cells (Raju et al., 2012). Furthermore, VacA activates two classes of MAPkinase, p38 and Erk1/2, along with the activating transcription factor 2 (ATF-2) pathways (Kim et al., 2012).

The *vacA* gene is present in all strains of *H. pylori* with varying proportions depending on the sequence diversity. These sequence diversity are associated with variations in the cytotoxicity and cellular responses. The gene itself can be categorized into four distinct regions: the signal sequence (s), intermediate (i), mid (m), and autotransporter region. Within each of these regions, polymorphic segments have been identified, with different allelic variants designated as s1 or s2, i1, i2, or i3, and m1 or m2, respectively. The s1m1 allelic form of VacA is more toxic to gastric epithelial cells than other allelic forms (Kim et al., 2012).

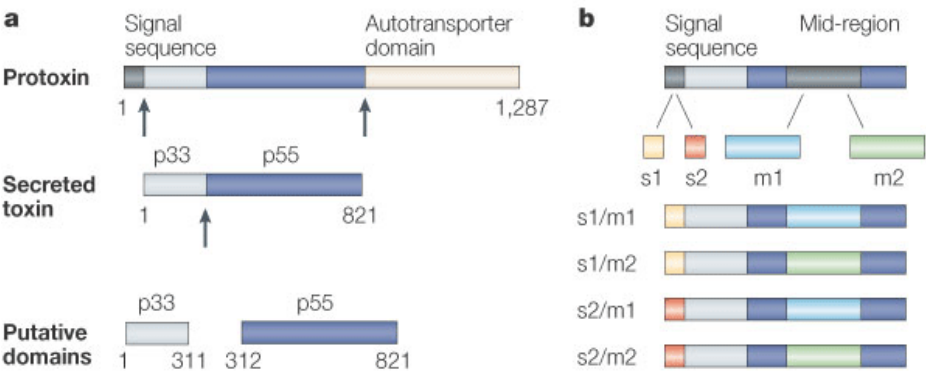


Figure12. (A) Vacuolating (VacA) protoxin cleaved into mature toxin. It is secreted into the extracellular spaces (B) Allelic diversity of VacA (Source: doi.org/10.1038/nrmicro1095)

The Cag Pathogenicity Island (*cagPAI*) and CagA

The discovery of the *cag* pathogenicity island (*cagPAI*) plays an important role in *H. pylori*'s virulence and its association with peptic ulcer disease in infected patients through the immunodominant protein CagA (Censini et al., 1996). Subsequently, in-depth analysis of the DNA regions surrounding the *cagA* gene was conducted, leading to the identification of the *cag* pathogenicity island (*cagPAI*). This significant finding was corroborated by extensive

research (**Akopyants et al., 1998**). The *cag*PAI exhibits several key characteristics commonly found in classic pathogenicity islands (**Censini et al., 1996, Hacker et al., 1997**). These characteristics include: **(i)** a distinct G + C content of 35 %, which diverges from the typical mean of 39 % found in the rest of the *H. pylori* genome; **(ii)** flanking direct repeats crucial for the integration of the approximately 40 kb locus into the genome; **(iii)** putative virulence genes and genes responsible for type IV secretion system; and **(iv)** insertion sequences.

The *cag*PAI is a ~40 kb region containing 31 genes. A number of these genes including *cagE* (homologue of *virB4*), *cagT* (*virB7*), *cagW* (*virB8*), *cagX* (*virB9*), *cagY* (*virB10*), *cagA* (*virB11*) and *cagβ* (*virD4*) have been shown to encode a type IV secretion system (TFSS) which might allow export of substances through bacterial outer membrane (**Asahi et al., 2000, Backert et al., 2001, Censini et al., 1996, Covacci et al., 2000**).

Individuals infected with *cag*⁺ strains of *H. pylori* face a significantly elevated risk of developing atrophic gastritis, peptic ulceration, and gastric adenocarcinoma compared with those with *cag*[–] strains (**Wirth et al., 1996**). However, in Asian populations, where the prevalence of *cag*⁺ strains is nearly ubiquitous among individuals, establishing a clear relationship of the *cag* gene with disease is difficult.

The *cagA* gene that encodes CagA is present at one end of the *cag*PAI. When *cagA*-positive *H. pylori* attaches to the gastric epithelial cells, the CagA protein is delivered directly into the host epithelial cells through the type IV secretion system encoded within the *cag*PAI (**Segal et al., 1999; Asahi et al., 2000**). CagA, ranging from 120 to 140 kDa, exhibits sequence diversity, which contains several distinctive Glu-Pro-Ile-Tyr-Ala (EPIYA) motifs. These EPIYA motifs, designated A through D, are differentiated by variations in the amino acid sequences surrounding the EPIYA motif itself (**Jones et al., 2010**).

Key signalling events triggered by CagA is the activation of the eukaryotic tyrosine phosphatase SHP-2. SHP-2 in turn activates the ERK1/2 MAP kinase, the Crk adaptor protein, and the C-terminal Src kinase pathway. Activation of these signalling pathways by CagA can lead to a variety of cellular changes, including: aberrant cell proliferation, decreased apoptosis, increased cell motility, disruption of cell-cell adhesion, and alteration of gene expression. These changes can contribute to the development of gastric cancer, which is associated with *H. pylori* infection. In addition, CagA can activate transcription factor nuclear factor (NF- κ B) that induces the release of pro-inflammatory cytokines such as interleukin-8 (IL-8), IL-6 and TNF α (Hatakeyama et al., 2014).

A central aspect of *H. pylori* pathogenesis lies in the ability of CagA and VacA to antagonize each other's effects, a phenomenon that holds significant implications in the process of gastric cancer development during *H. pylori* infection.

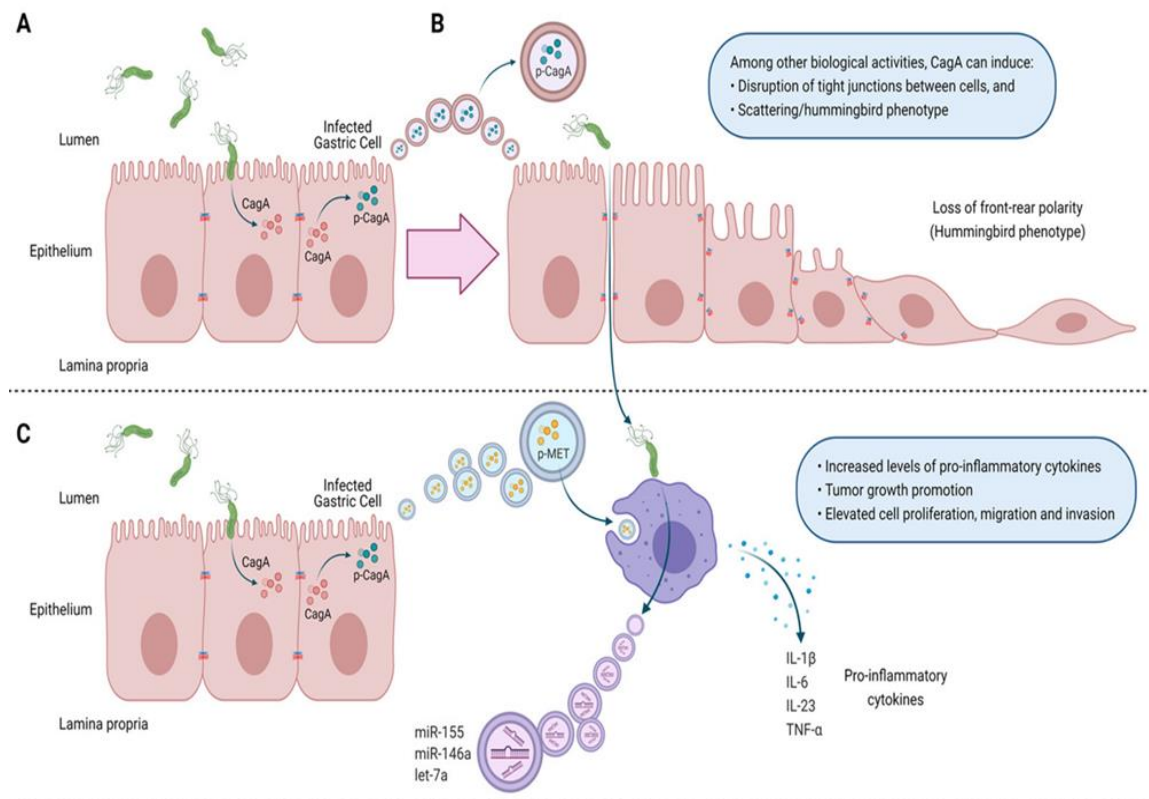


Figure13. *H. pylori* infected-host cells are associated with gastric cancer development. (Source: doi.org/10.3390/ijms22094823)

2.10 Immune Evasion by *H. pylori*

Once *H. pylori* successfully colonizes the gastric mucosal cells, it triggers host immune responses, involving both the innate and acquired, leading to the generation of specific antibodies and the activation of Th cells (Robinson et al., 2007). Additionally, it leads to the production of inflammatory regulators, reactive oxygen species (ROS), and cytokines (TNF- α , IL-6, IL-8, IL-17) into the lamina propria, which further activates the macrophages, dendritic cells, and various inflammatory mediators (Bagheri et al., 2015). *H. pylori* must evade these immune responses to establish and maintain colonization in the stomach for extended period of time. It is evident that the long-term persistence of *H. pylori* is a critical factor in its ability to colonise despite facing challenges from both innate and adaptive immune responses (Baldari et al., 2005; Robinson et al., 2007). Moreover, subsequent to *H. pylori* colonization, a portion of the infected population may develop autoimmune reactions or immune system abnormalities (Radic et al., 2014). These observations highlight the bidirectional effects between *H. pylori* and the human immune system. Over years of commensalism between host and *H. pylori*, the bacterium has evolved strategies to subvert the immune response, serving as a remarkable example of bacterial evolution to maintain its micro-territory within the human body (Chmiela et al., 2017). Persistent infection results in peptic ulcer and in severe cases stomach cancer. However, only 10–15% of individuals infected with *H. pylori* develop peptic ulcer disease, and a smaller fraction, about 1–3%, progress to gastric cancer (Kuipers et al., 1995). This shows the complex interplay among host factors, environmental conditions, and the bacteria, which collectively influences the process of carcinogenesis. Finally, bacterial persistence occurs only when *H. pylori* and the host immune system co-adapt after effective immune evasion.

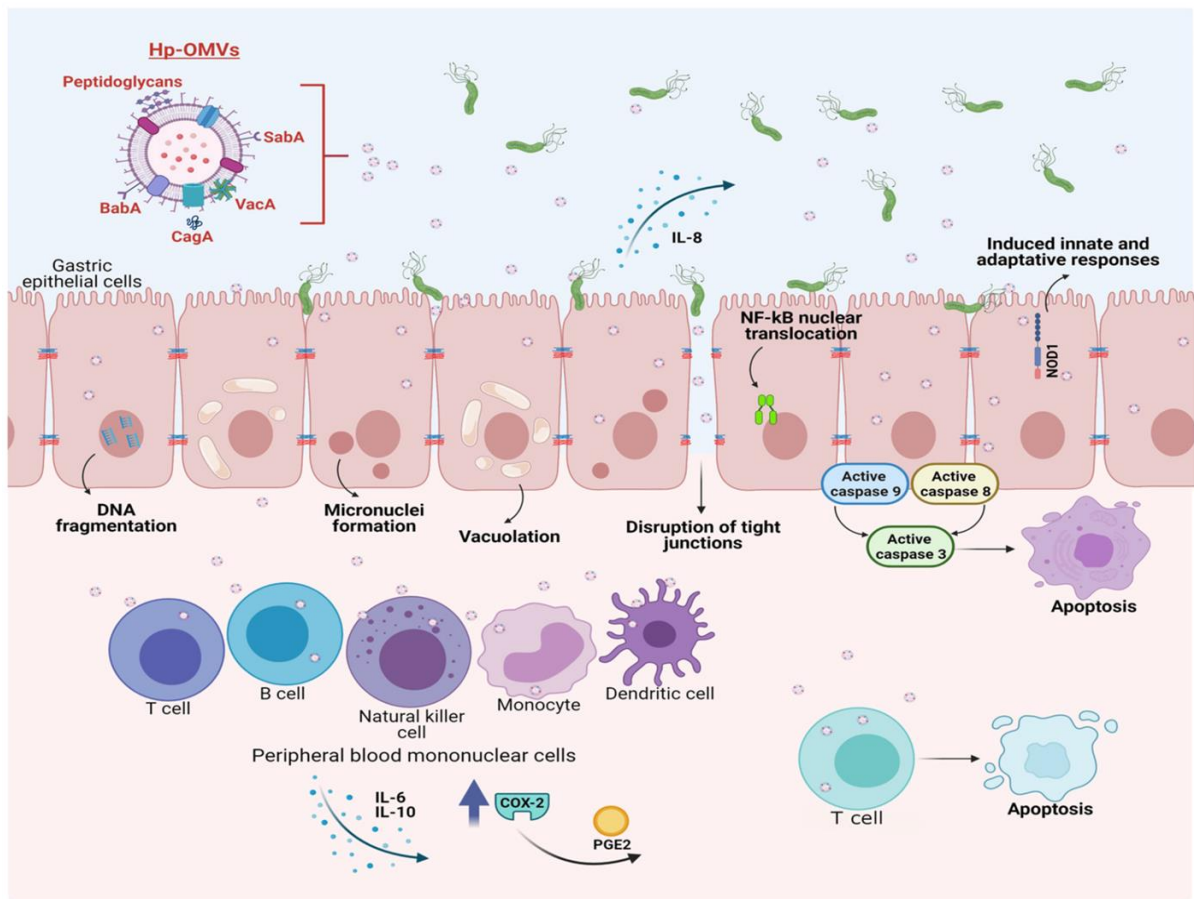


Figure14 Schematic representation of immune response against *H. pylori* infection in the gastric microenvironment. (Source: doi.org/10.3390/ijms22094823)

2.11 Autophagy: A Key Player in Immune Defense

Autophagy, an evolutionarily conserved catabolic process in eukaryotes, plays a crucial role in maintaining cellular homeostasis by facilitating the degradation of cargo, including long-lived proteins and damaged organelles. The resultant molecules are subsequently recycled to aid cells in adapting to various cellular stresses, such as nutrient starvation or growth factor depletion. There are three types of autophagy: (1) macro-autophagy (2) micro-autophagy and (3) chaperone-mediated autophagy. The difference in the types of autophagy lies in the mechanism of cargo delivery to the lysosome and the nature of the cargo or substrate (Mizushima and Levine, 2010; Galluzzi et al., 2017). The most explored among the three kinds of autophagy is macroautophagy. Our focus is on macroautophagy, referred to hereafter

as autophagy. The most distinctive feature of autophagy is the development of the double-membrane bound phagophore and autophagosome. The process starts with the phagophore formation which engulfs the material to be degraded and then elongates to form a double membrane known as an autophagosome. The autophagosome then fuses with the lysosome to destroy the engulfed material by acidic lysosomal hydrolases. Under normal conditions, it occurs at basal level that removes damaged cell organelles as well as unnecessary or misfolded proteins through a lysosomal -dependent pathway (**Li et al., 2012**). Autophagy is activated in response to various cellular stresses, such as nutrient or energy deficiency, protein aggregates, damaged organelle, oxidative stress or pathogen invasion. The cytoplasmic cargos breakdown into metabolites and are utilized in different biosynthetic pathways and energy production inducing cell survival. Therefore, autophagy is mainly thought of as a cyto-protective process, even though excessive self-degradation can potentially be harmful (a cyto-killing mechanism) (**Mehrpour et al., 2010**). Macroautophagy can alternatively be classified as bulk or selective autophagy. Under starvation conditions, nonselective autophagy is employed to turnover bulk cytoplasm, whereas selective autophagy specifically targets aggregated proteins (aggrephagy), damaged or excess organelles, such as mitochondria and peroxisomes, (mitophagy, lipophagy, chlorophagy, ribophagy, and pexophagy) as well as invasive microorganisms (xenophagy) (**Deffieu et al., 2009; Dunn et al., 2005**).

2.11.1 Molecular mechanism of Macroautophagy

Macroautophagy (hereinafter referred to as 'autophagy') begins with the formation of the phagophore, also known as the isolation membrane, which contains a lipid bilayer derived mostly from the ER and/or the trans-Golgi and endosomes in humans and PAS (preautophagosomal structure) in yeast (**Feng et al., 2014**). The membrane eventually generates a spherical autophagosome, where the intracellular cargos are sequestered, as the

phagophore swells and causes the membrane to bend. When selective autophagy occurs, the membrane appears to essentially wrap around the cargo and confirm to fit the specific target, but the processes that induce curvature of the membrane during non-specific autophagy are unknown (**Glick et al., 2010**).

2.11.2 Formation of Phagophore or nucleation

Several studies indicate that phagophore membranes are predominantly triggered by ER-associated structures known as omegasomes, as well as other cytosolic membrane structures such as the trans-Golgi and late endosomes. Atg8 was the first Atg protein identified as a phagophore and autophagosome marker (**Huang et al., 2000; Kirisako et al., 1999**). Subsequent investigations with GFP-tagged chimaeras revealed that the majority of Atg proteins, at least transiently, reside at this site (**Suzuki et al., 2001**). Phagophore assembly site (PAS) is postulated as the location where the phagophore assembles. The specific nature of the PAS in terms of protein and membrane composition, as well as the cause for its perivacuolar location, is unknown, however Atg protein assembly at the PAS happens in a hierarchical manner (**Reggiori et al., 2016**). ATG1 kinase in yeast creates a complex with ATG13 and ATG17 before recruiting the transmembrane protein ATG9, which increases lipid engagement for phagophore production. The energy-sensing TOR (target of rapamycin) kinase regulates this process by phosphorylating ATG13, which further inhibits binding with ATG1 and therefore initiates autophagy. The mammalian functional homologues of ATG1, ULK1 and ULK2 (Unc-51-like kinase-1 and -2), are required for autophagy initiation (**Wang et al., 2018**). Both ULK1 and ULK2 can interact with mTOR (mechanistic target of rapamycin) complex 1 (mTORC1) that inhibits ULK complex activity (**Kim et al., 2015**). When nutrients or growth factors are abundant, mTOR phosphorylates ULK1, inhibiting autophagy (**Sengupta et al., 2010**). Under nutritional deprivation conditions, on the other hand, ULK1 forms a stable complex with FIP200/ATG17 and ATG13.

The Class III phosphatidylinositol 3-kinase (PI3K) complex mediates phagophore membrane nucleation and assembly (**Hurley et al., 2017**). This complex is made up of PIK3C3 (phosphatidylinositol 3-kinase catalytic subunit type 3)/VPS34, its regulatory protein kinase PIK3R4/VPS15, Beclin 1 and ATG14 (**Reidick et al., 2017**). Beclin1 interacts with Bcl-2 family proteins via its BH3 (Bcl-2 homology 3) domain, including Bcl-2 (B-cell lymphoma 2), BclxL/ BCL2L1 (Bcl-2-like protein 1), and, to a lesser extent, Mcl-1 (myeloid cell leukaemia 1). In normal settings, for example, the interaction of anti-apoptotic Bcl-2 with Beclin1 limits autophagosome production (**Renault et al., 2014**). However, this inhibition is circumvented by MAPK8/JNK1-mediated phosphorylation of Bcl-2 in response to starvation-induced signalling, permitting autophagosome formation.

On the other hand, VPS34 phosphorylates phosphatidylinositols and stimulates the synthesis of phosphatidyl inositol 3-phosphate [PI(3)P], which is essential for the creation of phagophores. WIPI-1/2 (WD-repeat protein interacting with phosphoinositides 1 and 2) then interacts with PI(3)P in the phagophore membrane, initiating autophagosome elongation and maturation (**Mercer et al., 2018**).

2.11.3 Phagophore elongation and closure

During the phagophore elongation and closure process, two evolutionarily conserved Ub-like (UBL) conjugation systems are involved. These are the MAP1LC3B (microtubule-associated protein 1 light chain 3beta, or simply LC3; mammalian homologs of ATG8) and the ATG5-ATG12 complex. The complex then binds with ATG16L dimers and tethers to the growing phagophore, where ATG7 serves as an E1-like enzyme and ATG10 as an E2-like enzyme (**Otomo et al., 2013**), ATG7 activates ATG12 in an ATP-dependent manner by binding to the C-terminal glycine residue of ATG12 and transfers to ATG10, which enables the covalent attachment of ATG12 to the K130 residue of ATG5.

The second process involves the phosphatidyl ethanolamine (PE) conjugation of the soluble form of LC3, LC3-I, to produce the membrane bound form LC3-II, which is commonly used as a standard marker for autophagosome formation. When autophagy is induced, the cysteine protease ATG4 first cleaves LC3, exposing the C-terminal glycine residues for further activation by an E1-like enzyme ATG7 in an ATP-dependent manner. Next, the C-terminal glycine residues are transferred to another E2-like enzyme ATG3, and PE is then conjugated to the carboxyl glycine to produce processed lipidated LC3-II (**Otomo et al., 2013**). ATG8 has evolved into the LC3-family proteins, which include MAP1LC3A (2 splice variants), MAP1LC3B, MAP1LC3C, GABARAP (gammaaminobutyric acidreceptor associated protein), GABARAPL1 (GABA type A receptor a protein like 1), and GABARAPL2 (GABA type A receptor a protein like 2). One of these, MAP1LC3B, is the most researched family protein linked to the maturation and growth of autophagosomes and is frequently used to monitor the activation of autophagy in response to diverse cellular stressors. Given their high degree of similarity, additional LC3-family members are frequently assumed to have comparable roles (**Kabeya et al., 2004; Tanida et al., 2004**).

In addition, the chosen damaged cargo is often ubiquitinated, collected by the adaptor molecules -p62/SQSTM1 (sequestosome1), NDP52 and NBR1 (neighbour of BRCA1 gene 1), and finally delivered to autophagosomes via their LIR-motif (LC3-interacting-region) (**Rogov et al., 2014**).

2.11.4 Maturation and degradation

During maturation, autophagosomes fuses with lysosomes, generating an autolysosome, where acid hydrolases and cathepsins of lysosomes destroy the cargo. Before delivering to autolysosomal acid proteases, the pH of the autophagic vesicle is also reduced. RAB7, a member of the RAS oncogene family, is a tiny G-protein. In its GTP-bound state, the family plays an essential role in autolysosome formation (**Kuchitsu and Fukuda, 2018**).

Furthermore, two v-SNARE (vesicle-SNAP receptor) family proteins, VAMP3 and VAMP7 (vesicle associated membrane protein 3 and 7), are involved in autophagosome-lysosome fusion (Fader et al., 2019). The enzymes present such as Cathepsin proteases B and D within the lysosome destroy the selected cargo. LAMP-1 and LAMP-2 (lysosomal associated membrane proteins 1 and 2) are also required for functional autophagy at the lysosomal end (Eskelinen et al., 2002).

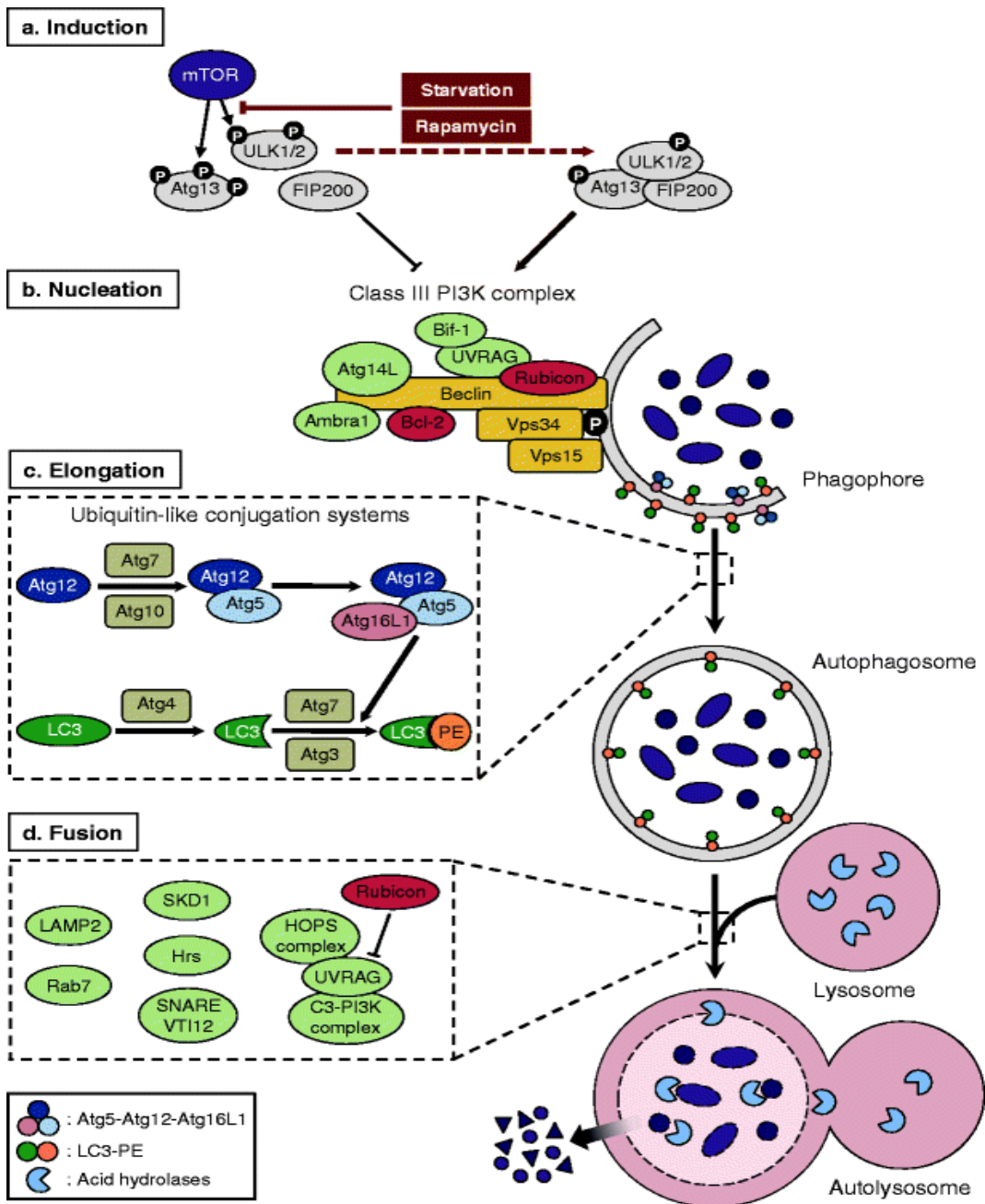


Figure 15. Stages of the autophagy pathway (Source: doi.org/10.1007/s00281-010-0226-8)

2.12 Multifaceted Roles of Autophagy in Infection and Immunity

Xenophagy, a selective form of autophagy that targets intracellular pathogens, plays a vital role in the innate and adaptive immune system responses to infection (**Capurro et al., 2020**). Upon entering host cells, invasive pathogens are promptly detected and subsequently degraded by the autophagic machinery. Not surprisingly, in order to establish persistent infections, intracellular bacteria have evolved specific strategies to evade the xenophagic response (**Mao et al., 2017; Hu et al., 2020**).

Three distinct outcomes have been observed. First, autophagy effectively restricts the growth of certain bacteria, such as by *Salmonella enterica* serovar Typhimurium and *Mycobacterium tuberculosis*. In the case of *M. tuberculosis*, the mycobacterial lipoprotein LpqH activates autophagy, which in turn targets phagosomes containing bacteria (**Shin et al., 2010**). Conversely, *Salmonella*-containing vacuoles are directed toward autophagosomes (**Birmingham et al., 2006**), leading to the degradation of bacteria within these autophagic compartments. Second, some bacteria have evolved mechanisms to evade autophagic degradation, as observed with *Shigella flexneri* and *Listeria monocytogenes* (**Ogawa et al. 2005; Dortet et al., 2011**). *Mycobacterium tuberculosis* and *Salmonella typhimurium* have also advanced and found new strategies to avoid autophagy (**Padhi et al., 2019; Xie et al., 2020**). For instance, *Shigella flexneri* employs the protein IcsB, which interferes with the interaction between IcsA and ATG5, a critical component of one of the ubiquitin-like conjugation systems, thus preventing the sequestration of bacteria into autophagosomes (**Ogawa et al. 2005**). Similarly, *Listeria monocytogenes* evades autophagic recognition through its protein internalin K (InlK), which binds to the host major vault protein complex, thereby inhibiting autophagic targeting (**Dortet et al., 2011**). Thirdly, certain bacteria have the ability to utilize autophagic vesicles as their intracellular niche. This phenomenon is exemplified by *Staphylococcus aureus* and *Anaplasma phagocytophilum*, both of which can

replicate within autophagosomes (Schnaith et al., 2007; Niu et al., 2008). Notably, all of these outcomes have been observed in the context of *H. pylori* infection. For instance, after the induction of autophagy by *H. pylori* the bacterium displays multiple strategies. It may evade autophagic degradation by downregulating autophagic proteins. Alternatively, *H. pylori* can exploit autophagosomes as their intracellular niche for survival or it may ultimately be degraded within autolysosomes (Raju et al., 2012; Yang et al., 2018 and Tang et al., 2012).

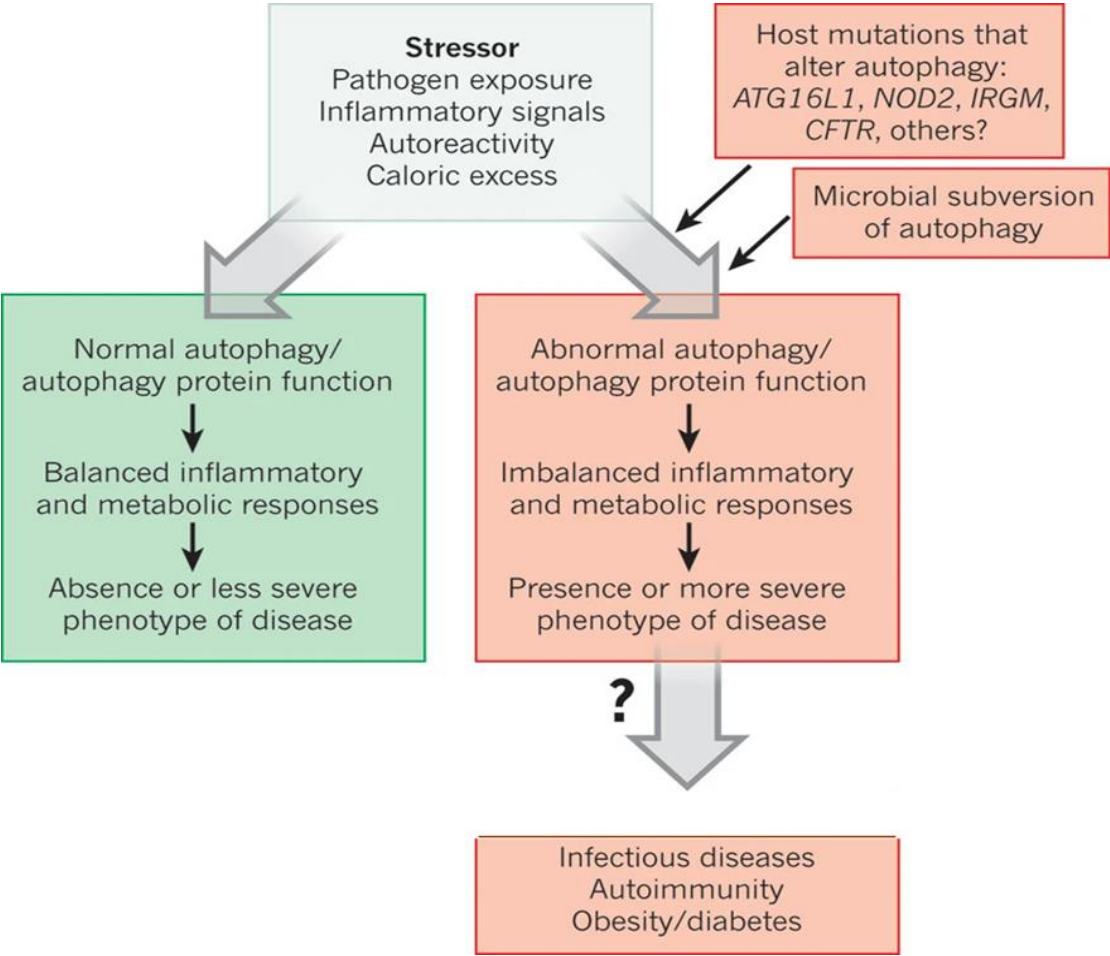


Figure16. Autophagy Levels and Proteins Regulating Disease in Response to Stressors
doi.org/10.1038/nature09782

2.13 Autophagy Modulation by *H. pylori* in gastric epithelial cells

The role of *H. pylori* in modulating the host's autophagy pathway has gained significant importance in understanding its pathogenesis. Numerous studies have confirmed that *H. pylori* infection triggers autophagy in both gastric epithelial cells (**Terebiznik et al., 2009; Chu et al., 2010**) and professional phagocytes (**Wang et al., 2009; Wang et al., 2010**). Accumulating evidences have demonstrated that *H. pylori* utilizes host autophagy to persist and even replicate within host cells, nevertheless, the specific mechanisms involved can vary depending on both the host cell type and the strain of the bacterium. Several virulence factors and host genes have been implicated in the regulation of *H. pylori*-induced autophagy. Of them, Terebiznik et al. originally discovered that VacA induces autophagy in the AGS cell line (**Terebiznik et al., 2009**). In gastric epithelial cells, VacA is adequate to induce autophagy. Research on VacA-mediated autophagy has revealed that VacA not only triggers autophagy but also disrupts autophagosome maturation with prolonged exposure to the toxin (**Raju et al., 2012**). However, how these virulence factors trigger autophagy is unknown. One clue is that VacA impairs mitochondrial function and depletes nutrients, which may be related to mTOR signalling suppression and autophagy induction (**Kim et al., 2019**). Exposure of VacA into the gastric epithelial cells leads to the accumulation of defective autophagosomes within the cell. Our understanding of the signalling events initiated by VacA to modulate autophagy is in its early stages of exploration. Reports demonstrate that VacA-induced ROS (Reactive Oxygen Species) stimulates the phosphorylation of AKT which in turn modulates autophagy (**Tsugawa et al., 2010**).

H. pylori is capable of modulating autophagy through other innovative mechanisms like miRNA. MIR30B directly targets ATG12 and BECN1, leading to the downregulation of autophagy and promoting the intracellular survival of *H. pylori* (**Tang et al., 2012**). An increasing body of evidences suggests the potential functional connection between the

virulence factors VacA and CagA. Several articles have indicated a correlation between diminished vacuolation and heightened CagA phosphorylation, indicating that the activation of VacA plays a pivotal role in CagA phosphorylation. Phosphorylation of CagA induces an inflammatory response and inhibits autophagy (Mimuro et al., 2002; Li et al., 2017; Eslami et al., 2019). A recent study has proposed that CagA exerts a negative regulatory influence on autophagy through the c-Met-PI3K/Akt-MTOR signaling pathway (Li et al., 2017). In this investigation, a noticeable difference was observed in patients infected with CagA-positive strains compared to those infected with CagA-negative strains, as indicated by a significant accumulation of SQSTM1/p62 in the gastric mucosa.

The expression of CagA is significantly elevated in CD44-positive gastric cancer cells primarily due to the ability of CD44-positive gastric cancer stem cells to suppress autophagy, subsequently leading to an increased expression of CagA (Tsugawa et al., 2012). Moreover, it's crucial to note that CagA-positive *H. pylori* strains have the capability to establish long-term colonization in gastric mucosal epithelial tissues. These strains can up-regulate inflammatory cytokines in individuals infected with *H. pylori*, and concurrently down-regulate the associated autophagy functions.

H. pylori gamma-glutamyl transpeptidase (HpGGT) is commonly present in all *H. pylori* strains. It plays a vital role in interactions with gastric mucosal epithelial cells (Chevalier et al., 1999). This enzyme acts as an autophagy inhibitor, facilitating the internalization of bacteria into gastric cells, thereby potentially leading to chronic gastric inflammation and even gastric tumors. Furthermore, there is evidence suggesting that HpGGT disrupts the autophagy flux by compromising lysosomal membrane integrity in AGS cells, resulting in a reduction of lysosomal cathepsin B activity (Bravo et al., 2019). In the later stages of infection, HpGGT diminishes cathepsin B activity and disrupts lysosomal degradation, thereby inhibiting the autophagic process. This disruption of lysosomal function ultimately

inhibits the autophagy process. This, in turn, creates an environment advantageous for the development of carcinogenesis.

Host genetics can indeed influence on autophagy with respect to *H. pylori* survival and persistence. Notably, individuals having ATG16L1*300A Crohn's disease risk allele have shown increased susceptibility to *H. pylori* infection, which correlates with their reduced autophagic response to VacA (Raju et al., 2012). Furthermore, a mutation associated with Crohn's disease, located within the NOD2 receptor, has been identified as a key player in *H. pylori's* intracellular survival and subsequent contribution to carcinogenesis (Rosenstiel et al., 2006).

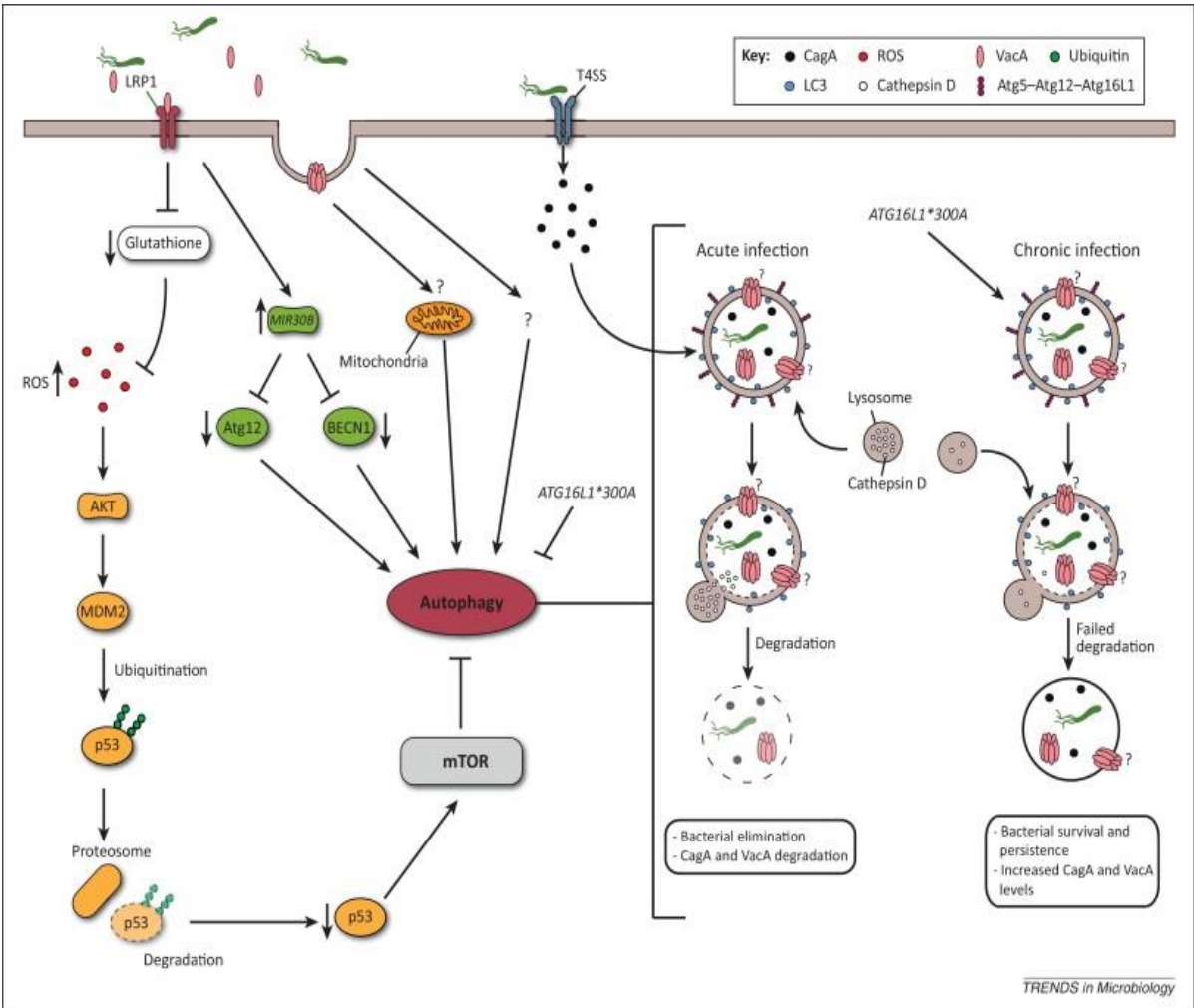


Figure17. Model summarizing current understanding of *Helicobacter pylori*-mediated autophagy. (Source: doi.org/10.1016/j.tim.2013.09.004)

2.14 Diagnostic tests

Diagnosis of *H. pylori* infection involves both invasive and non-invasive procedures (**Pilotto et al., 2014; Uotani et al., 2015; Smith et al., 2021; Bordin et al., 2021; Miftahussurur et al., 2016; Talebi Bezmin Abadi et al., 2018**). Invasive tests require the collection of biopsy samples during gastroduodenoscopy. These methods comprise the rapid urease test (RUT), histological assessment, bacterial culture, and the direct detection of *H. pylori* genetic material using techniques such as PCR, RT-PCR, or fluorescence in situ hybridization. Non-invasive approaches, on the other hand, include the ¹³C-urea breath test (UBT), serological detection of anti-*H. pylori* antibodies, the stool antigen test (SAT), and the direct detection of *H. pylori* genetic material in stool through PCR (**Bordin et al., 2021**).

2.15 *Helicobacter pylori* Treatment Guidelines Amidst Rising Antibiotic Resistance

Antibiotic resistance in *H. pylori* poses a significant global threat to human health. This resistance arises primarily due to chromosomally encoded mutations, but it is also driven by physiological alterations, including impaired regulation of drug uptake and efflux, as well as the formation of biofilms and the transition to coccoid forms (**Windham et al., 2018; Chen et al., 2019; Tsugawa et al., 2008**). There are medications, including antibiotics like amoxicillin, clarithromycin, metronidazole, tetracycline, levofloxacin, and rifabutin, particularly combination therapies made up of two or three of these antibiotics, an acid inhibitor, and/or a bismuth component that adds additional antibiotic effect to eradicate *H. pylori* (**Yamaoka et al., 2018; Malfertheiner et al., 2017**). Antibiotic that stands out as the foremost determinant of PPI-TT failure are metronidazole and clarithromycin resistance (**Malfertheiner et al., 2017; Fallone et al., 2016; Graham et al., 2010**). The prevalence of clarithromycin resistance has surged from 3% to around 11% at the turn of the century and

currently ranges from 15% to 30% globally (**Megraud et al., 2021**;; **Savoldi et al., 2018**;; **Lind et al., 1999**; **Meyer et al., 2002**; **Bujanda et al., 2021**; **Camargo et al., 2014**). Resistance to clarithromycin, metronidazole, and levofloxacin was 25%, 30%, and 20%, respectively, in 2,852 treatment-naïve patients from a European registry on *H. pylori* management (Hp-EuReg) (**Nyssen et al., 2021**; **Bujanda et al., 2021**). In the same study, resistance to tetracycline and amoxicillin was <1%. In addition, World Health Organization has classified clarithromycin-resistant *H. pylori* infection worldwide as a high-level threat among community-acquired infections (**Tacconelli et al., 2021**), prompting the abandonment of clarithromycin-based regimens when regional resistance exceeds 15% (**Malfertheiner et al., 2017**). Nevertheless, out of several therapeutic regimes designed to address clarithromycin resistance, including sequential therapy (PPI-dual followed by PPI-TT), hybrid therapy (PPI plus three antibiotics) and concomitant therapy (PPI plus simultaneous administration of three antibiotics) have emerged as proven approaches (**Molina-Infante et al., 2015**, **Liou et al., 2016**; **Crowe et al., 2016**; **Fallone et al., 2019**).

Treatment guidelines developed by expert organisations in Europe, Canada, and the United States, suggests:

- In regions with low clarithromycin resistance, the standard PPI-clarithromycin regimen remains the recommended first-line treatment (**Malfertheiner et al., 2012**). However, when therapy fails, most likely due to resistance to clarithromycin, levofloxacin, and/or metronidazole; they should be avoided in further eradication attempts.
- Second-line therapies should be bismuth quadruple therapy or levofloxacin triple therapy, depending on potential resistance, rifabutin-based triple and high-dose dual amoxicillin proton pump inhibitor therapy reserved for later treatment attempts (**Fallone et al., 2019**).

- In cases where the second-line therapy fails, the choice of *H. pylori* management regimen should ideally be guided by antimicrobial susceptibility testing (Malfertheiner et al., 2012).

Treatment failures with PPI-TT are primarily due to factors such as antibiotic resistance, inadequate acid suppression, and poor adherence to medication regimens 10. The crucial aspect of acid suppression, achieved through the use of PPIs (including omeprazole, esomeprazole, lansoprazole, pantoprazole, or rabeprazole), is essential. This acid suppression aims to elevate the intragastric pH to 6 or higher, a critical step that optimizes the stability, bioavailability, and effectiveness of antibiotics.

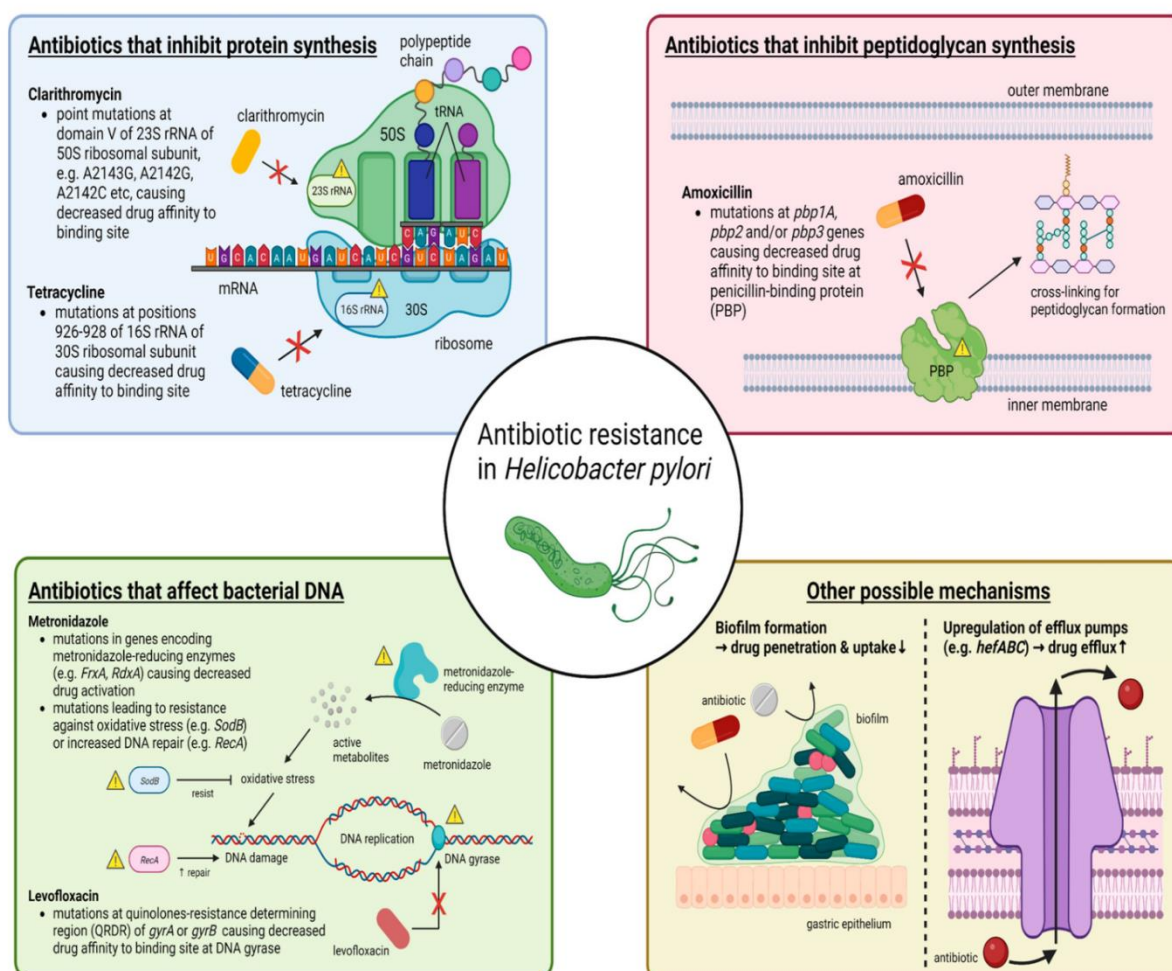


Figure18. Molecular mechanisms of antibiotic resistance in *H. pylori* are summarised. (Source: doi.org/10.3390/ijms241411708)

2.16 HMGB1: A Master Regulator of Host-Pathogen Interactions

Eukaryotic DNA is extremely condensed and organized within the nucleus to facilitate its crucial functions. This intact organisation is possible by a group of architectural proteins named as histones. In addition to histones, there is another class of architectural proteins known as the high mobility group (HMG) superfamily. HMG refers to a group of non-histone chromosome binding proteins. This nomenclature is derived from their characteristic features of having a low molecular weight and high mobility in gel electrophoresis (**Goodwin et al., 1973**). The HMG superfamily is divided into three families based on their DNA-binding domains: HMGA, HMGB, and HMGN proteins. The HMGB family consists of four members: HMGB1, HMGB2, HMGB3, and HMGB4, all of which exhibit over 80% sequence homology (**Goodwin et al., 1980; Lee et al., 2014**). HMGB1 is the most abundant nonhistone nucleoprotein member of the HMGB gene family. But, our primary focus is HMGB1.

The human HMGB1 protein consists of 215 amino acid (aa) residues, with a molecular weight ranging from 25 to 30 kDa. The majority of cells have HMGB1 proteins which are capable of non-sequence specific DNA binding (10–12) and bind to the minor groove of DNA. It comprises two homologous DNA-binding domains: the A-box , spanning amino acids 1 to 79, and the B-box, spanning amino acids 89 to 162 and a negatively charged C-terminal acidic tail, which contains amino acids 186 to 215 (**Lee et al., 2014; Bianchi et al., 1992**). The Box A domain binds DNA (**Stros et al., 1998**), the Box B domain binds and facilitates bending of DNA (**Belgrano et al., 2013**), and the C-terminal tail regulates the DNA binding and bending properties of HMGB proteins (**Blair et al., 2016**).

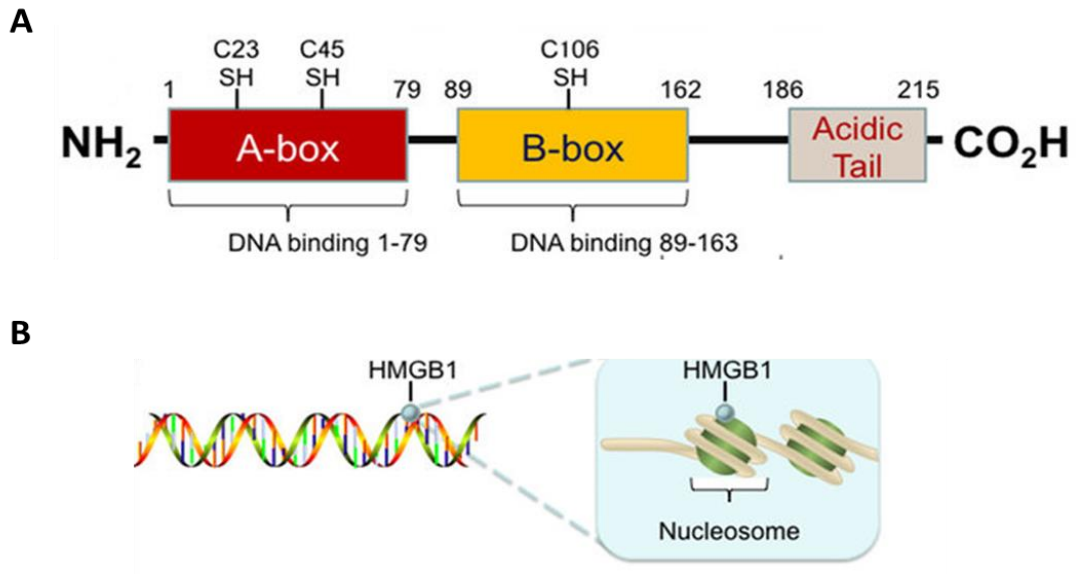


Figure19. Structure of the HMGB1 protein (Source:doi.org/10.18632/oncotarget.17885)

2.16.1 The HMGB1 Paradox: Alarmin and –Inflammatory Mediator

The biological function of HMGB1 is subjected to its specific subcellular localization as it shuttles back and forth from the nucleus to some amount in the cytoplasm and secreted into the extracellular space (**Muller et al., 2004**). It serves as both a nonhistone nucleoprotein when located within the nucleus and as an extracellular inflammatory cytokine when released into the extracellular environment. Within the nucleus it has role in DNA binding and maintaining its structural function, DNA replication or repair machinery, nucleosome assembly and transcriptional regulation. It binds to DNA with high affinity and helps to stabilize the DNA structure. It aids in the DNA replication or repair machinery and assists in the unwinding of DNA strands. By binding to specific regions of DNA, it participates in the regulation of gene expression at transcript level (**Kozlova et al., 2018; Reeves et al., 2003**).

Under cellular stress, HMGB1 translocate into the cytoplasm and has been implicated in the regulation of autophagy and apoptosis. It can have both promoting and inhibiting effects on autophagy depending on the context and cellular conditions. It can interact with proteins involved in the autophagic pathway, and influence autophagic activity. HMGB1 induces

autophagy by directly binding to the autophagy protein Beclin1 disrupting Beclin1/Bcl2 interaction through the activation of ERK/MAPK pathway (**Tang et al., 2010**). In normal conditions, Beclin1 can interact with anti-apoptotic protein called Bcl2 and inhibits the initiation of autophagy. Interestingly, competitive displacement of Bcl-2 by HMGB1, is likely to promote autophagy. On the other hand, HMGB1 can also modulate autophagy by regulating the autophagy flux. HMGB1-mediated inflammatory response can disrupt the normal autophagic process and lead to inhibition of autophagy (**Feng et al., 2021**).

In response to cellular stress, injury, or inflammation, HMGB1 can be actively secreted by immune cells or passively released from damaged or necrotic cells. Activated dendritic and NK cells, neutrophils, platelets, neutrophils, monocytes, and macrophages can all release HMGB1 in the extracellular space (**Wang et al., 1999; Dumitriu et al., 2005; Rouhiainen et al., 2000; Semino et al., 2005**). Once in the extracellular space, HMGB1 functions as a pro-inflammatory cytokine and stimulates inflammation. This is achieved through its binding to various receptors, including advanced glycation end products (RAGE) (**Cheng et al., 2014; Kohles et al., 2012**) and members of the toll-like receptor family (TLR, such as TLR2, TLR4, and TLR9) through MyD88 dependent and independent pathways; (**Zhou et al., 2013; Yan et al., 2012; Conti et al., 2013**). This binding activates the nuclear factor (NF)- κ B and mitogen-activated protein kinase (MAPK) pathways, subsequently triggering the production of multiple pro-inflammatory cytokines such as IL-6, IL-8, IL-1 β , IL-18 and tumor necrosis factor- α (TNF- α), primarily by activating NF- κ B pathways (**Ren et al., 2023; Liang et al., 2015**).

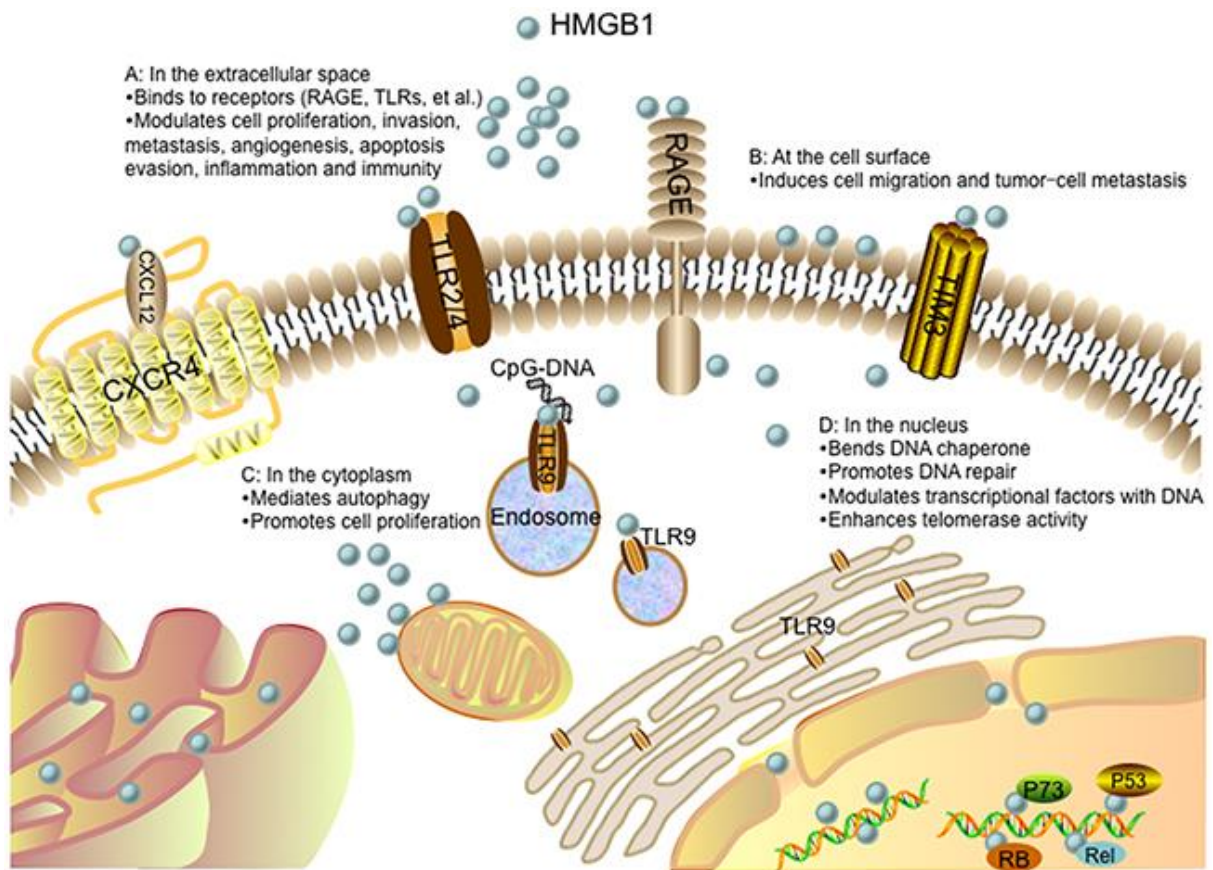


Figure20. HMGB1 during cancer progression (Source: doi.org/10.18632/oncotarget.17885)

2.16.3 HMGB1: A Promising Therapeutic Target

HMGB1, a protein that links cellular injury and immune response, is a promising target for drug development in a wide range of inflammatory diseases. Sepsis, a severe and potentially lethal inflammatory condition, is linked to a vicious cycle involving HMGB1 release (Ulloa et al., 2005). Elevated serum HMGB1 levels correlate with a worse prognosis in sepsis patients (Wang et al., 1999), but HMGB1 antagonists offer promising therapeutic potential (Yang et al., 2004). Even in acute conditions where microbes are not involved, such as hemorrhagic shock, HMGB1 antagonists show therapeutic promise (Ombrellino et al., 1999). Anti-HMGB1 antibodies ameliorates the severity of lung injury induced by acute blood loss in a mouse model, suggesting that HMGB1 plays a role in this condition (Kim et al., 2005). HMGB1-targeted therapy is a promising new treatment for rheumatoid arthritis, a

chronic inflammatory disease (**Pullerits et al., 2003**). HMGB1 is a protein that contributes to the development of arthritis in mice, and antibodies against HMGB1 have been shown to improve symptoms in mouse models of the disease (**Kokkola et al., 2003**).

Furthermore, the aberrant expression and release of HMGB1 has been demonstrated in numerous types of cancer, including colorectal cancer (**Moriwaka et al., 2010**), breast (**Stoetzer et al., 2013; Fersching et al., 2010**), lung (**Wang et al. 2012**), prostate (**Gnanasekar et al., 2009**), cervical (**Pang et al., 2014**), skin (**Mittal et al., 2010**), hepatocellular carcinoma (**Takeuchi et al., 2013; Wu et al., 1999**), gastric (**Song et al. 2012; Akaike et al., 2007**), pancreatic (**Soreide et al., 2015; Wittwer et al., 2013**), osteosarcoma (**Li et al., 2013**) and leukemia (**Jia et al., 2014**).

HMGB1 has multifaceted roles including modulating gene transcription and influencing several signaling pathways. Nonetheless, the roles of HMGB1 in cancer are intricate and paradoxical. In a murine model of glioma, blocking the signalling pathways mediated by RAGE or HMGB1 has been shown to inhibit tumor growth and metastasis (**Taguch et al., 2000**). Elevated levels of HMGB1 in tumors are associated with an increased potential for metastasis (**Nestl et al., 2001**). However, the role of HMGB1 in gastric cells during autophagy by *H. pylori* infection is not explored yet.

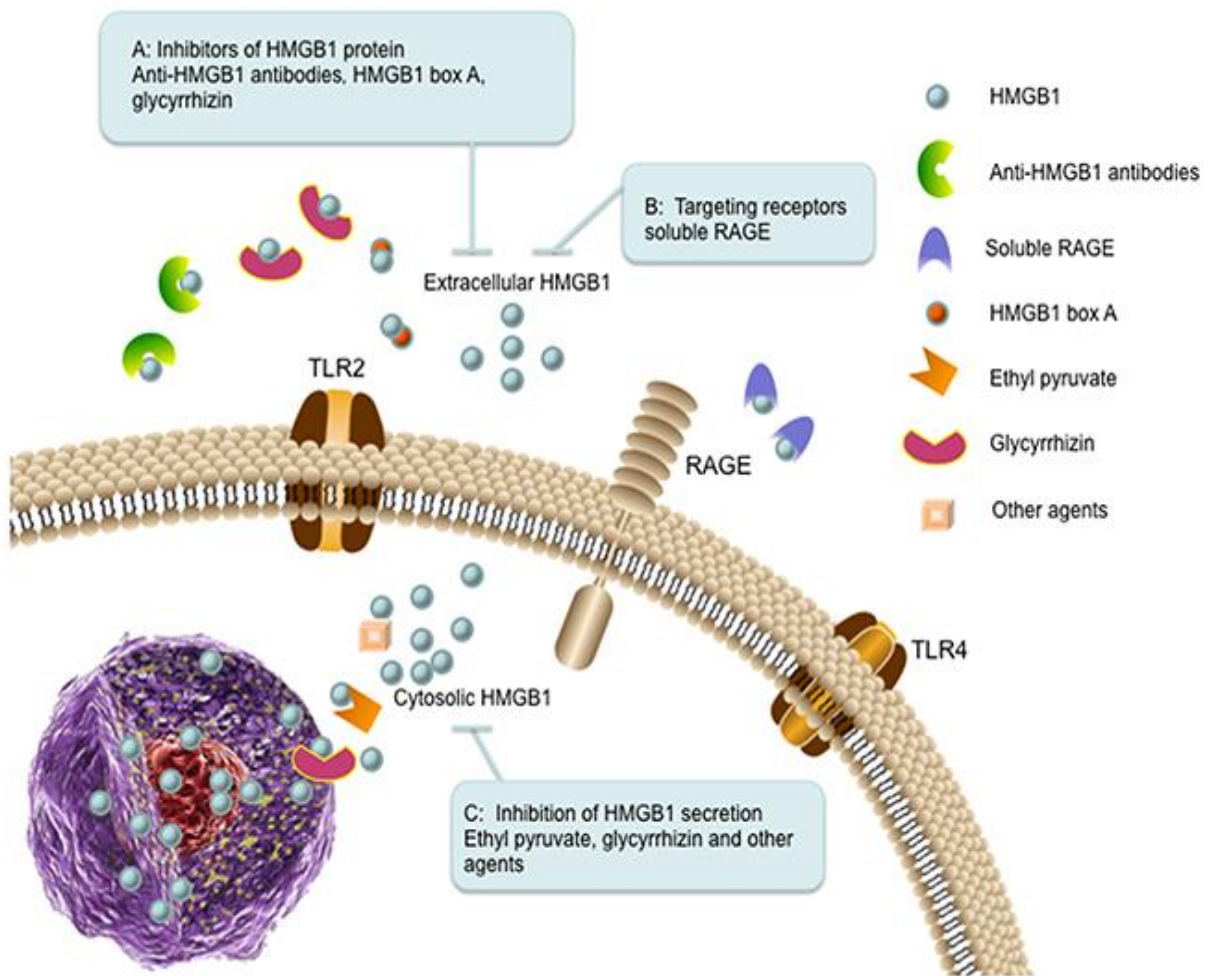


Figure21. The therapeutic strategies aimed at targeting HMGB1 in cancer. (Source: doi.org/10.18632/oncotarget.17885)

2.17 Glycyrrhizin: A Promising Approach to Inhibit HMGB1 and its cellular functions

Glycyrrhizin (GL), a triterpenoid glycoside, is the key biologically active component of licorice and it is extracted from the roots of the liquorice plant (*Glycyrrhiza glabra*). It has been recognized as a herbal remedy since ancient times and holds significant therapeutic value. Glycyrrhizin could inhibit the release of HMGB1 and can effectively attenuate the proinflammatory effects of HMGB1 by disrupting HMGB1 signalling (Vergoten et al., 2020; Su et al., 2017).

Glycyrrhizin is absorbed through the gastrointestinal tract after oral administration. Once ingested, glycyrrhizin is absorbed into the bloodstream through the intestines. Its oral bioavailability is only around 10%. After absorption, it is rapidly metabolized by the liver to glycyrrhetinic acid (GA), which is the active metabolite. Glycyrrhizin is excreted in the urine and bile (**Glavač and Kreft, 2004**). However, the pharmacokinetics of glycyrrhizin can be affected by a number of factors, including the dose, route of administration, and the presence of food.

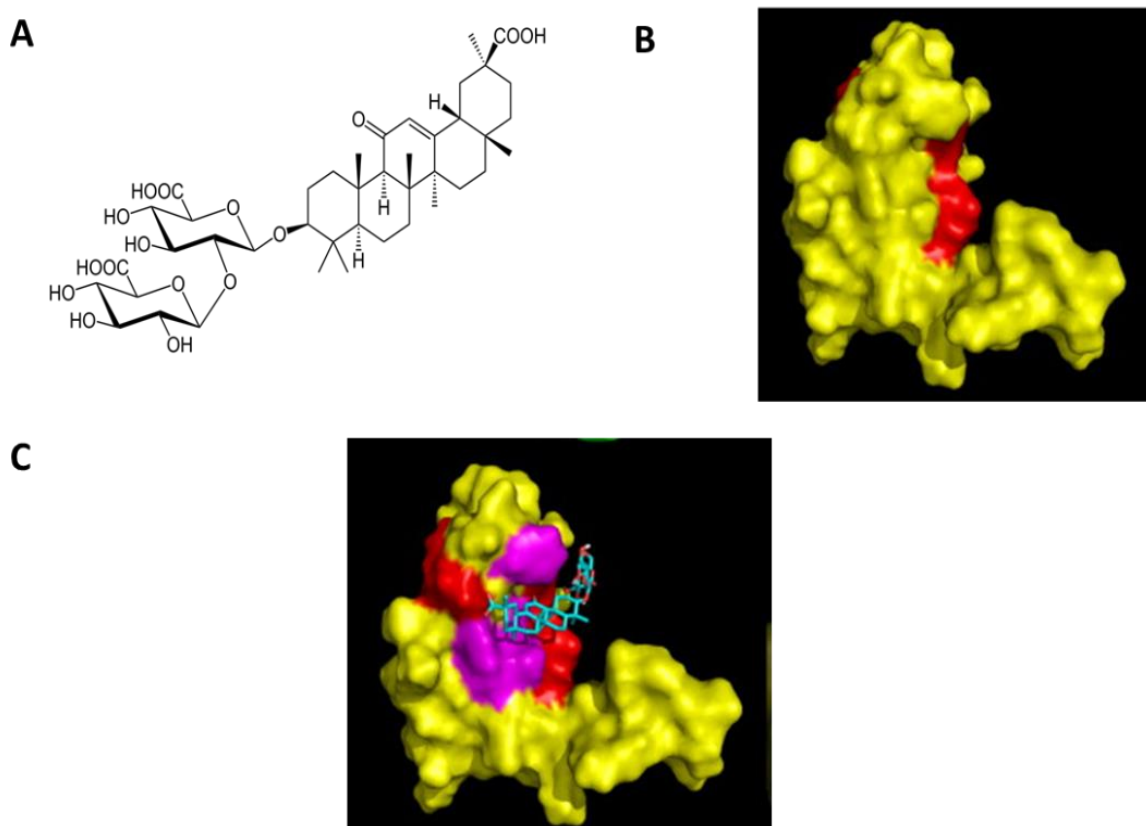


Figure22. Glycyrrhizin prevents the Chemotactic Activity of HMGB1. **A.** Structure of glycyrrhizin. **B.** (B) Surface representation of HMGB1 box A (PDB code: 1aab); **C.** Model of interaction of glycyrrhizin (cyan) binding with HMGB1; hydrophobic residues are shown in red and magenta. Glycyrrhizin (cyan) accommodates at the junction of the two arms of the L-shape fold. (Source: doi.org/10.1016/j.chembiol.2007.03.007)

2.17.1 Therapeutic effects

Glycyrrhizin has important functions in various biological activities, including immune regulation, apoptosis (Gwak et al., 2012), oxidative stress, autophagy and cell proliferation (Wahab et al., 2021). Glycyrrhizin and its metabolites also play important roles in antibacterial activities. Furthermore, it serves as an anti-inflammatory agent, diminishes allergic responses and safeguards against liver damage (Pastorino et al., 2018). Glycyrrhizin metabolites also have bactericidal activity against penicillin-resistant *Staphylococcus aureus* and can inhibit the expression of virulence genes (Wang et al., 2015). Recent studies have shown that glycyrrhizin plays an important role in both immune activation and immunosuppressive functions (Li et al., 2012; Zhou et al., 2021). For example, Glycyrrhizin can inhibit the production of proinflammatory cytokines such as IL-1 β and TNF- α (Zhang et al., 2021). It also enhances the production of the anti-inflammatory cytokine IL-10 (Zhou et al., 2021).

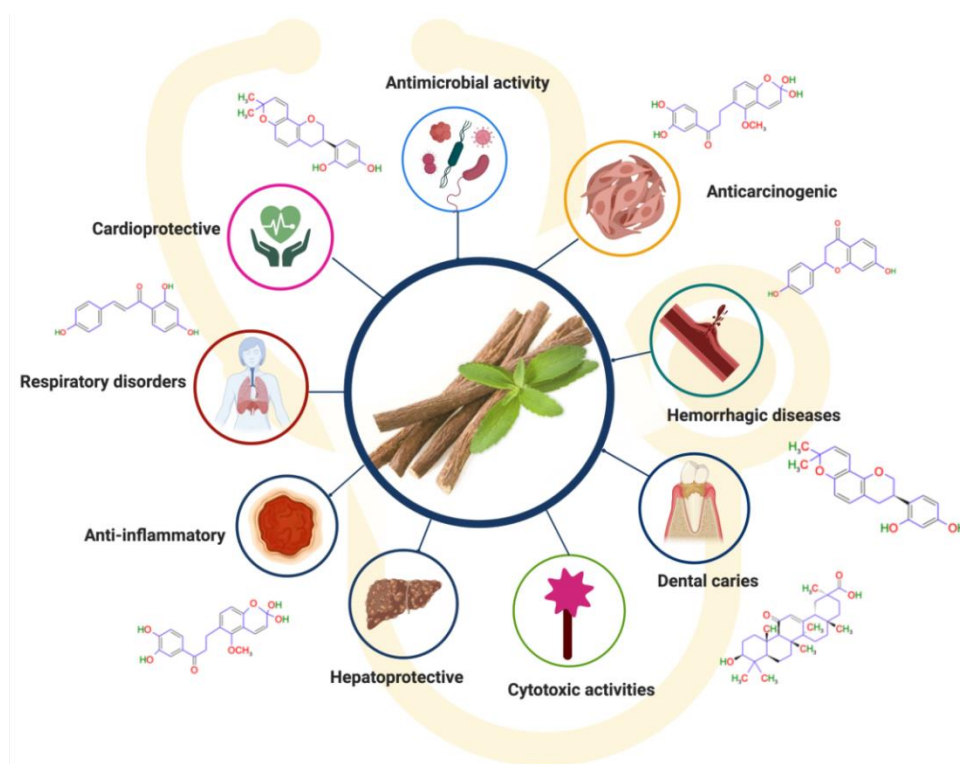


Figure23. Therapeutic effects of glycyrrhizin (Source: doi.org/10.3390/plants10122751)

Section 3

MATERIAL AND METHODS

1. Selective medium for *H. pylori* culture

Brain Heart Infusion Agar (BHIA) (Difco Laboratories, MI, USA) was used as the basal medium for the growth of *H. pylori*. BHIA was autoclaved for 15 min at 121° C. The medium was then allowed to cool to 50°C in a water bath before adding 5% horse serum (Invitrogen, NY, USA) aseptically to the BHIA in a horizontal laminar flow working chamber (ESCO Class II Biosafety Cabinet). Next, 0.4% isovitaleX (Becton Dickinson Microbiology Systems, MD, USA), trimethoprim (5µg/ml) (Sigma) soluble in alcohol, vancomycin (6µg/ml) soluble in water, and water soluble polymyxin B (10µg/ml) were added aseptically to the BHIA in a horizontal laminar flow working chamber (ESCO Class II Biosafety Cabinet). The antibiotic-supplemented blood/serum agar medium was thoroughly mixed and quickly poured (approximately 25ml per plate) in a sterile, disposable plastic petri dish (15 mm x 90 mm, Axygen, India) with aseptic technique. Once the agar solidified, the plates were stored in a cool, dark environment, typically in polythene bags, used within two weeks. Before usage, the plates were dried for about 1 hour at 37°C.

2. Growth conditions of *H. pylori*

H. pylori strains, including Sydney Strain SS1 (cagA+, vacA s2m2) and Strain 26695 (cagA+, vacA+ s1m1), were cultured on BHIA (Difco, USA) supplemented with 7% heat-inactivated horse serum (Invitrogen), antibiotics, and IsoVitaleX. These plates were incubated for 3 to 6 days at 37°C in a double-gas incubator (Double gas incubator, Heraeus, Langenselbold, Germany), with a calibrated gas composition of 5% O₂, 10% CO₂, and 85% N₂ to create an ideal microaerophilic environment. Additionally, a drug-resistant *H. pylori* strain, OT-14(3) vacA s2m2, (cagA-, resistant to clarithromycin and metronidazole), was isolated from a gastric cancer patient at IPGMER and SSKM Hospital, Kolkata, and cultured using the same protocol (Dr. Asish K Mukhopadhyay's Lab ICMR,NICED).

3. Preservation of bacterial strains

To preserve the exponentially growing *H. pylori* strains for future studies, approximately 3-4 loops of 24-hour-old culture were aseptically transferred into 1 ml cryovials containing 1 ml of sterile Brain Heart Infusion broth (BHI; Difco Laboratories, MI, USA) with the addition of 20% glycerol (Merck, India) to act as a cryopreservative. These vials were then stored at -70°C for long-term storage. For the revival of the organisms, a microfuge tube was removed from the freezer and rapidly thawed on ice. A small portion of the culture was aseptically extracted and streaked onto blood-serum agar plates, followed by the usual incubation process.

4. Maintenance of cell lines in culture

Human gastric cancer cell line AGS, HGC-27 (EP-CL-0107) and murine macrophage cell line RAW264.7 (ATCC TIB-71) were used. The AGS cell line was generously gifted by Dr. Asish Kumar Mukhopadhyay from ICMR-NICED, Kolkata, and is derived from a gastric adenocarcinoma patient. Source of HGC-27 is derived from metastatic lymph node of a gastric cancer patient. Both AGS and HGC-27 cells were cultured in F-12 media supplemented with 10% heat-inactivated fetal bovine serum (Sigma), 1% non-essential amino acids, and 1% pen-strep (containing penicillin at 100 units/ml and streptomycin at 100 µg/ml, Himedia, India). The incubation was carried out at 37°C in an atmosphere with 5% CO₂. The experiments were conducted using AGS and HGC-27 cells within a passage range of 5-10. RAW264.7 cells, on the other hand, were grown in RPMI1640 medium with 10% FBS and 1% penstrep. The experiments involving RAW264.7 cells were conducted with a maximum passage number of 3-5. These cells were also maintained in a humidified incubator at 37°C with 5% CO₂.

5. Freezing and thawing cells

For long-term storage, cells were preserved in liquid nitrogen. To freeze adherent cells, they were detached from the flask using an appropriate amount of 0.25% Trypsin-EDTA (Thermo Fisher Scientific Inc.), followed by centrifugation to pellet the cells. All cell types were centrifuged at 1800 rpm for 5 minutes using the Centrifuge. Approximately cells were resuspended in 1 ml of freezing medium, comprising 90% FBS (Gibco) and 10% dimethyl sulfoxide (DMSO, Thermo Fisher Scientific Inc). These cells were subsequently transferred into sterile cryovials (Corning Inc.) for storage at -80°C (at least 24 h) before transferring into liquid nitrogen tanks.

After quickly thawing the cryovials to ambient temperature and gradually adding 5 ml of normal culture media, the cells were recovered from liquid nitrogen. Cells were pelleted through centrifugation (as previously described), and the medium was removed before replacing it with fresh culture medium. The resuspended cells were allowed to culture for a period of 5-10 days, enabling them to recover before being used for experimental procedures.

6. *In vitro* Infection Assay

A cell density of 0.5×10^6 cells per 60mm cell culture dish was plated. The cells were starved for the entire night in 2 mL of incomplete F12 medium without antibiotics or FBS. The *H. pylori* SS1 or 26695 culture was suspended in sterile phosphate-buffered saline (PBS), and its optical density (OD) was adjusted to 1 at 600 nm. Subsequently, the suspension was centrifuged at 10,000 g for 10 min. For infection assay, cells were infected with *H. pylori* at a multiplicity of infection (MOI) of 1:100 for 4 h in all the experiments. Cells were then treated with gentamicin (100µg/ml) for 1 h in order to kill the extracellular bacteria.

Subsequently, cells were treated for 4 h with glycyrrhizin GLZ (200 µM) after being washed with PBS and cultured in fresh media. For CFU assay, in order to ascertain the number of bacteria that had infiltrated the AGS cells, cell lysis was carried out by adding 0.01% saponin

for 5 min at room temperature. Following preparation of the serial dilution, 100µL of the diluted solution was then plated on BHIA plates. Then, after 4-5 days of incubation, colonies were counted.

For the *H. pylori*-resistant strain [OT-14(3)], the same infection procedure was carried out. In case of chloroquine and bafilomycin treatment, cells were infected with or without *H. pylori* with a (MOI) 1:100 for 4 h, followed by gentamicin treatment for 1 h, and subsequent treatment was done with glycyrrhizin (200µM) and/or chloroquine (50µM) and/or bafilomycin (50 nM) for 4 h and/or 18 h.

7. Competent bacteria preparation

E. coli DH5α cells were initially cultured overnight in 1 ml of LB at 37°C. The following day, 500µl of the overnight culture was used to inoculate 50 ml of LB in a 1:1000 dilution, and these cells were grown at 37°C for an additional 3-4 h. Cells were kept on ice for 30 minutes before being centrifuged for 15 min at 4000 rpm and 4°C. After removing the supernatant, the cells were resuspended in 20 ml of 100mM CaCl₂, kept on ice for 30 min, and centrifuged under the same conditions. Once again, the supernatant was discarded, and the cells were resuspended in 500µl of 100mM CaCl₂ with 15% glycerol and finally stored at -80°C for future use.

8. DNA transformation into bacteria

All transformations were done using *E. coli* DH5α competent bacteria via the heat-shock method. DNA was directly mixed with 50µl of competent DH5α cells and kept on ice for 20 min. Following this, the cells were subjected to a brief incubation in a water bath at 42°C for 1.5 min and promptly transferred back onto ice. Next, 1 ml of LB medium was added, and the cells were placed in a shaking incubator at 37°C for 1 h. Subsequently, the cells were plated onto agar plates containing the appropriate antibiotics and incubated overnight in a 37°C incubator.

9. Plasmid DNA Isolation

Transformed DH5 α was grown overnight in LB medium at 37°C, and 10 ml of culture was used for plasmid DNA isolation using the QIAamp® DNA Mini Kit (Qiagen) according to the manufacturer's procedure. Briefly, the culture was centrifuged at 6000g for 15 minutes at 37°C. Supernatant was discarded, and the pellet was resuspended in 250 μ l of buffer P1 (containing RNase A). After vigorous shaking, 250 μ l of buffer P2 (lysis buffer) was added and inverted 4-6 times before being stored at room temperature for 5 minutes. 300 μ l of buffer P3 (neutralisation buffer) was added, stirred, and incubated on ice for 5 minutes. Genomic DNA was coagulated, and after 5 minutes of centrifugation at 13000rpm, clear supernatant containing plasmid DNA was quickly collected in a new tube. A QIAGEN-tip 20 column was equilibrated with buffer QBT, and plasmid DNA-containing supernatant was passed through it. The column was then washed three times with buffer QC before DNA was eluted with buffer QF. Isopropanol was used for alcohol precipitation, and plasmid DNA was recovered as a pellet. The DNA pellet was air dried before being dissolved in TE buffer (pH 8).

10. Plasmids

The GFP-LC3 plasmid was a gift from Prof. Parimal Karmakar (Department of Biotechnology, Jadavpur University, India). The tandem fluorescent LC3B (tfLC3B) plasmid was a gift from Dr. Dhiraj Kumar ICGEB, New Delhi, India. Myc-Tagged Empty Vector was a kind gift from Dr Santa Sabuj Das, ICMR, NICED, Kolkata. Myc-Tagged Hmgb1 Plasmid was bought RC205918 (Origene). The plasmids were transformed in DH5 α and purified using a Promega mini-prep plasmid isolation kit. The plasmid DNA was kept at -20°C in nuclease-free water.

Table2. Plasmids used in this study

Plasmid	Source
Tandem Fluorescent LC3b (tfLC3B) Plasmid	Dr. Dhiraj Kumar ICGB, New Delhi, India
GFP-LC3 Plasmid	Prof. Parimal Karmakar, Jadavpur University, India
Myc-Tagged Hmgb1 Plasmid	RC205918 (Origene)
Myc-Tagged Empty Vector	Dr Santa Sabuj Das, ICMR-NICED, Kolkata, India

11. siRNAs

The following siRNAs were purchased from ATG5siRNA, HMGB1 siRNA and nonspecific siRNA.

Table3. siRNAs used in this study

siRNAs	Source
Hmgb1 siRNA (Id Hs.Ri.Hmgb1.13.1)	IDT
Atg5 siRNA (Id Hs.Ri. Atg5.13.1)	IDT
Non-Specific siRNA	IDT

12. Lipofectamine mediated Transfection of plasmid and siRNA

Transfection of plasmids /or siRNA into AGS and RAW264.7 cells was carried out using Lipofectamine 2000 (Invitrogen). The cells were seeded in 6-well plates for 24 hours before the transfection process. For transfection, a mixture was prepared by combining 100µl of

OptiMEM (Invitrogen) with 5µl of Lipofectamine reagent, and the mixture was left to incubate at room temperature for 5-10 minutes. Next, 2µg of the chosen expression vector(s) /or 50nM siRNAs was diluted to a final volume of 100µl using OptiMEM and added to the Lipofectamine mixture. The mixture was gently mixed by tapping and then incubated at room temperature for 30 minutes. Subsequently, the Lipofectamine-plasmid DNA mixture /or Lipofectamine- siRNA, along with OptiMEM, was added to the cells. The cells were then placed in a CO₂ incubator at 37°C for a minimum of 6 hours. Following this incubation period, the transfection mixture was replaced with 2 ml of regular culture media.

13. Immunofluorescence

Cells were infected with *H. pylori* at a MOI of 1:100 for 4 h in all the experiments. Cells were then treated with gentamicin (100µg/ml) for 1 h in order to destroy the extracellular bacteria. Subsequently, cells were treated for a further 4 h with glycyrrhizin GLZ (200 µM) after being washed with PBS and cultured in fresh media. For immunofluorescence staining, cells were fixed in 4% paraformaldehyde at room temperature for 1 h and blocked in PBS containing 3% BSA and 0.01% Triton X100 for 1 hr. Next, coverslips were incubated with anti- LAMP1 and anti-Galectin-3 at 4°C overnight. Subsequently, secondary antibody incubation was done using TRITC-conjugated anti-rabbit secondary antibody (1:1000) (Cat# AP132R) and FITC- conjugated anti-mouse secondary antibody (1:1000). Lastly, the coverslips were mounted on glass slides by adding ProLong™ Gold Antifade reagent with DAPI (Thermo Fisher) and examined using an inverted confocal microscope (Carl Zeiss LSM 710). For immunofluorescence LAMP1, LC3B, HMGB1 and Beclin1 antibodies were used and same staining protocol was followed.

14. Live-cell confocal microscopy

AGS cells (2×10^5) were initially seeded in a round-bottom glass dish. After a 24h incubation period, the cells were exposed to *H. pylori* infection at a MOI of 100 for 4 h, followed by an additional 4h period of drug treatment.

-GFP-LAMP1

To monitor LAMP1 expression, *H. pylori*-infected and drug-treated AGS cells were subjected to live-cell imaging. This was achieved by adding 5µl of a baculovirus expressing the LAMP1-GFP construct (Cell Light™ Lysosomes-GFP, BacMam 2.0, #C10507) for a 16-hour incubation period. Subsequently, the cells were observed using a confocal microscope.(Zeiss model no.)

-LysoTracker staining

To study lysosomal acidification, cells were incubated with LysoTracker Red DND-99 (Invitrogen, L7528) for 30 minutes, followed by observation using an inverted confocal microscope.(Zeiss model no)

-Dextran staining

Lysosomal destabilization was assessed using Dextran, Alexa Fluor™ 488, with a molecular weight of 10,000 daltons (D22910, Invitrogen). After infection and drug treatment, cells were incubated with 200 µg/ml of dextran for 2 hours at 37°C and then observed under an inverted confocal microscope. (Carl Zeiss LSM 710).

15. Immunoblotting

Approximately 10^6 cells were harvested, washed with ice-cold 1X PBS and subsequently lysed in 0.5 ml of ice-cold RIPA buffer (Sigma-Aldrich Corp.) with the addition of a protease inhibitor cocktail. Protein concentrations were estimated using Lowry method. The samples were then boiled in 5X Laemmli buffer and separated by appropriate SDS-PAGE gels (**Table**

4 and 5). The resulting gel was transferred to a 0.22µm PVDF membrane (Sigma). Membranes were blocked in a solution of 5% skimmed milk dissolved in TBST buffer for 1 hour at room temperature. Subsequently, they were washed in TBST and incubated overnight with primary antibodies (**Table 6**) at 4°C.

Table4. Composition for Resolving gel (%)

Resolving gel (Composition)	Volume (ml) for 1 gel
30% acrylamide & bis-acrylamide (Solution A)	1.67
1.5M Tris-HCl (pH 8.8) (Solution B)	0.625
Water	2.5
10% SDS	0.15
10% APS	0.05
TEMED	0.05

Table5. Composition for Stacking Gel

Stacking Gel (Composition)	Volume (ml) for 1 gel
30% acrylamide & bis-acrylamide (Solution A)	0.66
1.5M Tris-HCl (pH 8.8) (Solution B)	1.26
Water	3.0
10% SDS	0.05
10% APS	0.025
TEMED	0.025

Table6. Primary antibodies used in the study.

Name	Specificity	Cat no.#	Dilution
Anti-HMGB1	Mouse monoclonal	ab77302	1:1000
Anti-SQSTM1/P62	Rabbit polyclonal	ab91526	1:3000
anti-LC3B	Rabbit polyclonal	ab51520	1:3000
Anti- ATG5	Rabbit monoclonal	ab228668	1:1000
Anti-Beclin 1	Rabbit monoclonal	ab207612	1:1000
Anti-LAMP1	Rabbit monoclonal	9091	1:3000
Anti-LAMP1	Mouse monoclonal	15665S	1:3000
Anti-UVRAG	Rabbit monoclonal	13115S	1:1000
Anti-WIPI2	Rabbit monoclonal	13571	1:1000
Anti-Beta actin	Mouse polyclonal	sc-47778	1:3000
Anti- α-Tubulin	Mouse polyclonal	BB-AB0118	1:3000

After the initial treatment with the primary antibody, the membranes were gently agitated on a shaker at room temperature for duration of 2 h. During this incubation, they were exposed to either horseradish peroxidase (HRP)-conjugated goat anti-rabbit secondary antibody (at a dilution of 1:10000) or goat anti-mouse secondary antibody (also at a dilution of 1:10000). Following this incubation, the membranes underwent a final wash using TBST for a period of 30 minutes. The resulting protein bands were visualized using the ChemiDoc MP Imaging System from Biorad. This visualization process was accomplished by utilizing the Millipore immobilon western chemiluminescent HRP substrate, which comprises luminol and hydrogen peroxide, serving as the substrate for the chemiluminescent reaction.

16. Protein estimation by Lowry method

A modified Lowry technique was used to estimate the protein concentration. Three different kinds of reagents were utilised for the measurement:

Reagent A: 2% Na_2CO_3 in 0.1M NaOH containing 0.16% Na-K tartrate + 0.1% SDS

Reagent B: 4% $\text{CuSO}_4 \cdot 5\text{H}_2\text{O}$

Reagent C was prepared by mixing 1 ml of reagent A and 10 μl of reagent B. 600 μl of reagent C was added to 200 μl of diluted proteins and allowed to stand at room temperature for 15 minutes. 1N Folin-Ciocalteu reagent was added and the mixture was maintained in the dark for 30 min. The OD was measured at 660nm, and the protein content was estimated using the following equation derived from the BSA standard curve: Protein concentration (g/ml) = $\text{OD}_{660} / 0.0026 \times \text{dilution factor}$.

17. Co-immunoprecipitation assay

After infection, the cells underwent two ice-cold 1 x PBS washes and were subsequently lysed using 0.5 ml of ice-cold RIPA buffer, which was supplemented with protease inhibitors. This lysis process occurred over a span of 30 min, with intermittent vortexing every 5–10 minutes, while the lysates were maintained on ice. Subsequently, the cell lysates were subjected to centrifugation at 13,000 rpm for 15 minutes at 4°C. Protein concentration was quantified using the Lowry reagent assay from 5 μl of each sample. Input samples were prepared from 5% of the lysates boiled with 2 x Laemmli buffer.

To facilitate pre-clearing of the lysates, control antibodies and 30 μL of 1:1 Protein-A agarose beads (Sigma) were used for 45 min at 4°C. The capture of the protein of interest was achieved by rotating the remaining lysate with 1 μg of a specific antibody overnight at 4°C. Immuno-complexes were then extracted using 30 μL magnetic Protein- A agarose beads, pelleted, and washed three times with ice-cold RIPA buffer. Both the input lysates and immunoprecipitation (IP) complexes were boiled in 2 x Laemmli buffer. Subsequently, they

were fractionated by SDS-PAGE and transferred to a 0.22µm PVDF membrane for Western blot analyses, as described previously.

18. *In Silico* Studies

String software, often referred to as STRING (Search Tool for the Retrieval of Interacting Genes/Proteins), is a bioinformatics tool and database designed for the analysis of protein-protein interactions (PPIs), functional annotations, and the construction of protein interaction networks.

19. RNA isolation

Total cellular RNA was extracted from AGS cell lines using Trizol reagent, RNAiso Plus (TaKaRa), following the manufacturer's protocol. RNA was quantified by measuring the absorbance at 260 nm. For adherent cells, the procedure involved aspirating the media, washing the cells with 1X PBS, and then adding 1-2ml of TRIzol, which was left at room temperature for 10-15 minutes. Lysed cells or tissues were centrifuged at 12,000g for 15 minutes, and supernatant was carefully collected after discarding the pellet. To this supernatant, 200µl of chloroform was added in a 1ml lysate, followed by another centrifugation step at 12,000g for 15 minutes at 4°C. Among the three layers formed during this process, the top liquid layer contains RNA, which was then carefully transferred into another tube. Subsequently, 500µl of isopropanol was added to the RNA-containing liquid and left at room temperature for 10 minutes. The mixture was subjected to centrifugation at 12,000g for 15 minutes at 4°C. After removing the supernatant, 500µl of 75% ethanol was added, and the RNA pellet was centrifuged at 7,500g for 5 minutes at 4°C. The supernatant was discarded, and the RNA pellet was allowed to dry. Finally, the RNA was dissolved in an appropriate volume (usually 30-50µl) of DNase and RNase-free water.

20. Calculation of DNA and RNA concentration

Concentration of both DNA and RNA was determined using a spectrophotometer. The absorbance at 260nm was measured, and the concentration was calculated using the following formulas:

For RNA: Concentration of RNA ($\mu\text{g/mL}$) = A260 measurement x 40 $\mu\text{g/mL}$ x dilution factor

For DNA: Concentration of DNA ($\mu\text{g/mL}$) = A260 measurement x 50 $\mu\text{g/mL}$ x dilution factor

It's important to note that 1 OD260 unit of RNA corresponds to 40 $\mu\text{g/mL}$, and 1 OD260 unit of DNA corresponds to 50 $\mu\text{g/mL}$.

The purity of both DNA and RNA was calculated by the ratio of OD260 to OD280. For pure DNA, the OD260/OD280 ratio is expected to be around 1.8, while for pure RNA, it should be approximately 2.0. Additionally, the purity of RNA was further evaluated by running a 1.2% agarose gel at 90V for 15 minutes. In the gel, the intensity ratio of the 28S rRNA band to the 18S rRNA band should ideally be 2:1 to indicate the presence of pure RNA.

21. cDNA synthesis

To prepare 1 μg of cDNA from RNA, the manufacturer's protocol was followed, using the Verso cDNA synthesis kit from Thermo Scientific. Initially, the RNA was denatured at 70°C for 10 minutes and then promptly placed on ice for 3 minutes. The RT-PCR master mix was prepared with the components listed below. This master mix was added to the RNA, and the PCR cycle was initiated. The cDNA synthesis step was carried out at 42°C for 30 minutes, followed by an inactivation step at 95°C for 2 minutes. After completion, the RT-PCR products were incubated at 40°C for 5 minutes and then stored at -20°C.

Table7. Requirements for cDNA synthesis using kit

Components	Volume (μl)
5X cDNA synthesis buffer	4
dNTP mix	2
RNA primer	1
RT enhancer	1
Verso enzyme mix	1
Template (RNA)	1-5
Nuclease free water	to make 20
Total volume	20

Table8. Requirements for RT - PCR

Components	Volume (μl)
1X SYBR green	10
Forward primer	1
Reverse primer	1
Template	variable
Water	To make 20
Total	20

22. Real-Time PCR

Real-Time Quantitative Reverse Transcription PCR was conducted to assess the expression levels of *H pylori* specific ribosomal 16s under various experimental conditions. The cDNA was amplified using a specific set of components using the following protocol. Primers were designed based on the target genes using IDT's PrimerQuest™ Tool. SYBR green served as the fluorescent dye, and Ct values were determined using the ABI 7500 Real-time PCR system. Each 20μl assay mixture included 1μg of cDNA. The expression patterns were analyzed using the $\Delta\Delta Ct$ method and were normalized to the internal control gene GAPDH. The $\Delta\Delta Ct$ values were calculated according to the formula: $\Delta\Delta Ct = (Ct \text{ value of the test} - Ct$

value of the internal control) - (Ct value of the test under control conditions). The relative density of *H. pylori* was quantified using semi-quantitative PCR by detecting *H. pylori*-specific 16S ribosomal DNA (rDNA) with the primers FP (5'-AGAGAAGCAATACTGTGAA-3') and RP (5'-CGATTACTAGCGATTCCA-3'). GAPDH was concurrently measured for normalization using the primers FP (5'-GTCTTCACCACCATGGAGAAGGC-3') and RP (5'-CATGCCAGTGAGCTTCCCGTTCA-3').

The thermal profile utilized consisted of the following steps: an initial denaturation cycle at 95°C for 10 minutes, followed by 40 amplification cycles with each cycle comprising denaturation at 95°C for 15 seconds and annealing/extension at 60°C for 1 minute. Subsequently, a dissociation curve was performed with the following parameters: 95°C for 1 minute, 55°C for 30 minutes, and 95°C for 30 seconds.

23. Enzyme-linked immunosorbent assay (ELISA)

The concentration of released pro-inflammatory cytokines (HMGB1, IL-8, IL-6 or TNF- α) in cell media and mouse serum was quantitated using an Indirect ELISA following the manufacturer's protocol provided by KRISHGEN Biosystems. Samples and standards were appropriately diluted in assay diluent, and the 96-well plate was coated and incubated at 37°C for 90 min. After three washes with a wash buffer, 100 μ l of the detection antibody was added to each well and incubated for 1 hour. Subsequently, 100 μ l of HRP-conjugate was added, followed by the addition of the TMB substrate, and the mixture was incubated until color development occurred. The reaction was halted by the addition of a stop solution, and the optical density (OD) was measured at 450nm using a spectrophotometer.

Standard curves were constructed using the provided standards with varying dilutions, and the curve equation was derived from the data obtained.

Concentration of proteins were determined using the equation and putting the OD values as “x”

Standard no.	Conc.of Standard (ng/ml)	Reaction
7	100	10µl stock (10µg/ml) + 990µl assay diluent
6	50	500µl standard 7 + 500µl assay diluent
5	25	500µl standard 6 + 500µl assay diluent
4	12.5	500µl standard 5 + 500µl assay diluent
3	6.25	500µl standard 4 + 500µl assay diluent
2	3.13	500µl standard 3 + 500µl assay diluent
1	0.5	500µl standard 2 + 500µl assay diluent

24. MTT Assay

Cells were cultured in 96-well plates at a density of 1×10^4 cells/ml. Cells were further exposed to different doses of Glycyrrhizin (50µM-200µM), while an untreated DMSO control was maintained. The cells were subsequently incubated for 24 hours. To assess cell viability, a MTT reagent (3-(4,5-dimethylthiazol-2-yl)-2,5-diphenyltetrazolium bromide) from Sigma was used. 20µl of MTT reagent were added to each well, and the cells were incubated for 4 h at 37°C in a CO₂ incubator. Following the incubation period, 100 µl of DMSO was added to dissolve the purple crystal formazan. Optical density (OD) was then measured at 590 nm, and the percentage of cell viability was calculated and visually represented on a graph.

25. Measurement of intracellular Reactive oxygen species (ROS)

Cells were cultured in 96-well plates at a density of 1×10^4 cells/ml. Cells were further treated with (DMSO control) or the drug of interest. To detect intracellular ROS levels, we employed the fluorescent probe 2,7-dichlorodihydrofluorescein diacetate (DCFDA) (Sigma-Aldrich).

After incubating with 20 μ M DCFDA for 30 minutes at 37°C, we utilized the Synergy H1 Multimode Microplate Reader (Molecular devices Spectramax M2) to measure fluorescence. Excitation was achieved using a blue filter (485 nm), and emission was measured with a green filter (528 nm). Each experiment was performed in triplicate and independently conducted two times.

26. Minimum inhibitory concentrations (MIC) determination with Glycyrrhizin

Frozen stock cultures were streaked onto BHI agar supplemented with 5% horse serum and incubated for 3 days under previously mentioned microaerophilic conditions. The isolates were subsequently restreaked on fresh BHI agar and incubated for 24 hours. Exponentially growing *H. pylori* cells were suspended in sterile phosphate-buffered saline (PBS) and adjusted to an optical density of 0.1 at 600nm. 10 μ l of this adjusted inoculum were then inoculated onto BHI agar plates containing various concentrations of glycyrrhizin (Millipore). Glycyrrhizin was dissolved in DMSO, and stock solutions with concentrations of 50 mg/ml were stored at -20°C. The final test concentrations included 5, 4, 3, 2 and 1mg/mL of glycyrrhizin. Growth control plates containing only BHI agar were included in each experiment. Petri plates incorporating the vehicle solvent DMSO were also included as a growth control to ensure the organism's viability was not affected by the solvent used to dissolve glycyrrhizin. Two standard *H. pylori* strains (26695, SS1) and two clinical isolates (OT-14(3), A88C1) were used for susceptibility testing. All plates were incubated under microaerophilic conditions at 37°C for 5 days. The minimum inhibitory concentration (MIC) was determined as the lowest concentration of the compound at which no visible growth was observed.

27. *H. pylori* infection in C57BL/6 mice and treatment with Glycyrrhizin

Mice were maintained in the animal house, following to a 12-hour light-dark cycle. Experiments were carried out in accordance with the guidelines established by the Institutional Animal Ethical Committee at NICED, Kolkata (Protocol Number PRO/157/-260, dated July 2022). Male C57BL/6 mice, 8 weeks old and bred in-house, were selected for these experiments. The mice were divided into three distinct experimental groups: Control group (CON) consisting of 5 mice, *H. pylori* SS1 infected group (HP) with 5 mice, and infected group treated with glycyrrhizin GLZ (HP+GLZ), also comprising 5 mice. Each group received daily antibiotic treatment over a span of seven days, which included Ciprofloxacin, Metronidazole, Erythromycin, and Albendazole. This antibiotic regimen was used to prevent potential bacterial or parasitic infections. A group of mice (HP and HP+GLZ) were subjected to inoculation with *H. pylori* SS1 at a dosage of 10^8 CFU per mouse per inoculation on alternate days. Meanwhile, another group of mice (CON) received PBS as a control. After two weeks of the initial inoculation, the HP+GLZ group received glycyrrhizin orally at a dosage of 10 mg/kg for a period of 4 weeks, while the CON group received sterile water. At the end of the fourth week, all mice were euthanized. Gastric tissues were isolated, and blood samples were collected for experimental purposes, following the methodology outlined in (Saha et al., 2022). These experiments were repeated three times, with a total of 15 mice in each set of experiments.

28. Histology

The antral regions of the stomachs from mice in the control, *H. pylori*-infected, and glycyrrhizin-treated groups were sectioned for histological analysis. These tissue samples were fixed in 10% formalin and subsequently embedded in paraffin. Sections with a thickness

of 5µm were then produced using a microtome. These sections were stained with hematoxylin and eosin and examined under a Zeiss microscope (model 1000 2026). Images were captured at original magnifications of 10x, 20x, and 40x using Progress CapturePro 2.6 software.

29. Statistical Analysis

All data were presented as mean \pm S.E.M. Statistical comparisons between two groups were performed using an Unpaired t-test, while multiple comparisons were conducted using one-way ANOVA. The significance level was indicated as follows: * for $p < 0.05$, indicating significance; ** for $p < 0.01$, indicating high significance; and *** for $p < 0.001$, indicating highly significant.

Section 4

**AIMS
AND
OBJECTIVES**

The objectives of the proposed study are as follows:

Objective 1: Investigating the role of HMGB1 in autophagy during *Helicobacter pylori* infection.

Objective 2: Unravelling the mechanism by which we can interlink autophagic targets with inflammation in *H. pylori* infection.

Objective 3: Dissecting the role of novel signature autophagic targets due to HMGB1 activation

Section 5

RESULTS

OBJECTIVE I.

Chapter 1

***H. pylori* infection augments HMGB1 expression and modulates autophagy in gastric epithelial cells.**

Background

Helicobacter pylori (*H. pylori*) is a predominant human pathogen that infects more than half of the world's population. *H. pylori* infection can cause a variety of health problems, including gastritis, stomach ulcers, and in severe cases gastric cancer (**Chu et al., 2019**). *H. pylori* was formerly considered as an extracellular bacterium, but nowadays it is considered as an intracellular pathogen (**Amieva et al., 2002**). It was discovered that this bacterium could survive and even multiply inside stomach epithelial cells (**Tang et al., 2012**) and immune cells like macrophages (**Wang et al., 2009**). However, the host often employs many cellular defence methods to eradicate the entering bacteria. Autophagy is one of the key mechanisms involved in the recognition and capture of intracellular microorganisms for degradation.

Autophagy is a highly conserved mechanism that destroys cellular components or invading pathogens in eukaryotic cells via lysosomes (**Dikic et al., 2018**). Cellular components such as damaged cell organelles, proteins, or invading microbes are engulfed by double-membrane-bound structure known as phagophore which begins to develop at both ends to generate an autophagosome. The autophagosome then merges with a lysosome to form a, membrane-enclosed vesicle known as autolysosome. Lysosomal enzymes then break down the membrane and the autolysosomal contents (**Shintani and Klionsky, 2004**).

The molecular mechanism of autophagy comprises of several stages: phagophore initiation, elongation, maturation, and cargo degradation. Each step requires a set of Atg (autophagy-related) proteins. Several autophagy-related proteins are involved in the process including LC3B, p62, ATG5 and Beclin-1. Beclin-1 forms an isolation membrane during the initiation of autophagy. ATG5 is another essential protein for the elongation of the phagophoric membrane in autophagic vesicles. It is stimulated by ATG7 and forms a complex with ATG12 and ATG16L1 (**Yang and Klionsky, 2010**). Microtubule-associated proteins 1A/1B

light chain 3B (MAP1LC3B) is the standard marker of autophagy and its expression reflects the number of autophagosome formation. SQSTM1/p62 is an important cargo receptor involved in selective autophagy whose degradation is a hallmark of autophagy activation **(Levine et al., 2011)**. Hence, there are several proteins in the initiation and maturation steps of autophagy.

According to the previous studies, infection with *H. pylori* induces autophagy in both gastric epithelial cells **(Terebiznik et al., 2009; Tang et al., 2012)** and immune cells **(Wang et al., 2009)**. Among the various virulence factors produced by *H. pylori*, those that mainly induce autophagy in gastric mucosal epithelial cells include VacA and CagA **(Raju et al., 2012)**. VacA and Cag A have antagonistic roles in autophagy. It has been reported earlier that VacA induces autophagy whereas Cag A inhibits autophagic maturation **(Li et al., 2017)**.

Several autophagy molecules are active during different stages of autophagy processes. HMGB1 is one of the crucial factors for autophagy. Primarily, HMGB1 is a nuclear protein but it has multiple functions according to its subcellular location. While inside the nucleus, it plays significant role in maintenance of structure and stability of the nucleosome and exerts control over transcription **(Ueda et al., 2010)**. In the cytoplasm, it regulates autophagy and apoptosis. In response to stimuli, it is secreted into the extracellular space and acts as a damage-associated molecular pattern (DAMP) molecule. Moreover, it activates immune response by binding to pattern recognition receptors (PRRs) as a chemokine or cytokine **(Andersson et al., 2018)**. Extracellular HMGB1 is either passively released by necrotic tissues or actively secreted by stressed cells **(Wang et al., 1999; Dumitriu et al., 2005; Rouhiainen et al., 2000; Semino et al., 2005)**. Additionally, studies have shown that it also plays a range of biological roles in pathological aspects. In its role as a cytokine, it contributes to the development of diseases associated with inflammation, such as cancer **(Wang et al., 2020)**. However, the role of HMGB1 in autophagy is not explored during *H.*

pylori infection in gastric cells. Substantial evidences have shown that HMGB1 is expressed abnormally in a variety of tumours, including gastric tumour. These features make HMGB1 a promising target as a biomarker for the study of gastric disorders. Here, we explain how HMGB1 regulates autophagy during *H. pylori* infection and investigates its role in pathogenesis.

Materials and Methods

Expression of autophagy proteins were checked by western blotting, levels of cytokine production was checked by ELISA. Autophagosome formation was observed under confocal microscopy. All methods were previously described in materials and methods section.

Results

1.1 *H. pylori*- infection activates HMGB1 expression in gastric epithelial cells

1.1.1 HMGB1 expression at different MOI of *H. pylori* 26695-infection in AGS cells

At first, we examined the effect of *H. pylori* infection on the expression of HMGB1 in gastric epithelial cells. AGS is the most common gastric cancer epithelial cell line obtained from the stomach tissue of a 54-year-old White female patient with gastric adenocarcinoma. To this end, we infected AGS cells with *H. pylori* strain 26695(*vacA*+, *cagA*+) at different MOIs (50, 100, 200, 400 & 600) for 4 h followed by treatment with 100 µg/ml gentamicin for 1 h to kill extracellular bacteria and finally incubated in fresh medium for another 3 h. AGS cell extracts were solubilized in RIPA buffer and further subjected to western blotting for analysis of proteins and beta actin was used as loading control. As demonstrated in **Figure 1.1A-B**, HMGB1 expression levels were significantly elevated in cells infected with *H. pylori* at MOI 100 and reduced at higher MOIs of 200, 400 and 600. Further, we determined the level of IL-8 as it is the strong indicator of inflammation during *H. pylori* infection. For this purpose, the cell culture medium collected after infection was subjected to ELISA for the measurement of released cytokines from infected cells. We found that the level of IL-8 increases during infection at different MOIs (50, 100, 200, 400 & 600) but were remarkably highest at MOI 100 (**Figure 1.1C**). These results suggest that MOI 100 of *H. pylori* 26695 is optimal for infection and HMGB1 overexpression in AGS cells.

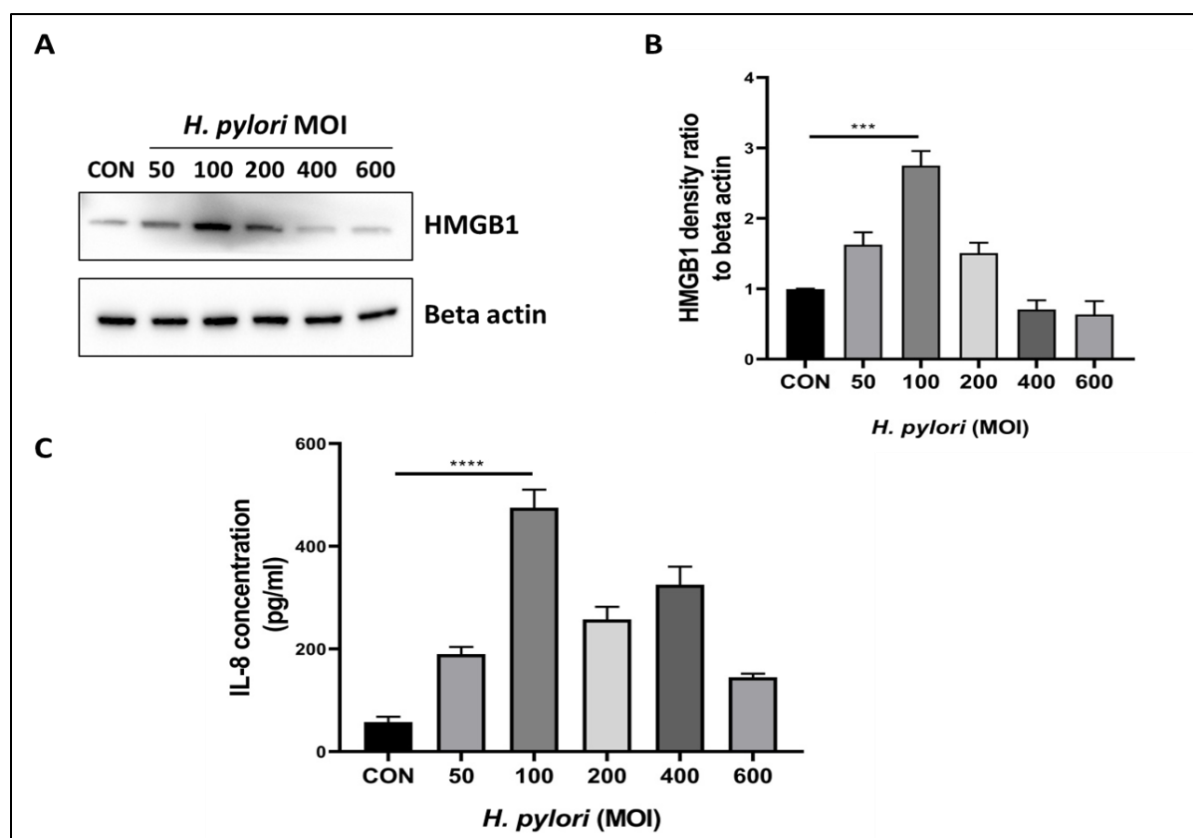


Figure1.1 Varying MOI of *H. pylori* stimulate HMGB1 expression in AGS cells. (A–C) AGS cells were uninfected (Con) or infected with varying MOIs (50, 100, 200, 400 & 600) of *H. pylori* for 6 h. (A) Cell lysates were prepared and expression level of HMGB1 was observed by western blot analysis. Beta-actin was used as protein loading control. (B) Densitometry analysis is represented graphically. (C) Cell culture medium of uninfected(Con) or infected with varying MOIs (50, 100, 200, 400 & 600) of *H. pylori* for 6 h was collected and IL-8 was determined using ELISA assay. Graphs were represented as mean±SEM (n=3); One-way ANOVA was performed and significance was calculated; *** $p < 0.0001$ and **** $p < 0.001$.

1.1.2 HMGB1 expression at different time points of *H. pylori* SS1- infection in AGS cells

AGS cells were also concurrently infected with another standard strain of *H. pylori* Sydney strain 1 SS1 [CagA+, VacA(s1/m1)] (with the same protocol of infection as of 26695) over a range of time interval (2, 4, & 6 h) at MOI 1: 100 and the expression levels of HMGB1 were investigated by western blot assay. Cells were infected with *H. pylori* strain SS1 at MOI: 100 for 4 h followed by treatment with 100 µg/ml gentamicin for 1 h and then incubated in fresh medium over a range of time interval (2, 4, & 6 h). Result showed that *H. pylori* SS1

infection to AGS cells induced HMGB1 expression that peaked at 4 h and decreased at 6 h (Figure 1.2A, B). These findings imply that both the strains of *H. pylori* 26695 & SS1 causes increased HMGB1 expression in AGS cells, and the MOI of 100 and 3- 4 h incubation period are ideal conditions for infection.

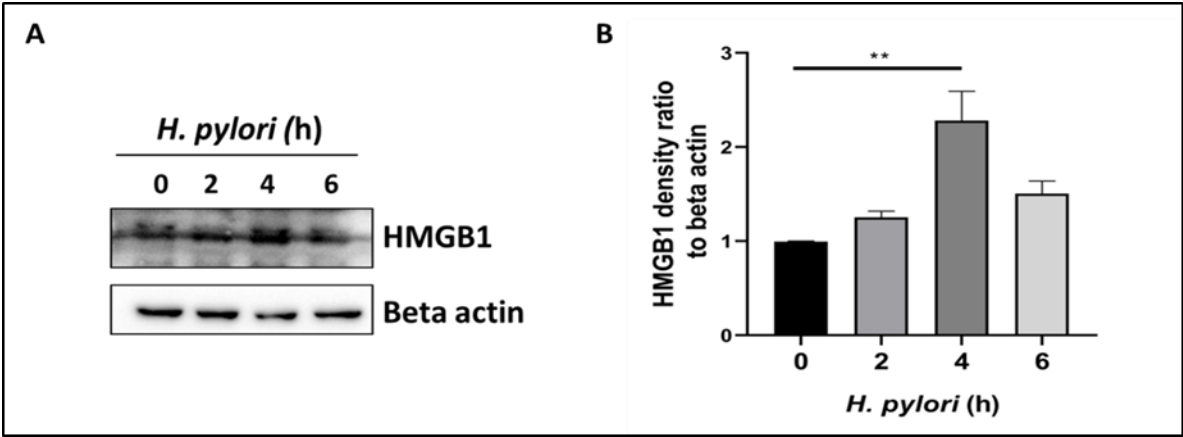


Figure1.2. *H. pylori* induces HMGB1 expression at different time points of infection. (A–C) AGS cells were uninfected (0) or infected with *H. pylori* for (2, 4 & 6 h. (A) Cell lysates were prepared and expression level of HMGB1 was observed by western blot analysis. Beta-actin was used as a protein loading control. (B) Densitometry analysis is represented graphically. Graphs were represented as mean±SEM (n=3); One-way ANOVA was performed and significance was calculated; ** p < 0.01.

1.1.3. Subcellular location of HMGB1 by *H. pylori* SS1- infection in AGS cells

Physiologically active HMGB1 can be translocated to the cytosol and extracellular space despite its predominant localization within the nucleus in most cells. In order to determine the effect of *H. pylori* infection in the nucleo-cytoplasmic translocation of HMGB1, AGS cells were infected with *H. pylori* SS1 for 4 h and immunofluorescence was performed using HMGB1 specific antibody. As shown in **Figure 1.3A**, we found green fluorescence was localised mainly in the nucleus but not in cytoplasm in case of un-infected cells (Con). However, the distribution of green fluorescence clearly demonstrated that HMGB1 was abundant in the cytoplasm of cells upon *H. pylori* SS1 infection.

Further to ascertain whether HMGB1 is released into the extracellular space, we collected the culture medium from experiment set up of **Figure 1.2** and subsequently ELISA was

performed to determine HMGB1 release. Consistent with the western blot results (**Figure 1.2A**), HMGB1 released from *H. pylori*- infected cells significantly increased in time-dependent manner but there was a drop in extracellular release after 4 h (**Figure 1.3B**). This indicates *H. pylori* infection helps in HMGB1 translocation into the cytoplasm and specifically the cytoplasmic HMGB1 is secreted in the extracellular space to mediate inflammation in gastric cells.

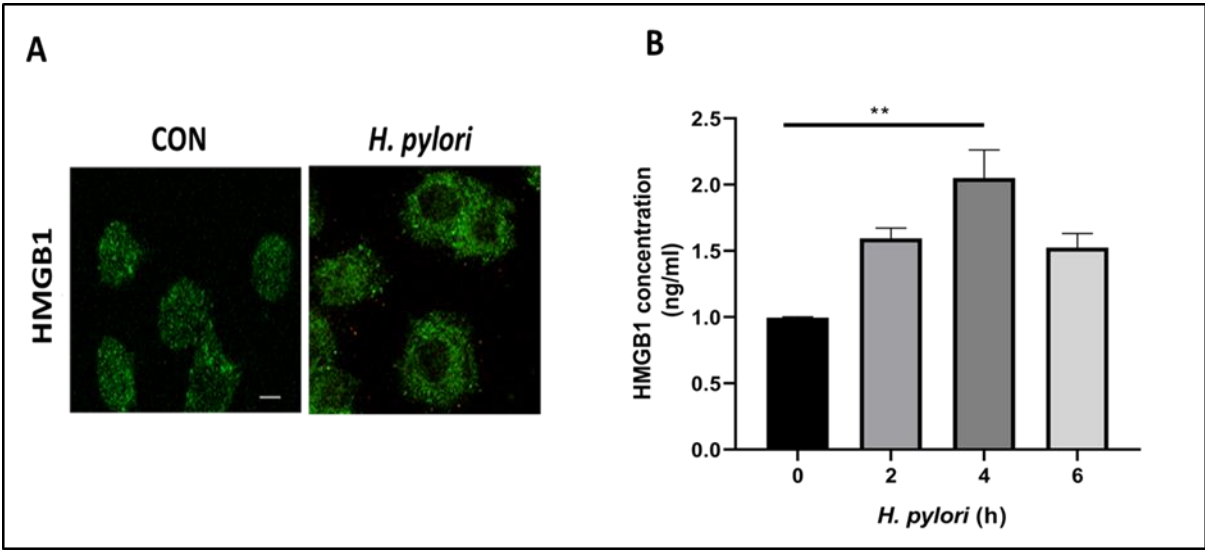


Figure 1.3 HMGB1 Location in response to *H. pylori* infection. (A) AGS cells were infected with *H. pylori* for 0, 2, 4 and 6 h. Immunofluorescence staining was performed in which cells were fixed and probed with antibody against HMGB1 (green). The stained samples were analyzed by confocal microscopy. Scale bars, 10 μ m. (B) Cell culture medium of infected cells was collected and HMGB1 was determined by ELISA assay. Graphs were represented as mean \pm SEM (n=3); One-way ANOVA was performed and significance was calculated; ** p < 0.001.

1.2 *H. pylori*- infection modulates autophagy in gastric epithelial cells

1.2.1 *H. pylori* 26695- modifies autophagy in AGS cells

According to several reports, *H. pylori* is known to invade gastric epithelial cells and *H. pylori* infection induces defective autophagy meaning it stimulates the autophagy in gastric epithelial cells during early infection, whereas the bacteria suppresses autophagy at later stages of infection in order to promote its survival and colonisation (Yang et al., 2018; Tang

et al., 2012). To evaluate the autophagic regulation, we infected AGS cells with *H. pylori* 26695 as described before and analysed the expression of autophagy proteins (LC3B, Beclin1 and P62) by western blotting. LC3B exists in two forms in the cell: unconjugated LC3B-I and lipid phosphatidylethanolamine-conjugated LC3B-II (**Kabeya et al., 2004; Meyer et al., 2013; Mizushima et al., 2002; Tanida et al., 2004**). The latter form is inserted into the expanding autophagosome's inner and outer membranes during the induction of autophagy. As a result, it serves as a crucial autophagy marker to track autophagy induction. We observed an increase in the expression of LC3B-II (**Figure 1.4A, B**), indicating enhanced autophagosome formation.

Parallely, we performed - confocal microscopy to verify the expression of LC3B in *H. pylori* infected cells. AGS cells were transiently transfected with GFP-tagged LC3B expression plasmid and 36 h post-transfection, cells were either uninfected or infected with *H. pylori* for another 4 h. Results demonstrated that there are few LC3B puncta (green fluorescence) in case of uninfected transfected cells indicating basal level of autophagy but the LC3B puncta formation significantly increased in *H. pylori*-infected cells consistent with the western blotting (**Figure 1.4C, D**). The increase in the LC3B puncta formation was calculated by measuring mean fluorescence intensity within a certain area of expression of LC3B puncta in case of uninfected (Control) & *H. pylori*-infected gastric cells. However, due to dynamic nature of autophagy, increased levels of LC3-II (Western blot analysis) or an accumulation of green fluorescent protein (GFP)-LC3B puncta (confocal analysis of cells transfected with a plasmid encoding GFP-LC3B) are indicative of either autophagy induction or a block in autophagosome fusion with lysosome, or decreased lysosomal degradation.

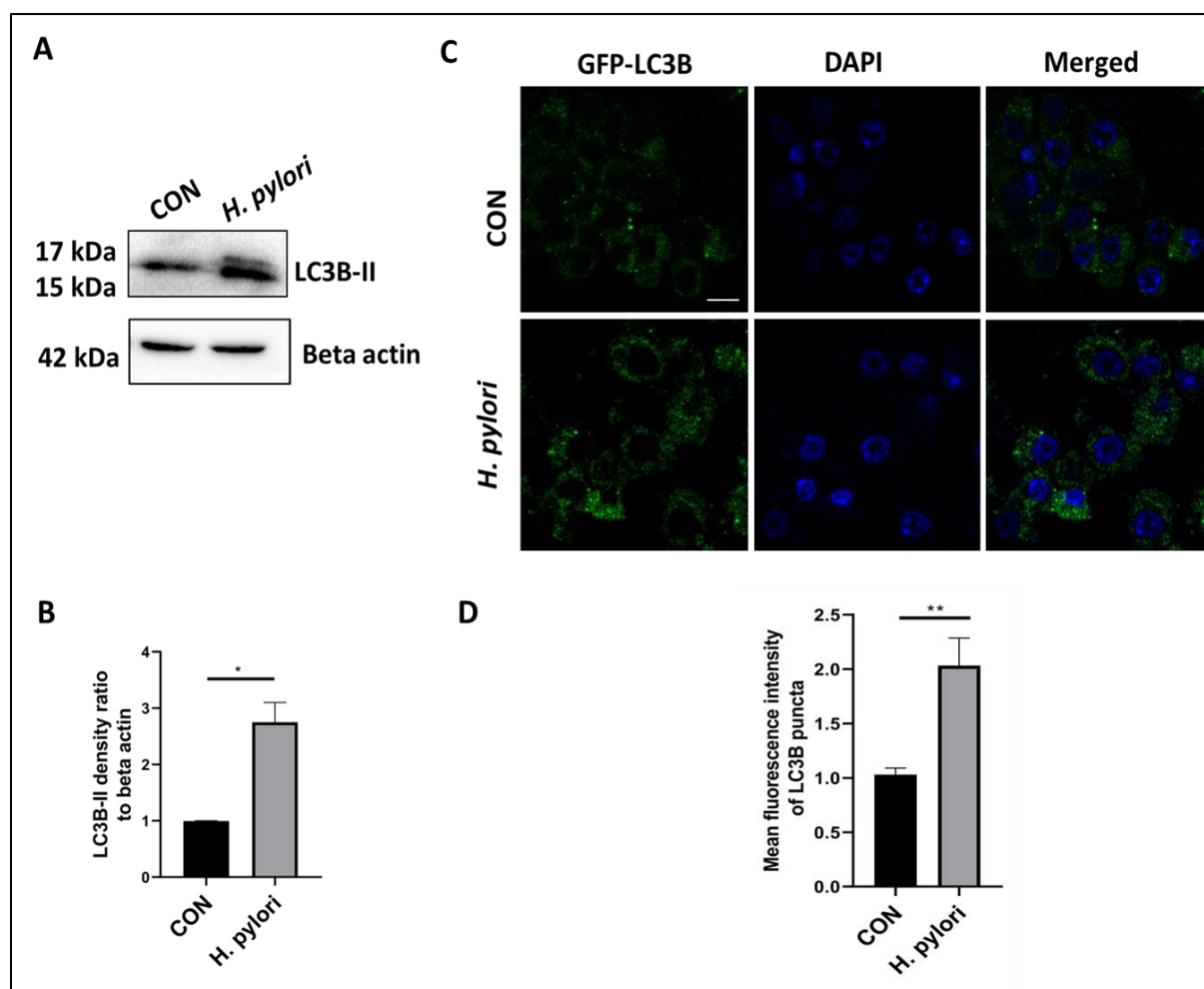


Figure 1.4 Infection with *H. pylori* 26695 (MOI 100) was performed in AGS cells for 4 h (A-D). Immunoblotting was performed for quantification of autophagy-associated marker proteins (LC3B-II). Beta-actin was used as a loading control. **(B)** Densitometry analyses are represented graphically. **(C)** AGS cells were transiently transfected with GFP-tagged LC3B expression plasmid & further infected with *H. pylori* for 4 h. Confocal microscopy showed LC3B puncta (green) formation in control (CON) & *H. pylori* infected cells and stained with DAPI (blue) to visualize cell nuclei. The stained samples were analyzed by confocal microscopy. Scale bars, 10 μ m. **(D)** Graphs were represented as mean \pm SEM (n=3); Unpaired t-test was done and significance was calculated; * $p < 0.05$, ** $p < 0.01$.

Subsequently, we assessed the expression of the autophagy-related protein Beclin-1, which is known to participate with LC3-II at the early stage of autophagy. Beclin1 was found to be increased as well. **(Figure 1.5A, B)**. Another autophagy marker, SQSTM1/p62, a key protein involved in autophagy was further examined to study more about the autophagy process during *H. pylori* infection. P62 degradation is a hallmark of induction of autophagy and we found a remarkable increase in the p62 indicating accumulation of autophagosomes during *H.*

pylori infection (**Figure 1.5A, C**). All together, the results indicate that dysregulation of autophagy during *H. pylori* 26695- infection in gastric cells.

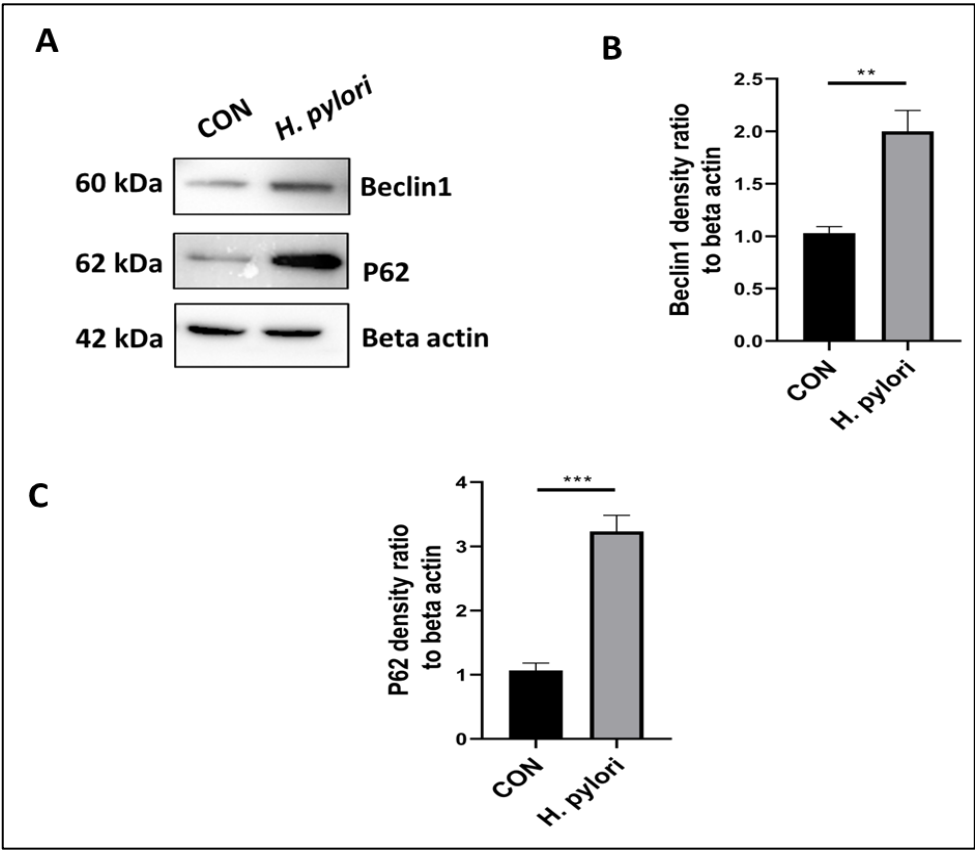


Figure 1.5 Infection with *H. pylori* (MOI 100) was performed in AGS cells for 4 h (A-C). Immunoblotting was performed for quantification of autophagy-associated marker proteins (Beclin1&P62). Beta-actin was used as a loading control. (B-C) Densitometry analyses are represented graphically. Unpaired t-test was done and significance was calculated; ** $p < 0.01$ and *** $p < 0.001$.

1.2.2 *H. pylori* SS1- regulates autophagy in AGS cells

Furthermore, we evaluated the autophagy mechanism by another standard strain of *H. pylori* i.e, SS1. In that context, we infected AGS cells with *H. pylori* SS1 with the same protocol as described before and studied the expression of autophagy proteins by western blotting and confocal microscopy analysis. As per **Figure 1.6A, B** there was a significant increase in the LC3B-II to beta actin ratio with the cells infected with *H. pylori*SS1 strain. To verify western blot data of LC3B-II, we performed confocal microscopy. The results showed augmented

expression of LC3B puncta in the AGS cells transfected with GFP-LC3B plasmid and infected with bacteria as compared to un-infected group (**Figure 1.6C, D**).

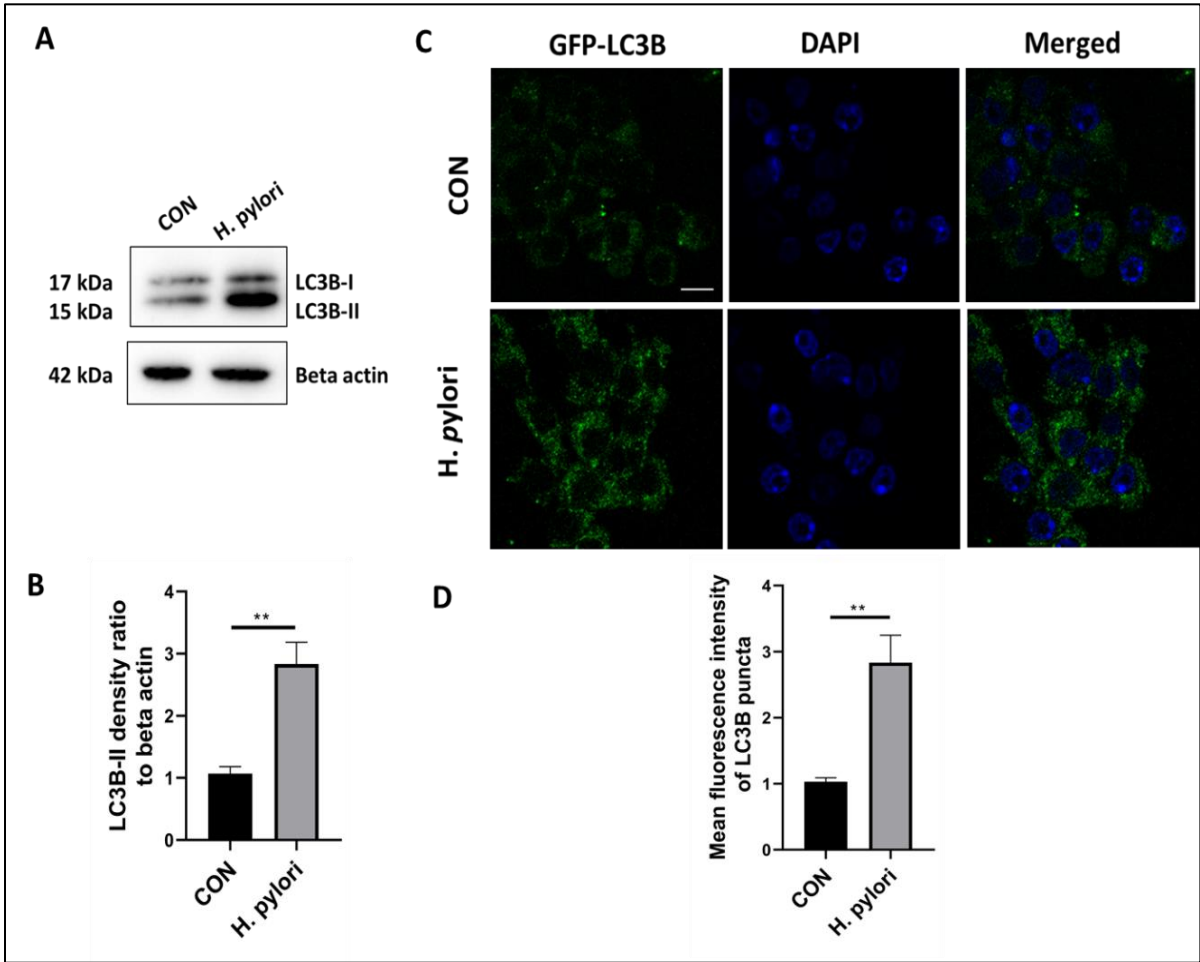


Figure 1.6 Infection with *H. pylori* SS1 (MOI 100) was performed in AGS cells (A-D). Immunoblotting was performed for quantification of autophagy-associated marker proteins (LC3B II.). Beta-actin was used as a loading control. (B) Densitometry analyses are represented graphically. (C) AGS cells were transiently transfected with GFP-tagged LC3B expression plasmid & further infected with *H. pylori* SS1 for 4 h. Confocal microscopy showed LC3B puncta (green) formation in control (CON) & *H. pylori* infected cells and stained with DAPI (blue) to visualize cell nuclei. The stained samples were analyzed by confocal microscopy. Scale bars, 10 μ m. (D) Graphs were represented as mean \pm SEM (n=3); Unpaired t-test was done and significance was calculated; ** p < 0.01.

To detect other important markers of autophagy, we performed western blot analysis to quantify the expression of Beclin1 and P62 in the gastric cells of un-infected and *H. pylori* SS1 infected group. Compared with the control group, we found an increased in the expression of Beclin1 (**Figure 1.7A, B**) and accumulated P62 under *H. pylori* infected group

(Figure 1.7A, C). Accumulated p62 often occurs in conjunction with impairment of autophagic degradation. The results indicate that autophagic markers accumulate due to the deregulation of autophagy during *H. pylori* SS1- infection. This is in line with *H. pylori* 26695 infection to gastric cells.

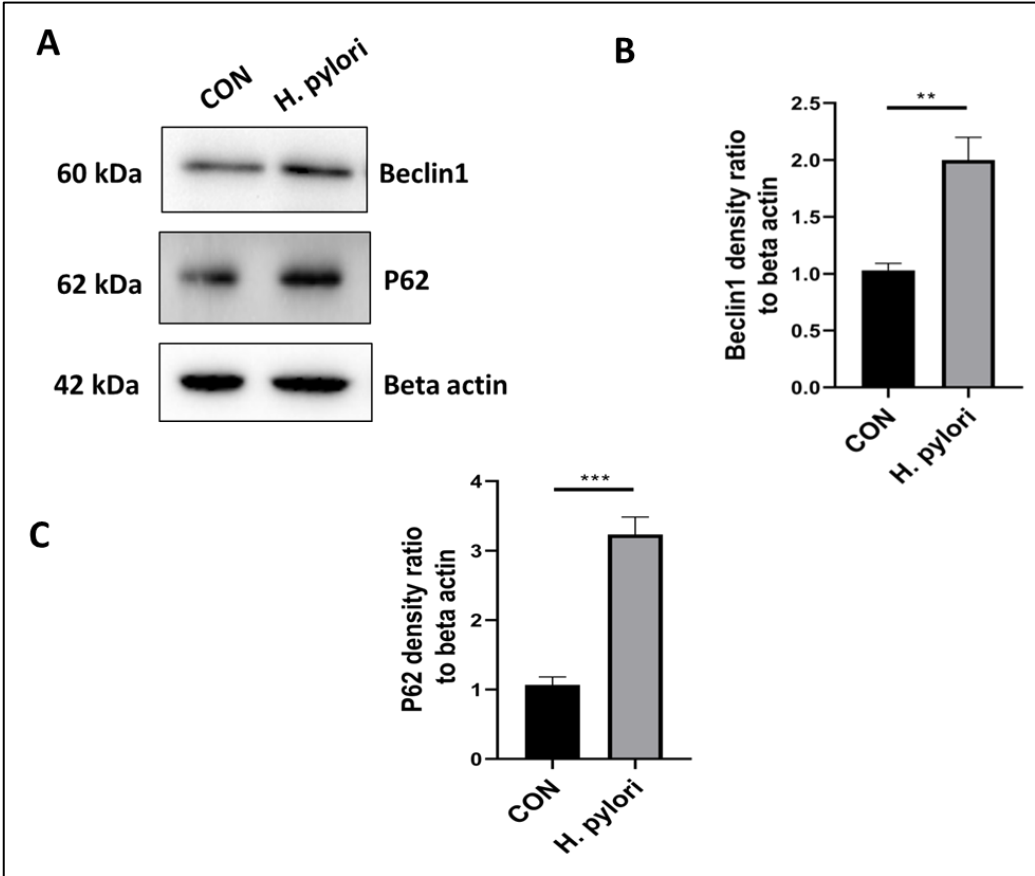


Figure 1.7 Infection with *H. pylori* (MOI 100) was performed in AGS cells (A-C). Immunoblotting was performed for quantification of autophagy-associated marker proteins (Beclin1&P62). Beta-actin was used as a loading control. (B-C) Densitometry analyses are represented graphically. Unpaired t-test was done and significance was calculated; ** $p < 0.01$ and *** $p < 0.001$.

1.3 HMGB1 expression and autophagy regulation by *H. pylori*-infection in HGC-27 cells

We next investigated HMGB1 expression or autophagy induction in another gastric cell line such as HGC-27. HGC-27 is a human cell line obtained from a metastatic lymph node of gastric cancer. To this end, we infected gastric epithelial cell line (HGC-27 cells) with *H.*

pylori 26695 at MOI 100 for 4 h and protein expression level was evaluated using western blot. We observed that an enhanced expression of HMGB1 (**Figure 1.8 A, B**) along with autophagic stimulation with an increase in the LC3B-II expression (**Figure 1.8 A, C**) in *H. pylori* infected HGC-27 cells as compared to control. Therefore, the results indicate that in line with infection in AGScells, overexpression of HMGB1 and modulation of autophagy in HGC-27 cells as well.

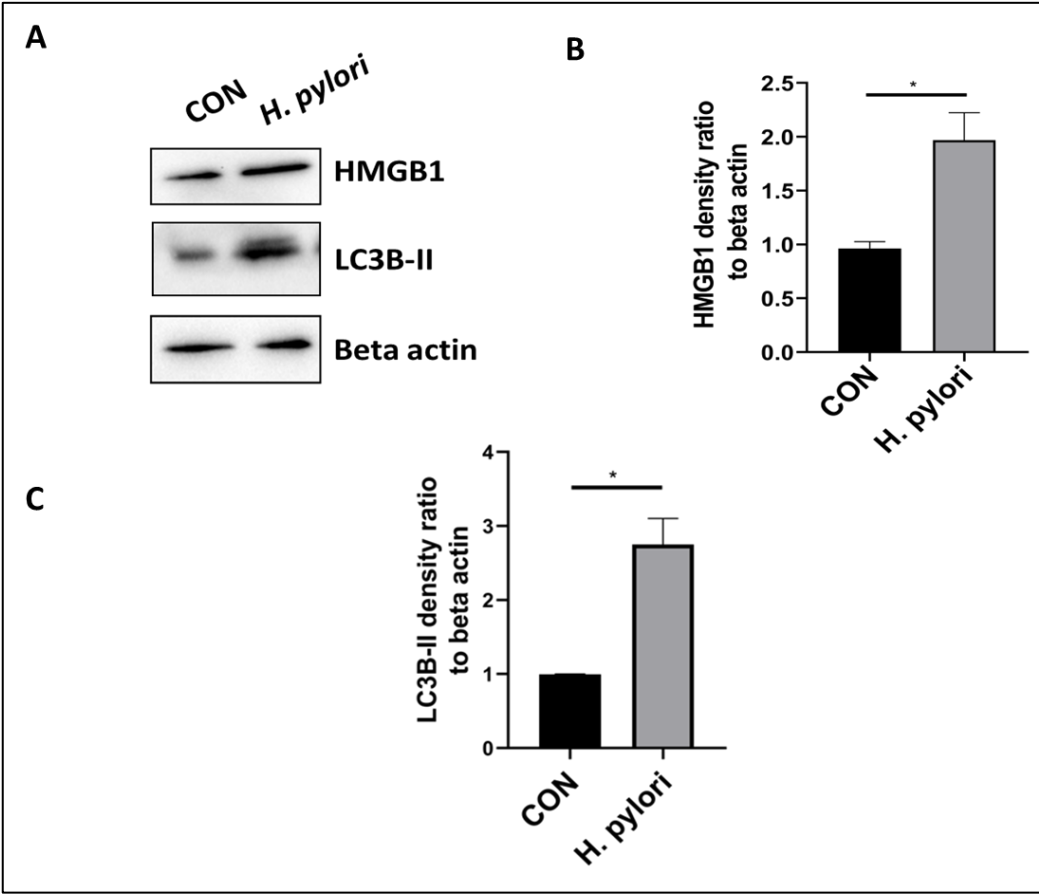


Figure 1.8 *H. pylori* induces HMGB1 expression in HGC-27 cells. (A-C) HGC-27 cells were uninfected or infected with *H. pylori* 26695 for 6 h. Cell lysates were prepared and expression level of HMGB1 and LC3B-II was observed by western blot analysis. Beta-actin was used as a protein loading control. (B-C) Densitometry analysis is represented graphically. Graphs were represented as mean±SEM (n=3); Unpaired t-test was done and significance was calculated; * $p < 0.05$.

1.4 *H. pylori*- infection induces HMGB1 expression and modifies autophagy in RAW 264.7 cells

Since *H. pylori* can also colonize and persist within immune cells like macrophages, an important mediator of gastritis during infection, we further questioned whether *H. pylori* infection could regulate autophagy and stimulate HMGB1 production in macrophages. To this end, we infected RAW 264.7 cells (mouse macrophage cell line) with *H. pylori* 26695 for 4 h and 8 h and performed western blot analysis to detect HMGB1 level. We found an increased expression of HMGB1 in macrophage cells at 4 h of *H. pylori* infection. While as we increased the time period of infection, expression level of HMGB1 is decreased at 8 h (Figure 1.9 A, B).

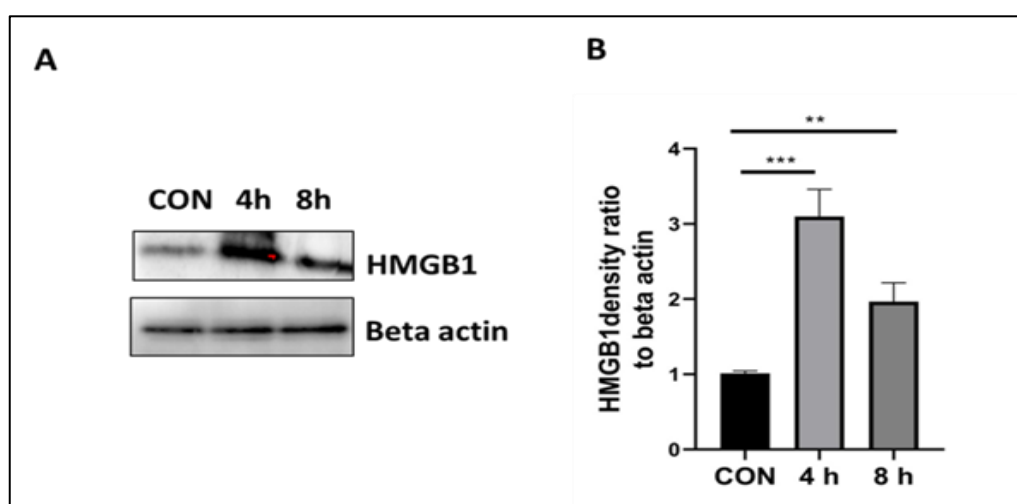


Figure 1.9 *H. pylori* 26695 stimulates HMGB1 expression in RAW264.7 cells. (A–B) RAW264.7 cells were uninfected or infected with *H. pylori* 26695 for (4 & 8 h). (A) Cell lysates were prepared and expression level of HMGB1 was observed by western blot analysis. Beta-actin was used as a protein loading control. (B) Densitometry analysis is represented graphically. Graphs were represented as mean \pm SEM (n=3); One-way ANOVA was performed and significance was calculated; ** $p < 0.01$, *** $p < 0.001$.

Accordingly, we performed western blotting to assess autophagy regulation in response to *H. pylori* infection in RAW 264.7 cells. We found a rise in the expression of LC3B-II at both 4 h and 8 h infection (Figure 1.10A, B) unlike as in AGS cells. Further we assessed the

expression of the autophagy-related protein Beclin-1, which is known to participate at the early stage of autophagy. Beclin1 was found to be increased with infection of *H. pylori* from 4h to 8h. (Figure 1.10A, C). Another autophagy marker, SQSTM1/p62, a key protein involved in autophagy was further examined. The expression of the p62 protein is elevated by *H. pylori* infection at 4 h but a decrease at 8 h infection (Figure 1.10A, D).

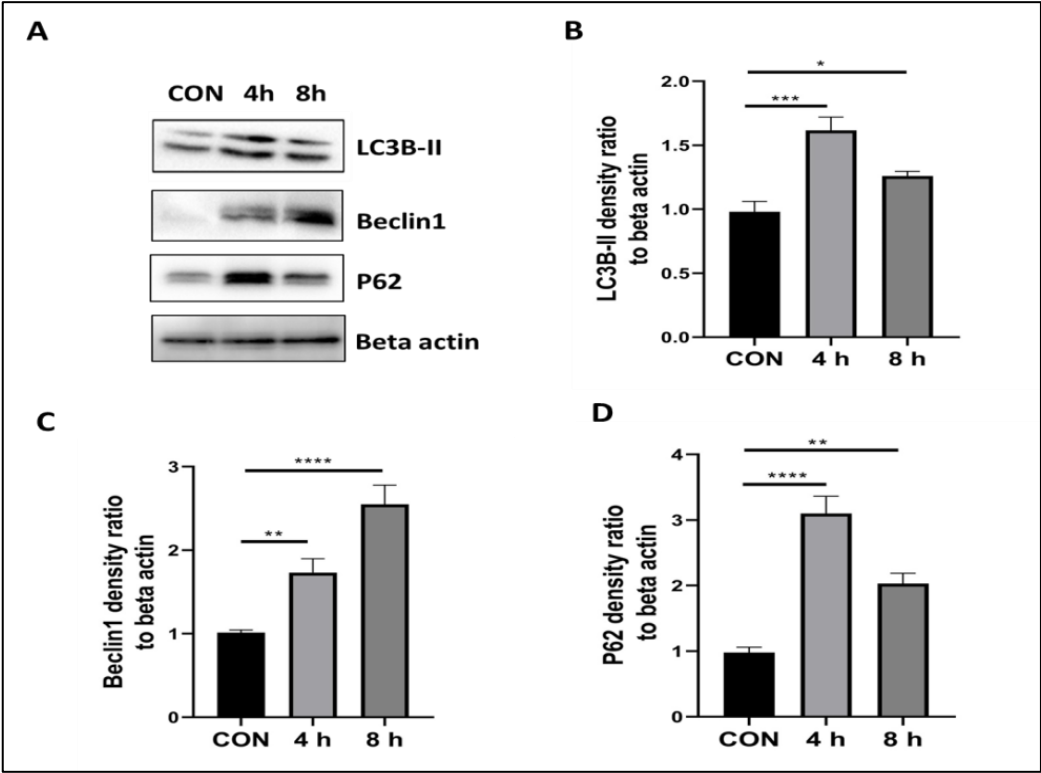


Figure 1.10 Infection with *H. pylori* (MOI 100) in macrophages (A-D). Immunoblotting was performed for quantification of autophagy-associated marker proteins (LC3B-II, Beclin1 & P62). Beta-actin was used as a loading control. (B-D) Densitometry analyses are represented graphically. One-way ANOVA was performed and significance was calculated; * $p < 0.05$, ** $p < 0.01$ and *** $p < 0.001$.

In parallel, we performed confocal microscopy to verify western blot data of LC3B in *H. pylori* infected RAW 264.7 cells. RAW 264.7 cells were transiently transfected with GFP-tagged LC3B expression plasmid and 36 h post-transfection, cells were infected with *H. pylori* for another 4 h and 8 h. Results demonstrated that there are few LC3B puncta (green fluorescence) in case of uninfected (control) transfected cells indicating basal level of autophagy but the LC3B puncta formation significantly increased in *H. pylori*-infected cells

consistent with the western blotting at both the time point of infection (4 & 8 h) (**Figure 1.11A, B**). However, increased levels of LC3II-B (Western blot analysis) or accumulation of green fluorescent protein (GFP)-LC3B puncta (confocal analysis of cells transfected with a plasmid encoding GFP-LC3B) indicates either autophagy induction, or a block in autophagosome fusion with lysosome, or decreased lysosomal degradation.

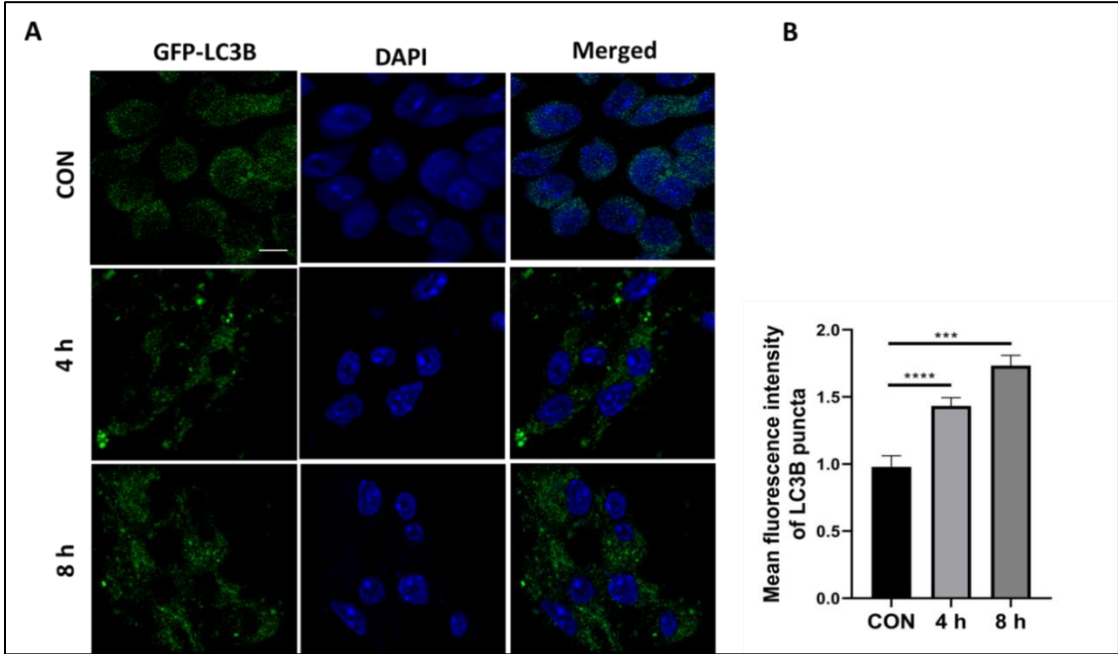


Figure 1.11 Infection with *H. pylori* 26695 (MOI 100) was performed in RAW264.7 cells for 4 h & 8 h. (A-B). (A) RAW264.7 cells were transiently transfected with GFP-tagged LC3B expression plasmid & further infected with *H. pylori* 26695 for 4 h and 8 h. Confocal microscopy showed LC3B puncta (green) formation in control (CON) & *H. pylori* infected cells and stained with DAPI (blue) to visualize cell nuclei. The stained samples were analyzed by confocal microscopy. Scale bars, 10 μ m. (B) Graphs were represented as mean \pm SEM (n=3); One-way ANOVA was performed and significance was calculated; *** p < 0.001.

Conclusion

All together the data demonstrated that *H. pylori* infection modulates pathway autophagy together with increase in expression of HMGB1 in the early hours of infection in both the human gastric cancer cell line (AGS & HGC-27) and the mouse macrophage cell line (RAW 264.7). Dysregulation of autophagy is also present at some time points. However, AGS cell line was used for the subsequent studies since it was reported to be more susceptible.

Chapter 2

**Autolysosomal degradation function was compromised due to
H. pylori infection**

Background

Autophagy is an evolutionary conserved process that can be separated into two phases. First, double-membrane autophagosomes sequester intracellular components. Second, the autophagosome fuses with the lysosome to form an autolysosome, which releases enzymes into the compartment, causing the autolysosomal contents to be degraded. Autophagy can be elicited by a variety of harmful stimuli and plays a crucial function in maintaining cellular homeostasis and also helps in defending against pathogen infection (**Haeussler et al., 2020, Prajsnar et al., 2021**). Several intracellular pathogens, including *Mycobacterium tuberculosis*, *Salmonella typhimurium*, *Shigella flexneri* and *Listeria monocytogenes*, have been found to regulate autophagy for their own propagation (**Xie et al., 2020; Ogawa et al., 2005; Padhi et al. 2019**). Primarily, autophagy is initiated due to infection, but is attenuated due to prolonged exposure to *H. pylori* infection, however the process by which the pathogen regulates host autophagy is still not well understood (**Terebiznik et al., 2006; Raju et al., 2012**). Importantly, *H. pylori* prevents the fusion of lysosomes with autophagosomes, thus inhibits the later stages of autophagy. Autophagy disruption by *H. pylori* lowers autophagic flux and may facilitate persistent infection into the gastric cells. However, it is still uncertain how *H. pylori* modulates autophagy and prolongs its survival from lysosomal degradation.

Lysosomes are highly acidic subcellular organelles that contain more than 50 soluble acid hydrolases and they are involved in the autophagosomal content degradation. LAMP1 (lysosomal associated membrane protein 1) is an important end stage marker of autophagy that is associated with the lysosomal membrane (**Lubke et al., 2009**).

Materials and Methods

Autophagy marker protein expression levels were checked using western blot. Live-cell imaging was performed to monitor the lysosomes expressing LAMP1 using LAMP1-GFP construct. Double-immunofluorescence assay was done using LC3B and LAMP1 antibodies to determine reduced fusion between autophagosomes and lysosomes. Autophagic flux was explored by (i) Western blotting in infected AGS cells followed by the treatment of Bafilomycin A1 in both infected and un-infected cells. (ii) Both autophagosomes and autolysosomes were examined by transfecting AGS cells with mRFP-GFP tandem fluorescent-tagged LC3B (tfLC3B) followed by *H. pylori* infection and subjected to confocal microscopy. Colony forming unit (CFU) assay was performed to check intracellular survival of *H. pylori*. Detailed methods are already described in the materials and methods section.

Results

2.1 Downregulation of late autophagy marker protein expression

Previous study has revealed that *H. pylori* can induce autophagy or inhibit autophagy, allowing *H. pylori* to multiply (Xie et al., 2020). Till now, we investigated the early stage markers of autophagy (LC3B, ATG5 and Beclin1) and found an induction of autophagy leading to the formation of autophagosomes as a result of *H. pylori* infection. Further, we intended to investigate the expression levels of late stage markers of autophagy. AGS cells were infected with *H. pylori* SS1 (with the same protocol of infection as described before for 4 h) and subjected to western blot analysis to delineate the expression levels of lysosomal-associated membrane protein 1 (LAMP1). LAMP1, a glycoprotein commonly expressed on the lysosomal membrane, is a frequent marker for estimating lysosomal integrity or morphology (Tsugawa et al., 2019). Results showed that the expression of the LAMP1 protein level significantly dropped at 4 h as compared to expression level of LAMP1 in control (**Figure 2.1A, B**).

Concurrently, LAMP1 western data was further verified with confocal microscopy in which *H. pylori* infected and uninfected AGS cells were subjected to live cell imaging using GFP-LAMP1 construct. GFP -LAMP1 allows for precise and focused targeting of cellular lysosomes irrespective of the pH of lysosomes. First, cells grown on glass bottom dishes were infected with *H. pylori* SS1 (with the same protocol of infection as described before) for 4 h followed by addition of GFP-LAMP1 construct overnight and subjected for live cell confocal microscopy analysis the next day. The results suggest that *H. pylori* infection down regulated the expression of LAMP1 as compared to control indicating decrease in the quantity of lysosomes during *H. pylori* infection for 4 h in gastric cells (**Figure 2.1C, D**).

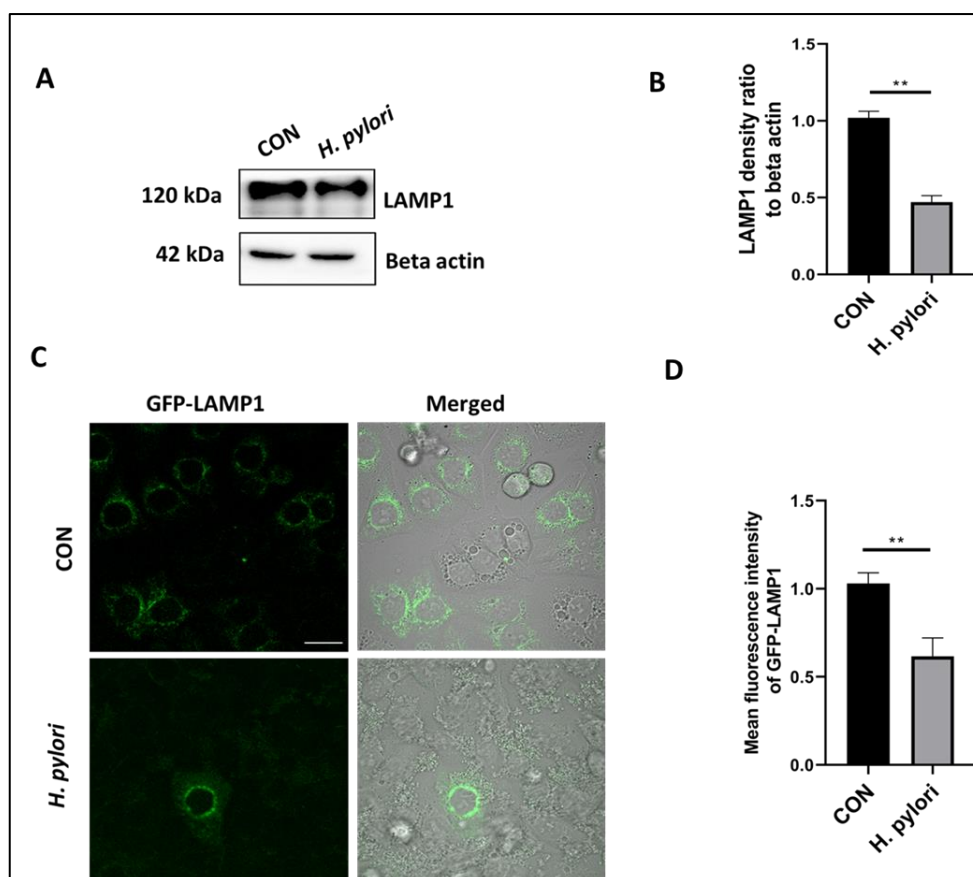


Figure. 2.1 Infection with *H. pylori* for lysosomal protein expression (A-D) Immunoblotting was performed for quantification of lysosomal-associated marker proteins (LAMP1). Beta-actin was used as a loading control. **(B)** Densitometry analyses are represented graphically **(C)** Live cell imaging was performed using a construct, LAMP1-GFP for labeling lysosomes under confocal microscopy. **(D)** Fold change in the mean fluorescence intensity of GFP-LAMP1 was calculated. Scale bar: 10µm. Graphs were represented as mean±SEM (n=3); Unpaired t-test was done and significance was calculated; ** p < 0.01.

2.2 *H. pylori* infection down-regulates autophagic flux

2.2.1 Autophagic flux downregulation

Since the process of autophagy is dynamic, increased expression levels of LC3B (Western blot or confocal analysis) and p62 (Western blot) are indicative of either block in autophagosome- lysosome fusion or disrupted lysosomal degradation. Given this ambiguity in understanding autophagy mechanism during *H. pylori* infection, autophagic flux was assessed. The fusion of the autophagosomes with lysosomes is a key stage of autophagic flux. AGS cells infected with *H. pylori* was followed by the chloroquine (CQ) treatment in both

infected and un-infected cells. CQ is a weak base that can accumulate in lysosomes, where it is protonated and raises the pH. This inhibits the activity of lysosomal enzymes which impairs autophagic flux and inhibits the fusion of autophagosomes with lysosomes, a necessary step in autophagy (Fedele et al., 2020). Result shows that both LC3B-II and p62 accumulates in the presence of CQ than without CQ implying decreased autophagic flux (Figure. 2.3A). However, there was no apparent significant increase in autophagic flux in either *H. pylori*-infected or only control cells as LC3B and p62 accumulation is present in infected cells. Thus, these findings support *H. pylori* infection led to disruption in the autolysosomal degradation function.

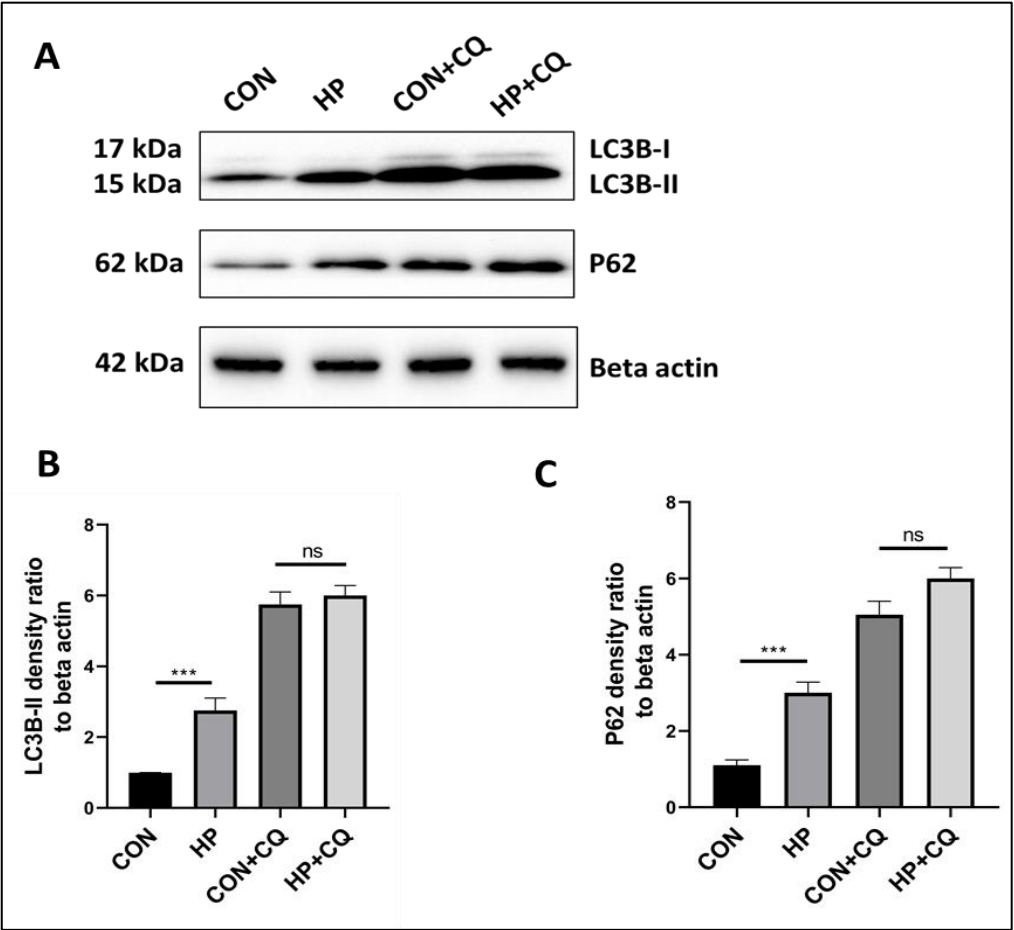


Figure.2.2 Infection with *H. pylori* reduces autophagic flux in AGS cells. (A-C) AGS cells incubated with *H. pylori* for 4 h followed by exposure to chloroquine CQ (50 μ M) and/or bafilomycin BAF (50nM) for 4h. (A) Cell lysates were subjected to western blot to determine P62 and LC3B-II protein levels Beta-actin was used as protein loading control. (B, C) Graphs were represented as mean \pm SEM (n=3); One-way ANOVA was performed and significance was calculated; *** p < 0.001.

2.2.2 Visualization of autophagic flux downregulation using confocal microscopy

Additionally, we visualized the decrease in the autophagic flux by confocal microscopy. Both autophagosomes and autolysosomes were examined by transfecting AGS cells with mRFP-GFP tandem fluorescent-tagged LC3B (tfLC3B) for 48h followed by *H. pylori* infection. GFP but not RFP-LC3B is unstable in acidic environment, gets quenched and loses its fluorescence in autolysosomes (**Figure 2.4A**). Due to the colocalization of GFP and RFP, autophagosomes appeared as yellow dots in *H. pylori*-infected gastric cells. However in rapamycin-treated infected cells, we detected more red intensity dots than green intensity dots as shown in (**Figure 2.4A**) which indicate that both the number of autolysosomes increased. Difference in the number of dots of GFP (green) and RFP (red) in each of control, *H. pylori* infected and rapamycin treated in *H. pylori* infected cells is graphically represented (**Figure 2.4B, C**).

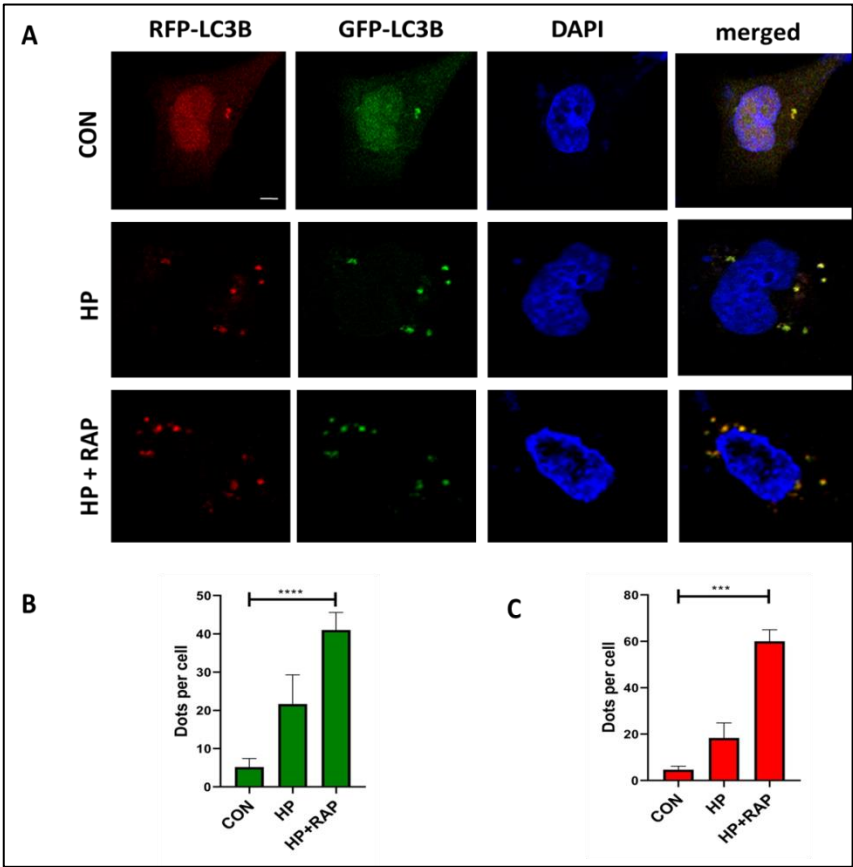


Figure 2.3 *H. pylori* infection lowers autophagic flux in AGS cells. (A) AGS cells were transfected with a tandem mRFP-GFP tag (tfLC3B) plasmid & further infected with *H. pylori* (MOI 100) for 4 h.

Confocal microscopy showed LC3B puncta formation in control (CON), *H. pylori* (HP) infected cells & Rapamycin treatment (500nM) in *H. pylori* cells (HP+RAP). The yellow puncta showed autophagosomes. The free red puncta are autolysosomes. Scale bar: 2µm. **(B)** Graph represents GFP-LC3B (Green) dots expression on autophagosomes only **(C)** Graph represents RFP-LC3B (Red) dots expression on both autophagosomes and autolysosomes. Graph represented as mean±SEM (n=3); Significance was determined by One-way ANOVA; *** $p < 0.001$, **** $p < 0.0001$.

2.3 *H. pylori* survive and replicate in AGS cells

Earlier *H. pylori* was considered as a non-invasive pathogen that adhered to the surface of the stomach epithelium. Mounting evidence suggests that *H. pylori* penetrates into the cells and causes infection (Dubois et al., 2007; Liu et al., 2012). To this end, we investigated that bacteria can invade into the gastric epithelium infected with *H. pylori*. Intracellular *H. pylori* levels were assessed by immunofluorescence labelling, western blotting and CFU assay. Cells were infected with *H. pylori* for 4 h followed by gentamicin treatment to kill extracellular bacteria and further incubated for another 4 h. Bacteria that were not cleared by gentamicin remain localised on the periplasmic membrane for 4 h of infection and then gradually migrated into the cytoplasm as the infection progressed, as shown in **Figure 2.5A**. The numbers of bacteria invading increased, as revealed by anti-*H. pylori* antibody staining (that is red bacterial dots stained with DAPI) showing that the bacteria are proliferating and moving from the membrane into the cytoplasm between 4 and 8 h after infection.

Further, we confirmed the intracellular *H. pylori* levels by CFU assay. Cells were infected with *H. pylori* followed by gentamicin treatment to kill extracellular bacteria and further incubated for 4 h & 8 h infection. AGS cells were lysed and serial dilution was prepared and then 100µL of dilutions were plated on BHIA plates. Colonies were then observed after 3-4 days of culture (CFU/ml). The number of *H. pylori* represents the number of live bacteria inside the cells. As shown in **Figure. 2.5B**, the number of CFU at 4 h shows the amount of *H. pylori* that invades the AGS cells. This number gradually increased from 4 h to 8 h infection. This suggests that the invading *H. pylori* can proliferate intracellularly.

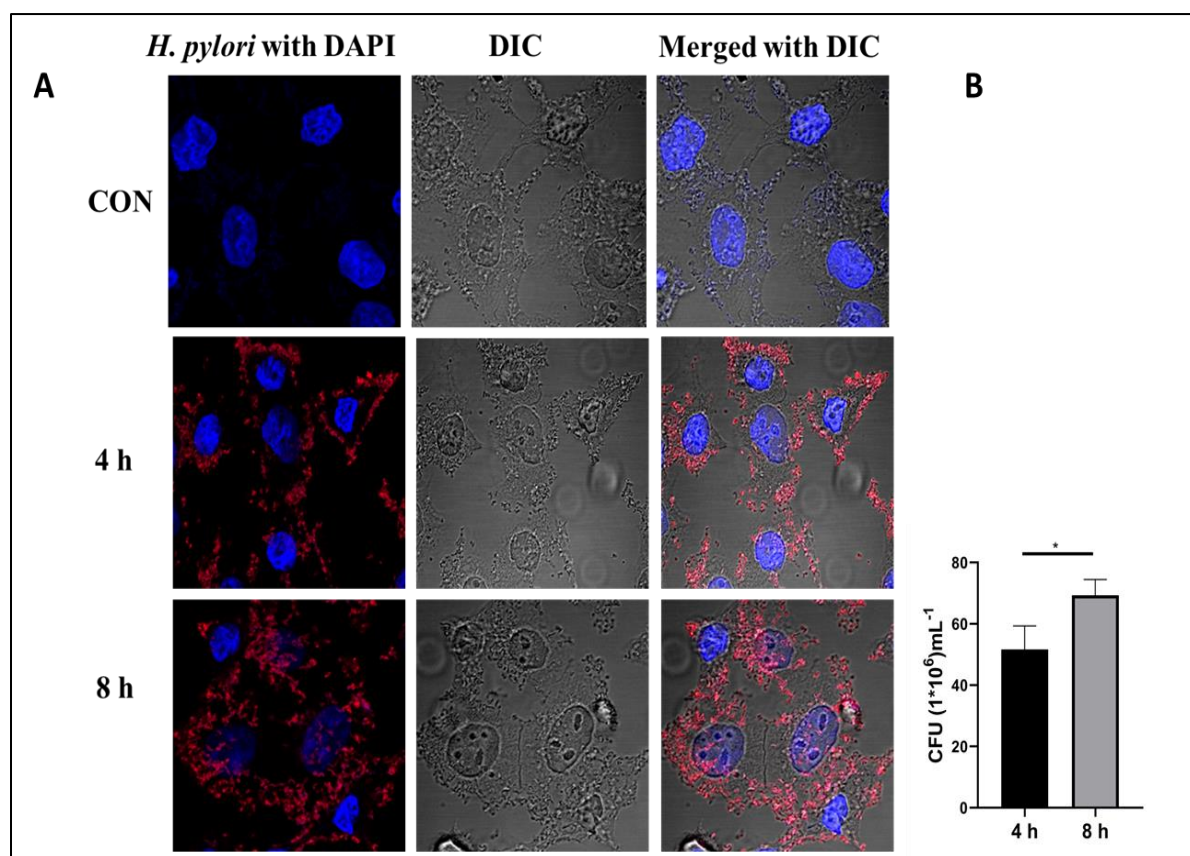


Figure 2.4 *H. pylori* persist and multiply in gastric cells. (A-B) Cells were infected with *H. pylori* SS1 strain (MOI 100) for 4 h followed by gentamicin treatment to kill extracellular bacteria and then incubated in fresh medium for 4h and 8h (A) Immunofluorescent staining of *H. pylori* in AGS cells. The infected cells were collected, fixed, and stained with anti-*H. pylori* antibody (red) and DAPI (blue). The samples were observed with confocal microscopy. (B) Colony forming assay was done in which cells were lysed and plated on BHIA plates with serial dilutions, for 4-5 days to count colony and CFU/ml was graphically represented. Scale bar: 5µm. Graph represented as mean±SEM (n=3); Significance was determined by Unpaired t-test; * p < 0.05.

2.4 *H. pylori* exploits autophagosomes as a survival niche in human stomachs

In order to examine whether engulfed *H. pylori* may survive in autophagosomes, ATG5 (autophagy-related protein 5) gene was specifically knocked down using siRNA ATG5 (Figure 2.6A, B). ATG5 is an indispensable component of the ATG5-ATG12-ATG16L1 complex, required for the autophagic vesicle formation. Autophagy can be inhibited or downregulated when ATG5 is knocked down indicating that ATG5 is essential for autophagy. As expected, results demonstrated an enhanced bacterial clearance effect after

ATG5 was suppressed (**Figure 2.6C**) in line with the previous findings where *H. pylori* was present in double-layered autophagosomes (**Dubois et al., 2007; Liu et al., 2012**). The data corroborates the idea that non- degradative autophagosomes serve as their niche for *H. pylori* growth in order to sustain intracellular infections by lowering autophagic flux.

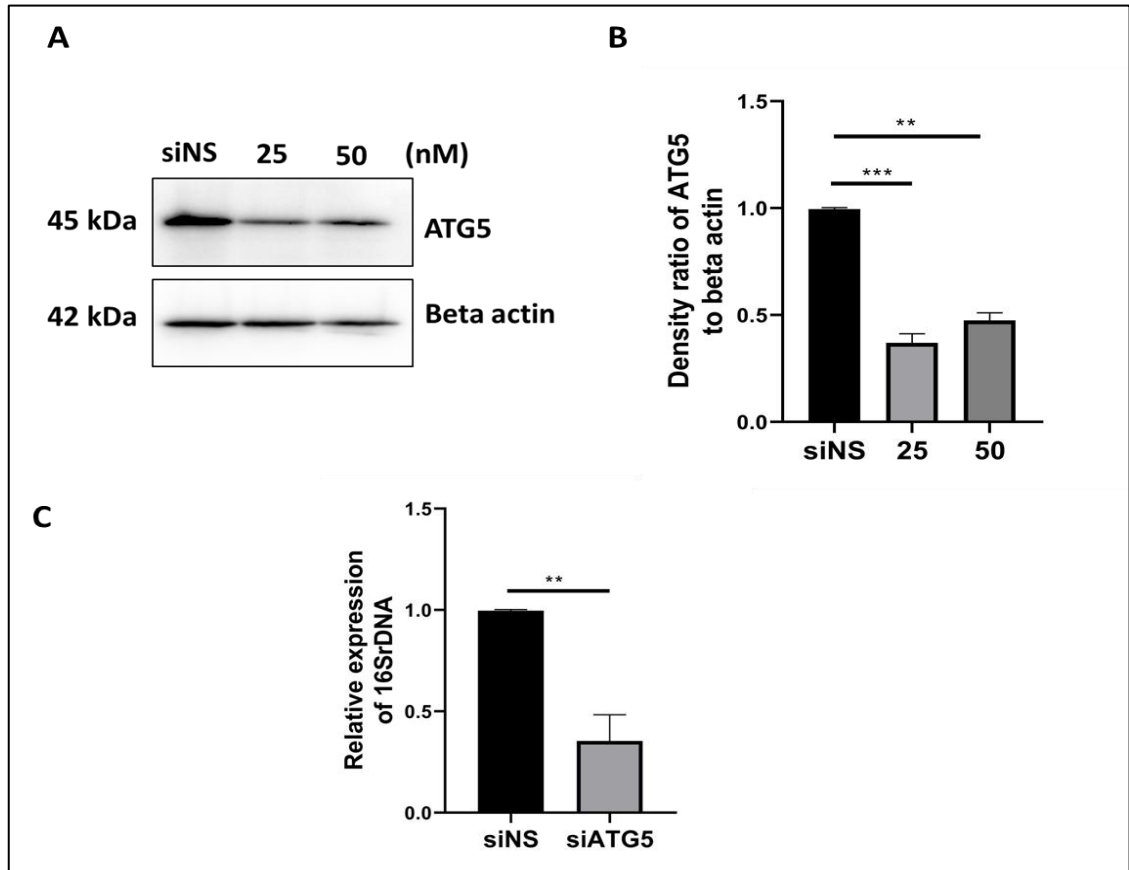


Figure 2.5 *H. pylori* occupy autophagosomes for survival in gastric cells. **(A)** Cells were transfected with non-specific siRNA (siNS) and ATG5 siRNA (siATG5) at two doses 25nM and 50nM for 48h. Immunoblotting was performed for quantification of ATG5 inhibition. Beta-actin was used as a loading control. **(B)** Densitometry graphs are represented. One-way ANOVA was performed **(C)** Cells were transfected with non-specific siRNA (siNS) and ATG5 siRNA (siATG5) & then infected with *H. pylori* SS1 strain for 4h, intracellular *H. pylori* DNA was measured by RT- PCR. GAPDH was kept as an internal control. Graphs were represented as mean±SEM (n=3); Unpaired t-test was performed and significance was calculated; ** p < 0.01, *** p < 0.001.

Conclusion

Our data showed a decrease in the late-stage marker of autophagy and an increase in the accumulation of p62 degradation. This provides clear evidence that *H. pylori* downregulates autophagic flux and employs non-degradative autophagosomes for its intracellular survival and replication within gastric epithelial cells

Chapter 3

**Inhibiting HMGB1 induces autolysosomal degradation function
in gastric cells.**

Background

Helicobacter pylori is a major cause of gastric complications and it is associated with gastric disorders. It is a gram-negative bacterium that has evolved with the ability to colonise and hide in stomach epithelial and immune cells (Khatoon et al., 2016; Li et al., 2017). This is thought to be one of the contributing factors for the rise in *H. pylori* antibiotic resistance (Tshibangu-Kabamba et al., 2021). In response to infection, host cells induce autophagy in order to maintain cellular homeostasis (Yang et al., 2016). However, *H. pylori* in turn, have evolved the ability to modulate the host's autophagic machinery in order to sustain intracellular infection (Li et al., 2017). This dysregulation of autophagy by *H. pylori* intrigued us to explore the role of host proteins that regulate the autophagy pathway. Among them High Mobility Group Box1 (HMGB1) is a critical regulator of autophagy.

HMGB1 is a nuclear non-histone protein that plays a major role in a variety of biological processes depending on its subcellular or extracellular distribution. HMGB1 has also been shown to stimulate pro-autophagic activities in the past (Yin et al., 2017; Tang et al., 2010). In some cancer cells, HMGB1 inhibits autophagy (Feng et al., 2021). It acts as a cytokine & contributes to the development of diseases associated with inflammation, such as cancer (Wang et al., 2020). Evidence suggests that HMGB1 is expressed abnormally in a number of malignancies, including gastric cancer (Lin et al., 2016). However, the role of HMGB1 in autophagy is not explored during *H. pylori* infection in gastric cells. These features make HMGB1 a promising target for identification as a biomarker in gastric disorders.

Considering the scenario of *H. pylori* infection and autophagy impairment, development of novel drugs or repurposing is unavoidable, as antibiotic resistance is well established. In our study, we employed glycyrrhizin (Mollica et al., 2007), an HMGB1 inhibitor, to investigate the role of the autophagy-lysosomal pathway during *H. pylori* infection in both *in vitro* and *in vivo* conditions.

Material and Methods

Western blots were performed to observe autophagic protein expression levels. Autophagosome formation was observed using confocal microscopy and Live-cell imaging was performed to monitor lysosomal integrity. RT-PCR and Colony forming unit (CFU) assay was performed to check intracellular survival of *H. pylori*. Si RNA and Tandem fluorescent-tagged LC3B transfection was performed with lipofectamine 2000. Double immunofluorescence assay was performed to check autophagic activity. Methods were already described in the materials and methods section.

Results

3.1 Glycyrrhizin induces autophagy in gastric adenocarcinoma cells

3.1.1 Induction of autophagic marker protein expression by western blot analysis

First, we wanted to check the effect of glycyrrhizin treatment on HMGB1 expression in our working conditions. We treated AGS cells with glycyrrhizin at different concentrations that is (50, 100, 200µM) for 4 h. Samples were analysed in western blot and we found that expression of HMGB1 is reduced in a dose dependent manner by glycyrrhizin treatment. Further, we tested the expression levels of various autophagy proteins upon glycyrrhizin treatment in AGS cells. Major autophagy marker proteins (such as LC3B-II, and LAMP1) increased (**Figure 3.1A, B**). Expression of LC3B-II and LAMP1 were almost identical at a 50µM glycyrrhizin dosage. Although LC3B-II and LAMP1 increased at a dose of 100µM glycyrrhizin treatment, this rise was not statistically significant. It's interesting to note that as glycyrrhizin concentration was enhanced further, at 200µM dose, both LC3B-II and LAMP1 expression elevated significantly (**Figure 3.1A, B**). Therefore, the dose that worked best was 200µM.

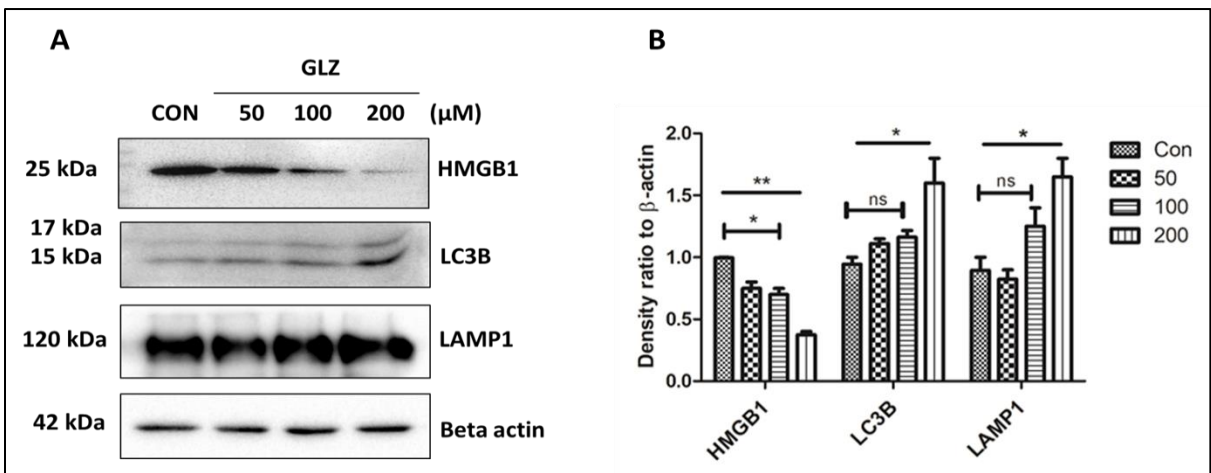


Figure 3.1 Glycyrrhizin treatment at different doses increases the level of autophagy protein. AGS cells were exposed with glycyrrhizin (GLZ) at varying doses (50, 100 & 200µM) or DMSO for 4 h (a) Western blot analysis was used to determine the expression levels of HMGB1 and autophagy marker proteins LC3B and LAMP1. The protein loading control was beta-actin. Densitometry

analyses are graphically represented and significance was calculated; * $p < 0.05$, ** $p < 0.01$, ns= nonsignificant.

3.1.2 Induction of autophagy by confocal microscopy

Subsequently, we used immunofluorescence of LC3IIB to establish that glycyrrhizin-induced autophagy. The formation of LC3IIB puncta was greatly increased after 4h drug treatment (**Figure 3.2A, B**). The impact of glycyrrhizin-induced autophagosomal maturation in gastric cancer cells was next evaluated. Since LAMP1 is a known indicator of lysosomal activity, we tagged lysosomes with the LAMP1-GFP construct following glycyrrhizin treatment. Glycyrrhizin then remarkably increased LAMP1 expression (green) in live cells as compared to control (**Figure 3.2C, D**). All of these findings imply that glycyrrhizin stimulates autophagy in gastric cancer cells.

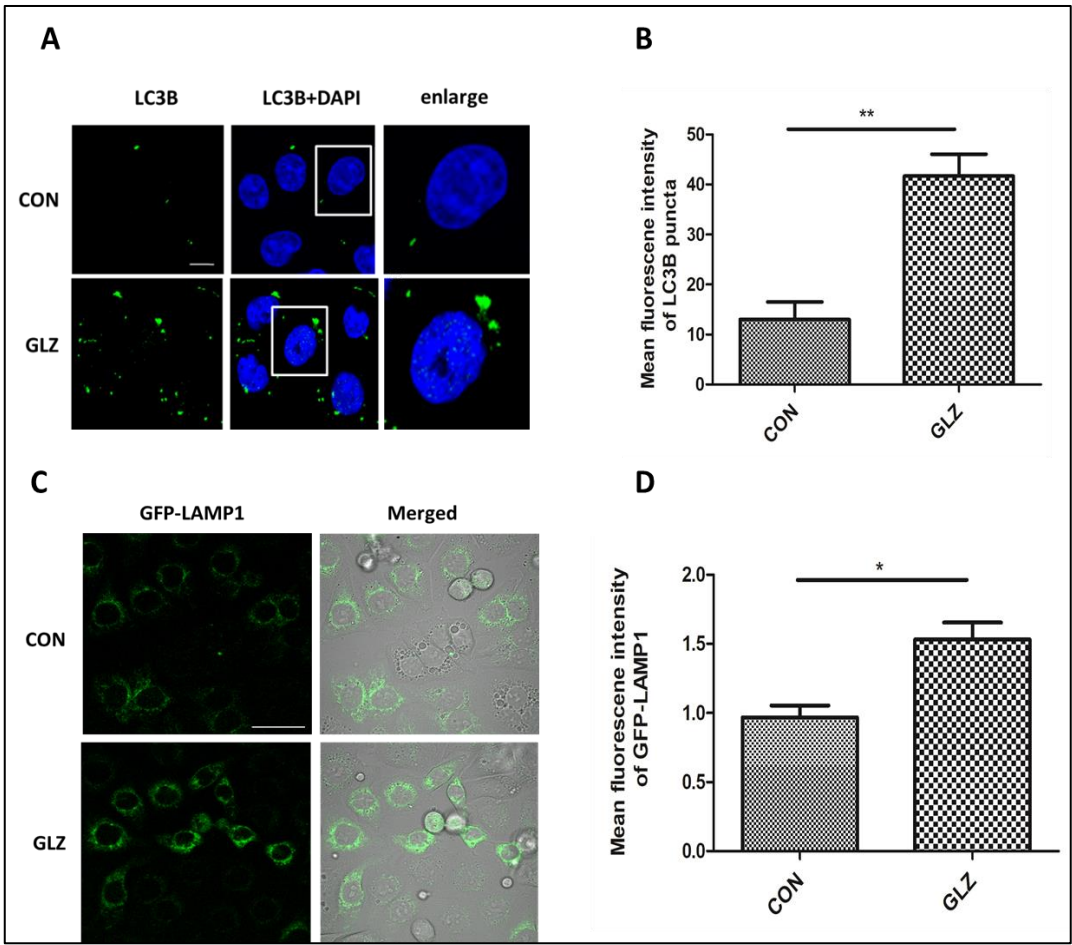


Figure 3.2 Glycyrrhizin treatment augments autophagy proteins in gastric cancer cells. AGS cells were exposed with glycyrrhizin (GLZ) (200 μ M) or DMSO for 4 h (**A, B**) Immunofluorescence was performed on control and drug-treated cells, and changes in mean fluorescence intensity were

calculated. Scale bar: 5µm. Confocal microscopy showed LC3B puncta (green) formation. LC3B puncta formation was quantified and graphically plotted. **(C, D)** Confocal microscopy was used to image live cells using the LAMP1-GFP construct for labelling lysosomes. The mean fluorescence intensity of GFP-LAMP1 was determined as a fold change. Scale bar: 10µm. Graphs were represented as mean±SEM (n=3); Unpaired t-test was done and significance was calculated; * $p < 0.05$, ** $p < 0.01$.

3.2 Activation of autophagy in *H. pylori*-infected gastric adenocarcinoma cells

3.2.1. Induction of autophagic protein expression by western blot analysis

As *H. pylori* is known to invade gastric epithelial cells, we used western blotting to investigate how drug treatment affected the expression of autophagy proteins in *H. pylori*-infected gastric cancer cells. Gastric cells were infected with the *H. pylori* Sydney Strain SS1 for 4 h and post treated with 200µM glycyrrhizin (4 h). We found an overexpression of LC3B-II and LAMP1 upon glycyrrhizin exposure as compared to only infected cells **(Figure3.3A- C)**.

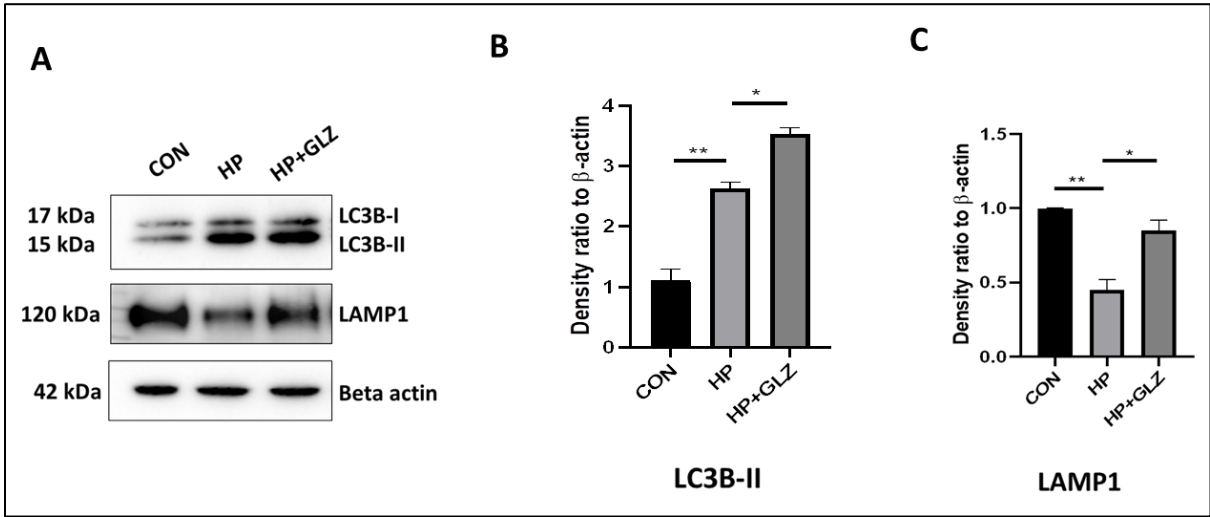


Figure 3.3 Activation of autophagy protein by glycyrrhizin treatment in *H. pylori* infected AGS cells. (A-C) Cells were infected with *H. pylori* SS1 strain (MOI 100) for 4 h and then exposed to glycyrrhizin (GLZ) (200µM). Autophagy-associated marker proteins (LC3B and LAMP1) were quantified by immunoblotting. As a loading control, beta-actin was used. Densitometry analyses are graphically represented. One way ANOVA was used and significance was calculated; * $p < 0.05$, ** $p < 0.01$.

3.2.2. Enhancement of autophagy due to drug treatment

Moreover we carried out immunofluorescence and live-cell imaging experiments of drug-treated *H. pylori*-infected cells to recapitulate the western blot results of LC3B-II and LAMP1 expression. As compared to untreated infected cells, glycyrrhizin treatment consistently resulted in higher LC3B puncta formation and elevated LAMP1 expression (**Figure3.4A-D**). The results demonstrated that glycyrrhizin increases lysosomal and autophagosomal activity in infected cells.

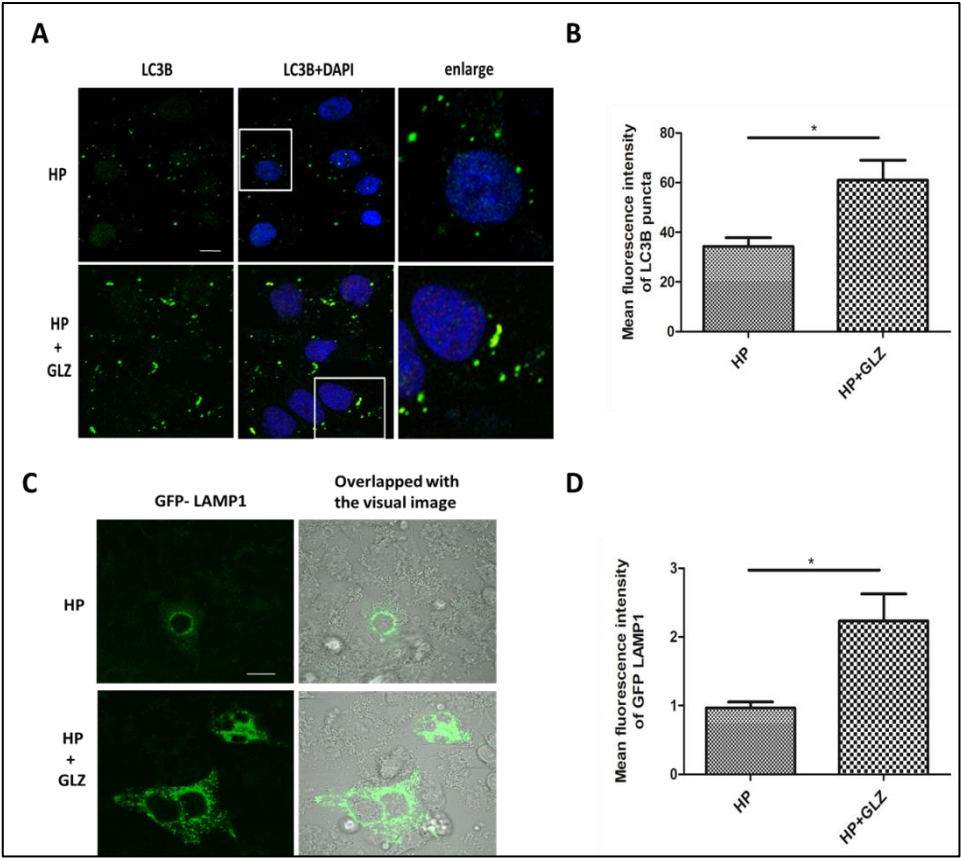


Figure 3.4 Glycyrrhizin treatment increases autophagy in *H. pylori* infected AGS cells. (A-D) Infection with *H. pylori* was performed in cells for 4 h and further exposed to glycyrrhizin (GLZ) (200µM) for 4 h. **(A)** Confocal microscopy showed LC3B puncta (green) in *H. pylori* (HP) infected & *H. pylori*+ glycyrrhizin (HP+GLZ) treated cells. After immunofluorescence, LC3B puncta formation was quantified and **(B)** graphically plotted. Scale bar: 5µm. **(C)** Live cell imaging of LAMP1 under confocal microscopy showed GFP-LAMP1 puncta formation and **(D)** graphically represented. Scale bar: 10µm. Unpaired t-test was performed and significance was calculated; * p < 0.05.

3.3 Glycyrrhizin stimulates autophagy flux in *H. pylori*-infected gastric adenocarcinoma cells

3.3.1. Regulation of autophagic flux by glycyrrhizin

SQSTM1/p62 is one of the primary targets of autophagic flux. As a result, we measured the expression of p62, a crucial protein involved in autophagy. Western blotting revealed that *H. pylori* infection increases p62 at 4h (**Figure 3.5**). This is because autolysosomal degradation is impaired. Glycyrrhizin, on the other hand, causes p62 degradation at 4h.

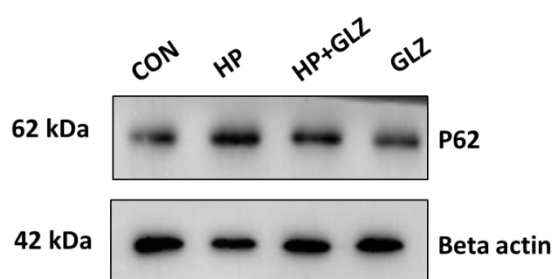


Figure 3.5 Activation of autophagy proteins by glycyrrhizin treatment in *H. pylori* infected AGS cells. Cells were infected with *H. pylori* SS1 strain (MOI 100) for 4 h and then exposed to glycyrrhizin (GLZ) (200μM). Cell lysates were subjected to western blot for examining P62 protein levels and as a loading control, beta-actin was used.

3.3.2. Visualization of fusion of autophagosomes and lysosomes using immunofluorescence

Since *H. pylori* infection contributes to impaired autophagy, we investigated the effect of glycyrrhizin on autophagic flux. We conducted a double immunofluorescence experiment for the proteins LC3B and LAMP1 in order to evaluate the stimulation of autophagic flux by glycyrrhizin. Results showed that both LC3B and LAMP1 puncta colocalized in glycyrrhizin-treated infected and only *H. pylori*-infected cells (**Figure 3.6A**). However, increase in the colocalization coefficient of the glycyrrhizin-treated cells indicated that glycyrrhizin-induced autophagosomal lysosomal maturation.

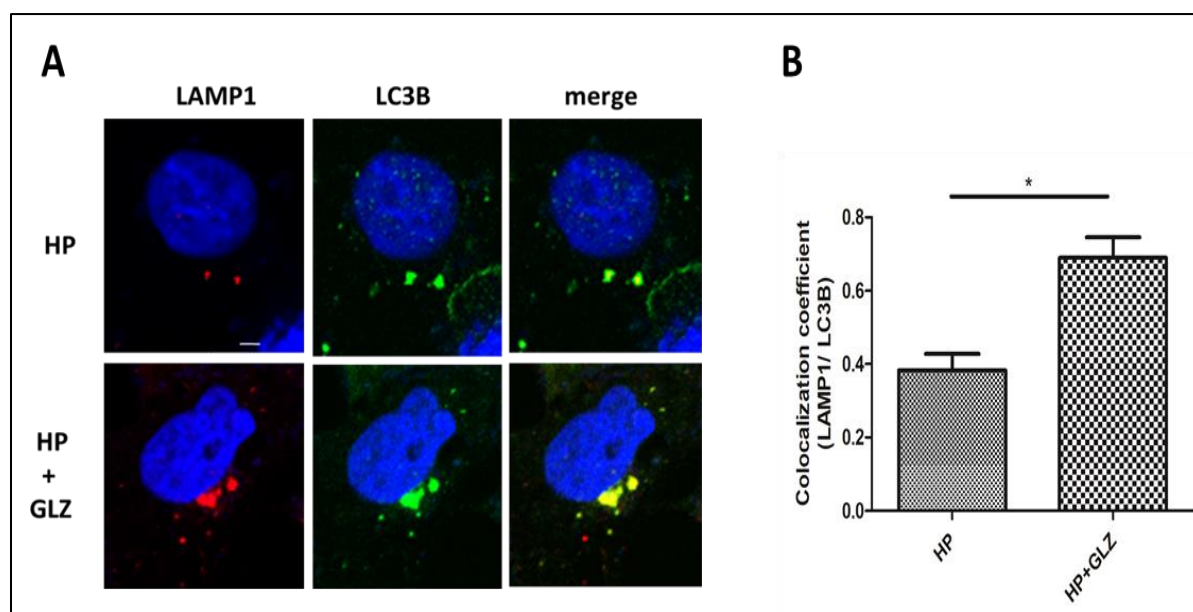


Figure 3.6 Glycyrrhizin induces autophagy flux in *H. pylori*-infected AGS cells (A-B) Double immunofluorescence for LAMP1 and LC3B was performed after GLZ (glycyrrhizin) exposure to *H. pylori*-infected cells for 4 h. Confocal microscopy revealed that LAMP1 (red) and LC3B (green) puncta colocalized to form yellow puncta. Change in the co-localization coefficient of each group was calculated. Scale bar: 2 μ m. Graph represented as mean \pm SEM (n=3); Significance was determined by Unpaired t-test; * p < 0.05.

3.3.3. Visualization of the formation of autophagosomes and autolysosomes

Next, to assess the amount of accumulated autolysosomes and autophagosomes by glycyrrhizin-treatment, we transfected the AGS cells with tandem fluorescent LC3B (tfLC3B) plasmid. Tandem fluorescent-tagged LC3B (mRFP-EGFP-LC3) is a simple technique for detecting autophagic flux that takes use of the differing pH stability of eGFP and mRFP fluorescent proteins. Autophagosomes appeared as yellow dots due to colocalization of both eGFP and mRFP. This has been observed in *H. pylori*-infected gastric cells whereas in glycyrrhizin-treated infected cells we observed more free red dots as GFP and RFP did not colocalize. Autolysosomes appears red due to the acidic pH of lysosomes which quench GFP (**Figure 7A, B**). All together, these results revealed that glycyrrhizin prevents *H. pylori*-mediated inhibition of autolysosome formation in the infected cells and thereby promotes autolysosomal maturation.

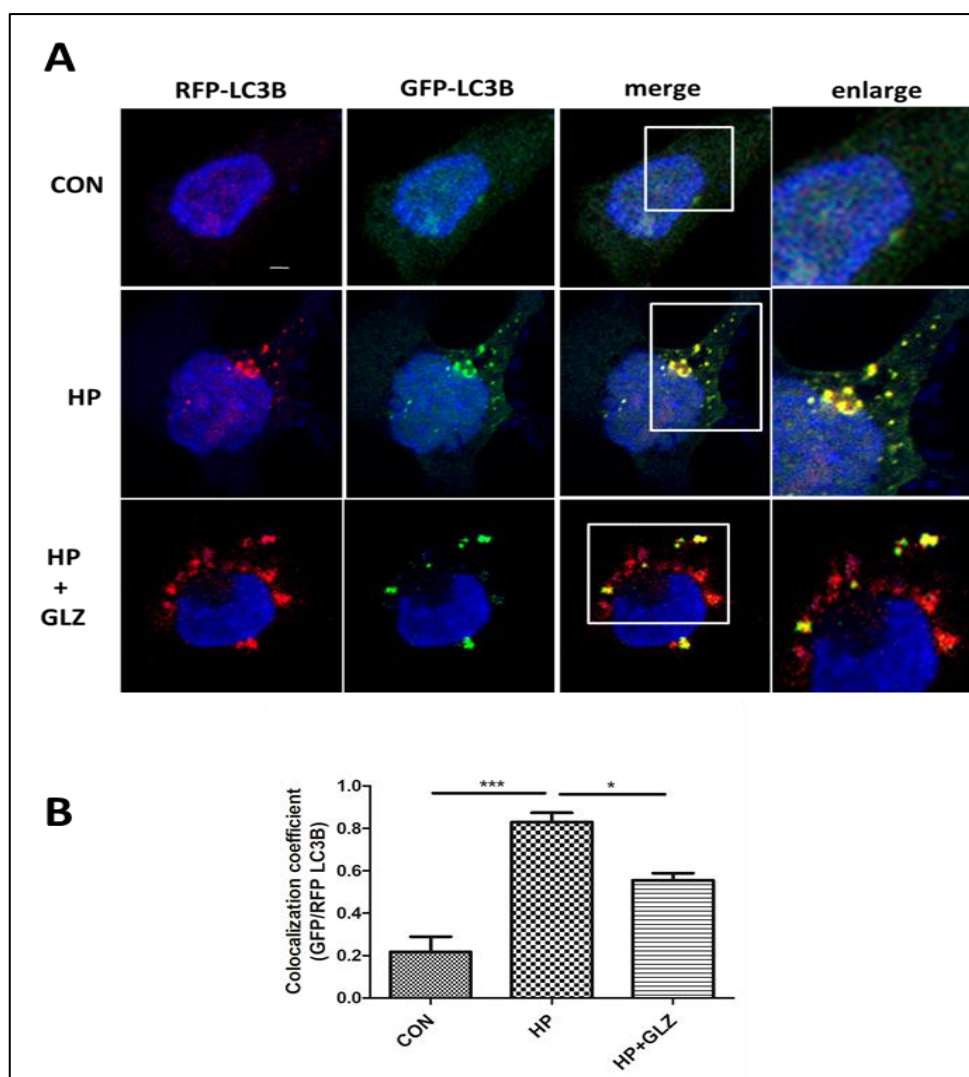


Figure 3.7 Confocal microscopy analysis of the formation of autophagosomes and autolysosomes (A) AGS cells were transfected with a tandem mRFP-GFP tag (tfLC3B) plasmid and then infected with *H. pylori* SS1 strain (MOI 100) for 4h and finally glycyrrhizin (GLZ) (200 μ M) treatment was done. Confocal imaging revealed the development of LC3B puncta in control, *H. pylori* and *H. pylori* + glycyrrhizin treated cells. Autophagosomes were visible in the yellow puncta. The free red puncta are autolysosomes. (B) Change in the co-localization coefficient of each group was calculated and graphically represented. Scale bar: 2 μ m. Significance was determined by one way ANOVA and significance was calculated; * $p < 0.05$, *** $p < 0.001$.

3.4 Anti- *H. pylori* action of glycyrrhizin by induced Autophagy

3.4.1 Determining the effect of glycyrrhizin on intracellular *H. pylori*

Till now, we investigated that glycyrrhizin induces autophagy in both the uninfected and infected AGS cells. Next, we looked at how autophagy induction affected intracellular bacterial proliferation. Intracellular *H. pylori* levels were assessed by RT-PCR and CFU

assay. Cells were first infected for 4 h with *H. pylori*, then treated with gentamicin, and then incubated for further 4 h with glycyrrhizin and an additional set of experiment was performed with 18 h drug treatment. We tested 16SrDNA that is unique to *H. pylori* using real-time PCR (RT-PCR). The glycyrrhizin treatment for 4 h and 18 h decreased intracellular *H. pylori* at a significant level (**Figure 3.8A**). We also conducted an interesting bacterial adhesion assay to investigate bacterial proliferation. In line with this, drug administration for 4 h and 18 h resulted in a considerable reduction in intracellular *H. pylori* burden (**Figure 3.8B**).

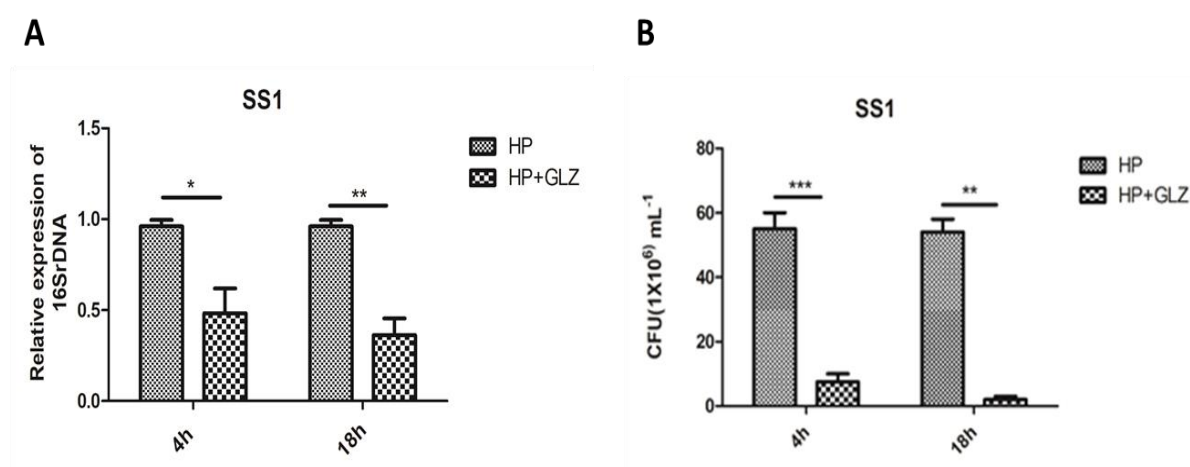


Figure 3.8 Glycyrrhizin inhibits intracellular *H. pylori* burden in AGS cells. (A, B) Cells were cultured with *H. pylori* SS1 strain (MOI 100) for 4 h followed by gentamicin treatment to kill extracellular bacteria. Finally, cells were exposed to glycyrrhizin GLZ (200 μ M) for 4 h and 18 h. (A) Real-time PCR was used to analyse the intracellular *H. pylori* DNA (16SrDNA). The internal control was GAPDH. (B) Cells were lysed, serially diluted and plated on BHIA plates for 4-5 days in order to count colonies. CFU/ml was then graphically displayed. Graph were represented as mean \pm SEM (n=3); Unpaired t-test was done and significance was calculated; * $p < 0.05$, ** $p < 0.01$, *** $p < 0.001$.

3.4.2 Determining the effect of glycyrrhizin on a resistant strain of *H. pylori* [OT-14 (3)]

Since the problem of *H. pylori* gaining antibiotic resistance is a major concern, we infected a resistant clinical strain of *H. pylori* [OT-14 (3)] in AGS cells for 4 h followed by glycyrrhizin treatment. In drug treated condition, multiplication of *H. pylori* reduced significantly (**Figure 3.9**).

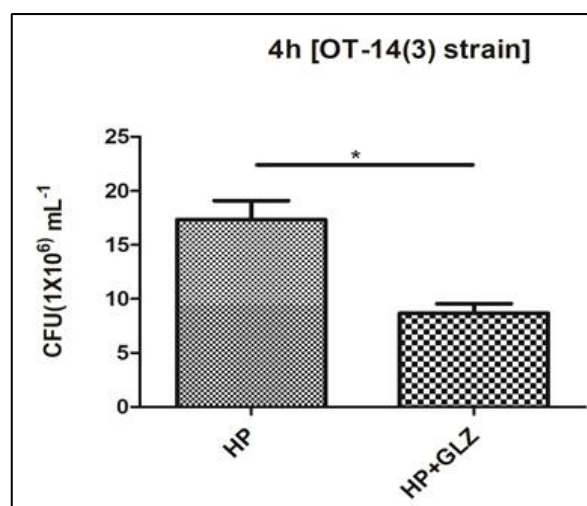


Figure 3.9 Glycyrrhizin inhibits intracellular *H. pylori* burden in AGS cells. Cells were cultured with *H. pylori* [OT-14 (3)] strain (MOI 100) for 4 h followed by gentamicin treatment to kill extracellular bacteria. Finally, cells were exposed to glycyrrhizin GLZ (200μM) for 4 h and 18 h. Cells were lysed, serially diluted and plated on BHIA plates for 4-5 days in order to count colonies. CFU/ml was then graphically displayed. Graph were represented as mean±SEM (n=3); Unpaired t-test was done and significance was calculated; * $p < 0.05$.

3.5 Activation of autophagy pathway by glycyrrhizin is mediated through HMGB1 suppression

To examine the possible involvement of HMGB1 in *H. pylori* infection, AGS cells were transiently transfected with both non-specific siRNA and HMGB1-specific siRNA. Subsequently, these transfected cells were infected with *H. pylori* for 4 hours and then subjected to immunoblotting analysis. Western blot analysis demonstrated effective silencing of HMGB1 in AGS cells 48 hours post-transfection (**Figure 3.10A**). Subsequently, HMGB1 knockdown led to a significant increase in the levels of LAMP1 and LC3IIB, as shown in **Figure 3.10B, C, D**. Additionally, we assessed the intracellular *H. pylori* load through RT-PCR and observed a substantial reduction in intracellular *H. pylori* burden following HMGB1 silencing (**Figure 3.10E**).

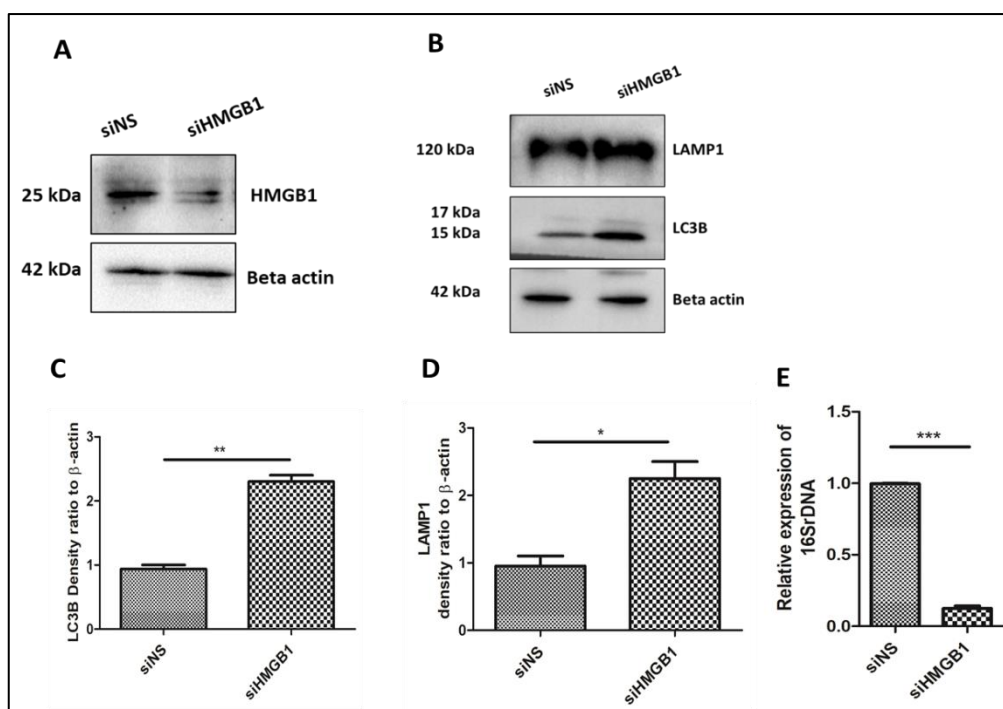


Figure 3.10 Inhibition of HMGB1 induces autophagy and suppresses bacterial growth (A-E) Cells were transfected for 48 h with non-specific siRNA (siNS) and HMGB1 siRNA, (A) Immunoblotting was conducted to quantify the extent of HMGB1 inhibition. (B) Afterwards, the cells were subjected to infection with the *H. pylori* (MOI of 100) for 4 h. Immunoblotting was conducted to assess the expression levels of LAMP1 (C) and LC3B (D). To ensure protein quantification, beta-actin was used as a loading control, and the results were visualized through graphical representation using densitometry analyses. (E) The quantification of intracellular *H. pylori* DNA (16S rDNA) was done using RT-PCR. GAPDH was employed as the internal control for normalization. Unpaired t-test was performed and significance was calculated; * $p < 0.05$, ** $p < 0.01$, *** $p < 0.001$.

3.6 Effect of glycyrrhizin on autophagic induction while using lysosomal inhibitors

In order to confirm the impact of glycyrrhizin on autophagic flux, we used chloroquine (CQ), a lysosomal inhibitor, and bafilomycin (BAF a vacuolar ATPase (V-ATPase) inhibitor that impairs autophagic flux by V-ATPase-dependent acidification and prevent autophagosome-lysosome fusion (Fedele et al., 2020). AGS cells infected with *H. pylori* was followed by the treatment of BAF and/or CQ in both infected and un-infected cells and glycyrrhizin in infected cells only. We assessed the level of SQSTM1/p62, a pivotal protein in the

autophagic process. Western blot analysis revealed an increase in p62 levels upon *H. pylori* infection at both the 4 h (**Figure 3.11A**) and 18 h (**Figure 3.11B**) time points. Prolonged exposure to *H. pylori* resulted in the accumulation of p62, indicative of impaired autolysosomal degradation. In contrast, glycyrrhizin treatment induced p62 degradation at both 4 h and 18 h (**Figure 3.11A, B**).

After administration of CQ and BAF, p62 accumulates in *H. pylori*-infected and uninfected cells treated with glycyrrhizin (**Figure 3.11A, B**). We also investigated how CQ affected glycyrrhizin-mediated *H. pylori* clearance. As expected CQ treatment to *H. pylori*-infected cells facilitates propagation of bacteria (**Figure 3.11C**). On the other hand, glycyrrhizin exposure diminishes the effect of CQ and decreases the *H. pylori* burden (**Figure 3.11C**), but it is not as significant as only glycyrrhizin in infected cells.

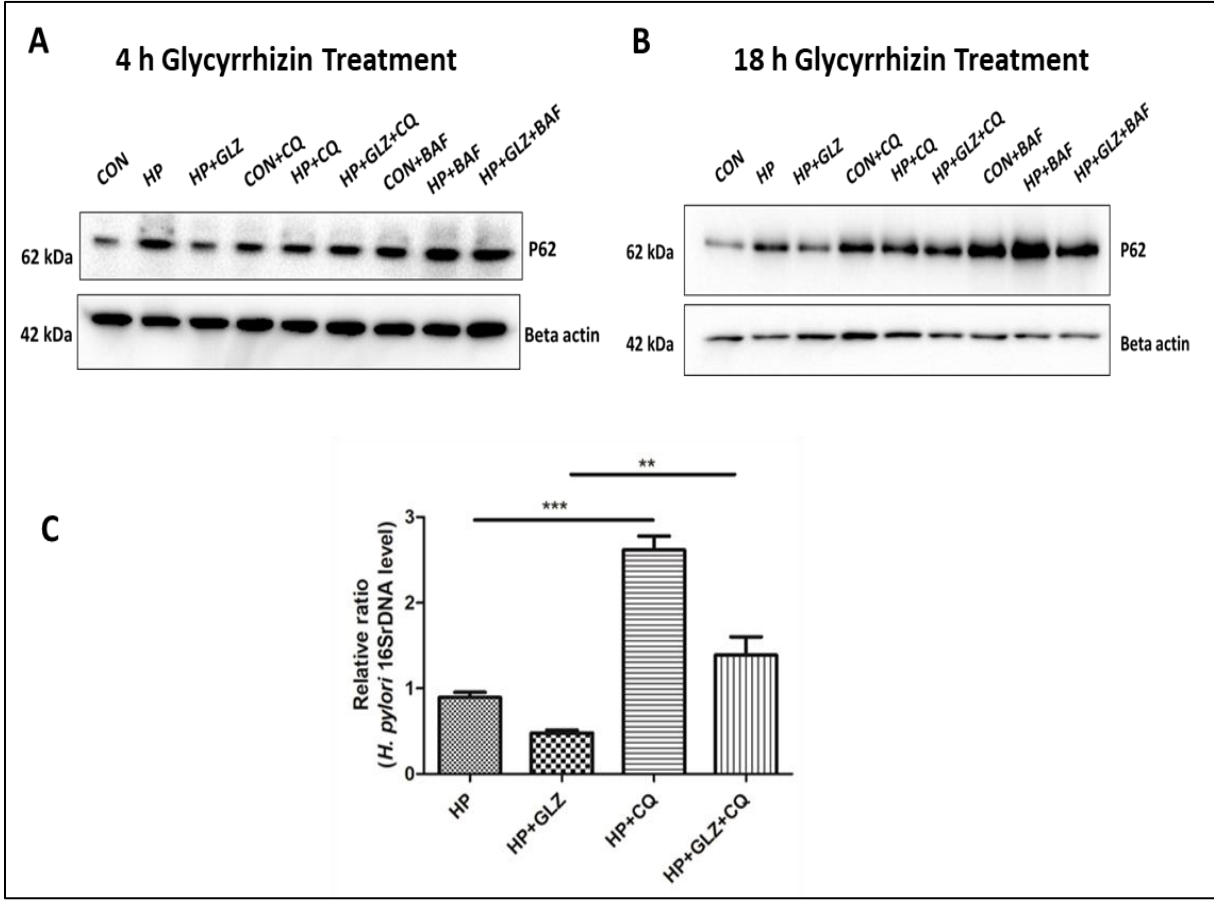


Figure 3.11 Glycyrrhizin's effect on autophagy while using lysosomal inhibitors. (A-B) AGS cells infected with *H. pylori* SS1 strain for 4h followed by exposure to glycyrrhizin GLZ (200μM) and/or

chloroquine CQ (50 μ M) and/or bafilomycin BAF (50nM)/ or untreated for 4h and 18h treatment respectively. Cell lysates were subjected to western blot for determining P62 protein levels for 4h (A) and (B) 18h. Beta-actin was used as a protein loading control. (C) AGS cells were incubated with the *H. pylori* SS1 strain for 4h followed by exposure to glycyrrhizin GLZ (200 μ M) and/or chloroquine CQ (50 μ M) for 4h. Intracellular *H. pylori* DNA (16SrDNA) was measured by RT- PCR. GAPDH was used as the internal control. One-way ANOVA was done and significance was calculated; ** $p < 0.01$, *** $p < 0.001$.

3.7 Analysis of the effects of different doses of glycyrrhizin on AGS cell viability

To analyze whether exposure of glycyrrhizin is toxic or affects the viability of AGS cells, glycyrrhizin was treated for 24 h at varying doses (50, 100 and 200 μ M) and subjected to MTT (3-4,5-dimethylthiazol-2,5-diphenyltetrazolium bromide) assay. The results showed that the treatment of glycyrrhizin did not result in any significant toxicity at various doses (50, 100, and 200 μ M) for 24 h (Figure 3.12).

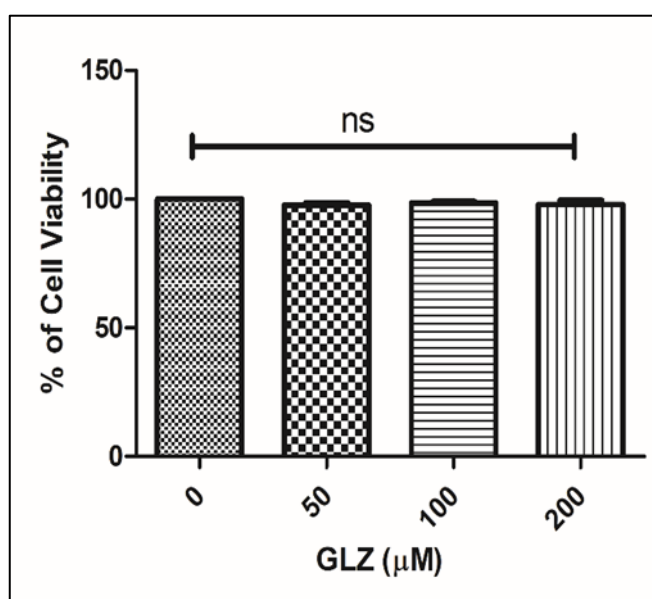


Figure 3.12 Cellular toxicity by glycyrrhizin treatment. (A) AGS cells were treated for 24 hours with glycyrrhizin (50-200 μ M) or DMSO. MTT assay was used to determine the viability percentage. Densitometric analyses are depicted graphically. GraphPad Prism 5 graphs were expressed as meanSEM (n=3); one-way ANOVA was done, and significance level was assessed, ns=nonsignificant.

3.8 Analysis of glycyrrhizin on *Helicobacter pylori* viability

To investigate whether 200 μ M dosage of glycyrrhizin have any direct bactericidal effect on bacteria, serial wise diluted suspension of *H. pylori* were spotted on BHIA medium containing glycyrrhizin of 200 μ M concentration along with control, where no glycyrrhizin was added. After 3-4 days of incubation period in the microaerophilic condition, no change in the number of bacterial colonies was observed as compared to control. The data suggest that glycyrrhizin was unable to inhibit the growth of *H. pylori* in BHIA (brain heart infusion agar) media, indicating that 200 μ M concentration has no bactericidal impact on the growth of *H. pylori* (Figure 3.13).

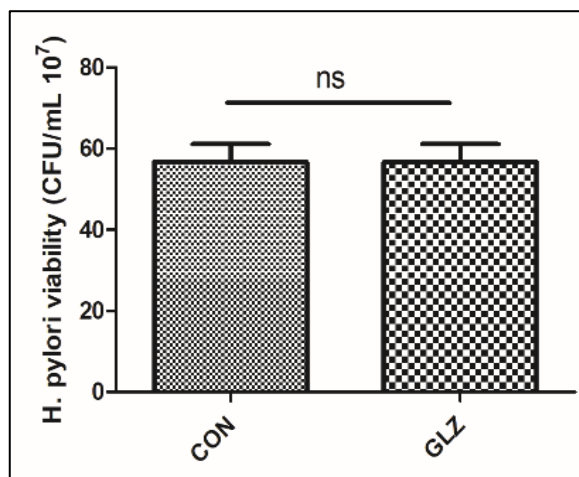


Figure 3.13 Standard agar dilution methods for determination of *Helicobacter pylori* viability. Briefly, serially diluted bacterial suspension of OD at 600nm 0.1 was spotted on BHIA medium containing glycyrrhizin of 200 μ M concentration along with control where no glycyrrhizin was added and incubated them in the microaerophilic condition for 3-4 days. *H. pylori* viability was determined by counting the number of bacterial colonies (CFU/mL) in the BHIA medium. Graphs generated using GraphPad Prism 5 were represented as mean \pm SEM (n=3); Unpaired t-test was performed and significance was calculated, ns=nonsignificant.

3.9 Determination of MIC of glycyrrhizin in BHIA plate

Minimum inhibitory concentrations (MICs) refer to the lowest concentration of compounds that can effectively inhibit the visible growth of a specific microorganism. MICs are primarily determined using the micro-dilution method, serving as a crucial tool to assess

bacterial resistance to drugs. MIC of glycyrrhizin was determined using standard agar dilution method according to protocol described by (De et al, 2018). Briefly, serially diluted bacterial suspension of OD at 600nm 0.1 were spotted on BHIA medium containing different concentration of glycyrrhizin (1, 2, 3, 4, and 5 mg/ml) along with control where no glycyrrhizin is added and incubated them in the microaerophilic conditions for 3-4 days.

Two standard strains of *H. pylori* (SS1 & 26695) and two highly antibiotic resistant strains (OT-14(3) & A88C1) were assessed for determining MIC and represented in tabular form (Figure 3.13).

Strain name	MIC (mg/ml)
SS1	3
26695	4
OT-14(3)	2
A88C1	2

Figure 3.14 Determination of MIC of glycyrrhizin. Microdilution assay was performed in BHIA plate using glycyrrhizin at varying concentrations against different strains of *H. pylori*. MICs were observed and represented.

Conclusion

Cumulatively, these data suggest that the inhibition of HMGB1 by using the inhibitor glycyrrhizin results in an increase in the late-stage markers of autophagy and the degradation of p62. This, in turn, effectively reduces intracellular *H. pylori* growth, even in the case of antibiotic-resistant strains. The overall effect is the promotion of the autophagy-lysosomal pathway within gastric epithelial cells.

OBJECTIVE II.

Chapter 4

Unraveling the mechanism to interlink autophagic targets with inflammation during *H. pylori* infection

Background

Autophagy activation is a crucial mechanism that destroys damaged organelles, misfolded proteins or invading pathogens and maintains cellular homeostasis (**Mizushima et al., 2007**).

Autophagy triggers the formation of a double-membrane autophagosome which further fuses with the lysosome to form autolysosome, and the cargo is destroyed by lysosomal acid hydrolases in autolysosome (**Malicdan et al., 2007**). As a result, autophagy inactivation occurs when the process is disrupted at any stage. One of the main causes of autophagy inactivation is lysosomal dysfunction, which results in the aggregation of proteins, including autophagy substrates leading to cellular toxicity (**Yim et al., 2020; Yu et al., 2013**).

Evasion of the host cell's autophagy by *H. pylori* has been a longstanding puzzle, but a recent study proposed that *H. pylori* virulence factor gamma-glutamyltranspeptidase (HpGGT) inhibited the late stages of autophagy by preventing its degradation in lysosomes (**Bravo et al., 2019**). This results in the accumulation of autophagosomes which can overburden the lysosomal degradation capacity. As a consequence, lysosomes are compromised, the lysosomal membranes are weakened and rupture along with lysosomal membrane permeabilization. Moreover, this lysosomal disturbance is also associated with inflammation often stimulated by HMGB1 activation (**Yuan et al. 2020**). HMGB1 acts as a pro-inflammatory cytokine when released from cells during injury or inflammation and the excessive levels of extracellular HMGB1 can also promote inflammation (**Cheng et al., 2014**). This inflammation in turn, inhibits autophagy and disrupts cellular homeostasis.

A recent report showed that HMGB1 activation causes lysosomal membrane permeabilisation (LMP) in diabetic retinopathy (**Feng et al., 2021**). Therefore, in line of both the findings of **Bravo** and **Feng**, we can recapitulate that *H. pylori* infection induces HMGB1 activation, that in turn causes inflammation, lysosomal dysfunction, and ultimately LMP (**Bravo et al., 2019 & Feng et al., 2021**). There is currently no specific treatment for lysosomal dysfunction. We

then questioned that whether inhibiting HMGB1 expression could reduce the lysosomal dysfunction and inhibit inflammation. In this context, for the first time we treated *H. pylori* infected cells with glycyrrhizin and elucidated the mechanism behind reducing HMGB1 inactivation and recovery from lysosomal dysfunction / LMP.

Materials and methods

Confocal microscopy and Live-cell imaging were performed to monitor lysosomal integrity. Double immunofluorescence assay and Confocal microscopy were done to monitor lysosomal membrane permeabilization (LMP). RT-PCR and Colony forming unit (CFU) assay were performed to check intracellular survival of *H. pylori*. Intracellular ROS levels were monitored by using 2,7-dichlorodihydrofluorescein diacetate (DCFDA). Pro-inflammatory cytokine (IL-8) levels from media were estimated using Enzyme-linked immunosorbent assay (ELISA). NF- κ B transcription factor assay was performed using NF- κ B transcription factor assay kit. Methods are already described in the materials and methods section.

Results

4.1. Glycyrrhizin restores lysosomal pH during *H. pylori*-infection

4.1.1. Evaluation of Lysosomal pH using Acridine orange

Acidic vesicles can be detected and imaged in cells using fluorescent proteins or fluorescently tagged probes. Acridine orange has long been used as a convenient tracer of acidic vesicles. Acridine orange labelling is used to monitor the acidic compartment of lysosomes in AGS cells. Reduced red signal intensity was observed in *H. pylori*-infected cells indicating impaired lysosomal acidification whereas glycyrrhizin treatment boosted red intensity by restoring lysosomal acidification (**Figure 4.1**).

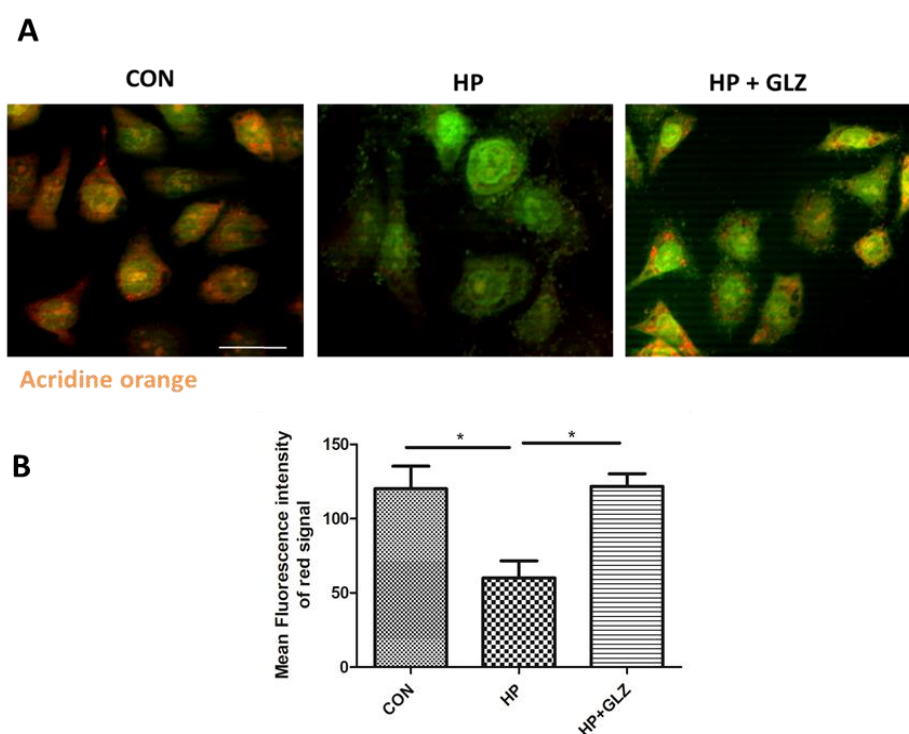


Figure 4.1 Glycyrrhizin restores lysosomal function using Acridine orange. (A-B) Infection with *H. pylori* SS1 strain (MOI 100) was performed for 4h followed by glycyrrhizin (GLZ) (200 μ M) exposure for another 4h. **(A)** Lysosomal membrane integrity was monitored by Acridine Orange (AO) staining in a fluorescence microscope. Briefly, cells were incubated with 10 μ g/ml of acridine orange (15 min) and examined. The mean fluorescence intensity of the red signal was determined and graphically represented. Scale bar: 10 μ m. **(B)** Fold change was quantified and graph is generated using GraphPad Prism 5 and represented as mean \pm SEM (n=3); Significance was calculated by one-way ANOVA; * p < 0.05.

4.1.2. Evaluation of Lysosomal pH using LysoTracker Red (LTR)

Additionally, we exposed the cells to LysoTracker Red (LTR), which selectively binds to vesicles with low pH, in order to assess lysosomal acidification. Cells are first grown on glass bottom dishes and then infected with *H. pylori* SS1 (with the same protocol of infection as described before) for 4 h followed by drug administration. After glycyrrhizin treatment, LTR was added for 30 min and subjected to live cell confocal microscopy analysis. Lysosomal pH of *H. pylori* infection was affected as fluorescent signals diminished which is evident by mean fluorescence intensity in comparison to the control. However, compared to only *H. pylori*-infected cells, glycyrrhizin treatment restored the acidic pH and red signals appeared in infected cells (**Figure 4.2**).

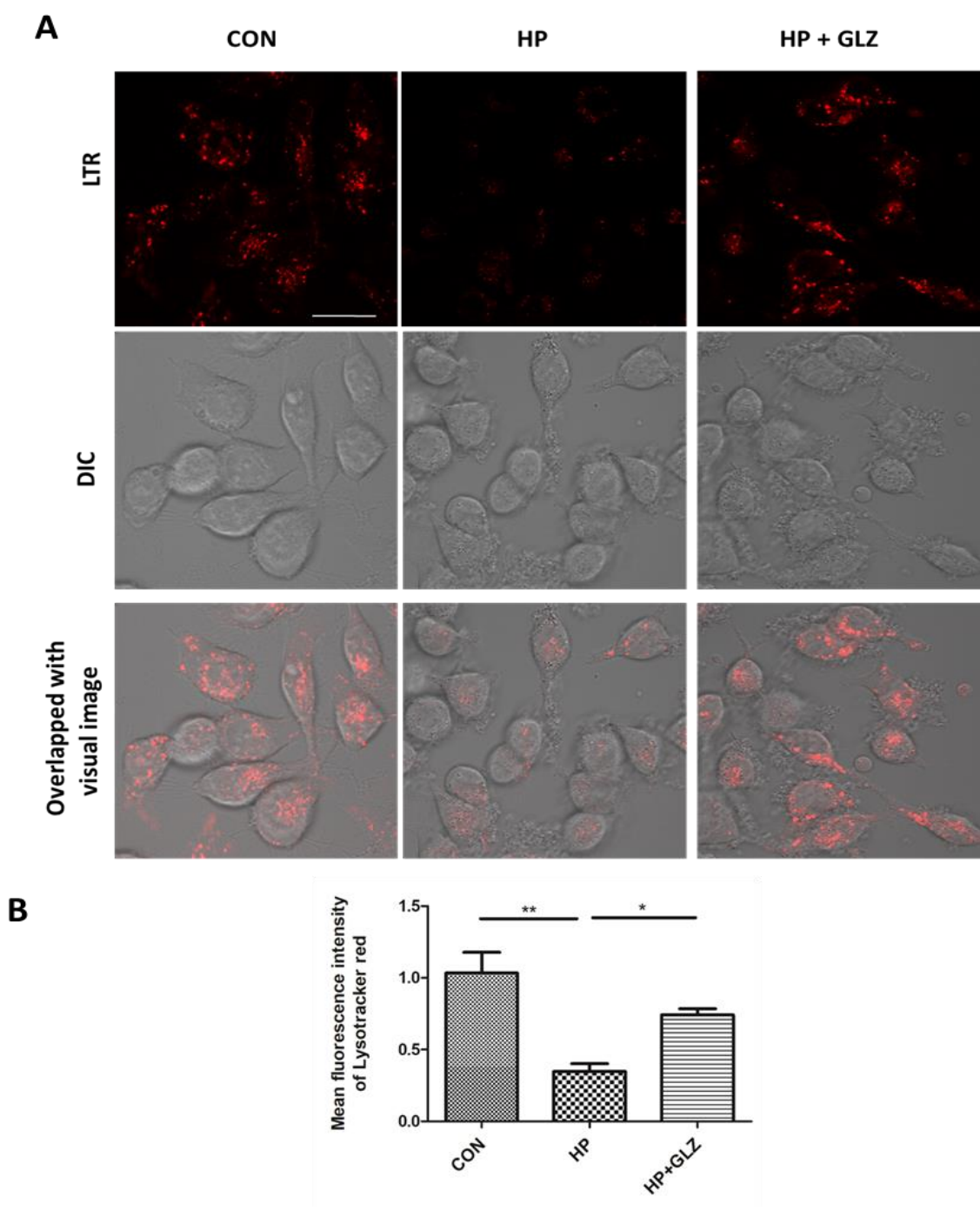


Figure 4.2 Lysosomal function is restored by glycyrrhizin. (A-B) Infection with *H. pylori* SS1 strain (MOI 100) was performed for 4h followed by glycyrrhizin (GLZ) (200 μ M) exposure for 4h. (A) Live cell imaging of drug-treated, infected and control cells was done with LysoTracker Red incubation (100 nM, 30 min) to label lysosomes and mean fluorescence intensity was assessed under the confocal microscope. Scale bar: 10 μ m. (B) Fold change was quantified and graphs were generated using GraphPad Prism 5 and represented as mean \pm SEM (n=3); Significance was calculated by one-way ANOVA; * $p < 0.05$, ** $p < 0.01$.

4.2 Glycyrrhizin promotes lysosomal degradation function by reducing lysosomal membrane permeabilization (LMP)

4.2.1 Determination of LMP using double immunofluorescence (Galectin3 & LAMP1)

Since LMP occurred in both *H. pylori* infection and HMGB1 activation, we explored whether glycyrrhizin treatment could help in LMP recovery. Double immunofluorescence assay was performed using galectin3 and LAMP1 antibody. Galectin3 colocalization with LAMP1 was significantly higher in *H. pylori* infection than in control cells because galectin3 binds to lysosomal membrane glycoproteins that are exposed during LMP. However, glycyrrhizin treatment of infected cells reduced co-localization of galectin3 and LAMP1, most likely due to LMP suppression (**Figure 4.3**).

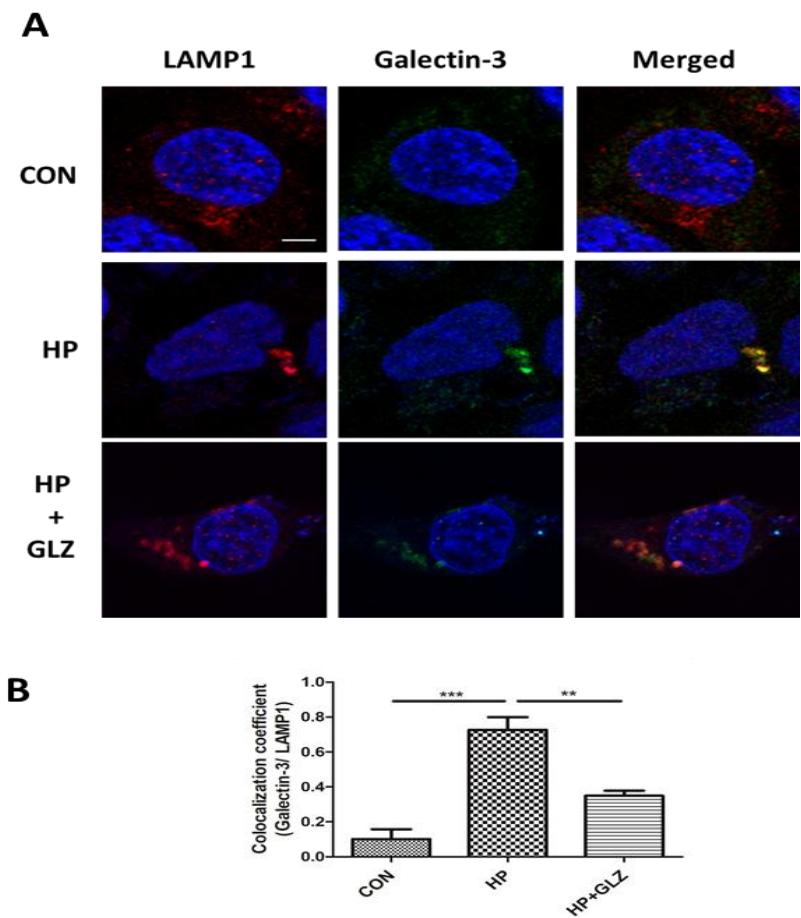


Figure 4.3 Glycyrrhizin restores the integrity of the lysosomal membrane. (A–B) Glycyrrhizin (GLZ) (200μM) treatment was used after 4h *H. pylori* infection (MOI 100). (**A**) To confirm LMP, double immunofluorescence assay using LAMP1 and Galectin-3 antibodies was performed. Cells

were examined using a confocal microscope, and the difference between each group's co-localization coefficients was calculated. Scale bar: 2µm. **(B)** Graphs were generated using GraphPad Prism 5 and represented as mean±SEM (n=3); Significance was calculated by one-way ANOVA; ** p < 0.01, *** p < 0.001

4.2.2 Determination of LMP using Alexa Fluor labelled dextran molecules

In the next step, to verify inhibition of LMP, we further loaded control, *H. pylori*-infected, and drug-treated cells with Alexa Fluor labelled dextran molecules. Dextran redistribution was seen in infected cells (diffuse staining), indicating lysosomal efflux, but not in infected cells treated with glycyrrhizin (**Figure 4.4**). Dextran's confined puncta formation in drug-treated cells exclusively indicated lysosomal localization.

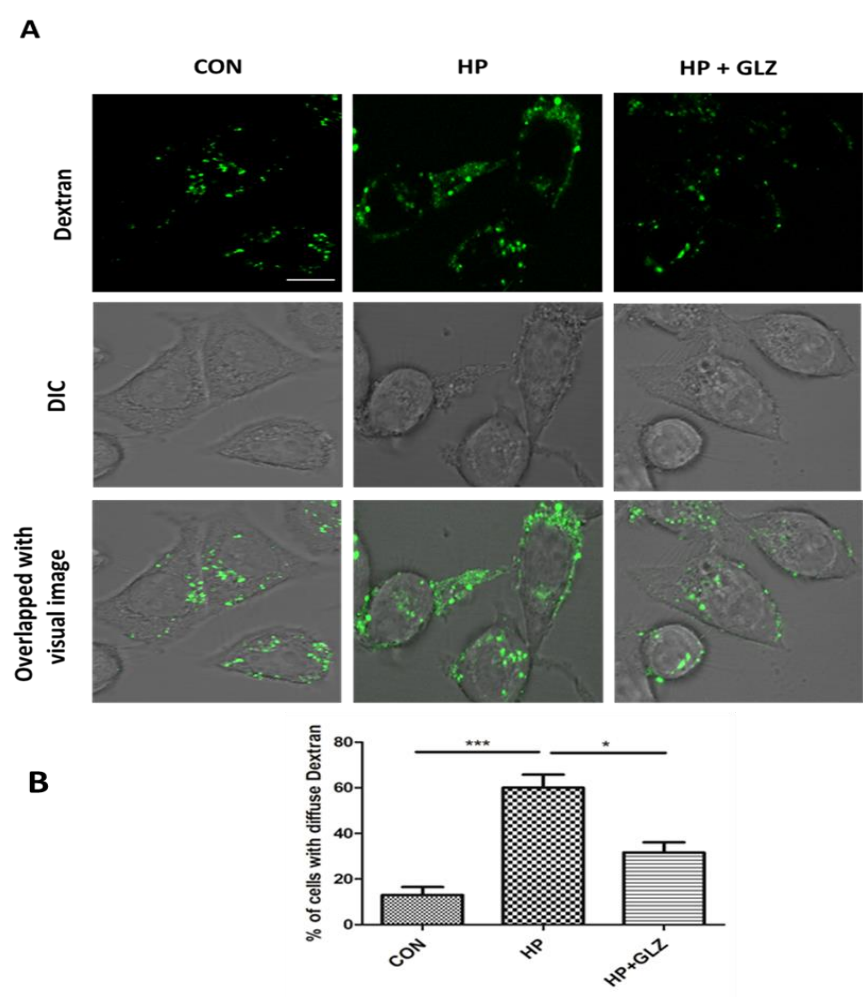


Figure 4.4 Lysosomal destabilization was assessed using live cell imaging. (A–B) Glycyrrhizin (GLZ) (200 M) treatment was done after 4h *H. pylori* infection (MOI 100). **(A)** Finally, after staining with dextran (0.5 mg/ml) for 2 hours, the amount of cells with diffused dextran was counted. **(B)**

Graphs were generated using GraphPad Prism 5 and represented as mean±SEM (n=3); Significance was calculated by one-way ANOVA; * $p < 0.05$, *** $p < 0.001$.

4.3 Glycyrrhizin suppresses reactive oxygen species (ROS) and inflammation in *H. pylori* infected gastric cells

Since inflammation and reactive oxygen species (ROS) generation triggers lysosomal disruption, we then examined whether glycyrrhizin inhibits *H. pylori* induced ROS and inflammatory cytokine production. In accordance, glycyrrhizin-exposed cells drastically decreased IL-8 release and ROS levels when compared to only infected-cells (**Figure4.5 A, B**).

In addition, as generation of ROS can activate NF- κ B signaling pathway (**Morgan et al., 2011**), our study explored the impact of glycyrrhizin on NF- κ B promoter activity. Hence, we subjected AGS cells to *H. pylori* infection followed by treatment with glycyrrhizin. Subsequently, we analyzed the nuclear extracts to ascertain the extent of NF- κ B's transcriptional activity. Expectedly, upon *H. pylori* infection, there was a notable increase in the binding of NF- κ B to NF- κ B response elements. Intriguingly, the exposure of glycyrrhizin exhibited a significant dampening effect on the *H. pylori*-induced NF- κ B DNA binding activity (**Figure4.5 C**). These data indicate that glycyrrhizin repair the lysosomal degradation activity by inhibiting LMP. Moreover, drug treatment reduced inflammation and ROS activation along with inhibition of LMP.

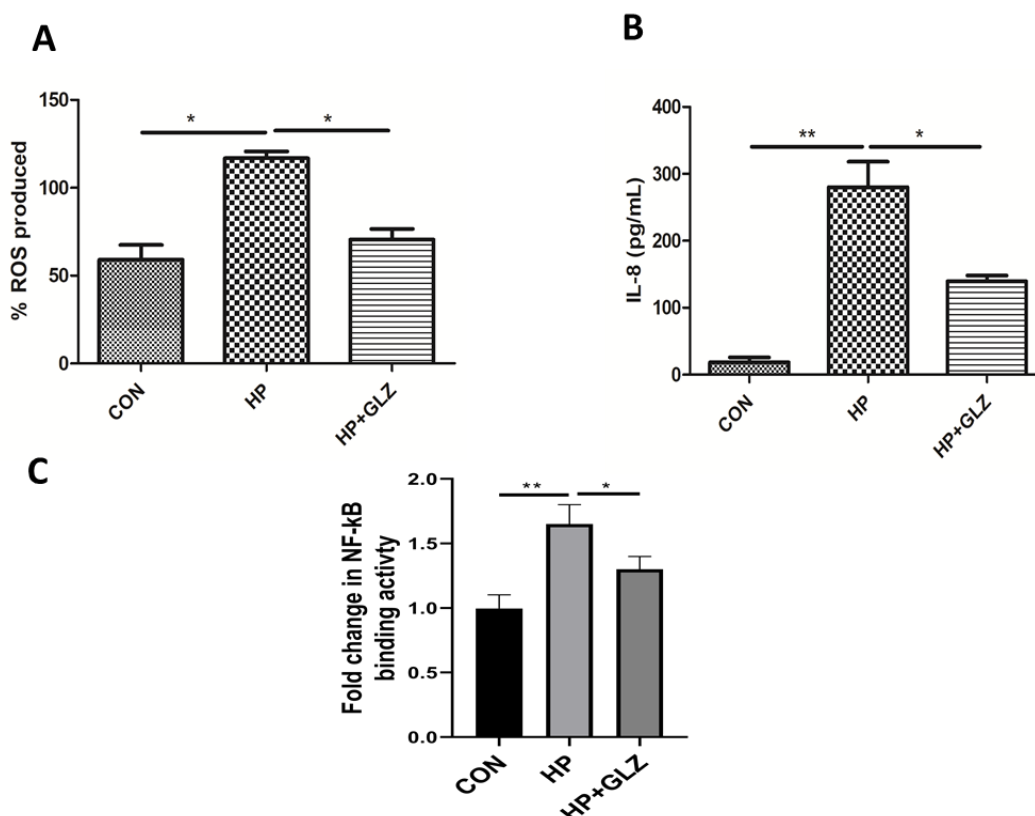


Figure 4.5 Glycyrrhizin reduces reactive oxygen species (ROS) and inflammation. (A) Expression of reactive oxygen species (ROS) in infected and drug treated cells was determined by DCFDA method for 30 min in a fluorimeter. (B) The expression of IL-8 from media collected after treatment was analysed by ELISA in a microplate reader. (C) The cell groups, Control (CON), *H. pylori* infected (HP), *H. pylori* infected and glycyrrhizin treated (HP + GLZ), were subjected to NF- κ B promoter assay, which aimed to demonstrate the activation of NF- κ B binding to the promoter sequence. Graphs were generated using GraphPad Prism 5 and represented as mean \pm SEM (n=3); Significance was calculated by one-way ANOVA; * $p < 0.05$, ** $p < 0.01$.

Conclusion:

Glycyrrhizin induces lysosomal acidification, by inhibiting LMP and thereby reduces *H. pylori* infection. This effect occurs in conjunction with restoration of the *H. pylori* -induced complex cascade of events, including the activation of NF- κ B, inflammation, and the generation of ROS and LMP. These findings strongly suggest the critical role of lysosomal acidification in the antimicrobial actions brought about by glycyrrhizin.

Chapter 5

Glycyrrhizin alleviates *H. pylori* infection in *in vivo* mice model

Background

Infection with *Helicobacter pylori* is associated with chronic active gastritis, peptic ulcer, and is a key risk factor for stomach adenocarcinoma development. Upon entry of the *H. pylori* in the stomach, host triggers an immune response in order to eliminate the bacteria. This immune response often involves the activation of NF- κ B. NF- κ B activation leads to the production of various pro-inflammatory cytokines, such as interleukins and tumor necrosis factor (TNF α), which recruit immune cells to the site of infection and initiate an inflammatory response. The molecular and cellular mechanisms by which *H. pylori* bacteria colonise the stomach and cause disorder have been studied using a number of rodent gastric models of *Helicobacter pylori* infection. Subsequently, we validated the *in vitro* activity of glycyrrhizin in *in vivo* mice model. SS1 strain of *H. pylori* was chosen as it is the standard mouse-adapted strain. C57BL/6 Mice were infected and treated with glycyrrhizin. Based on earlier research of glycyrrhizin (Lv et al., 2020 and Fu et al., 2014), the effective dose of the drug was established for *H. pylori*-infection in *in vivo* model.

Materials and Methods

Western blots were performed to observe change in the expression levels of autophagic marker proteins. ELISA was done to analyse the inflammatory cytokines. HE staining was done to observe the morphological changes in the gastric tissues. Methods are already described in the materials and methods section.

Results

5.1 Glycyrrhizin induces autophagy in an *in vivo* mice model

We conducted *in vivo* validation of glycyrrhizin's efficacy using a C57BL/6 mice model. In this model, mice were infected with the *H. pylori* SSI strain and subsequently treated with glycyrrhizin for a 30-day period at a dose of 10 mg/kg body weight (**Figure5.1**). The selection of this particular glycyrrhizin dosage for *H. pylori*-infected mice was based on prior studies by (Lv et al., 2020) and (Fu et al., 2014).

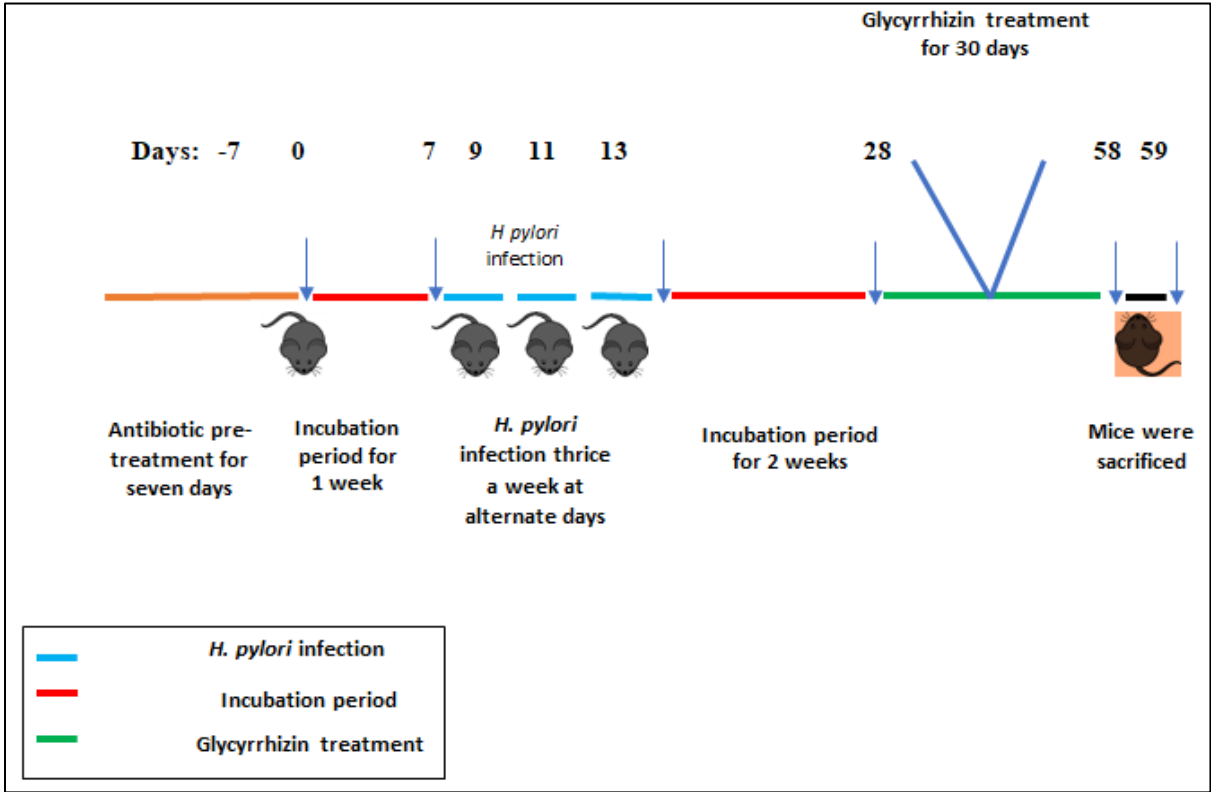


Figure 5.1 Treatment regime of glycyrrhizin in *H. pylori* infected C57BL/6 mice model. Antibiotic was orally gavaged to C57BL/6 mice (n = 5 per group) for every 7 days and then mice had a 7-day incubation period. The *H. pylori* SS1 strain was then oro-gastrically gavaged to mice three times a week at alternate days. After a 14-day incubation period, mice were treated with glycyrrhizin every other day for four weeks, with /without the incubation period. Mice were sacrificed at the end of treatment, & serum & stomach tissues were collected.

Mice stomach tissues of control, infected, and glycyrrhizin-treated were processed for western blot analysis in order to examine autophagy markers proteins. Glycyrrhizin being the

well-known inhibitor of HMGB1 decreased the level of HMGB1 (**Figure5.2A, B**). In addition, it causes the degradation of p62 protein, a hallmark of autophagy induction (**Figure5.2A, C**). ATG5 was increased due to infection and glycyrrhizin further enhanced the expression (**Figure5.2A, D**). In line, as compared to only infected cells, glycyrrhizin treatment consistently resulted in elevated LAMP1 expression level (**Figure5.2A, F**). But in case of Beclin1, glycyrrhizin reduced the level which was augmented due to infection (**Figure5.2A, E**). These data shows that glycyrrhizin induces autophagy in an *in vivo* mice model.

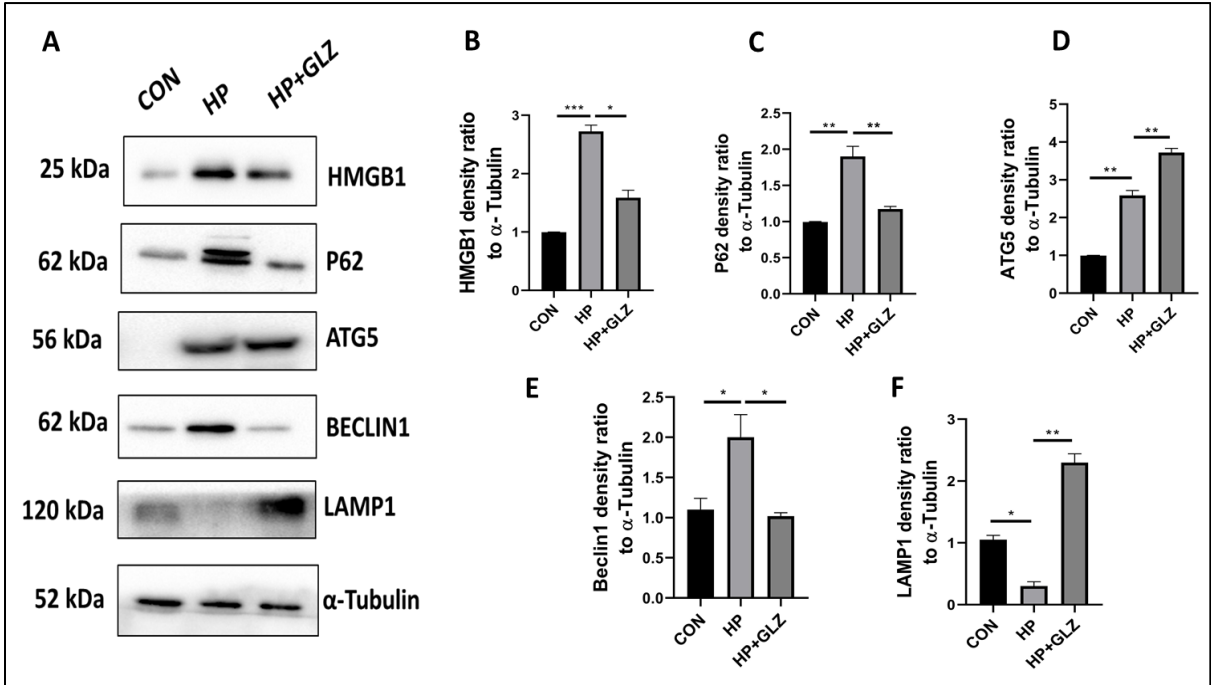


Figure5.2 Mice gastric tissues were processed to examine HMGB1 and autophagy marker proteins (P62, ATG5, Beclin1 and LAMP1) via Western blot. Protein loading was monitored using α -tubulin. Graphs were represented as mean \pm SEM (n=3); Significance was determined by one-way ANOVA; * $p < 0.05$, ** $p < 0.01$, *** $p < 0.001$.

5.2 Glycyrrhizin reduces the inflammatory cytokine levels during *H. pylori* infection

Since activation of NF- κ B contributes to the inflammation associated with *H. pylori* infection, we examined the effect of glycyrrhizin on inflammation. We next investigated the

effect of glycyrrhizin on inflammatory markers linked with NF- κ B activation. The serum obtained from mice samples were used to measure the levels of IL-6, TNF α and HMGB1 in ELISA. Expression of HMGB1 and IL-6 was considerably suppressed by glycyrrhizin treatment (**Figure5.3A, B**). However, the level of TNF α remains unchanged (**Figure5.3C**). Hence, inhibition of HMGB1 during *H. pylori* infection induces autophagy and reduces inflammation.

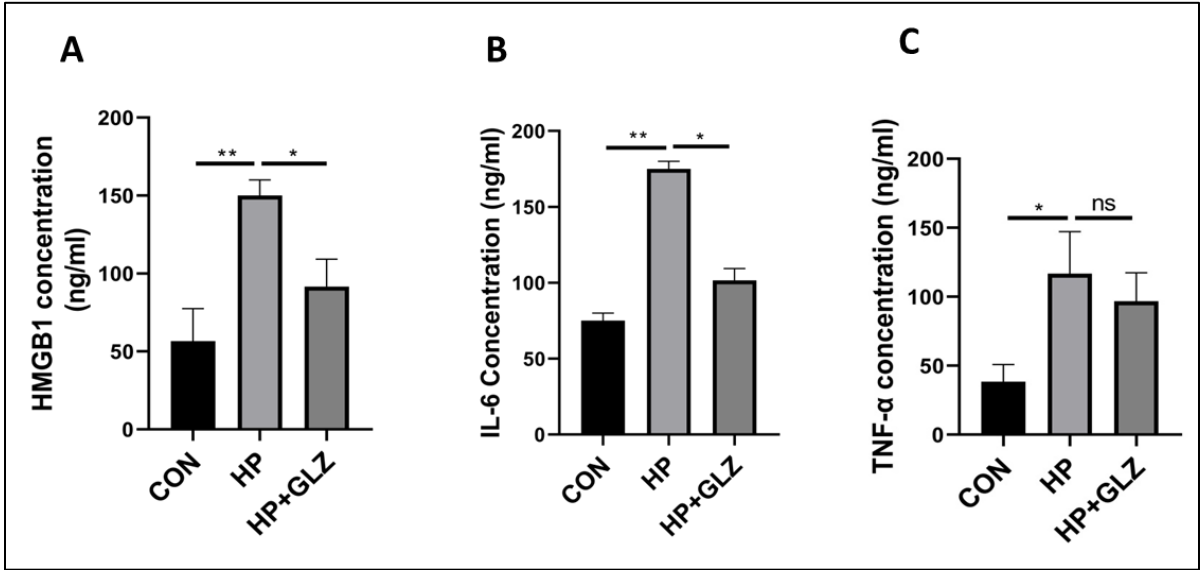


Figure 5.3 Treatment with glycyrrhizin affects the expression of NF- κ B and related inflammatory cytokines. (A-C) Serum samples from control, infected, and infected mice post-treated with glycyrrhizin were tested for HMGB1, IL-6, and TNF levels using ELISA. The expression of HMGB1 and cytokines was determined by ELISA in a microplate reader. Graphs were represented as mean \pm SEM (n=3); Significance was determined by one-way ANOVA; * p < 0.05, ** p < 0.01, *** p < 0.001, ns= nonsignificant.

5.3 Glycyrrhizin effectively reduces inflammation in gastric tissues

Further in order to assess the histopathological changes in post-glycyrrhizin treatment, gastric tissues were subjected to Hematoxylin and Eosin (HE) staining. In case of *H. pylori* infection, moderate signs of inflammation, including hyperplasia and inflammatory cell infiltration in stomach tissues were observed. Glycyrrhizin effectively reduced inflammation and contributed to partial recovery of the damaged tissue (**Figure5.4**).

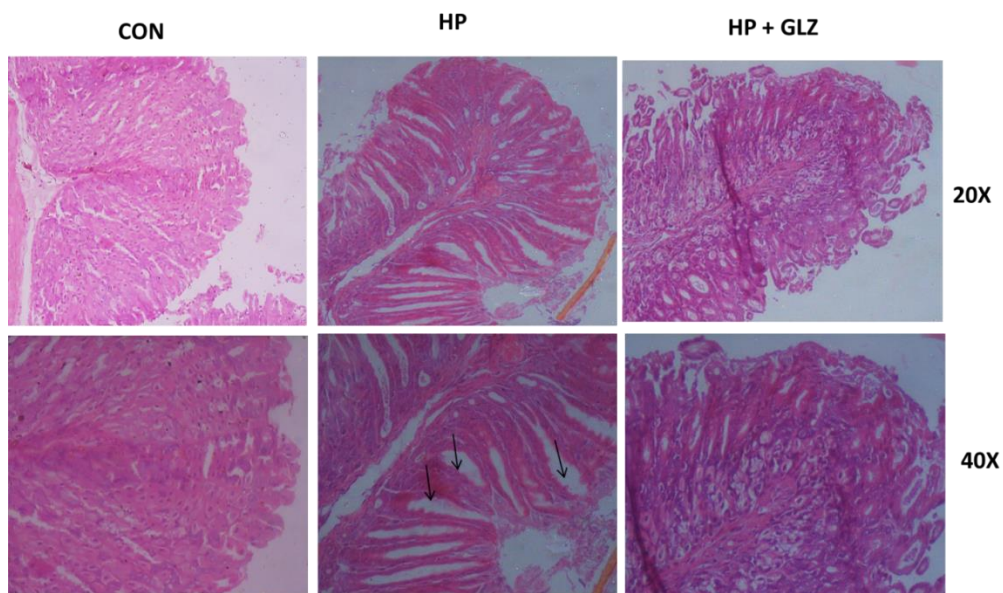


Figure 5.4 Glycyrrhizin reduces tissue damage in HE staining of infected- gastric tissues. The inflammatory changes are depicted in histology images of Control (CON), *H. pylori* (HP) infected, and *H. pylori*-infected plus glycyrrhizin treated (HP+GLZ) gastric tissues at 20X and 40X, respectively. Tissue injury is indicated by the black arrows (↑).

Conclusion

Glycyrrhizin, , stimulates autophagy in gastric tissues by inhibiting HMGB1 expression This, in turn, limits gastric tissue damages in an *in vivo* mouse model, aligning with the outcomes observed in our *in vitro* experiments.

OBJECTIVE III.

Chapter 6

**Dissecting the role of novel signature autophagic targets due to
HMGB1 activation**

Background

Autophagy plays a crucial role in maintaining cellular homeostasis by degrading and recycling damaged or dysfunctional cellular components, including organelles or proteins and defends against intracellular pathogens (**Dikic et al., 2018**). Autophagy is a complex process that is involved in a variety of cellular functions, and High mobility group box 1 (HMGB1) is one of the many factors that can regulate this process (**Zhao et al., 2020**). The role of HMGB1 in autophagy regulation varies as it can act as an anti-autophagic or a pro-autophagic factor based on specific cellular conditions and signalling pathways involved (**Khambu et al., 2020; Feng et al., 2021**). HMGB1 induces autophagy by directly binding to the autophagy protein Beclin1 disrupting Beclin1/Bcl2 interaction through the activation of ERK/MAPK pathway (**Tang et al., 2010**). During *H. pylori* infection in gastric cells we observed that, autophagy is inhibited and bacteria proliferate inside the autophagosomes (**Li et al., 2017**). Therefore, we assume that HMGB1 activation due to *H. pylori* infection has some definite role in autophagy. As HMGB1 is known to interact with several proteins, we hypothesized that HMGB1 might interact with autophagy proteins during the infection.

The exact role of HMGB1 in autophagy during *H. pylori* infection is complex. It is not yet completely understood. However, it is evident that HMGB1 has both promoting and inhibiting effects on autophagy (**Yin et al., 2017; Feng et al., 2021**). More research is required to determine HMGB1 mediated specific targets in autophagy and uncover the underlying mechanisms involved which can be therapeutically utilized in *H. pylori* infection.

In this context, the autophagic regulatory network and interaction between host factors were investigated and validated in *in vitro* conditions in gastric cancer and macrophage cell lines.

Material and methods

After infection with *H. pylori* 26695 strain, co-immunoprecipitation assays were performed in AGS and RAW 264.7 cells. Transfection was done with a myc-tagged HMGB1 plasmid and HMGB1 siRNA. Then cells were further subjected to infection with *H. pylori* 26695 strain for 6h, Western blot was performed. Co-Immunofluorescence studies were performed to confirm protein-protein interaction. Interaction of proteins was predicted by bioinformatic approach.

Results

6.1 Determination of autophagic targets of HMGB1 using Co-Immunoprecipitation

6.1.1 Using western blotting

To elucidate the possible involvement of autophagy proteins with HMGB1 during *H. pylori* infection, we infected AGS cells with *H. pylori* 26695 strain for 6h and performed co-immunoprecipitation experiments using HMGB1 antibody. We found that HMGB1 is interacting with Beclin1, an initiator of autophagy (**Figure6.1A**). Beclin1 recruits key autophagic proteins to a pre-autophagosomal structure, thereby forming the core complex consisting of Beclin1, Vps34, and Vps15. Additionally, HMGB1 was found to interact with two additional molecules, UV irradiation resistance-associated gene (UVRAG) and a WD-40 domain-containing protein (WIP1) (**Figure6.1B**). UVRAG and WIP1 are constituents of the human Vps34 complex, and their roles within the complex appear to serve as positive regulators of autophagy. This is a novel finding in HMGB1 regulated autophagic pathway during *H. pylori* infection.

Further, the association was strengthened by reverse pull-down assay, where immunoprecipitation using Beclin1 antibody was performed and significant interaction was observed with HMGB1 and UVRAG (**Kang et al., 2011**) respectively upon *H. pylori* infection (**Figure6.1B**).

Moreover, we used bioinformatic approach to study these interactions using String software. We observed direct interaction with HMGB1 and Beclin1 (**Figure6.1C**). This has been reported earlier (**Tang et al, (2010)**).

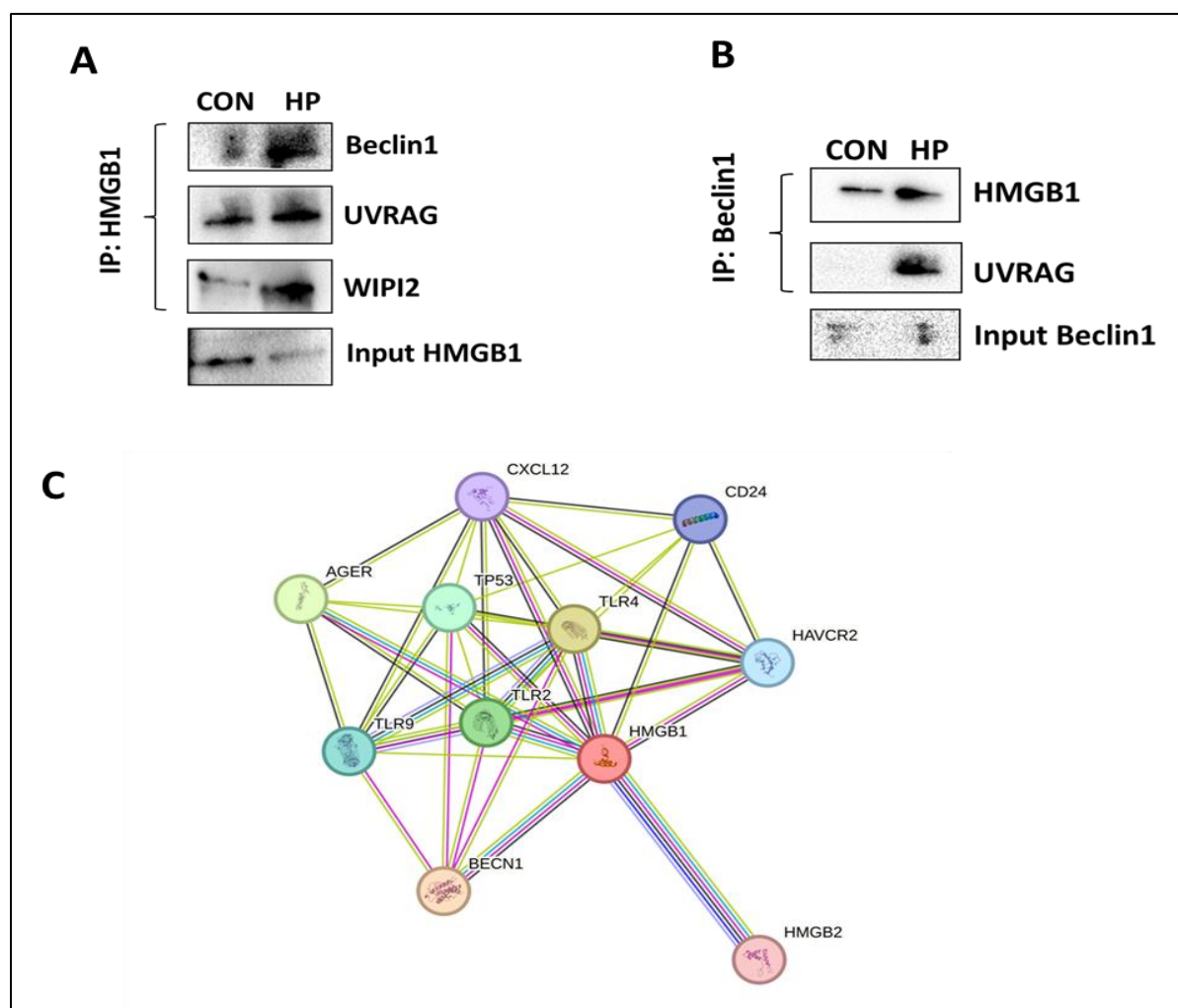


Figure 6.1 HMGB1 interacts with different autophagy proteins. (A-B) AGS cells infected with *H. pylori* for 6h were subjected to co-immunoprecipitation assay using specific antibody followed by western blot analysis with different antibodies. **(A)** Immunoprecipitated with HMGB1 antibody in *H. pylori* infected and/or un-infected cells followed by western blot to observe the interaction with Beclin1, UVRAG and WIPI2 antibodies. HMGB1 interacts with major autophagy proteins. 10% input was used & blotted with anti-HMGB1 antibody. **(B)** Immunoprecipitation with Beclin1 antibody in *H. pylori* infected and/or un-infected cells followed by western blot to observe the interaction with HMGB1 and UVRAG antibody. 10% input was used & blotted with anti-Beclin1 antibody. **(C)** Using string software we observed that HMGB1 directly binds to Beclin1.

6.1.2 Determining interaction of HMGB1 with Beclin1 by immunofluorescence

In addition, we performed immunofluorescence studies to visualize the interaction of HMGB1 with Beclin1. Cells were infected/ un-infected with *H. pylori* after which association was visualized by confocal microscopy using HMGB1 and Beclin1 specific antibodies.

HMGB1 remains inside the nucleus in case of control cells while upon infection HMGB1 localizes from nucleus to cytoplasm and binds with the Beclin1 protein (**Figure.6.2A, B**).

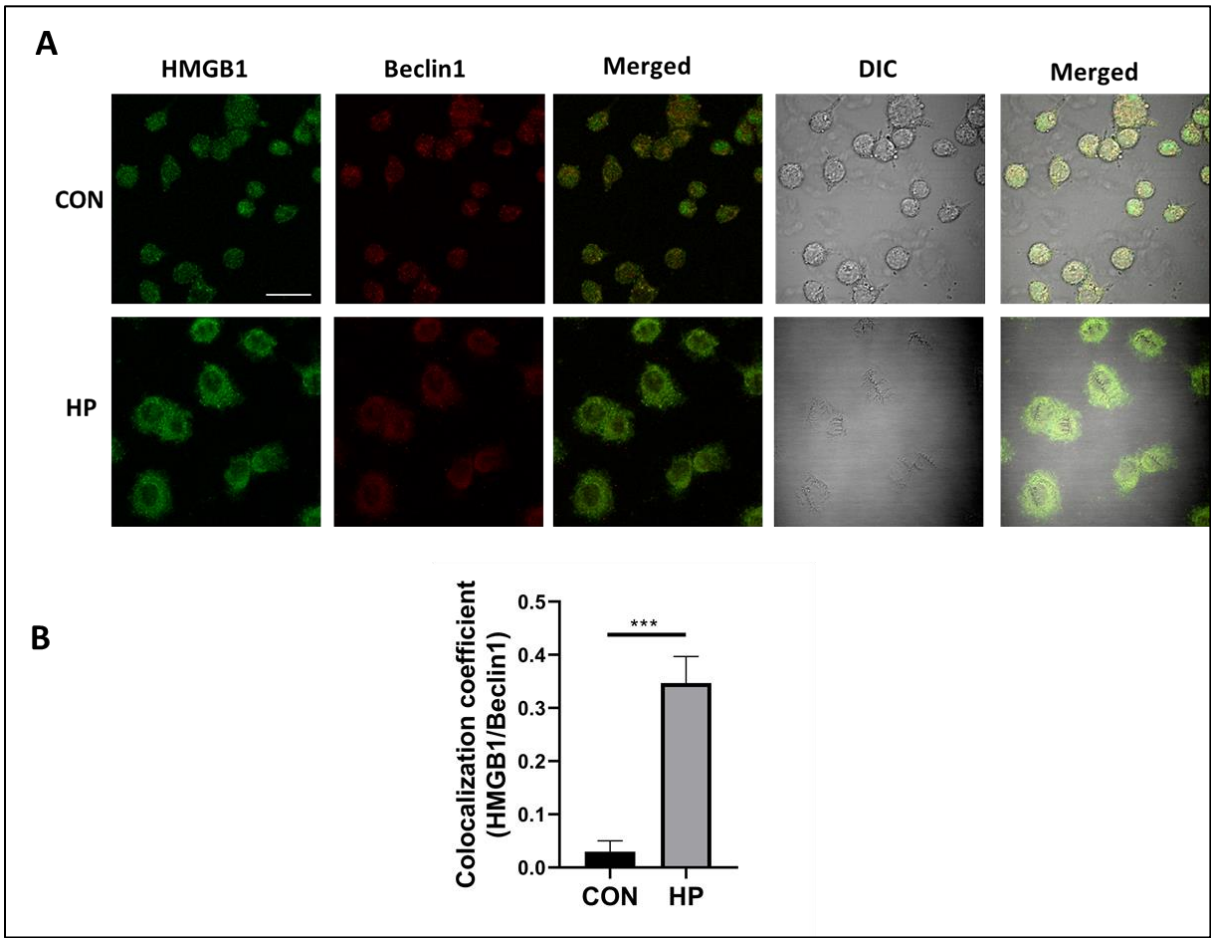


Figure 6.2 Immunofluorescence to detect HMGB1-Beclin1 interaction. (A-B) AGS cells were infected with *H. pylori* for 6h and subjected to double immunofluorescence using HMGB1 (green) and Beclin1 (red) antibody. Cells were examined using a confocal microscope, Scale bar: 10 μ m and (B) The difference between each group's co-localization coefficients was calculated. Graphs were represented as mean \pm SEM (n=3); Significance was determined by Unpaired t-test was performed; *** p < 0.001.

6.2 Interaction studies of HMGB1 and Beclin1 in overexpressed HMGB1 cells

6.2.1 Western blotting

In parallel, HMGB1 was overexpressed in AGS cells and the association between HMGB1 and Beclin1 was ascertained. Cells were transiently transfected with myc-tagged HMGB1

expression plasmid and 36 h post-transfection, were either infected or un-infected with *H. pylori* for another 6h. Immunoprecipitation of HMGB1 was performed in control and *H. pylori* infected cell lysates, and the presence of Beclin1 in the pull-down fraction confirmed their interaction in *H. pylori* infected cell lysates (**Figure6.3**).

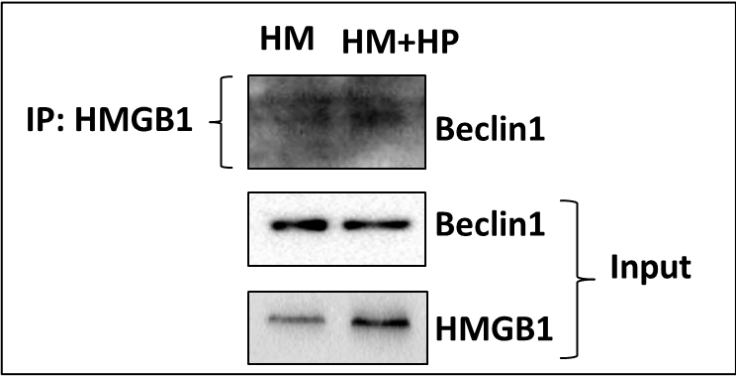


Figure 6.3 HMGB1 interacts with Beclin1 in overexpressed cells. (A) AGS cells were transfected with myc-tagged HMGB1 plasmid followed by infection with *H. pylori* for 6h and further subjected to co-immunoprecipitation with HMGB1 antibody. Finally,western blot analysis was performed with Beclin1 and HMGB1 antibodies. 10% input were used & blotted with anti-HMGB1 and anti-Beclin1 antibody.

6.2.2 Confocal microscopy

These interaction studies were further validated by colocalization of HMGB1 and Beclin1 in HMGB1 overexpressed cells. We performed coimmunofluorescence experiments with HMGB1 and beclin1 antibodies. The results demonstrated that HMGB1 remained concentrated inside the nucleus in most of the cells and there was no significant association of both the proteins in case of transfected un-infected group (**Figure6.4A, B**). While in case of *H. pylori* infected group, HMGB1 shuttles between nucleus and cytoplasm and colocalization coefficient of HMGB1 and Beclin1 was 0.785, thus establishing their interaction (**Figure6.4A, B**).

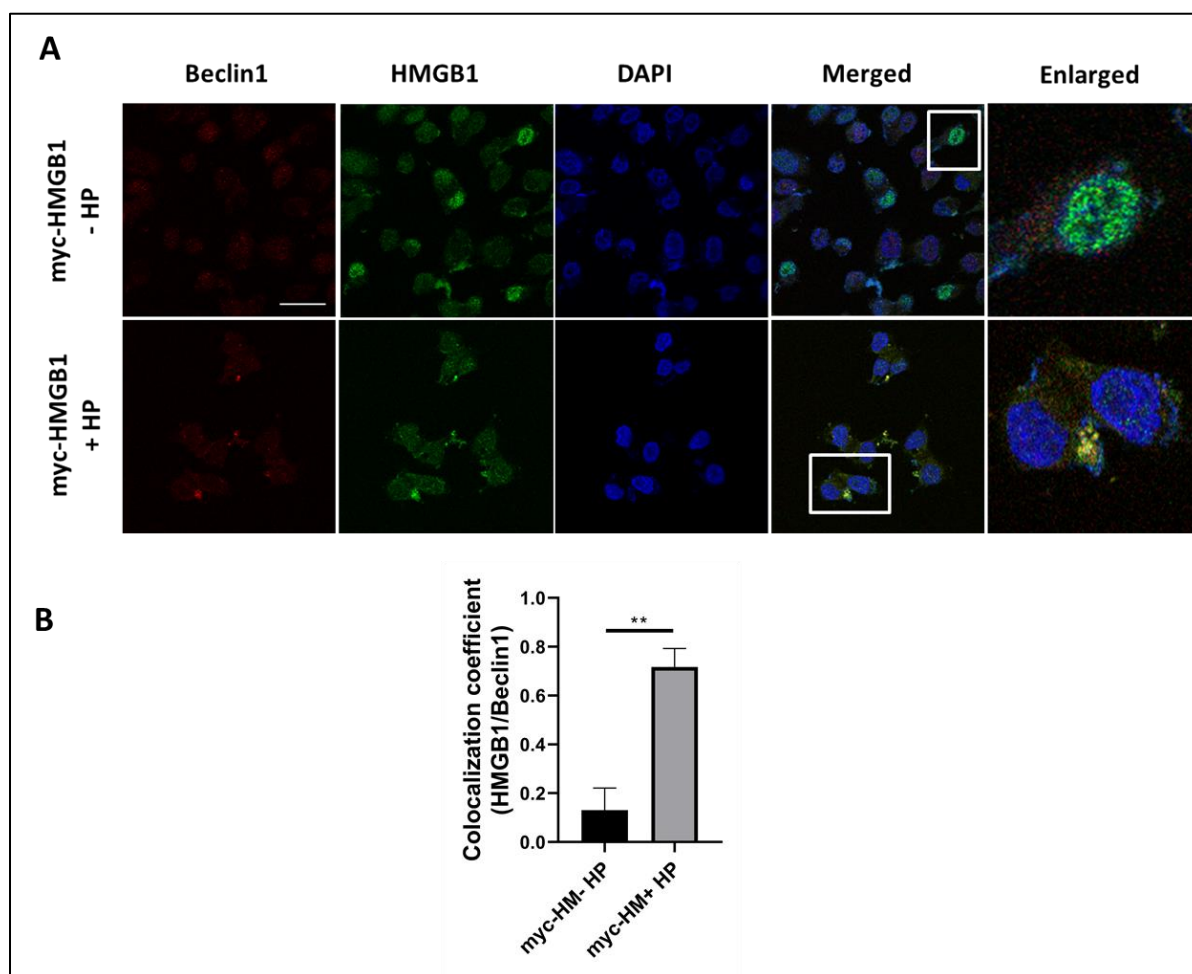


Figure 6.4 Immunofluorescence to detect HMGB1-Beclin1 interaction in HMGB1 overexpressed condition. (A-B) AGS cells transfected with myc-tagged HMGB1 plasmid followed by infection with *H. pylori* for 6h were subjected to double immunofluorescence using HMGB1(green) and Beclin1(red) antibody. Cells were examined using a confocal microscope, Scale bar: 10µm and (B) The difference between each group's co-localization coefficients was calculated. Graphs were represented as mean±SEM (n=3); Significance was determined by Unpaired t-test was performed; ** p < 0.01.

6.3 Autophagic targets interacting with HMGB1 in macrophages

Macrophages play a definitive role during *H. pylori* infection. *H. pylori* is known to activate macrophages and elicit cytokine production. We infected RAW 264.7 cells with *H. pylori* for 6h and performed co-immunoprecipitation experiment using anti-HMGB1 antibody. We found that HMGB1 is interacting with Beclin1 and UVRAG (**Figure6.5A**). However, in reverse pull down assay using UVRAG antibody, we observed that UVRAG significantly

interacts with Beclin1 in *H. pylori* infected group. But it is not interacting with HMGB1 suggesting that interaction with UVRAG is indirect while with Beclin1, there is direct interaction (**Figure6.5B**).



Figure 6.5 HMGB1 interacts with different autophagy proteins in RAW 264.7 cells. (A-B) RAW 264.7 cells were infected with *H. pylori* for 6h. (A) Co-Immunoprecipitation with anti-HMGB1 antibody was done followed by western blot analysis to observe interaction with Beclin1 and UVRAG. 10% input was used & blotted with anti-HMGB1 antibody. (B) Immuno-precipitation with UVRAG antibody in *H. pylori* infected and/or un-infected cells was done followed by western blot to observe the interaction with HMGB1 and Beclin1. 10% input were used & blotted with anti-HMGB1 and anti-UVRAG antibody.

6.4 Unraveling the Mechanism Regulated by HMGB1

Till now we observed that HMGB1 interact with multiple autophagy proteins, in order to modulate the autophagic mechanism during *H. pylori* infection. To determine the signaling pathways regulated by HMGB1 during *H. pylori* infection in gastric cells, cells were transiently transfected with myc-tagged HMGB1 (HM) expression plasmid and myc-tagged Empty vector (EV). 36 h post-transfection, cells were infected with *H. pylori* for another 6h. We examined kinases which can be regulated by HMGB1, including ERK1/2 and p38 MAPK. Our findings revealed a notable rise in the phosphorylation levels of ERK1/2 (**Figure6.6A, B**) and p38 MAPK (**Figure6.6C, D**), reflecting their activation during *H. pylori* infection.

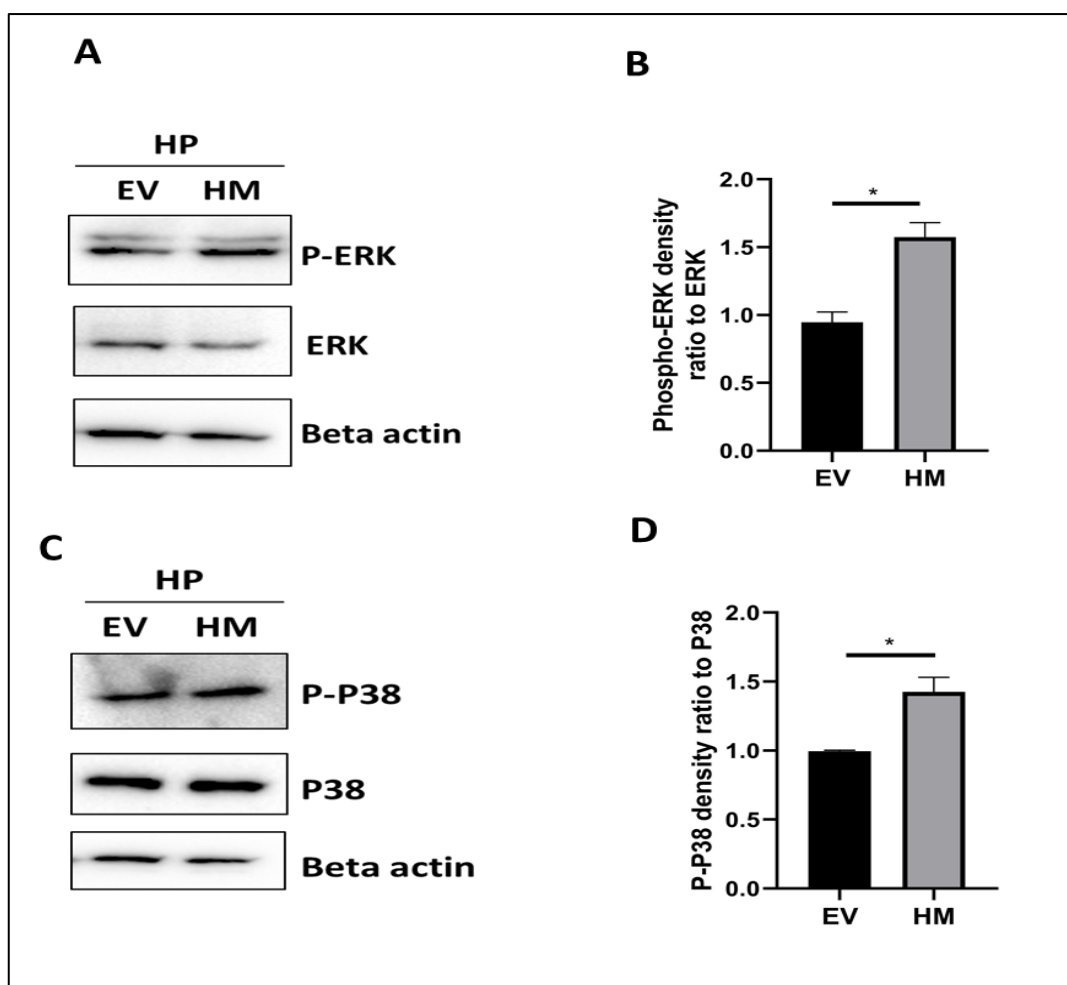


Figure 6.6 HMGB1 regulation via signaling pathways. (A-D) AGS cells were transfected with myc-tagged HMGB1 plasmid and myc-tagged Empty vector (EV). 36 h post-transfection, was followed by infection with *H. pylori* for 6h and further subjected to western blot analysis. Graphs were represented as mean \pm SEM (n=3); Significance was determined by Unpaired t-test was performed; * $p < 0.05$.

Conclusion

HMGB1 interacts with various autophagy proteins, including Beclin1, UVRAG, and WIPI2, suggesting that it might modulate the cellular mechanism in response to *H. pylori* infection within gastric cells by interacting with different autophagy proteins. HMGB1 activation further downstream activates ERK/P38 signalling axis.

Section 6

DISCUSSION

Eukaryotic cells get rid of damaged organelles and protein aggregates by the mechanism of autophagy to maintain cellular homeostasis. Moreover, it is the same mechanism used to destroy intracellular invaders (including viruses, bacteria, and protozoa). Autophagy is a common physiological process that begins with the formation of phagophores, which elongate and engulf portions of the cytoplasm to form double-membrane structures, autophagosomes. Subsequently, autophagosomes fuse with lysosomes to form degradative autolysosomes, where the engulfed contents are degraded by acidic lysosomal hydrolases (Orvedahl et al., 2009). In particular, autophagy that targets intracellular pathogens is termed xenophagy, and this is essential for the innate and adaptive immune responses of the host system to respond against infection (Deretic et al., 2005). As an evolutionary counterpoint, pathogens have evolved strategies to restrain and fight back against host defense mechanisms and ensure their survival. Several intracellular pathogens that are known to subvert autophagy are- *Salmonella*, *Shigella*, and *Mycobacterium* (Xie et al., 2014; Ogawa et al., 2005; Padhi et al., 2019). Boosting autophagy can strengthen the host's defense against intracellular pathogens. Research has demonstrated that small molecule enhancers of autophagy, such as rapamycin induce the autophagy pathway for efficient delivery of cargo (pathogens) to the lysosome (Floto et al., 2007; Lin et al., 2017). Therefore, exploring the intricate relationship between autophagy and intracellular pathogens might lead to the development of new therapies for infectious diseases.

H. pylori was previously recognized as an extracellular bacterium that adheres to the surface of the gastric epithelium. However, numerous *in vitro* studies have suggested the possibility of bacterial invasion into gastric epithelial cells (Dubois et al., 2007; Liu et al., 2012; Oh et al., 2005). Moreover, many electron microscopic studies of gastric biopsy samples from infected individuals have reported intact and degraded forms of the bacterium within epithelial cells (Hu et al., 2019). However, the mechanism by which *H. pylori* survives

within the cells still awaits elucidation. In this study, we showed that *H. pylori* infect and colonizes within human gastric cancer cells. *H. pylori* secretes two major virulence factors CagA and VacA, both of which play significant roles in pathogenesis. In our study, we have used two standard strains of *H. pylori* 26695 and SS1. *H. pylori* 26695 s1m1 type indicates *vacA*+ & *cagA*+ strain. *H. pylori* SS1 strain is *cagA*+, but it expresses a non-functional VacA and this strain is compatible with mice infection. It is important to note that earlier findings of **Terebiznik et al., (2009)** demonstrated that VacA induces autophagy, while **Raju et al., (2012)** have reported that prolonged exposure to VacA inhibits autophagy. Recent studies have provided further insights into CagA into the regulation of autophagy, suggesting that autophagy is down-regulated in *cagA*+ strains as compared to *cagA* mutant strains (**Li et al., 2017**). Hence, both VacA and CagA contribute to the modulation of autophagy which further leads to the disruption of autophagosome maturation and prevents fusion of autophagosomes with lysosomes. This may enhance intracellular *H. pylori* growth within the defective autophagosomes as observed in our study. In this manner, *H. pylori* manipulates the host cell's machinery to create intracellular replicative niches within the gastric epithelial cells of the stomach and these niches provide protection from antibiotics and immune responses, thus making it challenging for antibiotics to eradicate the bacterium (**Zhang et al., 2018**). These surviving bacteria can later re-emerge and recolonize the stomach once antibiotic treatment is completed, leading to recurrent infections (**Sarem et al., 2016**).

In our current study, we confirmed an increase in autophagosome numbers following *H. pylori* infection, consistent with several prior findings (**Chu et al., 2010; Hu et al., 2019**). Notably, we also observed a disruptive effect of *H. pylori* infection on lysosomal activities and autolysosomal degradation function accompanied by decrease in LAMP1 expression and accumulation of p62, aligning with the earlier work conducted by **Raju et al.**, which suggested a suppressive role of *H. pylori* in autolysosomal maturation (**Tsugawa et al., 2019**;

Hu et al., 2019). Specific mechanisms by which *H. pylori* accomplishes its survival are still being investigated, but it often involves the interaction between bacterial effector and host cell proteins. *H. pylori* also influences the signalling pathways that regulate autophagy in host cells. This involves the activation or inhibition of key signalling molecules that control the initiation and progression of autophagy. By altering these signalling pathways, *H. pylori* manipulates the host cell's autophagic response to its advantage.

High Mobility Group Box1 (HMGB1) is a key signalling molecule involved in the regulation of autophagy which varies as it can act as an anti-autophagic or a pro-autophagic factor based on the specific cellular conditions and signalling pathways involved (**Khambu et al., 2020; Feng et al., 2021**). When *H. pylori* colonizes the stomach lining, inflammation is induced in the gastric mucosa. This inflammatory response is the host's attempt to combat the infection (**Lamb et al., 2013**). During inflammation and cellular stress, cells may release HMGB1 into the extracellular space. HMGB1 is considered as a pro-inflammatory molecule extracellularly because it can activate immune responses and contribute to the inflammatory cascade (**Cheng et al., 2014**).

Previous studies have shown that HMGB1 plays diverse roles in various types of cancer including gastric (**Song et al. 2012**), colorectal (**Moriwaka et al., 2010**), breast (**Stoetzer et al., 2013; Fersching et al., 2010**), lung (**Wang et al., 2012**) etc. Hence, HMGB1 is often targeted as a potential biomarker and therapeutic candidate for investigating gastric disorders. However, the role of HMGB1 in gastric cells during *H. pylori* infection has not been explored till date. Several strategies are now being developed to directly or indirectly reduce HMGB1 expression, activity or its release in the treatment of various inflammatory diseases and cancer. For instance, anti-HMGB1 antibodies ameliorate the severity of lung injury induced by acute blood loss in a mouse model (**Kim et al., 2005**). HMGB1 knockdown utilising antisense technology decreases cancer cell proliferation and metastasis (**Chen et al., 2014; Li**

et al., 2014). In this study, we aimed to investigate the impact of HMGB1 inhibition on autophagy during *H. pylori* infection. Therefore, keeping in mind the fact of rise in antibiotic resistance, we focused on pharmacological drugs as an alternative to antibiotics for the treatment of *H. pylori* mediated gastric disorders. Natural compounds offer several advantages over synthetic compounds, notably a diminished risk of resistance development and a more environmentally friendly profile. To investigate the role of HMGB1 we used glycyrrhizin, a herbal compound that inhibits HMGB1 and thus, delineates the impact of HMGB1 inhibition during *H. pylori* infection in gastric cells. Glycyrrhizin has gained significant attention in recent times due to its antimicrobial properties. Glycyrrhizin has remarkable antibacterial activities against *Staphylococcus aureus*, *Mycobacterium tuberculosis*, and human immunodeficiency virus (HIV) (**Wang et al., 2015**).

This study provides evidence for the application of glycyrrhizin, an inhibitor of HMGB1 as a potential therapeutic agent. It shows negligible toxicity in AGS cells. This has significant importance, as toxicity is an important parameter for the development of novel antimicrobial agents. For the first time, glycyrrhizin demonstrated a reduction in the intracellular *H. pylori* burden in AGS gastric carcinoma cells. To gain deeper insights into the mechanism underlying bacterial clearance, we identified that glycyrrhizin induces the expression of major autophagy marker proteins such as Beclin1, LC3B, and LAMP1 in *H. pylori*-infected cells. This aligns with findings from prior research on glycyrrhizin's improved autophagy flux in myoblast cells (**Lv et al., 2020**). Moreover, the study shows that glycyrrhizin treatment induces autolysosome formation in infected cells. Autolysosomes are the vesicles where autophagosomes are fused with lysosomes and the autophagic cargo is degraded and recycled within the cell. It is considered an essential step in the autophagy process. This observation gains further support from western blot and confocal microscopic analyses, which reveal increased LAMP1 activity (**Tsugawa et al., 2019**) and remarkable increase in co-localization

of LC3B and LAMP1 in cells treated with the drug. Further autolysosome formation was confirmed by confocal microscopy and we observed enhanced fusion of autophagosomes with lysosomes in tandem fluorescent LC3B (tfLC3B) plasmid transfected AGS cells. Recent reports supported this mechanism of bacterial clearance by stimulation of autophagy, in which autophagy enhancers, such as vitamin D and statins, effectively control *H. pylori* infection (Hu et al., 2019; Liao et al., 2017). Further, we observed that siRNA-based knockdown of HMGB1 had similar effect with pharmacological inhibition of HMGB1. Similar results were obtained with glycyrrhizin treatment thus, confirming anti-HMGB1 activity to be responsible for autophagy induction.

Our studies have revealed a promising antimicrobial effect of glycyrrhizin against *H. pylori*, both at pharmacological and physiological concentrations. Furthermore, taking into consideration the significant issue of antibiotic resistance in *H. pylori* (Gene et al., 2003; Huang et al., 2017), this antimicrobial effect was extended to antibiotic-resistant strains, suggesting that glycyrrhizin holds significant potential as a therapeutic agent in the treatment of antibiotic-resistant *H. pylori* infections. The work underlines the potential of HMGB1 inhibition as a novel therapeutic approach for the treatment of intracellular bacterial infections. The data presented in this study suggest that glycyrrhizin may function as a specialized drug against intracellular bacteria and might have no direct impact on *H. pylori*. We observed that glycyrrhizin at similar concentration has no impact on *H. pylori* growth. However, it has been demonstrated that the anti-*H. pylori* effect of glycyrrhizin is autophagy-dependent by using autophagy inhibitors.

Apart from the earlier reported roles of VacA and CagA in modulating autophagy during *H. pylori* infection, a recent study revealed that another virulence factor GGT (gamma-glutamyltranspeptidase) inhibits the late stage of autophagy by inducing Lysosomal Membrane Permeabilization (LMP) Bravo et al (2019). LMP is a cellular event characterized

by the disruption or permeabilization of the lysosomal membrane leading to the release of lysosomal enzymes into the cytoplasm **(Johansson et al., 2010)**. This can cause cellular damage, lysosomal dysfunction and subsequently autophagy- lysosome pathway dysfunction. In this context, for the first time we performed glycyrrhizin treatment using two main methods- 1. Immunofluorescence with galectin3 and LAMP1 antibodies, 2. Alexa fluor conjugated dextran molecule showed that preventing HMGB1 activation could recover LMP in *H. pylori* infected cells and subsequently restored the degradative function of autophagy. This finding is similar with another recent study where LMP is prevented by HMGB1 downregulation in diabetic retinopathy **(Feng et al., 2021)**.

Since lysosomes are the principal degradative organelles within eukaryotic cells, they play crucial role in the efficient elimination of damaged cellular materials, including engulfed pathogens, to maintain homeostasis. Lysosome requires an acidic environment (pH 5.0) in its lumen to carry out its digestive function and export the recycled cargos **(Xu et al., 2015)**. Consequently, the maintenance of normal lysosomal acidification is of utmost importance for ensuring their optimal degradation function. However due to LMP, it was anticipated that certain hydrolytic enzymes, such as cathepsins, could be released into the cytosol. Although we did not directly assess the presence of these enzymes in the cytoplasm, we investigated the impact of LMP on the modification of lysosomal acidification. With the help of Acridine orange labelling and LysoTracker Red staining, we observed reduced red signal intensity which indicated impaired lysosomal acidification in *H. pylori*-infected cells **(Hu et al., 2019)**. In contrast, glycyrrhizin treatment restored lysosomal acidification.

Furthermore, LMP has an association with inflammation and formation of reactive oxygen species (ROS) due to *H. pylori*-infection and overexpression of HMGB1 **(Kavčič et al., 2017; Yuan et al., 2020)**. Glycyrrhizin effectively reduced the elevated ROS production and increased the levels of inflammatory cytokines during infections, as demonstrated by

Hardbower et al., in 2013. Thus, our findings support the conclusion that inhibiting HMGB1 with glycyrrhizin promotes autophagosomal maturation and lysosomal degradation in *H. pylori*-infected gastric cells, thereby rescuing them from LMP-induced damage.

Moreover, we corroborated our findings using an *in vivo* mouse model. In alignment with our *in vitro* results, we observed that suppressing HMGB1 expression by the treatment of glycyrrhizin stimulated autophagy in gastric tissues. Inflammation is a significant concern during *H. pylori* infection, as it leads to gastric tissue damage and exacerbates the disease complications (**Lamb et al., 2013**). In this context, glycyrrhizin also reduces inflammation while inducing autophagy. Additionally, glycyrrhizin effectively repaired damages in gastric tissues due to *H. pylori* infection.

The existing literature suggests that HMGB1 interacts with multiple autophagy proteins to modulate the autophagy mechanism during pathogenesis (**He et al., 2017; Tang et al., 2016**). In this regard, we focussed our attention on investigating the role of HMGB1 in autophagic regulatory network and uncover the underlying mechanism of autophagy modulation during *H. pylori*-infection. Our study showed for the first time that HMGB1 interacts with two positive regulators of autophagy, a UV irradiation resistance-associated gene (UVRAG) and a WD-40 domain-containing protein (WIPI2). These are the major constituents of the human Vps34 complex during autophagy (**Morris et al., 2015**). However, in reverse pull-down assay direct interaction was not observed suggesting the probability of indirect interaction. In addition, HMGB1 also interacts with another key autophagy protein, Beclin1. Beclin1 recruits key autophagic proteins to a pre-autophagosomal structure (**Morris et al., 2015**), thereby forming the core complex consisting of Beclin1, Vps34, and Vps15. HMGB1 induces autophagy by directly binding to the autophagy protein Beclin1 disrupting Beclin1/Bcl2 interaction through the activation of ERK/MAPK pathway (**Tang et al., 2010**). Thus, HMGB1 plays a major determining factor as it pulls down important autophagic proteins to

regulate autophagy during infection. Further studies are necessary to provide a more comprehensive understanding of how HMGB1 precisely regulates autophagic pathway by interacting with other proteins, and how inhibiting HMGB1 influences host autophagosome biogenesis in response to pathogen exposure.

Moreover, extensive pharmacokinetic and pharmacodynamics studies are required for the development of glycyrrhizin as an alternative therapeutic for *H. pylori* infection. Glycyrrhizin can also be used in combination with antibiotics for better treatment of *H. pylori*-related gastric disorders.

Section 7

CONCLUSION

This thesis aimed to investigate the role of HMGB1 and unravel the underlying mechanism involved during *Helicobacter pylori* infection in both *in vitro* and *in vivo* conditions. Conclusions of this study are as follows:

- *H. pylori* infection modulates autophagy pathway and increases the expression of HMGB1 in both gastric cancer and macrophage cell lines.
- *H. pylori* downregulates autophagic flux and employs non-degradative autophagosomes to facilitate its intracellular survival and replication within gastric epithelial cells.
- The autophagy-lysosomal pathway was compromised due to an increase in Lysosomal Membrane Permeabilization (LMP) during *H. pylori* infection.
- Glycyrrhizin, an inhibitor of HMGB1 restores autophagic flux to inhibit *H. pylori* infection in AGS cells.
- Glycyrrhizin is able to inhibit *H. pylori* infection by inducing host defense mechanisms such as autophagy.
- Glycyrrhizin reduces HMGB1 expression with an increase in concentration from 50μM to 200μM in AGS cells.
- Glycyrrhizin at 200μM dose has no effect on extracellular *H. pylori* growth.
- Glycyrrhizin at 200μM reduces the burden of intracellular *H. pylori* and is also effective in the case of antibiotic-resistant strains.
- Glycyrrhizin is less/non-toxic for cells at 200μM concentration.
- Glycyrrhizin also inhibits the *H. pylori*-induced complex cascade of events, including the activation of NF-κB, cytokine production, and the generation of ROS.
- It upregulates several autophagy proteins both in *in vitro* and *in vivo* conditions.
- Inhibition of HMGB1 by using the inhibitor glycyrrhizin prevents LMP
- Inhibition of LMP induces lysosomal acidification.

- The recovered lysosomal function in turn enhanced autolysosomal degradation and concomitantly attenuated the intracellular *H. pylori* growth.
- In an *in vivo* mice model, glycyrrhizin reduces HMGB1 expression and inflammation and limits gastric tissue damages.
- The activation of HMGB1 in response to *H. pylori* infection unveils novel autophagic targets that might modulate the autophagy mechanism in gastric cells and macrophages. Multiple autophagy proteins such as Beclin1, UVRAG, and WIPI2 interact with HMGB1 during *H. pylori* infection.

Section 8

REFERENCES

- Akaike, H., Kono, K., Sugai, H., Takahashi, A., Mimura, K., Kawaguchi, Y., & Fujii, H. (2007). Expression of high mobility group box chromosomal protein-1 (HMGB-1) in gastric cancer. *Anticancer research*, 27(1A), 449-457.
- Akopyants, N. S., Clifton, S. W., Kersulyte, D., Crabtree, J. E., Youree, B. E., Reece, C. A., & Berg, D. E. (1998). Analyses of the cag pathogenicity island of *Helicobacter pylori*. *Molecular microbiology*, 28(1), 37-53.
- Alm, R. A., & Trust, T. J. (1999). Analysis of the genetic diversity of *Helicobacter pylori*: the tale of two genomes. *Journal of molecular medicine*, 77, 834-846.
- Altobelli, A., Bauer, M., Velez, K., Cover, T. L., & Müller, A. (2019). *Helicobacter pylori* VacA targets myeloid cells in the gastric lamina propria to promote peripherally induced regulatory T-cell differentiation and persistent infection. *MBio*, 10(2), 10-1128.
- Amieva, M. R., Salama, N. R., Tompkins, L. S., & Falkow, S. (2002). *Helicobacter pylori* enter and survive within multivesicular vacuoles of epithelial cells. *Cellular microbiology*, 4(10), 677-690.
- Andersen, L. P., & Espersen, F. R. A. N. K. (1992). Immunoglobulin G antibodies to *Helicobacter pylori* in patients with dyspeptic symptoms investigated by the Western immunoblot technique. *Journal of clinical microbiology*, 30(7), 1743-1751.
- Andersen, L. P., Elsborg, L., & Justesen, T. (1988). *Campylobacter pylori* in peptic ulcer diseases. II: Endoscopy and microbiological findings. *Scandinavian Journal of Gastroenterology*, 23, 760-764.
- Andersen, L. P., Holck, S., Povlsen, C. O., Elsborg, L., & Justesen, T. (1987). *Campylobacter pyloridis* in peptic ulcer disease: I. Gastric and duodenal infection caused by *C. pyloridis*: histopathologic and microbiologic findings. *Scandinavian journal of gastroenterology*, 22(2), 219-224.
- Andersen, L. P., Nørgaard, A., Holck, S., Blom, J., & Elsborg, L. (1996). Isolation of a “*Helicobacter heilmanii*”-like organism from the human stomach. *European Journal of Clinical Microbiology and Infectious Diseases*, 15, 95-96.

- ANDERSEN, L. P., RASKOV, H., ELSBORG, L., HOLCK, S., JUSTESEN, T., HANSEN, B. F., ... & GAARSLEV, K. (1992). Prevalence of antibodies against heat-stable antigens from *Helicobacter pylori* in patients with dyspeptic symptoms and normal persons. *Apmis*, 100(7-12), 779-789.
- Andersson, U., Yang, H., & Harris, H. (2018, August). High-mobility group box 1 protein (HMGB1) operates as an alarmin outside as well as inside cells. In *Seminars in immunology* (Vol. 38, pp. 40-48). Academic Press.
- Arnold, M., Moore, S. P., Hassler, S., Ellison-Loschmann, L., Forman, D., & Bray, F. (2014). The burden of stomach cancer in indigenous populations: a systematic review and global assessment. *Gut*, 63(1), 64-71.
- Asahi, M., Azuma, T., Ito, S., Ito, Y., Suto, H., Nagai, Y., ... & Sasakawa, C. (2000). *Helicobacter pylori* CagA protein can be tyrosine phosphorylated in gastric epithelial cells. *The Journal of experimental medicine*, 191(4), 593-602.
- Backert, S., Müller, E. C., Jungblut, P. R., & Meyer, T. F. (2001). Tyrosine phosphorylation patterns and size modification of the *Helicobacter pylori* CagA protein after translocation into gastric epithelial cells. *PROTEOMICS: International Edition*, 1(4), 608-617.
- Bagheri, N., Azadegan-Dehkordi, F., Shirzad, H., Rafieian-Kopaei, M., Rahimian, G., & Razavi, A. (2015). The biological functions of IL-17 in different clinical expressions of *Helicobacter pylori*-infection. *Microbial pathogenesis*, 81, 33-38.
- Baldari, C. T., Lanzavecchia, A., & Telford, J. L. (2005). Immune subversion by *Helicobacter pylori*. *Trends in immunology*, 26(4), 199-207.
- Beier, D., & Frank, R. (2000). Molecular characterization of two-component systems of *Helicobacter pylori*. *Journal of Bacteriology*, 182(8), 2068-2076.
- Belgrano, F. S., de Abreu da Silva, I. C., Bastos de Oliveira, F. M., Fantappiè, M. R., & Mohana-Borges, R. (2013). Role of the acidic tail of high mobility group protein B1 (HMGB1) in protein stability and DNA bending. *PLoS One*, 8(11), e79572.
- Berthenet, E., Yahara, K., Thorell, K., Pascoe, B., Meric, G., Mikhail, J. M., ... & Sheppard, S. K. (2018). A GWAS on *Helicobacter pylori* strains points to genetic variants associated with gastric cancer risk. *BMC biology*, 16, 1-11.

- Bianchi, M. E., Falciola, L., Ferrari, S., & Lilley, D. (1992). The DNA binding site of HMG1 protein is composed of two similar segments (HMG boxes), both of which have counterparts in other eukaryotic regulatory proteins. *The EMBO journal*, *11*(3), 1055-1063.
- Birmingham, C. L., Smith, A. C., Bakowski, M. A., Yoshimori, T., & Brumell, J. H. (2006). Autophagy controls Salmonella infection in response to damage to the Salmonella-containing vacuole. *Journal of Biological Chemistry*, *281*(16), 11374-11383.
- Blair, R. H., Horn, A. E., Pazhani, Y., Grado, L., Goodrich, J. A., & Kugel, J. F. (2016). The HMGB1 C-terminal tail regulates DNA bending. *Journal of molecular biology*, *428*(20), 4060-4072.
- Blaser, M. J. (1990). Helicobacter pylori and the pathogenesis of gastroduodenal inflammation. *Journal of Infectious diseases*, *161*(4), 626-633.
- Blaser, M. J. (1992). Hypotheses on the pathogenesis and natural history of Helicobacter pylori-induced inflammation. *Gastroenterology*, *102*(2), 720-727.
- Blaser, M. J. (1997). Ecology of Helicobacter pylori in the human stomach. *The Journal of clinical investigation*, *100*(4), 759-762.
- Bordin, D. S., Voynovan, I. N., Andreev, D. N., & Maev, I. V. (2021). Current Helicobacter pylori diagnostics. *Diagnostics*, *11*(8), 1458.
- Bravo, J., Díaz, P., Corvalán, A. H., & Quest, A. F. (2019). A novel role for Helicobacter pylori gamma-glutamyltranspeptidase in regulating autophagy and bacterial internalization in human gastric cells. *Cancers*, *11*(6), 801.
- Brown, L. M. (2000). Helicobacter pylori: epidemiology and routes of transmission. *Epidemiologic reviews*, *22*(2), 283-297.
- Buck, G. E. (1990). Campylobacter pylori and gastroduodenal disease. *Clinical microbiology reviews*, *3*(1), 1-12.
- Bujanda, L., Nyssen, O. P., Vaira, D., Saracino, I. M., Fiorini, G., Lerang, F., ... & Hp-EuReg Investigators. (2021). Antibiotic resistance prevalence and trends in patients infected with Helicobacter pylori in the period 2013–2020: Results of the European Registry on H. pylori Management (Hp-EuReg). *Antibiotics*, *10*(9), 1058.

- Bukholm, G., Tannaes, T., Nedenskov, P., Esbensen, Y., Grav, H. J., Hovig, T., ... & Guldvog, I. (1997). Colony variation of *Helicobacter pylori*: pathogenic potential is correlated to cell wall lipid composition. *Scandinavian journal of gastroenterology*, 32(5), 445-454.
- Camargo, M. C., García, A., Riquelme, A., Otero, W., Camargo, C. A., Hernandez-García, T. & Rabkin, C. S. (2014). The problem of *Helicobacter pylori* resistance to antibiotics: a systematic review in Latin America. *The American journal of gastroenterology*, 109(4), 485.
- Capurro, M. I., Prashar, A., & Jones, N. L. (2020). MCOLN1/TRPML1 inhibition-a novel strategy used by *Helicobacter pylori* to escape autophagic killing and antibiotic eradication therapy in vivo. *Autophagy*, 16(1), 169-170.
- Caroff, M., & Novikov, A. (2019). LPS structure, function, and heterogeneity. *Endotoxin detection and control in pharma, limulus, and mammalian systems*, 53-93.
- Censini, S., Lange, C., Xiang, Z., Crabtree, J. E., Ghiara, P., Borodovsky, M., ... & Covacci, A. (1996). *cag*, a pathogenicity island of *Helicobacter pylori*, encodes type I-specific and disease-associated virulence factors. *Proceedings of the National Academy of Sciences*, 93(25), 14648-14653.
- Chambers, M. G., Pyburn, T. M., González-Rivera, C., Collier, S. E., Eli, I., Yip, C. K., ... & Ohi, M. D. (2013). Structural analysis of the oligomeric states of *Helicobacter pylori* VacA toxin. *Journal of molecular biology*, 425(3), 524-535.
- Chan WY, Hui PK, Leung KM, Chow J, Kwok F, Ng CS (October 1994). "Coccoid forms of *Helicobacter pylori* in the human stomach". *American Journal of Clinical Pathology*. **102** (4): 503–7
- Chen, X., Li, P., Shen, Y., Zou, Y., Yuan, G., & Hu, H. (2019). Rhamnolipid-involved antibiotics combinations improve the eradication of *Helicobacter pylori* biofilm in vitro: A comparison with conventional triple therapy. *Microbial pathogenesis*, 131, 112-119.
- Cheng, P., Dai, W., Wang, F., Lu, J., Shen, M., Chen, K., ... & Xu, L. (2014). Ethyl pyruvate inhibits proliferation and induces apoptosis of hepatocellular carcinoma via regulation of the HMGB1–RAGE and AKT pathways. *Biochemical and biophysical research communications*, 443(4), 1162-1168.

- Chevalier, C., Thiberge, J. M., Ferrero, R. L., & Labigne, A. (1999). Essential role of *Helicobacter pylori*-glutamyltranspeptidase for the colonization of the gastric mucosa of mice. *Molecular microbiology*, 31(5), 1359-1372.
- Chmiela, M., & Gonciarz, W. (2017). Molecular mimicry in *Helicobacter pylori* infections. *World journal of gastroenterology*, 23(22), 3964.
- Chu, T. H., Huang, S. T., Yang, S. F., Li, C. J., Lin, H. W., Weng, B. C., ... & Tai, M. H. (2019). Hepatoma-derived growth factor participates in *Helicobacter Pylori*-induced neutrophils recruitment, gastritis and gastric carcinogenesis. *Oncogene*, 38(37), 6461-6477.
- Chu, Y.T. et al. (2010) Invasion and multiplication of *Helicobacter pylori* in gastric epithelial cells and implications for antibiotic resistance. *Infect. Immun.* 78, 4157–4165
- Conti, L., Lanzardo, S., Arigoni, M., Antonazzo, R., Radaelli, E., Cantarella, D., ... & Cavallo, F. (2013). The noninflammatory role of high mobility group box 1/toll-like receptor 2 axis in the self-renewal of mammary cancer stem cells. *The FASEB Journal*, 27(12), 4731-4744.
- Cortes, M. C. C., Yamakawa, A., Casingal, C. R., Fajardo, L. S. N., Juan, M. L. G., De Guzman, B. B., ... & Azuma, T. (2010). Diversity of the *cagA* gene of *Helicobacter pylori* strains from patients with gastroduodenal diseases in the Philippines. *FEMS Immunology & Medical Microbiology*, 60(1), 90-97.
- Covacci, A., & Rappuoli, R. (1998). *Helicobacter pylori*: molecular evolution of a bacterial quasi-species. *Current opinion in Microbiology*, 1(1), 96-102.
- Covacci, A., & Rappuoli, R. (2000). Tyrosine-phosphorylated bacterial proteins: Trojan horses for the host cell. *The Journal of experimental medicine*, 191(4), 587-592.
- Crowe, S. E. (2019). *Helicobacter pylori* infection. *New England Journal of Medicine*, 380(12), 1158-1165.
- de Martel, C., Georges, D., Bray, F., Ferlay, J., & Clifford, G. M. (2020). Global burden of cancer attributable to infections in 2018: a worldwide incidence analysis. *The Lancet Global Health*, 8(2), e180-e190.
- Deffieu, M., Bhatia-Kissova, I., Salin, B., Galinier, A., Manon, S., & Camougrand, N. (2009). Glutathione participates in the regulation of mitophagy in yeast. *Journal of Biological Chemistry*, 284(22), 14828-14837.

- Didelot, X., Nell, S., Yang, I., Woltemate, S., Van der Merwe, S., & Suerbaum, S. (2013). Genomic evolution and transmission of *Helicobacter pylori* in two South African families. *Proceedings of the National Academy of Sciences*, 110(34), 13880-13885.
- Dikic, I., & Elazar, Z. (2018). Mechanism and medical implications of mammalian autophagy. *Nature reviews Molecular cell biology*, 19(6), 349-364.
- Dortet, L., Mostowy, S., Louaka, A. S., Gouin, E., Nahori, M. A., Wiemer, E. A., ... & Cossart, P. (2011). Recruitment of the major vault protein by InlK: a *Listeria monocytogenes* strategy to avoid autophagy. *PLoS pathogens*, 7(8), e1002168.
- Dubois, A., & Borén, T. (2007). *Helicobacter pylori* is invasive and it may be a facultative intracellular organism. *Cellular microbiology*, 9(5), 1108-1116.
- Dumitriu, I. E., Baruah, P., Valentinis, B., Voll, R. E., Herrmann, M., Nawroth, P. P., ... & Rovere-Querini, P. (2005). Release of high mobility group box 1 by dendritic cells controls T cell activation via the receptor for advanced glycation end products. *The Journal of Immunology*, 174(12), 7506-7515.
- Dunn, Jr, W. A., Cregg, J. M., Kiel, J. A., Klei, I. J. V. D., Oku, M., Sakai, Y., ... & Veenhuis, M. (2005). Pexophagy: the selective autophagy of peroxisomes. *Autophagy*, 1(2), 75-83.
- Ernst, E. (1999). Is garlic an effective treatment for *Helicobacter pylori* infection?. *Archives of internal medicine*, 159(20), 2484-2485.
- Eskelinen, E. L., Illert, A. L., Tanaka, Y., Schwarzmann, G., Blanz, J., Von Figura, K., & Saftig, P. (2002). Role of LAMP-2 in lysosome biogenesis and autophagy. *Molecular biology of the cell*, 13(9), 3355-3368.
- Eslami, M., Yousefi, B., Kokhaei, P., Arabkari, V., & Ghasemian, A. (2019). Current information on the association of *Helicobacter pylori* with autophagy and gastric cancer. *Journal of cellular physiology*, 234(9), 14800-14811.
- Fader, C. M., Sánchez, D. G., Mestre, M. B., & Colombo, M. I. (2009). TI-VAMP/VAMP7 and VAMP3/cellubrevin: two v-SNARE proteins involved in specific steps of the autophagy/multivesicular body pathways. *Biochimica et Biophysica Acta (BBA)-Molecular Cell Research*, 1793(12), 1901-1916.

- Fallone, C. A., Chiba, N., van Zanten, S. V., Fischbach, L., Gisbert, J. P., Hunt, R. H., ... & Marshall, J. K. (2016). The Toronto consensus for the treatment of *Helicobacter pylori* infection in adults. *Gastroenterology*, *151*(1), 51-69.
- Fallone, C. A., Moss, S. F., & Malfertheiner, P. (2019). Reconciliation of recent *Helicobacter pylori* treatment guidelines in a time of increasing resistance to antibiotics. *Gastroenterology*, *157*(1), 44-53.
- Fan X., Long A., Goggins M., Fan X., Keeling P. W., Kelleher D. (1996). Expression
- Fann, J. C. Y., Chiang, T. H., Yen, A. M. F., Lee, Y. C., Wu, M. S., & Chen, H. H. (2018). Personalized risk assessment for dynamic transition of gastric neoplasms. *Journal of Biomedical Science*, *25*, 1-10.
- Fedele, A. O., & Proud, C. G. (2020). Chloroquine and bafilomycin A mimic lysosomal storage disorders and impair mTORC1 signalling. *Bioscience reports*, *40*(4), BSR20200905.
- Feng, L., Liang, L., Zhang, S., Yang, J., Yue, Y., & Zhang, X. (2022). HMGB1 downregulation in retinal pigment epithelial cells protects against diabetic retinopathy through the autophagy-lysosome pathway. *Autophagy*, *18*(2), 320-339.
- Feng, L., Liang, L., Zhang, S., Yang, J., Yue, Y., & Zhang, X. (2022). HMGB1 downregulation in retinal pigment epithelial cells protects against diabetic retinopathy through the autophagy-lysosome pathway. *Autophagy*, *18*(2), 320-339.
- Feng, Y., He, D., Yao, Z., & Klionsky, D. J. (2014). The machinery of macroautophagy. *Cell research*, *24*(1), 24-41.
- Fersching, D. M., Stoetzer, O. J., Siegele, B., Nagel, D., & Holdenrieder, S. (2010, August). Nucleosomes, rage and hmgbl in predicting response to neoadjuvant chemotherapy in breast cancer patients. In *TUMOR BIOLOGY* (Vol. 31, pp. S99-S99). VAN GODEWIJCKSTRAAT 30, 3311 GZ DORDRECHT, NETHERLANDS: SPRINGER.
- Fox, J. G. (1995). Non-human reservoirs of *Helicobacter pylori*. *Alimentary pharmacology & therapeutics*, *9*, 93-103.
- Fu, Y., Zhou, E., Wei, Z., Liang, D., Wang, W., Wang, T., ... & Yang, Z. (2014). Glycyrrhizin inhibits the inflammatory response in mouse mammary epithelial cells and a mouse mastitis model. *The FEBS journal*, *281*(11), 2543-2557.

- Galluzzi, L., Bravo-San Pedro, J. M., Levine, B., Green, D. R., & Kroemer, G. (2017). Pharmacological modulation of autophagy: therapeutic potential and persisting obstacles. *Nature reviews Drug discovery*, 16(7), 487-511.
- Gao, L., Weck, M. N., Nieters, A., & Brenner, H. (2009). Inverse association between a pro-inflammatory genetic profile and *Helicobacter pylori* seropositivity among patients with chronic atrophic gastritis: enhanced elimination of the infection during disease progression?. *European journal of cancer*, 45(16), 2860-2866.
- Glick, D., Barth, S., & Macleod, K. F. (2010). Autophagy: cellular and molecular mechanisms. *The Journal of pathology*, 221(1), 3-12.
- Gnanasekar, M., Thirugnanam, S., & Ramaswamy, K. (2009). Short hairpin RNA (shRNA) constructs targeting high mobility group box-1 (HMGB1) expression leads to inhibition of prostate cancer cell survival and apoptosis. *International journal of oncology*, 34(2), 425-431.
- González, C. A., & López-Carrillo, L. (2010). *Helicobacter pylori*, nutrition and smoking interactions: their impact in gastric carcinogenesis. *Scandinavian journal of gastroenterology*, 45(1), 6-14.
- Goodwin CS, McConnell W, McCulloch RK, McCullough C, Hill R, Bronsdon MA and Kasper G (1989a) Cellular fatty acid composition of *Campylobacter pylori* from primates and ferrets compared with those of other *campylobacters*. *J Clin Microbiol*. 27:938-943.
- Goodwin, C. S., & Armstrong, J. A. (1990). Microbiological aspects of *Helicobacter pylori* (*Campylobacter pylori*). *European Journal of Clinical Microbiology and Infectious Diseases*, 9, 1-13.
- Goodwin, C. S., & Worsley, B. W. (1993). Microbiology of *Helicobacter pylori*. *Gastroenterology Clinics of North America*, 22(1), 5-19.
- Goodwin, C. S., McCulloch, R. K., Armstrong, J. A., & Wee, S. H. (1985). Unusual cellular fatty acids and distinctive ultrastructure in a new spiral bacterium (*Campylobacter pyloridis*) from the human gastric mucosa. *Journal of medical microbiology*, 19(2), 257-267.

- Goodwin, G. H., Sanders, C., & Johns, E. W. (1973). A new group of chromatin-associated proteins with a high content of acidic and basic amino acids. *European Journal of Biochemistry*, 38(1), 14-19.
- Graham, D. Y., & Fischbach, L. (2010). Helicobacter pylori treatment in the era of increasing antibiotic resistance. *Gut*, 59(8), 1143-1153.
- Gu, H. (2017). Role of Flagella in the Pathogenesis of Helicobacter pylori. *Current microbiology*, 74, 863-869.
- Hachem, C. Y., Clarridge, J. E., Evans, D. G., & Graham, D. Y. (1995). Comparison of agar based media for primary isolation of Helicobacter pylori. *Journal of clinical pathology*, 48(8), 714-716.
- Hacker, J., Blum-Oehler, G., Mühldorfer, I., & Tschäpe, H. (1997). Pathogenicity islands of virulent bacteria: structure, function and impact on microbial evolution. *Molecular microbiology*, 23(6), 1089-1097.
- Haeussler, S., Köhler, F., Witting, M., Premm, M. F., Rolland, S. G., Fischer, C., ... & Conradt, B. (2020). Autophagy compensates for defects in mitochondrial dynamics. *PLoS genetics*, 16(3), e1008638.
- Haque, M., Hirai, Y., Yokota, K., Mori, N., Jahan, I., Ito, H., ... & Oguma, K. (1996). Lipid profile of Helicobacter spp.: presence of cholesteryl glucoside as a characteristic feature. *Journal of bacteriology*, 178(7), 2065-2070.
- Hatakeyama, M. (2017). Structure and function of Helicobacter pylori CagA, the first-identified bacterial protein involved in human cancer. *Proceedings of the Japan Academy, Series B*, 93(4), 196-219.
- Hazell, S. L., & Graham, D. Y. (1990). Unsaturated fatty acids and viability of Helicobacter (Campylobacter) pylori. *Journal of clinical microbiology*, 28(5), 1060-1061.
- He, Z. W., Qin, Y. H., Wang, Z. W., Chen, Y., Shen, Q., & Dai, S. M. (2013). HMGB1 acts in synergy with lipopolysaccharide in activating rheumatoid synovial fibroblasts via p38 MAPK and NF- κ B signaling pathways. *Mediators of inflammation*, 2013.
- Henriksen, T. H., Brorson, Ö., Schøyen, R., Thoresen, T., Setegn, D., & Madebo, T. (1995). Rapid growth of Helicobacter pylori. *European journal of clinical microbiology and infectious diseases*, 14, 1008-1011.

- Hooi, J. K., Lai, W. Y., Ng, W. K., Suen, M. M., Underwood, F. E., Tanyingoh, D., ... & Ng, S. C. (2017). Global prevalence of *Helicobacter pylori* infection: systematic review and meta-analysis. *Gastroenterology*, 153(2), 420-429.
- Howitt, M. R., Lee, J. Y., Lertsethtakarn, P., Vogelmann, R., Joubert, L. M., Ottemann, K. M., & Amieva, M. R. (2011). ChePep controls *Helicobacter pylori* infection of the gastric glands and chemotaxis in the Epsilonproteobacteria. *MBio*, 2(4), 10-1128.
- Hu, W., Chan, H., Lu, L., Wong, K. T., Wong, S. H., Li, M. X., ... & Zhang, L. (2020, May). Autophagy in intracellular bacterial infection. In *Seminars in cell & developmental biology* (Vol. 101, pp. 41-50). Academic Press.
- Huang, W. P., Scott, S. V., Kim, J., & Klionsky, D. J. (2000). The itinerary of a vesicle component, Aut7p/Cvt5p, terminates in the yeast vacuole via the autophagy/Cvt pathways. *Journal of Biological Chemistry*, 275(8), 5845-5851.
- Hurley, J. H., & Young, L. N. (2017). Mechanisms of autophagy initiation. *Annual review of biochemistry*, 86, 225-244.
- Ihamaki, T., Kekki, M., Sipponen, P., & Siurala, M. (1985). The sequelae and course of chronic gastritis during a 30-to 34-year bioptic follow-up study. *Scandinavian journal of gastroenterology*, 20(4), 485-491.
- Ilver, D., Arnqvist, A., Ogren, J., Frick, I. M., Kersulyte, D., Incecik, E. T., ... & Borén, T. (1998). *Helicobacter pylori* adhesin binding fucosylated histo-blood group antigens revealed by retagging. *Science*, 279(5349), 373-377.
- Jia, L., Clear, A., Liu, F. T., Matthews, J., Uddin, N., McCarthy, A., ... & Gribben, J. G. (2014). Extracellular HMGB1 promotes differentiation of nurse-like cells in chronic lymphocytic leukemia. *Blood, The Journal of the American Society of Hematology*, 123(11), 1709-1719.
- Jiang, S. J., Liu, W. Z., Zhang, D. Z., Shi, Y., Xiao, S. D., Zhang, Z. H., & Lu, D. Y. (1987). Campylobacter-like organisms in chronic gastritis, peptic ulcer, and gastric carcinoma. *Scandinavian journal of gastroenterology*, 22(5), 553-558.
- Jones, K. R., Whitmire, J. M., & Merrell, D. S. (2010). A tale of two toxins: *Helicobacter pylori* CagA and VacA modulate host pathways that impact disease. *Frontiers in microbiology*, 1, 115.

- Jorgensen, M., Daskalopoulos, G., Warburton, V., Mitchell, H. M., & Hazell, S. L. (1996). Multiple strain colonization and metronidazole resistance in *Helicobacter pylori*-infected patients: identification from sequential and multiple biopsy specimens. *Journal of infectious Diseases*, 174(3), 631-635.
- Kang, R., Livesey, K. M., Zeh, III, H. J., Loze, M. T., & Tang, D. (2010). HMGB1: a novel Beclin 1-binding protein active in autophagy. *Autophagy*, 6(8), 1209-1211.
- Kabeya, Y., Mizushima, N., Yamamoto, A., Oshitani-Okamoto, S., Ohsumi, Y., & Yoshimori, T. (2004). LC3, GABARAP and GATE16 localize to autophagosomal membrane depending on form-II formation. *Journal of cell science*, 117(13), 2805-2812.
- Khambu, B., Hong, H., Liu, S., Liu, G., Chen, X., Dong, Z., ... & Yin, X. M. (2020). The HMGB1-RAGE axis modulates the growth of autophagy-deficient hepatic tumors. *Cell Death & Disease*, 11(5), 333.
- Khatoon, J., Rai, R. P., & Prasad, K. N. (2016). Role of *Helicobacter pylori* in gastric cancer: Updates. *World journal of gastrointestinal oncology*, 8(2), 147.
- Kim, I. J., & Blanke, S. R. (2012). Remodeling the host environment: modulation of the gastric epithelium by the *Helicobacter pylori* vacuolating toxin (VacA). *Frontiers in cellular and infection microbiology*, 2, 37.
- Kim, J. Y., Park, J. S., Strassheim, D., Douglas, I., Diaz del Valle, F., Asehnoune, K., ... & Abraham, E. (2005). HMGB1 contributes to the development of acute lung injury after hemorrhage. *American Journal of Physiology-Lung Cellular and Molecular Physiology*, 288(5), L958-L965.
- Kim, J., Kundu, M., Viollet, B., & Guan, K. L. (2011). AMPK and mTOR regulate autophagy through direct phosphorylation of Ulk1. *Nature cell biology*, 13(2), 132-141.
- Kirisako, T., Baba, M., Ishihara, N., Miyazawa, K., Ohsumi, M., Yoshimori, T., ... & Ohsumi, Y. (1999). Formation process of autophagosome is traced with Apg8/Aut7p in yeast. *The Journal of cell biology*, 147(2), 435-446.
- Kivi, M., Tindberg, Y., Sörberg, M., Casswall, T. H., Befrits, R., Hellström, P. M., ... & Granström, M. (2003). Concordance of *Helicobacter pylori* strains within families. *Journal of clinical microbiology*, 41(12), 5604-5608.

- Klionsky, D. J. (2008). Autophagy revisited: a conversation with Christian de Duve. *Autophagy*, 4(6), 740-743.
- Kohles, N., Nagel, D., Jüngst, D., Stieber, P., & Holdenrieder, S. (2012). Predictive value of immunogenic cell death biomarkers HMGB1, sRAGE, and DNase in liver cancer patients receiving transarterial chemoembolization therapy. *Tumor Biology*, 33, 2401-2409.
- Kojima, K. K., Furuta, Y., Yahara, K., Fukuyo, M., Shiwa, Y., Nishiumi, S., ... & Kobayashi, I. (2016). Population evolution of *Helicobacter pylori* through diversification in DNA methylation and interstrain sequence homogenization. *Molecular biology and evolution*, 33(11), 2848-2859.
- Kokkola, R., Li, J., Sundberg, E., Aveberger, A. C., Palmblad, K., Yang, H., ... & Harris, H. E. (2003). Successful treatment of collagen-induced arthritis in mice and rats by targeting extracellular high mobility group box chromosomal protein 1 activity. *Arthritis & Rheumatism: Official Journal of the American College of Rheumatology*, 48(7), 2052-2058.
- Kozlova, A. L., Valieva, M. E., Maluchenko, N. V., & Studitsky, V. M. (2018). HMGB proteins as DNA chaperones that modulate chromatin activity. *Molecular Biology*, 52, 637-647.
- Krauss-Etschmann, S., Gruber, R., Plikat, K., Antoni, I., Demmelmair, H., Reinhardt, D., & Koletzko, S. (2005). Increase of antigen-presenting cells in the gastric mucosa of *Helicobacter pylori*-infected children. *Helicobacter*, 10(3), 214-222.
- Kuchitsu, Y., & Fukuda, M. (2018). Revisiting Rab7 functions in mammalian autophagy: Rab7 knockout studies. *Cells*, 7(11), 215.
- Kuipers, E. J., Thijs, J. C., & Festen, H. P. (1995). The prevalence of *Helicobacter pylori* in peptic ulcer disease. *Alimentary pharmacology & therapeutics*, 9, 59-69.
- Kumar, S., Metz, D. C., Ellenberg, S., Kaplan, D. E., & Goldberg, D. S. (2020). Risk factors and incidence of gastric cancer after detection of *Helicobacter pylori* infection: a large cohort study. *Gastroenterology*, 158(3), 527-536.
- Lam, S. Y., Mommersteeg, M. C., Yu, B., Broer, L., Spaander, M. C., Frost, F., ... & Peppelenbosch, M. P. (2022). Toll-like receptor 1 locus re-examined in a genome-

- wide association study update on anti-*Helicobacter pylori* IgG titers. *Gastroenterology*, 162(6), 1705-1715.30.
- Lanas, A., & Chan, F. K. (2017). Peptic ulcer disease. *The Lancet*, 390(10094), 613-624.
- Lee, S. A., Kwak, M. S., Kim, S., & Shin, J. S. (2014). The role of high mobility group box 1 in innate immunity. *Yonsei medical journal*, 55(5), 1165-1176.
- Levine, B., Mizushima, N., & Virgin, H. W. (2011). Autophagy in immunity and inflammation. *Nature*, 469(7330), 323-335.
- Li, B., Jiang, S. D., Zheng, X. F., Ni, B. B., Yang, Y. H., Chen, J. W., ... & Jiang, L. S. (2013). Expression of the inflammatory molecule hmgb1 in human osteosarcoma and its clinical relevance. *European Journal of Inflammation*, 11(1), 61-73.
- Li, N., Tang, B., Jia, Y. P., Zhu, P., Zhuang, Y., Fang, Y., ... & Zou, Q. M. (2017). *Helicobacter pylori* CagA protein negatively regulates autophagy and promotes inflammatory response via c-Met-PI3K/Akt-mTOR signaling pathway. *Frontiers in cellular and infection microbiology*, 7, 417.
- Li, W. W., Li, J., & Bao, J. K. (2012). Microautophagy: lesser-known self-eating. *Cellular and molecular life sciences*, 69, 1125-1136.
- Li, Y., Wandering-Ness, A., Goldenring, J. R., & Cover, T. L. (2004). Clustering and redistribution of late endocytic compartments in response to *Helicobacter pylori* vacuolating toxin. *Molecular biology of the cell*, 15(4), 1946-1959.
- Liang, Y., Hou, C., Kong, J., Wen, H., Zheng, X., Wu, L., ... & Chen, Y. (2015). HMGB1 binding to receptor for advanced glycation end products enhances inflammatory responses of human bronchial epithelial cells by activating p38 MAPK and ERK1/2. *Molecular and cellular biochemistry*, 405, 63-71.
- Lin, H. J., Hsu, F. Y., Chen, W. W., Lee, C. H., Lin, Y. J., Chen, Y. Y. M., ... & Lai, C. H. (2016). *Helicobacter pylori* activates HMGB1 expression and recruits RAGE into lipid rafts to promote inflammation in gastric epithelial cells. *Frontiers in Immunology*, 7, 341.
- Lind, T., Mégraud, F., Unge, P., Bayerdörffer, E., O'Morain, C., Spiller, R., ... & Cederberg, C. (1999). The MACH2 study: role of omeprazole in eradication of *Helicobacter pylori* with 1-week triple therapies. *Gastroenterology*, 116(2), 248-253.

- Liou, J. M., Fang, Y. J., Chen, C. C., Bair, M. J., Chang, C. Y., Lee, Y. C., ... & Wu, M. S. (2016). Concomitant, bismuth quadruple, and 14-day triple therapy in the first-line treatment of *Helicobacter pylori*: a multicentre, open-label, randomised trial. *The Lancet*, 388(10058), 2355-2365.
- Liou, J. M., Lin, J. T., Wang, H. P., Huang, S. P., Lee, Y. C., Chiu, H. M., ... & Wu, M. S. (2007). IL-1B-511 C→ T polymorphism is associated with increased host susceptibility to *Helicobacter pylori* infection in Chinese. *Helicobacter*, 12(2), 142-149.
- Liou, J. M., Malfertheiner, P., Lee, Y. C., Sheu, B. S., Sugano, K., Cheng, H. C., ... & El-Omar, E. M. (2020). Screening and eradication of *Helicobacter pylori* for gastric cancer prevention: the Taipei global consensus. *Gut*, 69(12), 2093-2112.
- Liu, H., Semino-Mora, C., & Dubois, A. (2012). Mechanism of *H. pylori* intracellular entry: an in vitro study. *Frontiers in Cellular and Infection Microbiology*, 2, 13.
- Logan, R. P., & Berg, D. E. (1996). Genetic diversity of *Helicobacter pylori*. *The Lancet*, 348(9040), 1462-1463.
- Lübke, T., Lobel, P., & Sleat, D. E. (2009). Proteomics of the lysosome. *Biochimica et Biophysica Acta (BBA)-Molecular Cell Research*, 1793(4), 625-635.
- Lv, X., Zhu, Y., Deng, Y., Zhang, S., Zhang, Q., Zhao, B., & Li, G. (2020). Glycyrrhizin improved autophagy flux via HMGB1-dependent Akt/mTOR signaling pathway to prevent Doxorubicin-induced cardiotoxicity. *Toxicology*, 441, 152508.
- Mahdavi, J., Sondén, B., Hurtig, M., Olfat, F. O., Forsberg, L., Roche, N., ... & Borén, T. (2002). *Helicobacter pylori* SabA adhesin in persistent infection and chronic inflammation. *Science*, 297(5581), 573-578.
- Malaty, H. M., El-Kasabany, A., Graham, D. Y., Miller, C. C., Reddy, S. G., Srinivasan, S. R., ... & Berenson, G. S. (2002). Age at acquisition of *Helicobacter pylori* infection: a follow-up study from infancy to adulthood. *The Lancet*, 359(9310), 931-935.
- Malfertheiner, P., Chan, F. K., & McColl, K. E. (2009). Peptic ulcer disease. *The lancet*, 374(9699), 1449-1461.
- Malfertheiner, P., Megraud, F., O'Morain, C. A., Atherton, J., Axon, A. T., Bazzoli, F., ... & European *Helicobacter* Study Group. (2012). Management of *Helicobacter pylori* infection—the Maastricht IV/Florence consensus report. *Gut*, 61(5), 646-664.

- Malfertheiner, P., Megraud, F., O'morain, C. A., Gisbert, J. P., Kuipers, E. J., Axon, A. T., ... & El-Omar, E. M. (2017). Management of *Helicobacter pylori* infection—the Maastricht V/Florence consensus report. *Gut*, 66(1), 6-30.
- Malicdan MC, Noguchi S, Nishino I (2007) Autophagy in a mouse model of distal myopathy with rimmed vacuoles or hereditary inclusion body myopathy. *Autophagy* 3:396–398.
- Malicdan, M. C. V., Noguchi, S., & Nishino, I. (2007). Autophagy in a mouse model of distal myopathy with rimmed vacuoles or hereditary inclusion body myopathy. *Autophagy*, 3(4), 396-398.
- Mao K, Klionsky DJ. (2017). Xenophagy: a battlefield between host and microbe, and a possible avenue for cancer treatment. *Autophagy* 13(2), 223–24.
- Marshall, B. J., Armstrong, J. A., McGeachie, D. B., & Clancy, R. J. (1985). Attempt to fulfil Koch's postulates for pyloric *Campylobacter*. *Medical Journal of Australia*, 142(8), 436-439.
- Martínez, L. E., Hardcastle, J. M., Wang, J., Pincus, Z., Tsang, J., Hoover, T. R., & Salama, N. R. (2016). *Helicobacter pylori* strains vary cell shape and flagellum number to maintain robust motility in viscous environments. *Molecular microbiology*, 99(1), 88-110.
- Mayerle, J., den Hoed, C. M., Schurmann, C., Stolk, L., Homuth, G., Peters, M. J., ... & Kuipers, E. J. (2013). Identification of genetic loci associated with *Helicobacter pylori* serologic status. *Jama*, 309(18), 1912-1920.
- McGowan, C. C., Necheva, A. S., Forsyth, M. H., Cover, T. L., & Blaser, M. J. (2003). Promoter analysis of *Helicobacter pylori* genes with enhanced expression at low pH. *Molecular microbiology*, 48(5), 1225-1239.
- Megraud, F., Coenen, S., Versporten, A., Kist, M., Lopez-Brea, M., Hirschl, A. M., ... & Glupczynski, Y. (2013). *Helicobacter pylori* resistance to antibiotics in Europe and its relationship to antibiotic consumption. *Gut*, 62(1), 34-42.
- Mehrpour, M., Esclatine, A., Beau, I., & Codogno, P. (2010). Overview of macroautophagy regulation in mammalian cells. *Cell research*, 20(7), 748-762.
- Mendz GL, Burns BP and Hazell SL (1995) Characterisation of glucose transport in *Helicobacter pylori*. *Biochim Biophys Acta*. **1244**:269-276.

- Mendz, G. L., & Hazell, S. L. (1991). Evidence for a pentose phosphate pathway in *Helicobacter pylori*. *FEMS microbiology letters*, 84(3), 331-336.
- Mendz, G. L., & Hazell, S. L. (1996). The urea cycle of *Helicobacter pylori*. *Microbiology*, 142(10), 2959-2967.
- Mendz, G. L., Hazell, S. L., & Burns, B. P. (1994). The Entner-Doudoroff pathway in *Helicobacter pylori*. *Archives of biochemistry and biophysics*, 312(2), 349-356.
- Mendz, G. L., Hazell, S. L., & Srinivasan, S. (1995). Fumarate reductase: a target for therapeutic intervention against *Helicobacter pylori*. *Archives of biochemistry and biophysics*, 321(1), 153-159.
- Mercer, T. J., Gubas, A., & Tooze, S. A. (2018). A molecular perspective of mammalian autophagosome biogenesis. *Journal of biological chemistry*, 293(15), 5386-5395.
- Meyer, G., Czompa, A., Reboul, C., Csepanyi, E., Czegledi, A., Bak, I., ... & Lekli, I. (2013). The cellular autophagy markers Beclin-1 and LC3B-II are increased during reperfusion in fibrillated mouse hearts. *Current pharmaceutical design*, 19(39), 6912-6918.
- Meyer, J. M., Silliman, N. P., Wang, W., Siepmann, N. Y., Sugg, J. E., Morris, D., ... & Hopkins, R. J. (2002). Risk factors for *Helicobacter pylori* resistance in the United States: the surveillance of *H. pylori* antimicrobial resistance partnership (SHARP) study, 1993–1999. *Annals of internal medicine*, 136(1), 13-24.
- Miftahussurur, M., & Yamaoka, Y. (2016). Diagnostic methods of *Helicobacter pylori* infection for epidemiological studies: critical importance of indirect test validation. *BioMed research international*, 2016.
- Mimuro, H., Suzuki, T., Tanaka, J., Asahi, M., Haas, R., & Sasakawa, C. (2002). Grb2 is a key mediator of *Helicobacter pylori* CagA protein activities. *Molecular cell*, 10(4), 745-755.
- Mittal, D., Saccheri, F., Vénéreau, E., Pusterla, T., Bianchi, M. E., & Rescigno, M. (2010). TLR4-mediated skin carcinogenesis is dependent on immune and radioresistant cells. *The EMBO journal*, 29(13), 2242-2252.
- Mizushima, N. (2007). Autophagy: process and function. *Genes & development*, 21(22), 2861-2873.

- Mizushima, N., & Levine, B. (2010). Autophagy in mammalian development and differentiation. *Nature cell biology*, 12(9), 823-830.
- Mobley, H. L., Island, M. D., & Hausinger, R. P. (1995). Molecular biology of microbial ureases. *Microbiological reviews*, 59(3), 451-480.
- Molina-Infante, J., Lucendo, A. J., Angueira, T., Rodriguez-Tellez, M., Perez-Aisa, A., Balboa, A., ... & Prados, S. (2015). Optimised empiric triple and concomitant therapy for *Helicobacter pylori* eradication in clinical practice: the OPTRICON study. *Alimentary pharmacology & therapeutics*, 41(6), 581-589.
- Molinari, M., Salio, M., Galli, C., Norais, N., Rappuoli, R., Lanzavecchia, A., & Montecucco, C. (1998). Selective inhibition of Ii-dependent antigen presentation by *Helicobacter pylori* toxin VacA. *The Journal of experimental medicine*, 187(1), 135-140.
- Mollica, L., De Marchis, F., Spitaleri, A., Dallacosta, C., Pennacchini, D., Zamai, M., ... & Bianchi, M. E. (2007). Glycyrrhizin binds to high-mobility group box 1 protein and inhibits its cytokine activities. *Chemistry & biology*, 14(4), 431-441.
- Monteiro, M. A. (2001). *Helicobacter pylori*: a wolf in sheep's clothing: the glycotype families of *Helicobacter pylori* lipopolysaccharides expressing histo-blood groups: structure, biosynthesis, and role in pathogenesis.
- Moran, A. P., & Prendergast, M. M. (2001). Molecular mimicry in *Campylobacter jejuni* and *Helicobacter pylori* lipopolysaccharides: contribution of gastrointestinal infections to autoimmunity. *Journal of autoimmunity*, 16(3), 241-256.
- Moran, A. P., Knirel, Y. A., Sof'ya, N. S., Widmalm, G., Hynes, S. O., & Jansson, P. E. (2002). Phenotypic Variation in Molecular Mimicry between *Helicobacter pylori* Lipopolysaccharides and Human Gastric Epithelial Cell Surface Glycoforms: ACID-INDUCED PHASE VARIATION IN LEWISX AND LEWISY EXPRESSION BY H. PYLORI LIPOLYSACCHARIDES. *Journal of Biological Chemistry*, 277(8), 5785-5795.
- Morbiato, L., Tombola, F., Campello, S., Del Giudice, G., Rappuoli, R., Zoratti, M., & Papini, E. (2001). Vacuolation induced by VacA toxin of *Helicobacter pylori* requires

the intracellular accumulation of membrane permeant bases, Cl⁻ and water. *FEBS letters*, 508(3), 479-483.

Morgan, M. J., & Liu, Z. G. (2011). Crosstalk of reactive oxygen species and NF- κ B signaling. *Cell research*, 21(1), 103-115.

Moriwaka, Y., Luo, Y., Ohmori, H., Fujii, K., Tatsumoto, N., Sasahira, T., & Kuniyasu, H. (2010). HMGB1 attenuates anti-metastatic defense of the lymph nodes in colorectal cancer. *Pathobiology*, 77(1), 17-23.

Morris, A. J., Ali, M. R., Nicholson, G. I., Perez-Perez, G. I., & Blaser, M. J. (1991). Long-term follow-up of voluntary ingestion of *Helicobacter pylori*. *Annals of internal medicine*, 114(8), 662-663.

Morris, B., & Warren, J. R. (1984). Unidentified curved bacilli in the stomach of patients with gastritis and peptic ulceration. *The lancet*, 323(8390), 1311-1315.

Moss, S. F. (2017). The clinical evidence linking *Helicobacter pylori* to gastric cancer. *Cellular and molecular gastroenterology and hepatology*, 3(2), 183-191.

Muller, S., Ronfani, L., & Bianchi, M. E. (2004). Regulated expression and subcellular localization of HMGB1, a chromatin protein with a cytokine function. *Journal of internal medicine*, 255(3), 332-343.

Myran, L., & Zarbock, S. D. (2018). Management of *Helicobacter pylori* infection. *US Pharm*, 43(4), 27-32.

Nedenskov-Sørensen, P., Bjørneklett, A., Fausa, O., Bukholm, G., Aase, S., & Jantzen, E. (1988). *Campylobacter pylori* infection and its relation to chronic gastritis: an endoscopic, bacteriologic, and histomorphologic study. *Scandinavian journal of gastroenterology*, 23(7), 867-874.

Nestl, A., Von Stein, O. D., Zatloukal, K., Thies, W. G., Herrlich, P., Hofmann, M., & Sleeman, J. P. (2001). Gene expression patterns associated with the metastatic phenotype in rodent and human tumors. *Cancer research*, 61(4), 1569-1577.

Nichols, L., Sughayer, M., Degirolami, P. C., Balogh, K., Pleskow, D., Eichelberger, K., & Santos, M. (1991). Evaluation of diagnostic methods for *Helicobacter pylori* gastritis. *American journal of clinical pathology*, 95(6), 769-773.

- Niu, H., Yamaguchi, M., & Rikihisa, Y. (2008). Subversion of cellular autophagy by *Anaplasma phagocytophilum*. *Cellular microbiology*, *10*(3), 593-605.
- No, L. (1986). 20: Validation of the publication of new names and new combinations previously effectively published outside the IJSB. *Int. J. Syst. Bacteriol*, *36*, 354-356.
- Nyssen, O. P., Bordin, D., Tepes, B., Pérez-Aisa, Á., Vaira, D., Caldas, M., & Gisbert, J. P. (2021). European Registry on *Helicobacter pylori* management (Hp-EuReg): patterns and trends in first-line empirical eradication prescription and outcomes of 5 years and 21 533 patients. *Gut*, *70*(1), 40-54.
- Odenbreit, S., Till, M., Hofreuter, D., Faller, G., & Haas, R. (1999). Genetic and functional characterization of the *alpAB* gene locus essential for the adhesion of *Helicobacter pylori* to human gastric tissue. *Molecular microbiology*, *31*(5), 1537-1548.
- of CD44 and its Variants on Gastric Epithelial Cells of Patients With *Helicobacter Pylori* Colonisation. *Gut* *38* (4), 507–512.
- Ogawa, M., Yoshimori, T., Suzuki, T., Sagara, H., Mizushima, N., & Sasakawa, C. (2005). Escape of intracellular *Shigella* from autophagy. *Science*, *307*(5710), 727-731.
- Ombrellino, M., Wang, H., Ajemian, M. S., Talhouk, A., Scher, L. A., Friedman, S. G., & Tracey, K. J. (1999). Increased serum concentrations of high-mobility-group protein 1 in haemorrhagic shock. *The Lancet*, *354*(9188), 1446-1447.
- Otomo, C., Metlagel, Z., Takaesu, G., & Otomo, T. (2013). Structure of the human ATG12~ATG5 conjugate required for LC3 lipidation in autophagy. *Nature structural & molecular biology*, *20*(1), 59-66.
- Padhi, A., Pattnaik, K., Biswas, M., Jagadeb, M., Behera, A., & Sonawane, A. (2019). *Mycobacterium tuberculosis* LprE suppresses TLR2-dependent cathelicidin and autophagy expression to enhance bacterial survival in macrophages. *The Journal of Immunology*, *203*(10), 2665-2678.
- Pan, T., Kondo, S., Le, W., & Jankovic, J. (2008). The role of autophagy-lysosome pathway in neurodegeneration associated with Parkinson's disease. *Brain*, *131*(8), 1969-1978.
- Pang, X., Zhang, Y., Wei, H., Zhang, J., Luo, Q., Huang, C., & Zhang, S. (2014). Expression and effects of high-mobility group box 1 in cervical cancer. *International journal of molecular sciences*, *15*(5), 8699-8712.

- Parkin, D. M., Bray, F., Ferlay, J., & Pisani, P. (2005). Global cancer statistics, 2002. *CA: a cancer journal for clinicians*, 55(2), 74-108.
- Parsonnet, J., Friedman, G. D., Vandersteen, D. P., Chang, Y., Vogelman, J. H., Orentreich, N., & Sibley, R. K. (1991). *Helicobacter pylori* infection and the risk of gastric carcinoma. *New England Journal of Medicine*, 325(16), 1127-1131.
- Parsonnet, J., Shmueli, H., & Haggerty, T. (1999). Fecal and oral shedding of *Helicobacter pylori* from healthy infected adults. *Jama*, 282(23), 2240-2245.
- Pilotto, A., & Franceschi, M. (2014). *Helicobacter pylori* infection in older people. *World journal of gastroenterology: WJG*, 20(21), 6364.
- Prajsnar, T. K., Serba, J. J., Dekker, B. M., Gibson, J. F., Masud, S., Fleming, A., ... & Meijer, A. H. (2021). The autophagic response to *Staphylococcus aureus* provides an intracellular niche in neutrophils. *Autophagy*, 17(4), 888-902.
- Pullerits, R., Jonsson, I. M., Verdrengh, M., Bokarewa, M., Andersson, U., Erlandsson-Harris, H., & Tarkowski, A. (2003). High mobility group box chromosomal protein 1, a DNA binding cytokine, induces arthritis. *Arthritis & Rheumatism: Official Journal of the American College of Rheumatology*, 48(6), 1693-1700.
- Radić, M. (2014). Role of *Helicobacter pylori* infection in autoimmune systemic rheumatic diseases. *World Journal of Gastroenterology: WJG*, 20(36), 12839.
- Raju, D., Hussey, S., Ang, M., Terebiznik, M. R., Sibony, M., Galindo-Mata, E., ... & Jones, N. L. (2012). Vacuolating cytotoxin and variants in Atg16L1 that disrupt autophagy promote *Helicobacter pylori* infection in humans. *Gastroenterology*, 142(5), 1160-1171.
- Reeves, R. (2010). HMG nuclear proteins: linking chromatin structure to cellular phenotype. *Biochimica et biophysica acta*, 1799(1-2), 3.
- Reggiori, F., & Mauthe, M. (2016). At the Center of Autophagy: Autophagosomes. *Encyclopedia of Cell Biology*, 243.
- Reidick, C., Boutouja, F., & Platta, H. W. (2017). The class III phosphatidylinositol 3-kinase Vps34 in *Saccharomyces cerevisiae*. *Biological Chemistry*, 398(5-6), 677-685.
- Ren, W., Zhao, L., Sun, Y., Wang, X., & Shi, X. (2023). HMGB1 and Toll-like receptors: potential therapeutic targets in autoimmune diseases. *Molecular Medicine*, 29(1), 117.

- Renault, T. T., Elkholi, R., Bharti, A., & Chipuk, J. E. (2014). B cell lymphoma-2 (BCL-2) homology domain 3 (BH3) mimetics demonstrate differential activities dependent upon the functional repertoire of pro-and anti-apoptotic BCL-2 family proteins. *Journal of Biological Chemistry*, 289(38), 26481-26491.
- Robinson, K., Argent, R. H., & Atherton, J. C. (2007). The inflammatory and immune response to *Helicobacter pylori* infection. *Best practice & research Clinical gastroenterology*, 21(2), 237-259.
- Rogov, V., Dötsch, V., Johansen, T., & Kirkin, V. (2014). Interactions between autophagy receptors and ubiquitin-like proteins form the molecular basis for selective autophagy. *Molecular cell*, 53(2), 167-178.
- Roh, Y. S., & Seki, E. (2013). Toll-like receptors in alcoholic liver disease, non-alcoholic steatohepatitis and carcinogenesis. *Journal of gastroenterology and hepatology*, 28, 38-42.
- Rosenstiel, P. et al. (2006) Influence of polymorphisms in the NOD1/ CARD4 and NOD2/CARD15 genes on the clinical outcome of *Helicobacter pylori* infection. *Cell. Microbiology*. 8, 1188–1198
- Rouhiainen, A., Imai, S., Rauvala, H., & Parkkinen, J. (2000). Occurrence of amphoterin (HMG1) as an endogenous protein of human platelets that is exported to the cell surface upon platelet activation. *Thrombosis and haemostasis*, 84(12), 1087-1094.
- Saha, K., Sarkar, D., Khan, U., Karmakar, B. C., Paul, S., Mukhopadhyay, A. K., ... & Bhattacharya, S. (2022). Capsaicin inhibits inflammation and gastric damage during *H pylori* infection by targeting NF- κ B–miRNA axis. *Pathogens*, 11(6), 641.
- Satin, B., Norais, N., Rappuoli, R., Telford, J., Murgia, M., Montecucco, C., & Papini, E. (1997). Effect of *Helicobacter pylori* vacuolating toxin on maturation and extracellular release of procathepsin D and on epidermal growth factor degradation. *Journal of Biological Chemistry*, 272(40), 25022-25028.
- Savoldi, A., Carrara, E., Graham, D. Y., Conti, M., & Tacconelli, E. (2018). Prevalence of antibiotic resistance in *Helicobacter pylori*: a systematic review and meta-analysis in World Health Organization regions. *Gastroenterology*, 155(5), 1372-1382.

- Schnaith, A., Kashkar, H., Leggio, S. A., Addicks, K., Kronke, M., & Krut, O. (2007). Staphylococcus aureus subvert autophagy for induction of caspase-independent host cell death. *Journal of Biological Chemistry*, 282(4), 2695-2706.
- Schöttker, B., Adamu, M. A., Weck, M. N., & Brenner, H. (2012). Helicobacter pylori infection is strongly associated with gastric and duodenal ulcers in a large prospective study. *Clinical gastroenterology and hepatology*, 10(5), 487-493.
- Schwarz, S., Morelli, G., Kusecek, B., Manica, A., Balloux, F., Owen, R. J., ... & Suerbaum, S. (2008). Horizontal versus familial transmission of Helicobacter pylori. *PLoS pathogens*, 4(10), e1000180.
- Segal, E. D., Cha, J., Lo, J., Falkow, S., & Tompkins, L. S. (1999). Altered states: involvement of phosphorylated CagA in the induction of host cellular growth changes by Helicobacter pylori. *Proceedings of the National Academy of Sciences*, 96(25), 14559-14564.
- Semino, C., Angelini, G., Poggi, A., and Rubartelli, A. (2005). NK/iDC interaction results in IL-18 secretion by DCs at the synaptic cleft followed by NK cell activation and release of the DC maturation factor HMGB1. *Blood* 106, 609–616.
- Sengupta, S., Peterson, T. R., & Sabatini, D. M. (2010). Regulation of the mTOR complex 1 pathway by nutrients, growth factors, and stress. *Molecular cell*, 40(2), 310-322.
- Shin, D. M., Yuk, J. M., Lee, H. M., Lee, S. H., Son, J. W., Harding, C. V., & Jo, E. K. (2010). Mycobacterial lipoprotein activates autophagy via TLR2/1/CD14 and a functional vitamin D receptor signalling. *Cellular microbiology*, 12(11), 1648-1665.
- Smith, S. I., Ajayi, A., Jolaiya, T., Onyekwere, C., Setshedi, M., Schulz, C., ... & Arigbabu, A. (2022). Helicobacter pylori infection in Africa: update of the current situation and challenges. *Digestive Diseases*, 40(4), 535-544.
- Song, B., Song, W. G., Li, Z. J., Xu, Z. F., Wang, X. W., Wang, C. X., & Liu, J. (2012). Effect of HMGB1 silencing on cell proliferation, invasion and apoptosis of MGC-803 gastric cancer cells. *Cell biochemistry and function*, 30(1), 11-17.
- Søreide, K., & Sund, M. (2015). Epidemiological-molecular evidence of metabolic reprogramming on proliferation, autophagy and cell signaling in pancreas cancer. *Cancer letters*, 356(2), 281-288.

- Sorimachi, K., & Okayasu, T. (2004). Classification of eubacteria based on their complete genome: where does Mycoplasmataceae belong?. *Proceedings of the Royal Society of London. Series B: Biological Sciences*, 271(suppl_4), S127-S130.
- Stark RM, Gerwig GJ, Pitman RS, Potts LF, Williams NA, Greenman J, et al. (February 1999). "Biofilm formation by *Helicobacter pylori*". *Letters in Applied Microbiology*. **28** (2): 121–6
- Stefano, K., Marco, M., Federica, G., Laura, B., Barbara, B., Gioacchino, L., & Gian, L. D. A. (2018). *Helicobacter pylori*, transmission routes and recurrence of infection: state of the art. *Acta Bio Medica: Atenei Parmensis*, 89(Suppl 8), 72.
- Stoetzer, O. J., Fersching, D. M., Salat, C., Steinkohl, O., Gabka, C. J., Hamann, U., ... & Holdenrieder, S. (2013). Circulating immunogenic cell death biomarkers HMGB1 and RAGE in breast cancer patients during neoadjuvant chemotherapy. *Tumor Biology*, 34, 81-90.
- Stros, M. (1998). DNA bending by the chromosomal protein HMG1 and its high mobility group box domains: effect of flanking sequences. *Journal of Biological Chemistry*, 273(17), 10355-10361.
- Suerbaum, S., & Michetti, P. (2002). *Helicobacter pylori* infection. *New England Journal of Medicine*, 347(15), 1175-1186.
- Suzuki, K., Kirisako, T., Kamada, Y., Mizushima, N., Noda, T., & Ohsumi, Y. (2001). The pre-autophagosomal structure organized by concerted functions of APG genes is essential for autophagosome formation. *The EMBO journal*, 20(21), 5971-5981.
- Syam, A. F., Waskito, L. A., Rezkitha, Y. A. A., Simamora, R. M., Yusuf, F., Danchi, K. E., ... & Yamaoka, Y. (2021). *Helicobacter pylori* in the Indonesian Malay's descendants might be imported from other ethnicities. *Gut Pathogens*, 13(1), 36.
- Szabò, I., Brutsche, S., Tombola, F., Moschioni, M., Satin, B., Telford, J. L., ... & Zoratti, M. (1999). Formation of anion-selective channels in the cell plasma membrane by the toxin VacA of *Helicobacter pylori* is required for its biological activity. *The EMBO journal*, 18(20), 5517-5527.
- Tacconelli, E., Carrara, E., Savoldi, A., Harbarth, S., Mendelson, M., Monnet, D. L., ... & Zorzet, A. (2018). Discovery, research, and development of new antibiotics: the WHO

- priority list of antibiotic-resistant bacteria and tuberculosis. *The Lancet infectious diseases*, 18(3), 318-327.
- Taguchi, A., Blood, D. C., del Toro, G., Canet, A., Lee, D. C., Qu, W., ... & Schmidt, A. M. (2000). Blockade of RAGE–amphoterin signalling suppresses tumour growth and metastases. *Nature*, 405(6784), 354-360.
- Takeuchi, T., Sakazume, K., Tonooka, A., Zaitzu, M., Takeshima, Y., Mikami, K., & Uekusa, T. (2013). Cytosolic HMGB1 expression in human renal clear cell cancer indicates higher pathological T classifications and tumor grades. *Urology journal*, 10(3), 960.
- Talebi Bezmin Abadi, A. (2018). Diagnosis of *Helicobacter pylori* using invasive and noninvasive approaches. *Journal of pathogens*, 2018.
- Tang, B., Li, N., Gu, J., Zhuang, Y., Li, Q., Wang, H. G., & Mao, X. H. (2012). Compromised autophagy by MIR30B benefits the intracellular survival of *Helicobacter pylori*. *Autophagy*, 8(7), 1045-1057.
- Tang, D., Kang, R., Livesey, K. M., Cheh, C. W., Farkas, A., Loughran, P., ... & Lotze, M. T. (2010). Endogenous HMGB1 regulates autophagy. *Journal of Cell Biology*, 190(5), 881-892.
- Tanida, I., Ueno, T., & Kominami, E. (2004). LC3 conjugation system in mammalian autophagy. *The international journal of biochemistry & cell biology*, 36(12), 2503-2518..
- Tannæs, T., & Bukholm, G. (2005). Cholesteryl-6-O-acyl- α -D-glucopyranoside of *Helicobacter pylori* relate to relative lysophospholipid content. *FEMS microbiology letters*, 244(1), 117-120.
- Taylor, J. A., Bratton, B. P., Sichel, S. R., Blair, K. M., Jacobs, H. M., DeMeester, K. E., ... & Salama, N. R. (2020). Distinct cytoskeletal proteins define zones of enhanced cell wall synthesis in *Helicobacter pylori*. *elife*, 9, e52482.
- Teneberg, S. (2009). The multiple carbohydrate binding specificities of *Helicobacter pylori*. *Glycoscience and Microbial Adhesion*, 121-138.
- Terebiznik, M. R., Raju, D., Vázquez, C. L., Torbricki, K., Kulkarni, R., Blanke, S. R., ... & Jones, N. L. (2009). Effect of *Helicobacter pylori*'s vacuolating cytotoxin on the autophagy pathway in gastric epithelial cells. *Autophagy*, 5(3), 370-379.

- Terry, K., Williams, S. M., Connolly, L., & Ottemann, K. M. (2005). Chemotaxis plays multiple roles during *Helicobacter pylori* animal infection. *Infection and immunity*, 73(2), 803-811.
- Tomb, J. F., White, O., Kerlavage, A. R., Clayton, R. A., Sutton, G. G., Fleischmann, R. D., & Venter, J. C. (1997). The complete genome sequence of the gastric pathogen *Helicobacter pylori*. *Nature*, 388(6642), 539-547.
- Tshibangu-Kabamba, E., & Yamaoka, Y. (2021). *Helicobacter pylori* infection and antibiotic resistance—from biology to clinical implications. *Nature Reviews Gastroenterology & Hepatology*, 18(9), 613-629.
- Tsugawa, H. et al. (2012) Reactive oxygen species-induced autophagic degradation of *Helicobacter pylori* CagA is specifically suppressed in cancer stem-like cells. *Cell Host Microbe* 12, 764–777
- Tsugawa, H., Mori, H., Matsuzaki, J., Sato, A., Saito, Y., Imoto, M., ... & Suzuki, H. (2019). CAPZA1 determines the risk of gastric carcinogenesis by inhibiting *Helicobacter pylori* CagA-degraded autophagy. *Autophagy*, 15(2), 242-258.
- Tsugawa, H., Suzuki, H., Nakagawa, I., Nishizawa, T., Saito, Y., Suematsu, M., & Hibi, T. (2008). Alpha-ketoglutarate oxidoreductase, an essential salvage enzyme of energy metabolism, in coccoid form of *Helicobacter pylori*. *Biochemical and biophysical research communications*, 376(1), 46-51.
- Typas, A., Banzhaf, M., Gross, C. A., & Vollmer, W. (2012). From the regulation of peptidoglycan synthesis to bacterial growth and morphology. *Nature Reviews Microbiology*, 10(2), 123-136.
- Ueda, T., & Yoshida, M. (2010). HMGB proteins and transcriptional regulation. *Biochimica et Biophysica Acta (BBA)-Gene Regulatory Mechanisms*, 1799(1-2), 114-118.
- Ulloa, L., & Tracey, K. J. (2005). The ‘cytokine profile’: a code for sepsis. *Trends in molecular medicine*, 11(2), 56-63.
- Ulloa, L., Ochani, M., Yang, H., Tanovic, M., Halperin, D., Yang, R., ... & Tracey, K. J. (2002). Ethyl pyruvate prevents lethality in mice with established lethal sepsis and systemic inflammation. *Proceedings of the National Academy of Sciences*, 99(19), 12351-12356.

- Uotani, T., & Graham, D. Y. (2015). Diagnosis of *Helicobacter pylori* using the rapid urease test. *Annals of translational medicine*, 3(1).
- Vale, F. F., Vadivelu, J., Oleastro, M., Breurec, S., Engstrand, L., Perets, T. T., ... & Lehours, P. (2015). Dormant phages of *Helicobacter pylori* reveal distinct populations in Europe. *Scientific reports*, 5(1), 14333.
- Venneman, K., Huybrechts, I., Gunter, M. J., Vandendaele, L., Herrero, R., & Van Herck, K. (2018). The epidemiology of *Helicobacter pylori* infection in Europe and the impact of lifestyle on its natural evolution toward stomach cancer after infection: A systematic review. *Helicobacter*, 23(3), e12483.
- Villako, K., Kekki, M., Maaroos, H. I., Sipponen, P., Uibo, R., Tammur, R., & Tamm, A. (1991). Chronic gastritis: progression of inflammation and atrophy in a six-year endoscopic follow-up of a random sample of 142 Estonian urban subjects. *Scandinavian Journal of Gastroenterology*, 26(sup186), 135-141.
- Wang, C., Fei, G., Liu, Z., Li, Q., Xu, Z., & Ren, T. (2012). HMGB1 was a pivotal synergistic effector for CpG oligonucleotide to enhance the progression of human lung cancer cells. *Cancer biology & therapy*, 13(9), 727-736.
- Wang, C., Wang, H., Zhang, D., Luo, W., Liu, R., Xu, D., & Liu, Z. (2018). Phosphorylation of ULK1 affects autophagosome fusion and links chaperone-mediated autophagy to macroautophagy. *Nature communications*, 9(1), 3492.
- Wang, H., Bloom, O., Zhang, M., Vishnubhakat, J. M., Ombrellino, M., Che, J., ... & Tracey, K. J. (1999). HMG-1 as a late mediator of endotoxin lethality in mice. *Science*, 285(5425), 248-251.
- Wang, S., & Zhang, Y. (2020). HMGB1 in inflammation and cancer. *Journal of hematology & oncology*, 13(1), 1-4.
- Wang, Y. H., Gorvel, J. P., Chu, Y. T., Wu, J. J., & Lei, H. Y. (2010). *Helicobacter pylori* impairs murine dendritic cell responses to infection. *PloS one*, 5(5), e10844.
- Wang, Y. H., Wu, J. J., & Lei, H. Y. (2009). The autophagic induction in *Helicobacter pylori*-infected macrophage. *Experimental biology and medicine*, 234(2), 171-180.
- Warren, J. R., & Marshall, B. (1983). Unidentified curved bacilli on gastric epithelium in active chronic gastritis. *The lancet*, 321(8336), 1273-1275.

- Watari, J., Chen, N., Amenta, P. S., Fukui, H., Oshima, T., Tomita, T., & Das, K. M. (2014). *Helicobacter pylori* associated chronic gastritis, clinical syndromes, precancerous lesions, and pathogenesis of gastric cancer development. *World Journal of Gastroenterology: WJG*, 20(18), 5461.
- Wen, Y., Marcus, E. A., Matrubutham, U., Gleeson, M. A., Scott, D. R., & Sachs, G. (2003). Acid-adaptive genes of *Helicobacter pylori*. *Infection and immunity*, 71(10), 5921-5939.
- Weyermann, M., Rothenbacher, D., & Brenner, H. (2009). Acquisition of *Helicobacter pylori* infection in early childhood: independent contributions of infected mothers, fathers, and siblings. *Official journal of the American College of Gastroenterology/ACG*, 104(1), 182-189.
- Williams, K. L. (Ed.). (2019). *Endotoxin Detection and Control in Pharma, Limulus, and Mammalian Systems*. Springer.
- Windham, I. H., Servetas, S. L., Whitmire, J. M., Pletzer, D., Hancock, R. E., & Merrell, D. S. (2018). *Helicobacter pylori* biofilm formation is differentially affected by common culture conditions, and proteins play a central role in the biofilm matrix. *Applied and Environmental Microbiology*, 84(14), e00391-18.
- Wirth, H. P., Yang, M., Karita, M., & Blaser, M. J. (1996). Expression of the human cell surface glycoconjugates Lewis x and Lewis y by *Helicobacter pylori* isolates is related to *cagA* status. *Infection and immunity*, 64(11), 4598-4605.
- Wittwer, C., Boeck, S., Heinemann, V., Haas, M., Stieber, P., Nagel, D., & Holdenrieder, S. (2013). Circulating nucleosomes and immunogenic cell death markers HMGB1, sRAGE and DNase in patients with advanced pancreatic cancer undergoing chemotherapy. *International journal of cancer*, 133(11), 2619-2630.
- Xie, Z., Zhang, Y., & Huang, X. (2020). Evidence and speculation: the response of *Salmonella* confronted by autophagy in macrophages. *Future Microbiology*, 15(13), 1277-1286.
- Xie, C., Li, N., Wang, H., He, C., Hu, Y., Peng, C., ... & Lu, N. (2020). Inhibition of autophagy aggravates DNA damage response and gastric tumorigenesis via Rad51 ubiquitination in response to *H. pylori* infection. *Gut Microbes*, 11(6), 1567-1589.

- Yamaguchi, H., Osaki, T., Kurihara, N., Taguchi, H., Hanawa, T., Yamamoto, T., & Kamiya, S. (1997). Heat-shock protein 60 homologue of *Helicobacter pylori* is associated with adhesion of *H. pylori* to human gastric epithelial cells. *Journal of medical microbiology*, 46(10), 825-831.
- Yamaoka, Y. (2018). How to eliminate gastric cancer-related death worldwide?. *Nature Reviews Clinical Oncology*, 15(7), 407-408.
- Yamaoka, Y. (Ed.). (2008). *Helicobacter pylori: molecular genetics and cellular biology*. Horizon Scientific Press.
- Yan, W., Chang, Y., Liang, X., Cardinal, J. S., Huang, H., Thorne, S. H., ... & Tsung, A. (2012). High-mobility group box 1 activates caspase-1 and promotes hepatocellular carcinoma invasiveness and metastases. *Hepatology*, 55(6), 1863-1875.
- Yang, H., Ochani, M., Li, J., Qiang, X., Tanovic, M., Harris, H. E., ... & Tracey, K. J. (2004). Reversing established sepsis with antagonists of endogenous high-mobility group box 1. *Proceedings of the National Academy of Sciences*, 101(1), 296-301.
- Yang, L., Li, C., & Jia, Y. (2018). MicroRNA-99b promotes *Helicobacter pylori*-induced autophagy and suppresses carcinogenesis by targeting mTOR. *Oncology letters*, 16(4), 5355-5360.
- Yang, X. J., Si, R. H., Liang, Y. H., Ma, B. Q., Jiang, Z. B., Wang, B., & Gao, P. (2016). Mir-30d increases intracellular survival of *Helicobacter pylori* through inhibition of autophagy pathway. *World journal of gastroenterology*, 22(15), 3978.
- Yang, Z., & Klionsky, D. J. (2010). Eaten alive: a history of macroautophagy. *Nature cell biology*, 12(9), 814-822.
- Yim, W. W. Y., & Mizushima, N. (2020). Lysosome biology in autophagy. *Cell discovery*, 6(1), 6.
- Yin, H., Yang, X., Gu, W., Liu, Y., Li, X., Huang, X., ... & He, W. (2017). HMGB1-mediated autophagy attenuates gemcitabine-induced apoptosis in bladder cancer cells involving JNK and ERK activation. *Oncotarget*, 8(42), 71642.
- Yu, C., Huang, X., Xu, Y. E., Li, H., Su, J., Zhong, J., ... & Sun, L. (2013). Lysosome dysfunction enhances oxidative stress-induced apoptosis through ubiquitinated protein accumulation in Hela cells. *The Anatomical Record: Advances in Integrative Anatomy and Evolutionary Biology*, 296(1), 31-

- Yuan, C. et al. (2022). The global prevalence of and factors associated with *Helicobacter pylori* infection in children: a systematic review and meta-analysis. *The Lancet Child Adolescent Health* 6, 185–194
- Yuan, X., Bhat, O. M., Lohner, H., Zhang, Y., & Li, P. L. (2020). Downregulation of lysosomal acid ceramidase mediates HMGB1-induced migration and proliferation of mouse coronary arterial myocytes. *Frontiers in Cell and Developmental Biology*, 8, 111.
- Zhao, Z., Hu, Z., Zeng, R., & Yao, Y. (2020). HMGB1 in kidney diseases. *Life Sciences*, 259, 118203.
- Zhou, T. B. (2014). Role of high mobility group box 1 and its signaling pathways in renal diseases. *Journal of Receptors and Signal Transduction*, 34(5), 348-350.

Section 9

ABBREVIATIONS

- aa- Amino acids
- µg - Microgram
- µl - Microlitre
- ANOVA – One way analysis of variance
- APS- Ammonium persulfate
- Bax - Bcl-2-associated X protein
- CFU – Colony forming Unit
- ATGs Autophagy-related genes
- BafA1 Bafilomycin A1
- CQ Chloroquine
- DAPI – 4',6-diamidino-2'-phenylindole
- DCFDA - 2,7-Dichlorofluorescein diacetate
- DMSO – Dimethyl sulfoxide
- DNA – Deoxyribonucleic Acid
- ELISA- Enzyme linked immunosorbant assay
- FBS- Fetal Bovine serum
- H₂O₂ - Hydrogen peroxide
- HRP - Horseradish peroxidase
- h - Hour
- LAMP-1- lysosomal associated membrane protein 1
- p62/SQSTM1- sequestosome 1
- mTOR- mechanistic target of rapamycin kinase
- MAP1LC3B- Microtubule-associated protein 1 light chain 3beta
- UVRAG- UV radiation resistance-associated gene
- HCl - Hydrochloric acid
- IHC - Immunohistochemistry
- IL-1β - Interleukin-1β
- IL-6 - Interleukin-6
- l – Litre
- MIC – Minimum Inhibitory Concentration
- min - Minutes
- ml – Mili litre

- mM – Milimolar
- MOI – Multiplicity of infection
- mRNA- Messenger Ribonucleic Acid
- MTT – 3-(4, 5-Dimethylthiazol-2-yl)-2, 5-Diphenylte-Trazolium Bromide
- nm – Nano metre
- NO - Nitric oxide
- PAGE – Polyacrylamide gel electrophoresis
- PBS – Phosphate buffered saline
- PMSF – Phenyl methane sulfonyl fluoride
- RIPA – Radioimmune precipitation assay
- p53 – Tumour protein p53
- RNA- Ribonucleic Acid
- ROS – Reactive Oxygen Species
- RPM- Rotations Per Minute
- RT-PCR – Reverse transcriptase Polymerase chain reaction
- SDS – Sodium dodecyl sulfat
- S.E.M. – Standard error of mean
- TNF- α – Tumor necrosis factor alpha
- WHO- World Health Organization

Section 10

PUBLICATIONS

AND

CONFERENCES

JOURNAL ARTICLES PUBLISHED

- **Khan, U.,** Karmakar, B. C., Basak, P., Paul, S., Gope, A., Sarkar, D., ... & Bhattacharya, S. (2023). Glycyrrhizin, an inhibitor of HMGB1 induces autolysosomal degradation function and inhibits *Helicobacter pylori* infection. *Molecular Medicine*, 29(1), 1-15.
- Saha, K., Sarkar, D., **Khan, U.,** Karmakar, B. C., Paul, S., Mukhopadhyay, A. K., ... & Bhattacharya, S. (2022). Capsaicin inhibits inflammation and gastric damage during H pylori infection by targeting NF-kB–miRNA axis. *Pathogens*, 11(6), 641.
- Basak, P., Maitra, P., **Khan, U.,** Saha, K., Bhattacharya, S. S., Dutta, M., & Bhattacharya, S. (2022). Capsaicin Inhibits *Shigella flexneri* Intracellular Growth by Inducing Autophagy. *Frontiers in pharmacology*, 13.

CONFERENCES ATTENDED


- Participated in an oral presentation entitled as “Therapeutic targeting of autophagy in gastric cancer” in the Young Scientists Conference organized during 22.12.2020 to 24.12.2020 as a part of **India International Science Festival-2020** by the Ministry of Health And Family Welfare, Govt. of India in collaboration with Vijnana Bharati (VIBHA).
- Participated in a poster presentation entitled as “Phytochemical, an inhibitor of HMGB1 induces autolysosomal degradation function and inhibits *H. pylori* infection” in the **15th Asian conference on Diarrhoeal disease and Nutrition (ASCODD)** Conference organized held at The Westin Kolkata Rajarhat India from 11.11.2022 to 13.11.2022, organized by ICMR – National Institute Of Cholera And Enteric Diseases, Kolkata.
- Participated in a poster presentation entitled as “Inhibition of HMGB1 abates *Helicobacter pylori* infection by promoting autolysosomal degradation activity” in the **91st Annual meeting of the Society of Biological Chemists (India) on “Life at the Confluence of Biology & Chemistry”**. Conference organized at the Biswa Bangla Convention Centre, New Town, Kolkata, from 08.12.2022 to 11.12.2022, organized by Bose Institute, CSIR-IICB, NIBMG and SNU Kolkata.

RESEARCH ARTICLE

Open Access



Glycyrrhizin, an inhibitor of HMGB1 induces autolysosomal degradation function and inhibits *Helicobacter pylori* infection

Uzma Khan¹, Bipul Chandra Karmakar², Priyanka Basak¹, Sangita Paul², Animesh Gope³, Deotima Sarkar¹, Asish Kumar Mukhopadhyay², Shanta Dutta² and Sushmita Bhattacharya^{1*} 

Abstract

Background *Helicobacter pylori* is a key agent for causing gastric complications linked with gastric disorders. In response to infection, host cells stimulate autophagy to maintain cellular homeostasis. However, *H. pylori* have evolved the ability to usurp the host's autophagic machinery. High mobility group box1 (HMGB1), an alarmin molecule is a regulator of autophagy and its expression is augmented during infection and gastric cancer. Therefore, this study aims to explore the role of glycyrrhizin (a known inhibitor of HMGB1) in autophagy during *H. pylori* infection.

Main methods Human gastric cancer (AGS) cells were infected with the *H. pylori* SS1 strain and further treatment was done with glycyrrhizin. Western blot was used to examine the expression of autophagy proteins. Autophagy and lysosomal activity were monitored by fluorescence assays. A knockdown of HMGB1 was performed to verify the effect of glycyrrhizin. *H. pylori* infection in in vivo mice model was established and the effect of glycyrrhizin treatment was studied.

Results The autophagy-lysosomal pathway was impaired due to an increase in lysosomal membrane permeabilization during *H. pylori* infection in AGS cells. Subsequently, glycyrrhizin treatment restored the lysosomal membrane integrity. The recovered lysosomal function enhanced autolysosome formation and concomitantly attenuated the intracellular *H. pylori* growth by eliminating the pathogenic niche. Additionally, glycyrrhizin treatment inhibited inflammation and improved gastric tissue damage in mice.

Conclusion This study showed that inhibiting HMGB1 restored lysosomal activity to ameliorate *H. pylori* infection. It also demonstrated the potential of glycyrrhizin as an antibacterial agent to address the problem of antimicrobial resistance.

Keywords *Helicobacter pylori*, Autophagy, Glycyrrhizin, HMGB1, LMP

Background

Infection with *Helicobacter pylori* is one of the key factors responsible for causing gastric disorders and a major risk factor for progression to gastritis and gastric cancer. It is a gram-negative bacterium that has evolved with the ability to colonize and take refuge in epithelial cells of the stomach (Khatoun et al. 2016; Li et al. 2017; Jung et al. 2017; González et al. 2021). This is considered as one of the possible reasons owing to the rise of antibiotic resistance

*Correspondence:
Sushmita Bhattacharya
durgasushmita@gmail.com

¹ Division of Biochemistry ICMR-NICED, ICMR-National Institute of Cholera and Enteric Diseases (ICMR-NICED), Kolkata 700010, India

² Division of Bacteriology ICMR-NICED, ICMR-National Institute of Cholera and Enteric Diseases (ICMR-NICED), Kolkata 700010, India

³ Division of Clinical Medicine, ICMR-NICED, ICMR-National Institute of Cholera and Enteric Diseases (ICMR-NICED), Kolkata, India



© The Author(s) 2023. **Open Access** This article is licensed under a Creative Commons Attribution 4.0 International License, which permits use, sharing, adaptation, distribution and reproduction in any medium or format, as long as you give appropriate credit to the original author(s) and the source, provide a link to the Creative Commons licence, and indicate if changes were made. The images or other third party material in this article are included in the article's Creative Commons licence, unless indicated otherwise in a credit line to the material. If material is not included in the article's Creative Commons licence and your intended use is not permitted by statutory regulation or exceeds the permitted use, you will need to obtain permission directly from the copyright holder. To view a copy of this licence, visit <http://creativecommons.org/licenses/by/4.0/>.

of *H. pylori* (Tshibangu-Kabamba et al. 2021; Thung et al. 2016). On account of this, WHO has considered *H. pylori* in the high-priority pathogens list (Shrivastava et al. 2018). Mounting evidence suggests that reprogramming host cellular pathways are an obligatory facet of *H. pylori* infection (Chmiela et al. 2017; Libânio et al. 2015; Sierra et al. 2020). On the other end of the spectrum, to eliminate an incoming pathogen, the host often deploys several cellular defense strategies. Autophagy is one of the important pathways involved in recognizing and capturing intracellular bacteria for their degradation (Yang et al. 2016, 2018; Raju et al. 2012). *H. pylori* infection in epithelial cells often induces the host autophagic machinery during early infection while survival and colonization of *H. pylori* are favoured by inhibition of autophagy at later stages (Yang et al. 2018, 2022; Tang et al. 2012; Kim et al. 2018). *H. pylori* secreted effector proteins like CagA and VacA have an impact on autophagy during infection. CagA inhibits autophagy and helps in the survival of bacteria within the host (Terebiznik et al. 2009 and Tsugawa et al. 2019). Moreover, autophagy is dynamically altered in response to infection (Levine et al. 2011).

Prior studies have shown that High mobility group box 1 (HMGB1) is augmented during *H. pylori* infection (Lin et al. 2016). Research over the past has also established that HMGB1 induces pro-autophagic activities (Yin et al. 2017; Tang et al. 2010). However, the role of HMGB1-mediated autophagy in *H. pylori* infection is unknown. Keeping in mind this scenario of *H. pylori* infection and autophagy impairment; drug designing is inevitable as antibiotic resistance is well known. In this study, we have used an inhibitor of HMGB1, glycyrrhizin (Mollica et al. 2007) to explore the role of the autophagy-lysosomal pathway during *H. pylori* infection in both in vitro and in vivo conditions. Here, we observed that pharmacological inhibition of HMGB1 reduces *H. pylori* infection by inducing autophagosomal lysosomal maturation.

Methods

Helicobacter pylori culture

Helicobacter pylori, Sydney Strain SS1 (*cagA*+, *vacA* s2m2) were grown on brain heart infusion (BHI) agar (Difco, USA) containing 7% heat-inactivated horse serum (Invitrogen), antibiotics, and IsoVitaleX as mentioned previously (Saha et al. 2022). Plates were kept in a microaerophilic atmosphere at 37 °C for five to six days. Stock cultures were stored at − 70 °C for further usage. Isolates were re-streaked on fresh BHI agar and incubated for 24 h which was used for experimental studies. *H. pylori* resistant strain [OT-14(3)] (*cagA*−, *vacA* s2m2), (clarithromycin, metronidazole resistant) isolated from

a gastric cancer patient at IPGMER and SSKM hospital, Kolkata was cultured with the same protocol.

Cell culture

The human gastric cancer cell line AGS was gifted by Dr. Asish Kumar Mukhopadhyay (ICMR-NICED, Kolkata). AGS cells were grown in F12 media (Sigma-Aldrich) supplemented with 10% heat-inactivated FBS (Sigma, USA), 1% penicillin–streptomycin (Sigma, USA), and maintained in an incubator at 37 °C and 5% CO₂.

In vitro infection assay

A cell density of 0.5×10^6 per 60 mm cell culture dish was plated. *H. pylori* SS1 culture was dissolved in sterile phosphate-buffered saline (PBS) and adjusted to an OD of 1 at 600 nm followed by centrifugation at 10,000 g for 10 min. The cells were starved overnight in 2 mL antibiotic and FBS-free incomplete F12 media. Cells were further infected with or without *H. pylori* with a multiplicity of infection (MOI) 1:100 for 4 h followed by gentamicin (100 µg/ml) treatment for 1 h, to kill the extracellular bacteria. Cells were then washed with PBS and incubated in fresh medium and treatment was done with glycyrrhizin GLZ (200 µM) for another 4 h. Cell lysis was performed by adding 0.1% saponin for 15 min at room temperature and serial dilution was prepared and then 100 µL of diluted suspension were plated on BHI agar plates to determine the number of invaded bacteria into the AGS cells. Colonies were then counted after 5–7 days of incubation. The CFU was determined by plating various serial dilutions of these bacterial suspensions on BHI agar plates (Hu et al. 2019). A similar assay was also performed for the *H. pylori*-resistant strain [OT-14(3)] with or without glycyrrhizin for 4 h. In the case of chloroquine and bafilomycin treatment, cells were infected with or without *H. pylori* with an (MOI) 1:100 for 4 h followed by gentamicin treatment for 1 h and further treatment was done with glycyrrhizin (200 µM) and/or chloroquine (50 µM) and/or bafilomycin (50 nM) for 4 h and/or 18 h.

Real-time PCR

Further, cDNA was prepared from RNA utilizing a Thermo Scientific cDNA synthesis kit. SYBR green kit of Applied Biosystems was used for Quantitative PCR. $\Delta\Delta C_t$ method was used to calculate and normalization was performed with the housekeeping gene control GAPDH. $\Delta\Delta C_t = \text{test} - \text{internal control} - \text{test control}$. The relative density of *H. pylori* was quantified by performing semi-quantitative PCR, detecting *H. pylori*-specific 16S-ribosomal DNA (rDNA) primer, FP (5'-AGAGAA GCAATACTGTGAA-3') & RP (5'-CGATTACTAGCG ATTCCA-3'). GAPDH was measured for normalization, FP (5'-GTCTTCACCACCATGGAGAAGGC-3'), and RP

(5'-CATGCCAGTGAGCTTCCCGTTCA-3'). The PCR efficiency for both the test gene (93%) and GAPDH (96%) are within the desired efficiency range which is 90–105% (Kralik et al. 2017).

Immunofluorescence

For immunofluorescence staining, cells were fixed in 4% paraformaldehyde at room temperature for 1 h and blocked in PBS containing 3% BSA and 0.01% Triton X100 for 1 h. Next, coverslips were incubated with anti-LAMP1 and anti-Galectin-3 at 4 °C overnight. Subsequently, secondary antibody incubation was done using TRITC-conjugated anti-rabbit secondary antibody (1:1000) (Cat# AP132R) and FITC-conjugated anti-mouse secondary antibody (1:1000). Lastly, the coverslips were mounted on glass slides by adding ProLong™ Gold Antifade reagent with DAPI (Thermo Fisher) and examined using an inverted confocal microscope (Carl Zeiss LSM 710). For LAMP1 and LC3B immunofluorescence staining, the same protocol was followed.

Transfection of plasmid and siRNA

The tandem fluorescent LC3B (tfLC3B) plasmid was a gift from Dr. Dhiraj Kumar ICGEB, New Delhi, India. To examine autophagosomes and autolysosomes, AGS cells were transiently transfected with tf-LC3B plasmid using Lipofectamine 2000 (Invitrogen). 48 h after transfection, cells were incubated with or without *H. pylori* and treated with glycyrrhizin. In the end, coverslips were mounted on ProLong™ Gold Antifade reagent with DAPI (Thermo Fisher) and imaged using an inverted confocal microscope. The following siRNAs were purchased from IDT: ATG5siRNA (ID hs.Ri. ATG5.13.1) and HMGB1 siRNA (ID hs.Ri.HMGB1.13.1) and used for transfection at 70% confluence with siRNA/ Non-specific siRNA using lipofectamine 2000 in a 35 mm dish. 48 h after transfection, cells were infected with or without *H. pylori* as described.

Live-cell confocal microscopy

AGS cells (2×10^5) were seeded on coverslips. After 24 h, cells were incubated with *H. pylori* (MOI 100) for 4 h followed by drug treatment for 4 h.

GFP-LAMP1

To monitor the lysosomes expressing LAMP1, *H. pylori*-infected and drug-treated AGS cells were subjected to live-cell imaging by adding 5 µl of baculovirus expressing Lamp1-GFP construct (Cell Light™ Lysosomes-GFP, BacMam 2.0, #C10507) for 16 h. Finally, cells were observed in the confocal microscope.

LysoTracker staining

To investigate the acidification of lysosomes, cells were incubated with LysoTracker Red DND-99 (Invitrogen, L7528) for 30 min. Cells were then observed under an inverted confocal microscope.

Dextran staining

Lysosomal destabilization was examined using Dextran, Alexa Fluor™ 488, and 10,000 MW (D22910, Invitrogen). Cells were incubated with 200 µg/ml dextran for 2 h at 37 °C after infection and drug treatment was then observed under an inverted confocal microscope.

MTT assay

Cellular toxicity was examined using a Colorimetric Cell Viability Kit (MTT) (Promokine) in 96-well plates. MTT reagent (3-(4,5-dimethylthiazol-2-yl)-2,5-diphenyltetrazolium bromide) was added and kept for 4 h. Purple crystal formazan formed was solubilized with DMSO. The amount of formazan salt was measured in a microplate reader (Bio-Rad Serial no. 19901) at an OD of 590 nm.

Measurement of reactive oxygen species (ROS) levels

Intracellular ROS levels were monitored by using 2,7-dichlorodihydrofluorescein diacetate (DCFH-DA). 10 µM of DCFH-DA was added to control, infected, and drug-treated cells for 30 min and kept at 37 °C. Excess DCFH-DA was washed with PBS three times. Finally, fluorescence was monitored (Ex-485 nm and Em-520 nm) using a multimode reader, Molecular devices Spectramax M2.

Immunoblotting

Control, drug-treated and infected cells were lysed in RIPA (Radio immunoprecipitation assay buffer) lysis buffer containing protease and phosphatase inhibitors. After cell lysis, centrifugation was done at 7000 rpm for 20 min at 4 °C. Further, protein level was determined and run on 10% or 12.5% SDS-PAGE gel at 120 V. Gels were further transferred to the PVDF membrane. 5% skimmed milk dissolved in TBST (20 mM Tris-HCl, 150 mM NaCl, 0.1% Tween20) buffer was used for blocking and incubated for 1 h at room temperature. In the next step, the membranes were kept overnight with primary antibodies at 4 °C. Eventually, after secondary antibody incubation, membranes were developed and scanned in a ChemiDoc. The primary antibodies used are rabbit polyclonal Anti-SQSTM1/p62 antibody (Cat# ab91526), rabbit monoclonal anti-ATG5 (Cat# ab228668), mouse monoclonal anti-LAMP1 (Cat# 15665S), rabbit monoclonal anti-beclin1 antibody (Cat

#ab207612), rabbit polyclonal anti-LC3B antibody (Cat#ab51520), mouse polyclonal anti- β -actin (Cat #sc-47778), mouse monoclonal anti-Galectin-3 (Cat #sc-53127), rabbit polyclonal anti- α -Tubulin (Cat #BB-AB0118), anti-rabbit secondary HRP-conjugate (Cat #12-348), anti-mouse secondary HRP-conjugate (Cat #12-349).

Enzyme-linked immunosorbent assay (ELISA)

Pro-inflammatory cytokine (IL-8, IL-6) levels from media and serum were estimated using the Krishgen Biosystems kit as per the manufacturer's instructions. All experiments were done in triplicate.

H. pylori infection in C57BL/6 mice and treatment with glycyrrhizin

Mice were maintained in the animal house under 12-h dark–light cycles. Experiments were conducted under the guidelines of the Institutional Animal Ethical Committee, NICED, Kolkata (PRO/157/- 260 July 2022). 8 weeks of male C57BL/6 mice bred in-house were used for the experiments. Three different experimental sets of mice were grouped: Control group (CON), $n=5$, *H. pylori* SS1 infected group (HP), $n=5$, infected group treated with GLZ (HP + GLZ), $n=5$. All groups of mice were treated every day for seven days with an antibiotic cocktail (Ciprofloxacin, Metronidazole, Erythromycin, Albendazole) to avoid any other bacterial/ parasite infections. A Group of mice (HP & HP + GLZ) were inoculated with 10^8 CFU/mouse/inoculation of *H. pylori* SS1 on three alternative days or PBS (CON). After two weeks of inoculation, a group of mice (HP + GLZ) was orally injected with glycyrrhizin (10 mg/kg) for 4 weeks, while a group of mice (CON) received sterile water. At the end of week 4, all mice were sacrificed. Gastric tissues were isolated and blood was collected for experimental purposes as described previously (Saha et al. 2022). Experiments were repeated three times. The total number of mice in each set of experiments was 15.

Statistical analysis

All data were represented as mean \pm S.E.M. Two groups were compared using an Unpaired t-test, and multiple comparisons were done by one-way ANOVA. The significance level has been marked as, * for $p < 0.05$, which implies significance, ** for $p < 0.01$, which implies very significance, and *** for $p < 0.001$, which implies highly significant.

Results

Glycyrrhizin induces autophagy in gastric epithelial cells

Previous reports indicated that glycyrrhizin induces autophagy in myoblast cells but there are no such reports

in gastric cells till date (Lv et al. 2020). Here, we checked the expression levels of different autophagy proteins upon glycyrrhizin treatment in AGS gastric cancer cells. Glycyrrhizin treatment for 4 h elevated the expression of autophagy proteins LC3B-II and LAMP1 in a dose-dependent manner (100 μ M, 200 μ M). At 50 μ M dose of glycyrrhizin, expression of LC3B-II and also LAMP1 was found to be almost the same. At 100 μ M dose of glycyrrhizin treatment, although LC3B-II and LAMP1 increased but it was not statistically significant (p value for LC3B-II is 0.2334 and for LAMP1 is 0.3152). Interestingly, further increase in glycyrrhizin concentration e.g., at 200 μ M dose, expression of LC3B-II increased significantly by 1.5 fold change (p value: 0.0136) and LAMP1 increased by 1.65 fold change (p value: 0.0419). On the other hand, glycyrrhizin reduced HMGB1 expression with an increase in concentration such as at 50 μ M by 1.3 fold change (p value: 0.0332), at 100 μ M by 1.4 fold change (p value: 0.0175) and at 200 μ M by 2.4 fold change (p value: 0.0011) respectively (Fig. 1A). The most effective dose was 200 μ M. To examine the possibility of toxicity of glycyrrhizin on AGS cells, we checked the effect of glycyrrhizin on the viability of AGS cells (Additional file 1: Fig. S1A). Glycyrrhizin treatment for 24 h at different concentrations (50, 100, 200 μ M) did not show significant toxicity. Further, we confirmed glycyrrhizin-induced autophagy by immunofluorescence of LC3B. Drug treatment for 4 h showed a significant enhancement of LC3B puncta formation by 3.2 fold change (unpaired t-test and p value: 0.0071) (Fig. 1B). Subsequently, we assessed the effect of glycyrrhizin-induced autophagosomal maturation in gastric cancer cells. LAMP1 is known to be a marker for lysosomal activity, therefore, we labeled lysosomes with LAMP1-GFP construct after exposure to glycyrrhizin treatment. Subsequently, glycyrrhizin induced LAMP1 expression significantly by a factor of 1.587 (p value: 0.0191) in live cells as compared to control (Fig. 1C). Together, these results suggest that glycyrrhizin induces an autophagic response in gastric cells.

Glycyrrhizin-induced autophagy inhibits intracellular *H. pylori* growth

Since *H. pylori* is known to invade gastric epithelial cells, we examined the effect of drug treatment on the expression of autophagy proteins by immunoblotting in *H. pylori*-infected gastric cancer cells. *H. pylori* Sydney Strain SS1 was used for infection in gastric cells for 4 h and post-treatment was done with 200 μ M glycyrrhizin (4 h). We observed upregulation of LC3B-II by 1.38 fold (p value: 0.0254) and LAMP1 by 1.74 (p value: 0.0028) in glycyrrhizin-treated *H. pylori*-infected cells as compared to the only *H. pylori*-infected cells (Fig. 2A). Moreover, LC3B-II by 1.63 fold (p value: 0.0123) and LAMP1 by

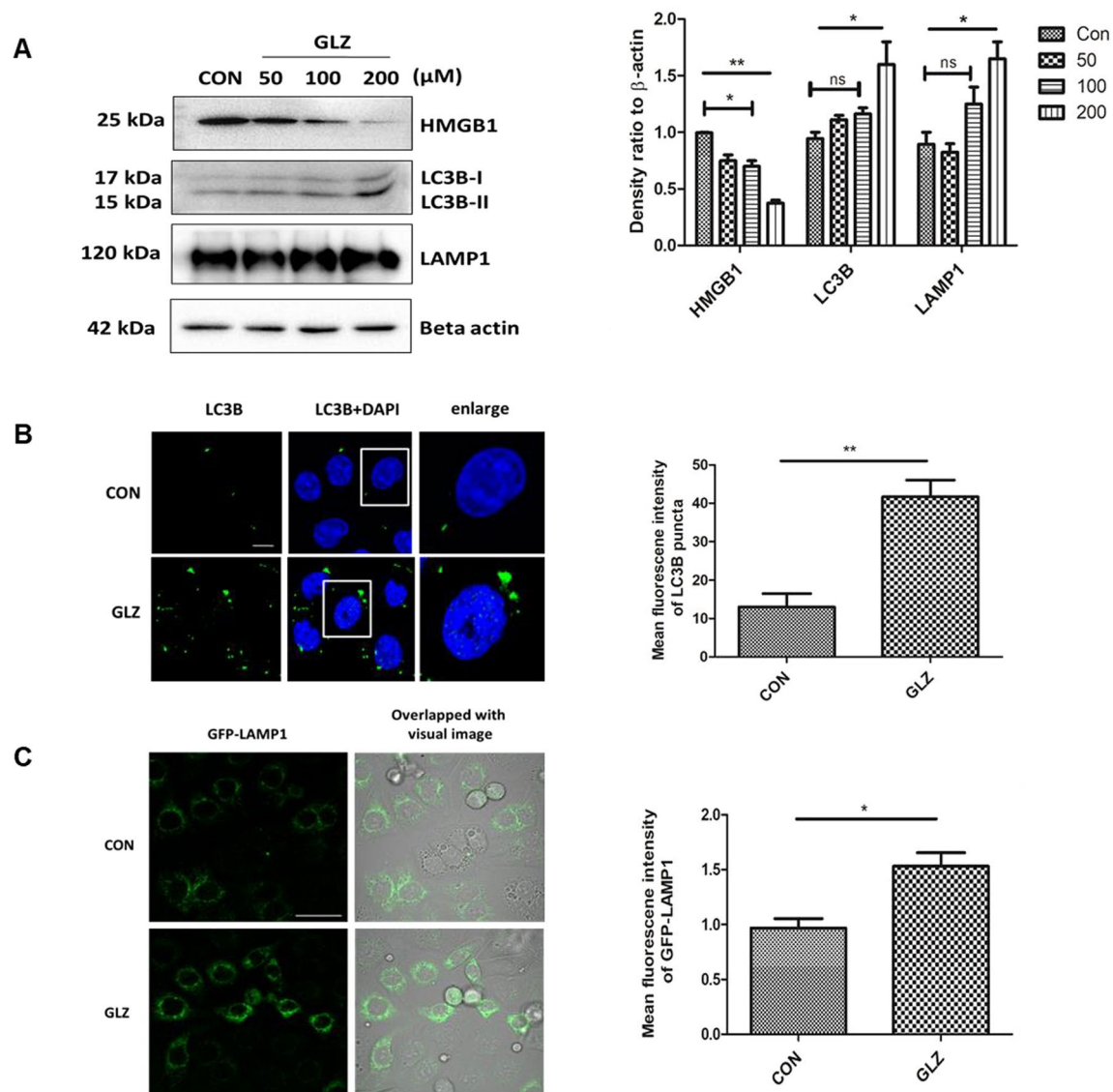


Fig. 1 Glycyrrhizin treatment overexpresses autophagy proteins. AGS cells were treated with glycyrrhizin GLZ (200 μM) or DMSO for 4 h **a** Cell lysates were prepared and expression level of HMGB1 and autophagy marker proteins LC3B-II and LAMP1 was observed by western blot analysis. Beta-actin was used as a protein loading control. Densitometry analyses are represented graphically. **b** Control and drug-treated cells were subjected to immunofluorescence and changes in the mean fluorescence intensity were measured. Scale bar: 5 μm. Confocal microscopy showed LC3B puncta (green) formation. LC3B puncta formation was quantified and graphically plotted. **c** Live cell imaging was performed using a construct, LAMP1-GFP for labeling lysosomes under confocal microscopy. Fold change in the mean fluorescence intensity of GFP-LAMP1 was calculated. Scale bar: 10 μm. Graphs were represented as mean ± SEM (n = 3); Unpaired t-test was done and significance was calculated; *p < 0.05 and **p < 0.01

1.5 fold (p value: 0.0002) were also upregulated in glycyrrhizin-treated control cells as previously explained in (Fig. 1A, B). To verify the findings of LC3B and LAMP1 expression, we additionally performed an immunofluorescence assay and live-cell analysis of drug-treated and *H. pylori*-infected cells. Consistently, in comparison to untreated infected cells, glycyrrhizin treatment resulted in 2.5 fold (p value: 0.0252) increased LC3B puncta formation and 2.3 fold (p value: 0.0347) higher

LAMP1 expression (Fig. 2B, C). The results showed that autophagosomal and lysosomal activities are increased by glycyrrhizin.

Next, we sought to examine the effect of autophagy induction on intracellular bacterial growth. We performed real-time PCR (RT-PCR) and checked *H. pylori*-specific 16SrDNA. Intracellular *H. pylori* level was significantly reduced by glycyrrhizin treatment for 4 h by 2.08 fold (p value: 0.0381) and 18 h by 2.7 fold (p value: 0.0037)

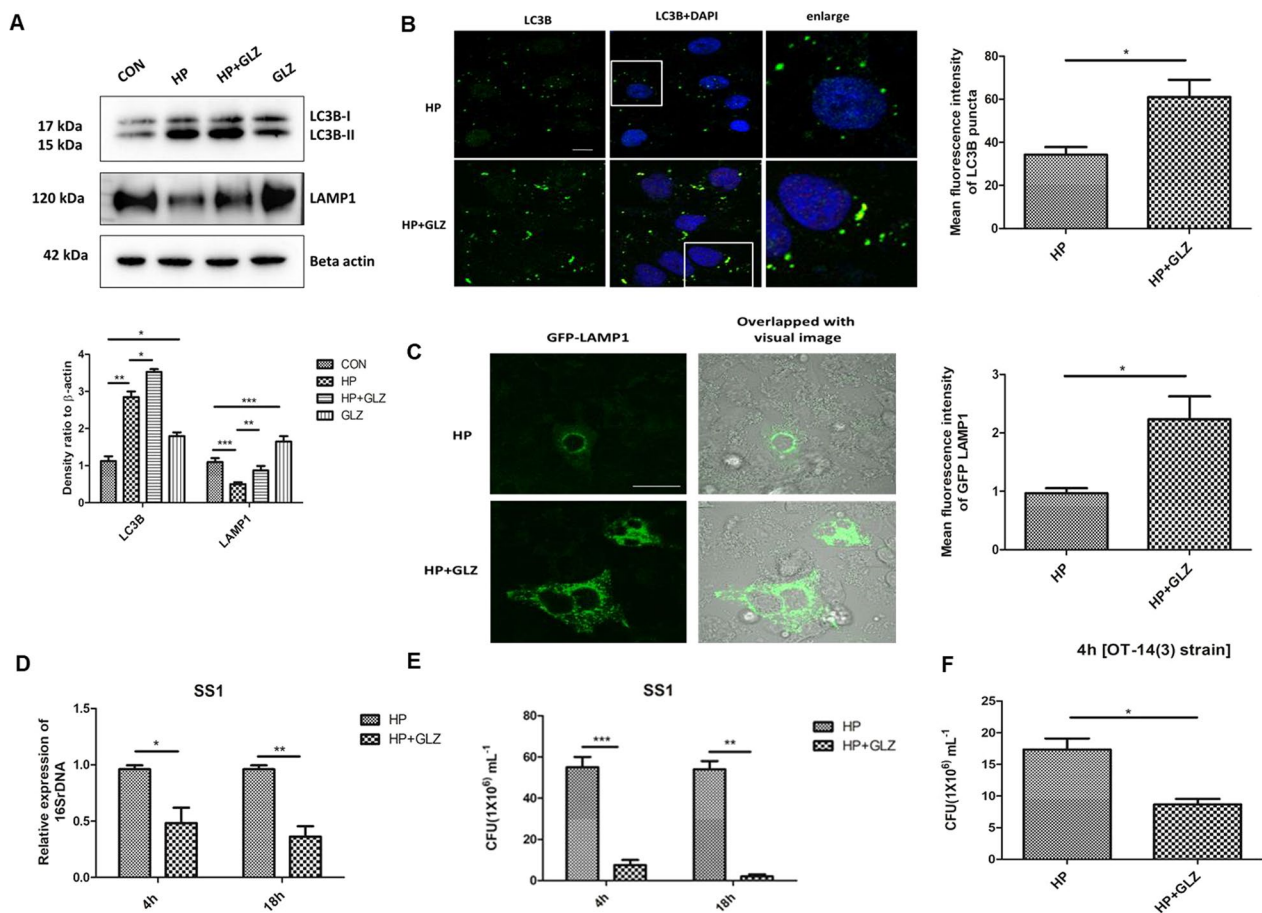


Fig. 2 Exposure to Glycyrrhizin reduces intracellular *H. pylori* growth in AGS cells. **a–c** Infection with *H. pylori* SS1 strain (MOI 100) was performed in cells for 4 h and further exposed to glycyrrhizin (GLZ) (200 μ M) for 4 h. **a** Immunoblotting was performed for quantification of autophagy-associated marker proteins (LC3B-II and LAMP1). Beta-actin was used as a loading control. Densitometry analyses are represented graphically. One-way ANOVA was performed. **b** Confocal microscopy showed LC3B puncta (green) in *H. pylori* (HP) infected & *H. pylori* + glycyrrhizin (HP + GLZ) treated cells, LC3B puncta formation was quantified and change in the mean fluorescence intensity was measured and graphically plotted. Scale bar: 5 μ m. **c** Live cell imaging of LAMP1 under confocal microscopy showed GFP-LAMP1 puncta formation. Fold change in the mean fluorescence intensity of GFP-LAMP1 was calculated, unpaired t-test was performed and graphically represented Scale bar: 10 μ m. **d, e** Cells were incubated with *H. pylori* SS1 strain (MOI 100) for 4 h followed by gentamicin treatment to kill extracellular bacteria. Finally, cells were treated with glycyrrhizin GLZ (200 μ M) at two different time points for 4 h and 18 h **d** Intracellular *H. pylori* DNA (16S rDNA) was determined by real-time PCR. GAPDH was used as the internal control. **e** Cells were lysed and plated on BHIA plates with serial dilutions, for 4–5 days for counting colonies and CFU/ml was graphically represented. **f** Infection with *H. pylori* resistant strain [OT-14(3)] (MOI 100) for 4 h was performed in gastric cells followed by glycyrrhizin GLZ (200 μ M) treatment for 4 h and CFU/ml was graphically represented. Graph were represented as mean \pm SEM (n = 3); Unpaired t-test was done and significance was calculated; *p < 0.05, **p < 0.01 and ***p < 0.001

(Fig. 2D). Of interest, we additionally examined the bacterial proliferation by bacterial adhesion assay. In line, intracellular *H. pylori* burden decreased significantly due to drug exposure for 4 h by tenfold (p value: 0.0005) and 18 h by 14.7 (p value: 0.0011) (Fig. 2E). Since antimicrobial resistance is a problem to curb *H. pylori* infection, we treated a resistant strain of *H. pylori* with glycyrrhizin for 4 h in AGS cells. Glycyrrhizin significantly reduced the growth of *H. pylori*-resistant strain [OT-14 (3)] by a factor

of 2.0 (p value: 0.0117) (Fig. 2F). However, glycyrrhizin failed to reduce *H. pylori* growth in BHIA media which indicates glycyrrhizin has no direct bactericidal effect on *H. pylori* at 200 μ M concentration (Additional file 1: Fig. S2A). Taken together, these data indicate that glycyrrhizin induces autophagy in gastric cancer cells and inhibits intracellular *H. pylori* growth.

Enhancement of autophagic flux by glycyrrhizin contributed to anti-*H. pylori* activity

As *H. pylori* infection is involved in defective autophagosomal lysosomal maturation and degradation, we determined the effect of glycyrrhizin on autophagic flux. To assess the activation of autophagic flux by glycyrrhizin, we performed a double-immunofluorescence assay for both LC3B and LAMP1 protein. Results demonstrated that both LC3B and LAMP1 colocalized in *H. pylori*-infected and glycyrrhizin-treated infected cells (Fig. 3A). The data indicated that glycyrrhizin-induced autophagosomal lysosomal maturation by 1.8 fold (p value: 0.0125).

Next, we examined the stage of glycyrrhizin-mediated autophagic degradation in both autophagosomes and lysosomes by transfecting the AGS cells with tandem fluorescent LC3B (tfLC3B) plasmid. In the case of *H. pylori*-infected gastric cells, autophagosomes appeared as yellow dots due to the colocalization of both GFP and RFP (fold change: 3.8 and p value: 0.0004). On the other hand, we observed more free red dots as GFP and RFP did not colocalize in infected cells followed by glycyrrhizin treatment (fold change: 1.5 and p value: 0.0238). Autolysosomes appear red due to the acidic pH of lysosomes which quench GFP (Fig. 3B). All together, these

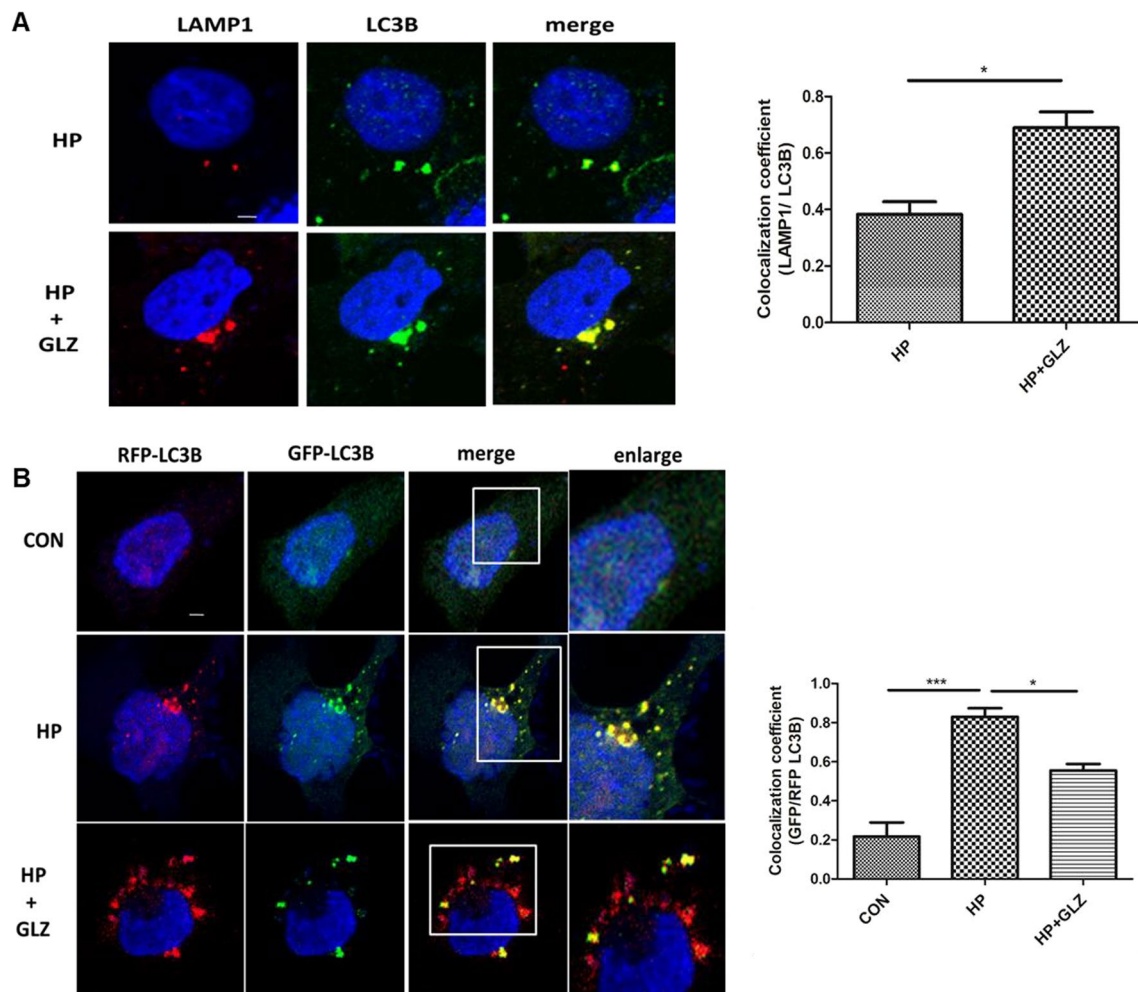


Fig. 3 Activation of autophagic flux by glycyrrhizin treatment (**a**, **b**) Cells were incubated with *H. pylori* SS1 strain (4 h) followed by glycyrrhizin GLZ (200 μ M) exposure for 4 h. **a** Glycyrrhizin (GLZ) exposure to *H. pylori*-infected cells for 4 h was subjected to LAMP1 and LC3B double immunofluorescence. Confocal microscopy showed yellow puncta with co-localization of LC3B puncta (green) & LAMP1 (red). Change in the co-localization coefficient of each group was calculated. Scale bar: 2 μ m. **b** AGS cells were transfected with a tandem mRFP-GFP tag (tfLC3B) plasmid & further infected with *H. pylori* SS1 strain (MOI 100) for 4 h and finally, glycyrrhizin (GLZ) (200 μ M) treatment was done for 4 h. Confocal microscopy showed LC3B puncta formation in control (CON), *H. pylori* (HP) infected & *H. pylori* + glycyrrhizin (HP + GLZ) treated cells. The yellow puncta showed autophagosomes. The free red puncta are autolysosomes. Change in the co-localization coefficient of each group was calculated. Scale bar: 2 μ m. Graph represented as mean \pm SEM (n = 3); Significance was determined by Unpaired t-test; *p < 0.05, ***p < 0.001

results revealed that glycyrrhizin prevents *H. pylori*-mediated inhibition of autolysosome formation in the infected cells by promoting lysosomal maturation.

Anti- *H. pylori* effect and autophagic degradation by glycyrrhizin is mediated through HMGB1 inhibition

To confirm or rule out the possible involvement of HMGB1 in *H. pylori* infection, AGS cells were transiently transfected with non-specific siRNA and HMGB1-specific siRNA followed by infection with *H. pylori* for 4 h and subjected to immunoblotting. Western blot revealed that HMGB1 is silenced in AGS cells after 48 h transfection (Additional file 1: Fig. S3A). HMGB1 knockdown

elevated the level of LC3B-II by 2.2 fold change (p value: 0.0073) and LAMP1 by 1.3 fold (unpaired t-test and p value: 0.0018) significantly (Fig. 4A, B). In addition, we examined the level of intracellular *H. pylori* by RT-PCR. HMGB1 silencing attenuated intracellular *H. pylori* burden significantly by 5.9 fold (p value: 0.0001) (Fig. 4C).

Further, we confirmed the effect of glycyrrhizin on autophagic flux. One of the best targets of autophagic flux is p62. Hence, we checked the level of SQSTM1/p62, a key protein involved in autophagy. Western blotting showed that p62 is increased due to *H. pylori* infection at both 4 h (Fig. 4D) and 18 h (Fig. 4E) time points. Long-term exposure to *H. pylori*, resulted in p62 accumulation.

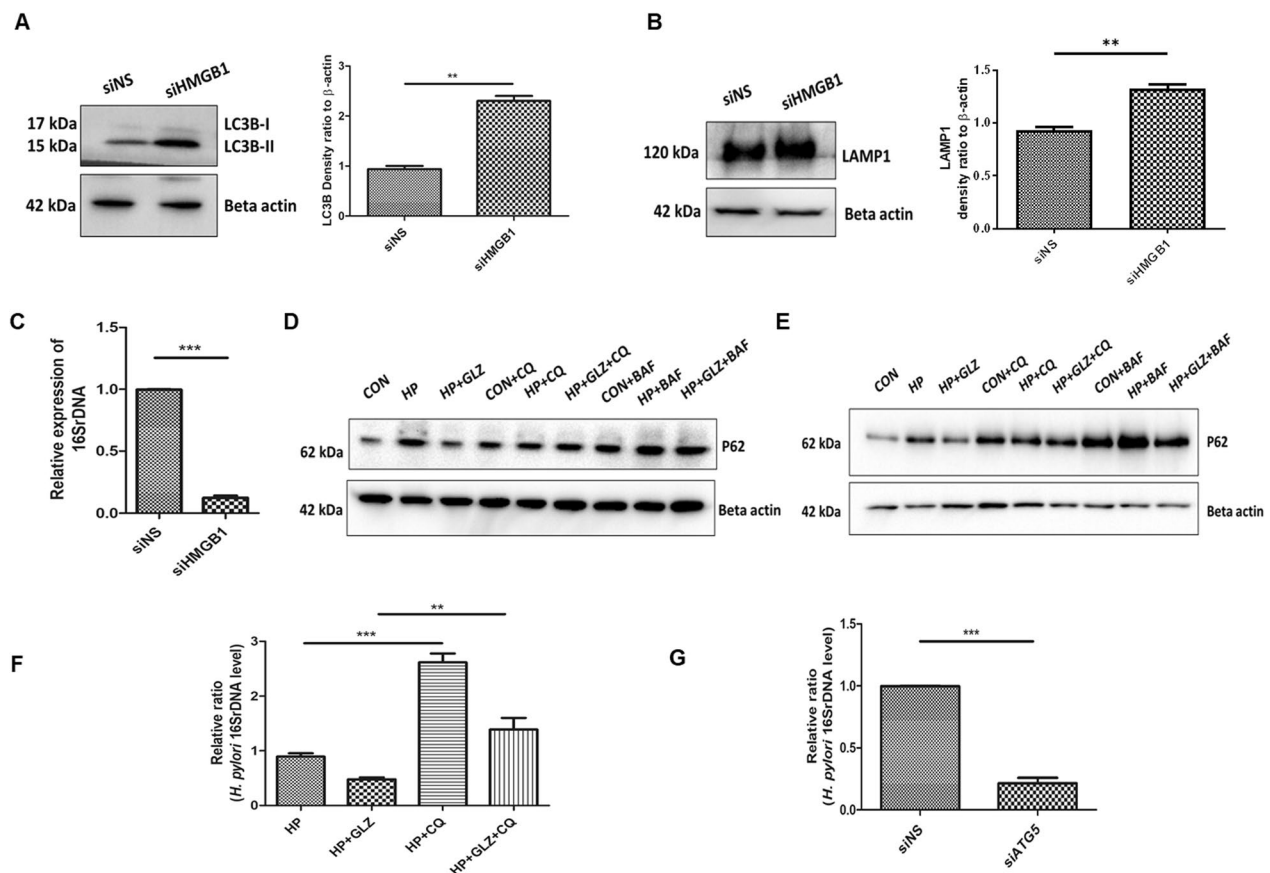


Fig. 4 HMGB1 inhibition reduces bacterial growth while impairment of lysosomal activity induces bacterial survivability. **a–c** After transfection for 48 h, nonspecific siRNA (siNS) and HMGB1 siRNA (siHMGB1) transfected cells were further infected with *H. pylori* SS1 strain (MOI of 100) for 4 h. **a**, **b** Immunoblotting was performed in infected cell lysates for expression of LC3B-II and LAMP1. Beta-actin was used as a protein loading control. Densitometry analyses are represented graphically. **c** Intracellular *H. pylori* DNA (16SrDNA) was determined by RT-PCR. GAPDH was used as the internal control. Unpaired t-test was performed. **(d, e)** AGS cells incubated with the *H. pylori* SS1 strain for 4 h and 18 h followed by exposure to glycyrrhizin GLZ (200 μ M) and/or chloroquine CQ (50 μ M) and/or bafilomycin BAF (50 nM) for 4 h and 18 h treatment respectively. Cell lysates were subjected to a western blot to determine P62 protein levels for 4 h (**d**) and 18 h (**e**). Beta-actin was used as a protein loading control. **f** AGS cells were incubated with the *H. pylori* SS1 strain for 4 h followed by exposure to glycyrrhizin GLZ (200 μ M) and/or chloroquine CQ (50 μ M) for 4 h. Intracellular *H. pylori* DNA (16SrDNA) was measured by RT-PCR. GAPDH was used as the internal control. **g** Cells were transfected with non-specific siRNA (siNS) and ATG5 siRNA (siATG5) & then incubated with *H. pylori* SS1 strain for 4 h, and intracellular *H. pylori* DNA was measured by RT-PCR. GAPDH was kept as an internal control. Graphs were represented as mean \pm SEM (n = 3); One-way ANOVA was performed and significance was calculated; **p < 0.01, ***p < 0.001

This is evident due to the impairment of autolysosomal degradation. On the other hand, glycyrrhizin treatment induces p62 degradation at 4 h and 18 h.

To validate the effect of glycyrrhizin on autophagic flux, we treated the AGS cells with chloroquine (CQ), a potent lysosomal inhibitor, and bafilomycin (BAF), specific for inhibition of autophagosomal lysosomal fusion and acidification. P62 accumulates in both *H. pylori*-infected and uninfected cells treated with glycyrrhizin after exposure to CQ and BAF. Additionally, we analyzed the effect of CQ on glycyrrhizin-mediated *H. pylori* clearance. Due to the blocking of autophagic flux, CQ promptly elevated *H. pylori* infection by 2.9 fold and counteracted the antimicrobial action of glycyrrhizin (p value: 0.0074) (Fig. 4F).

According to previous reports, *H. pylori* can survive within non-digestive autophagosomes (Raju et al. 2012). We analyzed the effect of Atg5 knockdown (Atg5 is an autophagy marker protein required for autophagosome

formation) on intracellular *H. pylori* survival. Western blot showed that Atg5 is silenced in AGS cells after 48 h transfection (Additional file 1: Fig. S3B). Consistently, bacterial clearance occurred significantly by 4.6 fold due to the silencing of Atg5 (p value: 0.0001) (Fig. 4G). Cumulatively, these data demonstrated that *H. pylori* proliferate within autophagosomes inside the host while glycyrrhizin, an inhibitor of HMGB1 promotes autophagosomal lysosomal degradation which in turn reduces intracellular *H. pylori* growth.

Lysosomal acidification was recovered by glycyrrhizin

Further, we investigated in detail the restored lysosomal degradation capacity of glycyrrhizin. We performed Acridine Orange staining to monitor the acidic compartment of lysosomes in AGS cells. A lower red signal in *H. pylori*-infected cells was observed as compared to control because lysosomal acidification was compromised

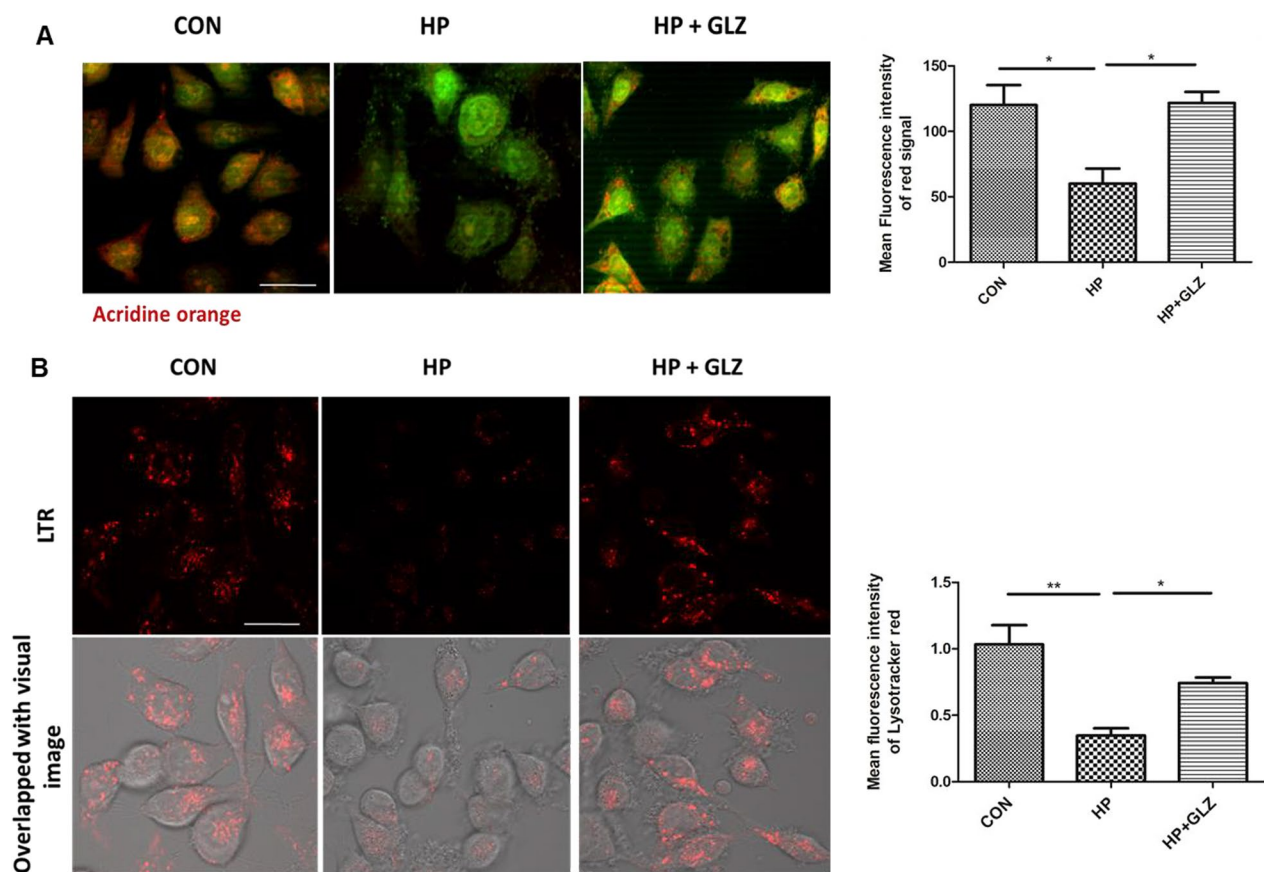


Fig. 5 Lysosomal function is restored by glycyrrhizin. **a–b** Infection with *H. pylori* SS1 strain (MOI 100) was performed for 4 h followed by glycyrrhizin (GLZ) (200 μ M) exposure for 4 h. **a** Lysosomal membrane integrity was monitored by Acridine Orange (AO) staining in a fluorescence microscope. Briefly, cells were incubated with 10 μ g/ml of acridine orange (15 min) and examined. The mean fluorescence intensity of the red signal was determined and graphically represented. Scale bar: 10 μ m. **b** Live cell imaging of drug-treated, infected and control cells was done with LysoTracker Red incubation (100 nM, 30 min) to label lysosomes and mean fluorescence intensity was assessed under the confocal microscope. Scale bar: 10 μ m. Fold change was quantified and graphs were generated using GraphPad Prism 5 and represented as mean \pm SEM (n = 3); Significance was calculated by one-way ANOVA; *p < 0.05, **p < 0.01

whereas glycyrrhizin treatment increased red intensity by restoring lysosomal acidification by a factor of 2.0 (p value: 0.0263) (Fig. 5A). Additionally, to evaluate lysosomal acidification, we exposed the cells to LysoTracker Red which selectively binds to vesicles that have low pH. Here, *H. pylori* infection affected lysosomal pH and reduced the fluorescent signals as compared to the control. Glycyrrhizin exposure restored the acidic pH and showed red signals in infected cells as compared to only infected cells (fold change: 2.139 and p value: 0.0495) (Fig. 5B). The data indicates that glycyrrhizin restored the disrupted lysosomal function during *H. pylori*-infection.

Glycyrrhizin enhanced lysosomal degradation by inhibiting lysosomal membrane permeabilization (LMP)

According to previous reports, *H. pylori* reduced lysosomal degradation capacity due to lysosomal membrane

permeabilization (LMP) (Bravo et al. 2019). Moreover, HMGB1 is also involved in LMP (Feng et al. 2022). Therefore, we determined whether the effect of glycyrrhizin in restoring lysosomal function is mediated by LMP. We performed double immuno-fluorescence of galectin3 and LAMP1. Colocalization of galectin3 with LAMP1 remarkably increased in *H. pylori* infection than control as galectin3 binds to lysosomal membrane glycoproteins which are exposed after LMP. But, glycyrrhizin treatment in infected cells reduced co-localization of galectin3 and LAMP1 probably due to inhibition of LMP (fold change: 2.07 and p value: 0.0074) (Fig. 6A). Additionally, we validated LMP by loading control, *H. pylori*-infected and drug-treated cells with Alexa Fluor conjugated dextran molecules. The redistribution of dextran was observed in infected cells (diffuse staining) indicating lysosomal efflux but not in the case of glycyrrhizin-treated infected

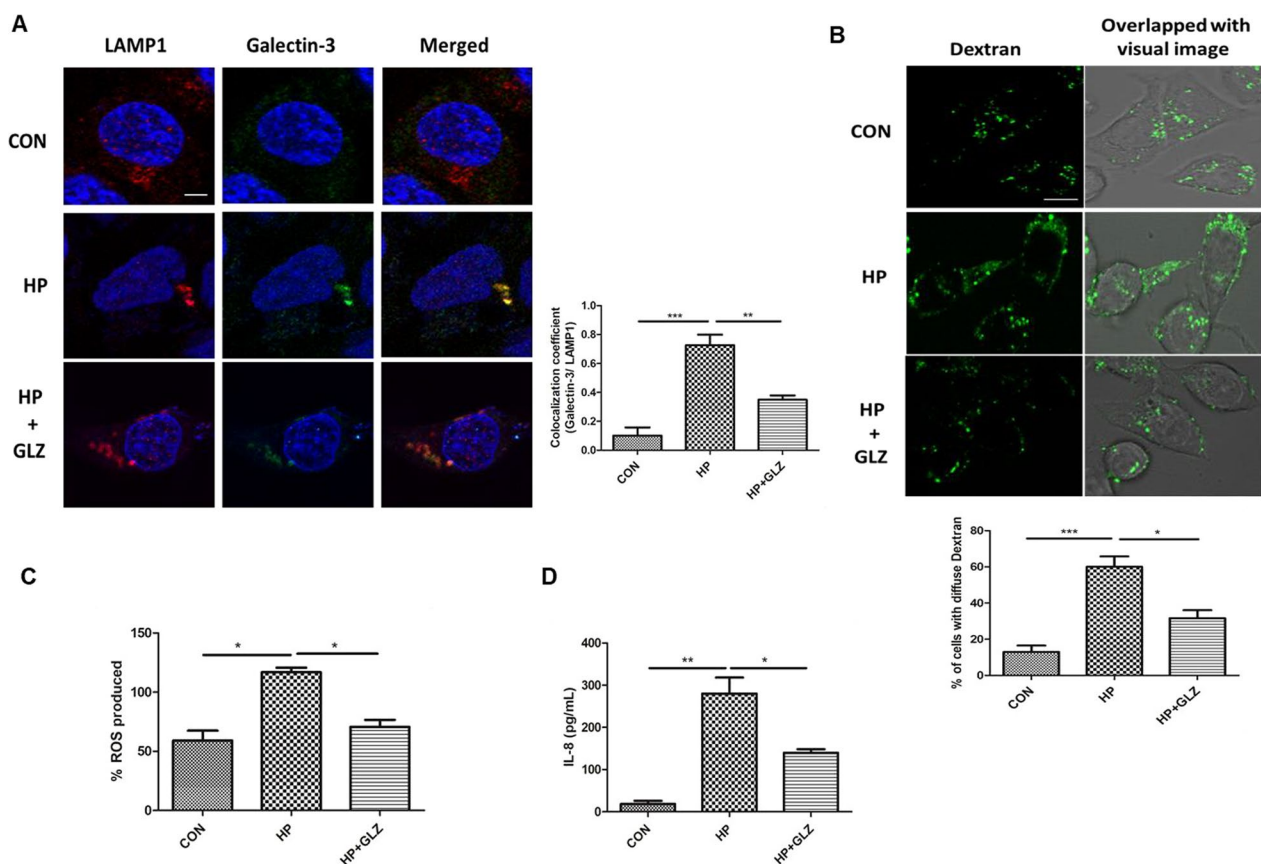


Fig. 6 Lysosomal membrane integrity is restored by glycyrrhizin. **a–d** Infection with *H. pylori* SS1 strain (MOI 100) was performed for 4 h followed by glycyrrhizin (GLZ) (200 μ M) treatment (4 h). **a** Double immunofluorescence was done with LAMP1 & Galectin-3 antibodies to confirm LMP. Cells were observed under the confocal microscope and the difference in the co-localization coefficient of each group was calculated. Scale bar: 2 μ m. **b** Lysosomal destabilization was estimated using live cell imaging after staining with dextran (0.5 mg/ml) for 2 h under the confocal microscope and the number of cells with diffused dextran was counted. Scale bar: 5 μ m. **c** Expression of reactive oxygen species (ROS) in infected and drug-treated cells was determined by DCFDA methods for 30 min in a fluorimeter. **d** The expression of IL-8 from media collected after treatment was analyzed by ELISA in a microplate reader. Graphs were generated using GraphPad Prism 5 and represented as mean \pm SEM (n = 3); Significance was calculated by one-way ANOVA; *p < 0.05, **p < 0.01, ***p < 0.001

cells. Confined punctate structures of dextran indicated exclusive lysosomal localization in drug-treated cells (Fig. 6B). Subsequently, we examined the effect of the inhibition of LMP by glycyrrhizin on ROS and inflammatory cytokines as LMP is linked to inflammation and oxidative stress. In line, glycyrrhizin-exposed cells dramatically reduced both ROS levels (fold change: 1.65 and *p* value: 0.0289) and IL-8 secretion (fold change: 2 and *p* value: 0.0456) significantly as compared to only infected cells (Fig. 6C, D). Taken together, these data indicate that glycyrrhizin improved lysosomal degradation activity and induced protective effects by inhibiting LMP.

In vivo mice model, glycyrrhizin induces autophagy and reduces gastric damages

Eventually, we validated the activity of glycyrrhizin in in vivo mice model. We have infected mice with the *H. pylori* SSI strain. After infection, mice were treated with

glycyrrhizin for 30 days at a 10 mg/kg body weight dose (Additional file 1: Fig. S4A). The effective dose of glycyrrhizin was determined for *H. pylori*-infected mice from previous data on glycyrrhizin (Lv et al. 2020; Fu et al. 2014). We performed western blots with control, infected, and glycyrrhizin-treated-infected gastric tissues. Glycyrrhizin reduced the level of HMGB1 significantly by 1.64 fold (*p* value: 0.0262) and induced p62 degradation by 1.73 fold (*p* value: 0.0010) which is a marker of autophagosomal lysosomal degradation. It also strongly augmented LAMP1 expression by 7.55 fold (*p* value: 0.003) (Fig. 7A). Furthermore, we checked the effect of glycyrrhizin on IL-6 levels in the serum collected from treated mice. Glycyrrhizin significantly reduced IL-6 expression by a factor of 1.6 (*p* value: 0.0086) (Fig. 7B). To further assess the anti-*H. pylori* effect of glycyrrhizin, we examined gastric tissues for changes in morphology. There were changes in the gastric histopathology when

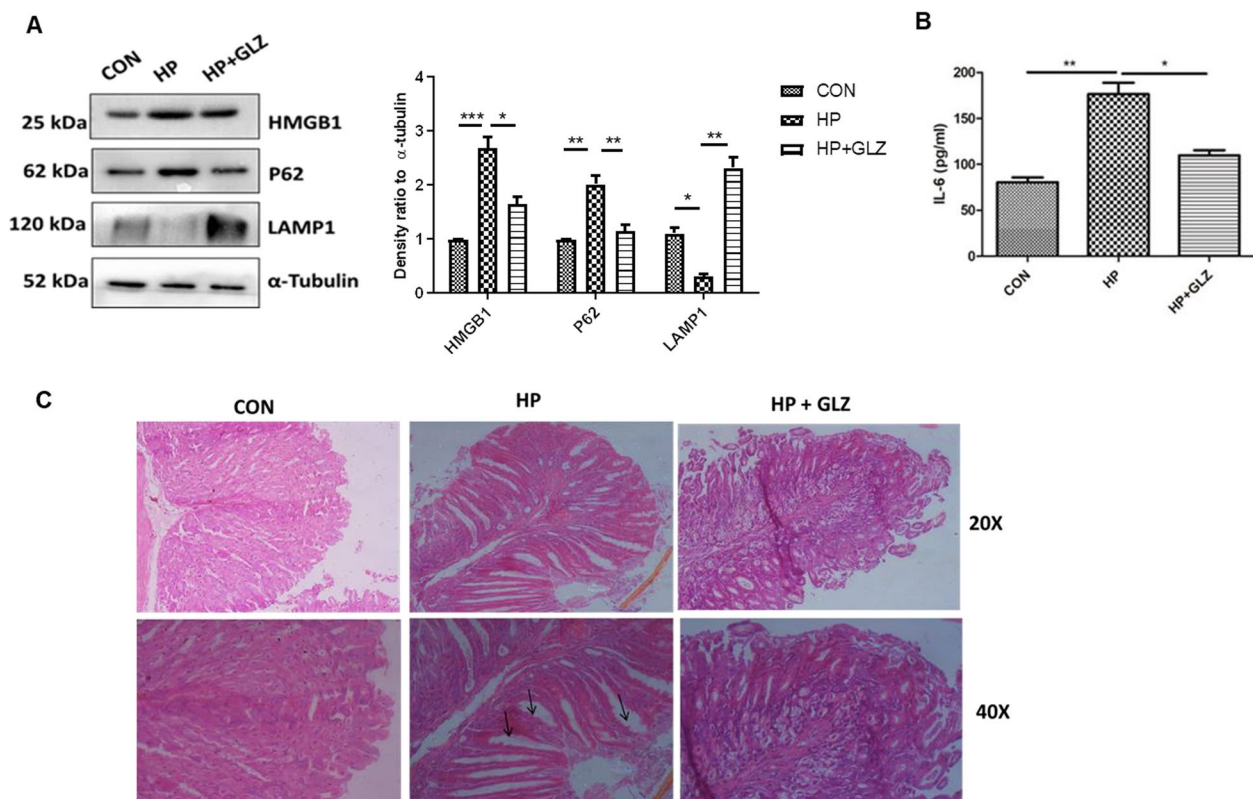


Fig. 7 Glycyrrhizin treatment induces autophagy in *H. pylori*-infected mice and ameliorates gastric tissue damage (**a–c**) C57BL/6 mice (*n* = 5 per group) were treated with antibiotics every 7 days. Then after 7 days incubation period, mice were infected with the *H. pylori* SSI strain thrice a week on alternate days. Mice were incubated for 14 days and then administered with or without glycyrrhizin GLZ (10 mg /kg body weight), every day for 4 weeks. After treatment mice were sacrificed, and gastric tissues and serum were collected. **a** Immunoblot showing the expression of HMGB1 and autophagy proteins (HMGB1, P62, LAMP1) of mouse gastric tissues. α-tubulin was used as a protein loading control. Densitometry analyses are represented graphically. **b** The expression of IL-6 was determined by ELISA in a microplate reader. **c** Histology images of Control (CON), *H. pylori* (HP) infected, and *H. pylori*-infected plus glycyrrhizin treated (HP + GLZ) gastric tissues at 20X and 40X respectively representing the inflammatory changes. Black arrows (↑) indicate gastric tissue damages. Graphs were represented as mean ± SEM (*n* = 3); Significance was determined by one-way ANOVA; **p* < 0.05, ***p* < 0.01, ****p* < 0.001

compared with a control group for *H. pylori*-infected gastric tissues (Fig. 7C). *H. pylori*-induced inflammation and inflammatory cell infiltration in gastric tissues caused epithelial cell damage whereas glycyrrhizin reduced inflammation and repaired tissue damage. Hence, collectively these data revealed that glycyrrhizin induced autophagy and consequently decreased inflammation and gastric tissue damage in in vivo mice model.

Discussion

Current evidence suggests that autophagy plays a major role to protect the host from bacterial pathogens (Giraud-Gatineau et al. 2020; Kim et al. 2012). But the pathogens have their mechanisms to subvert autophagy and persistently invade the host and promote intracellular survival. *Salmonella*, *Shigella*, and *Mycobacterium* are known to avoid autophagy (Xie et al. 2020; Ogawa et al. 2005; Basak et al. 2022; Padhi et al. 2019). However, there are reports which showed that *H. pylori* induce autophagy at the beginning but gradually it inhibits autophagy (Yang et al. 2018; Tang et al. 2012). The mechanisms behind initial activation and subsequent impairment involve a complex interplay between host and bacterial factors. *H. pylori* secretes virulent factors like CagA and VacA (Raju et al. 2012). Both these factors contribute to pathogenesis. Although previous literature suggests that VacA induces autophagy but later it has been reported by Raju et al. that prolonged exposure to VacA inhibits autophagy (Raju et al. 2012; Terebiznik et al. 2009). Recent studies have also revealed that autophagy is down-regulated in *cagA* + strains as compared to *cagA* mutant strains. This inhibition of autophagy is accompanied by the accumulation of p62 and decreased LAMP1 expression (Li et al. 2017). Henceforth, in the current study, we have used the *H. pylori* SS1 strain which is *cagA* positive but expresses non-functional *vacA* and this strain is also capable of mice infection.

Here, we investigated the effect of HMGB1 inhibition during *H. pylori* infection. HMGB1 is reported to be overexpressed in *H. pylori*-infected gastric cells (Lin et al. 2016). Recent reports suggested that HMGB1 causes impairment of autophagy by inducing lysosomal membrane permeabilization (LMP) in diabetic retinopathy (Feng et al. 2022). Hence, we have targeted HMGB1 for treating *H. pylori* infection. Here, glycyrrhizin, an inhibitor of HMGB1 decreased the intracellular *H. pylori* burden in gastric cancer cells. To find out the details behind bacterial clearance, we observed that glycyrrhizin induces autophagy in gastric cells. This is consistent with previous studies of glycyrrhizin in myoblast cells (Lv et al. 2020). Glycyrrhizin treatment attenuated *H. pylori* infection and also induced the expression of autophagy marker proteins. Moreover, glycyrrhizin showed co-localization

of both LC3B and LAMP1 in *H. pylori*-infected gastric cancer cells. We also observed that LAMP1 expression has increased due to glycyrrhizin treatment. This indicates autolysosome formation as LAMP1 expression is necessary for autophagosomal maturation (Tsugawa et al. 2019). Keeping in mind that antibiotic resistance of *H. pylori* is a major problem (Gene et al. 2003; Huang et al. 2017), glycyrrhizin was tested for its ability to eradicate the growth of resistant *H. pylori* strain in in vitro conditions. Glycyrrhizin successfully showed clearance of antibiotic-resistant *H. pylori*. In addition, transient knock-down of HMGB1 resulted in parallel to glycyrrhizin treatment, hence the probable mechanism behind the induction of autophagy by glycyrrhizin is due to its inherent anti-HMGB1 property. Bacterial clearance by autophagy induction is a general mechanism as recent reports revealed that autophagy inducers like vitamin D and statin controlled *H. pylori* infection (Hu et al. 2019; Liao et al. 2017). Further, we determined the effect of glycyrrhizin in the later stages of autophagy. Consistent with the results of initial autophagy induction, our results demonstrated that glycyrrhizin treatment augments lysosomal degradation resulting in reduced bacterial burden. It is reported that *H. pylori* induce p62 accumulation which is a characteristic feature of inhibition of autophagic flux. In contrast, glycyrrhizin treatment augmented p62 degradation to improve the autophagic flux. Subsequently, p62 accumulation was observed due to the inhibition of autophagosomal maturation and flux by chloroquine and bafilomycin. Glycyrrhizin further is unable to inhibit *H. pylori* growth due to CQ treatment indicating the involvement of autophagic flux during infection (Hu et al. 2019). To gain a deeper insight into autophagic activity by glycyrrhizin we searched for the probable mechanisms. Previous studies suggested that *H. pylori* survived in undigested autophagosomes (Raju et al. 2012). Consistently, we proved that Atg5 knock-down inhibited *H. pylori* growth as Atg5 is responsible for autophagosome formation. Furthermore, the accumulation of undigested autophagosomes results in lysosomal membrane permeabilization (LMP) (Feng et al. 2022). HMGB1 is associated with LMP causing defective lysosomal activity and *H. pylori* is also reported to have impairment of lysosomal acidification by inducing LMP (Bravo et al. 2019; Feng et al. 2022). In this study, inhibition of HMGB1 by glycyrrhizin rescued LMP in *H. pylori*-infected cells and further restored the degradative capacity of autophagy proving that LMP is responsible for the inhibition of autophagosome degradation. Moreover, we observed that lysosomal pH has been restored by glycyrrhizin using LysoTracker Red staining as acidic pH is extremely important for the proper digestive action of lysosomes. Further, we examined Alexa Fluor conjugated

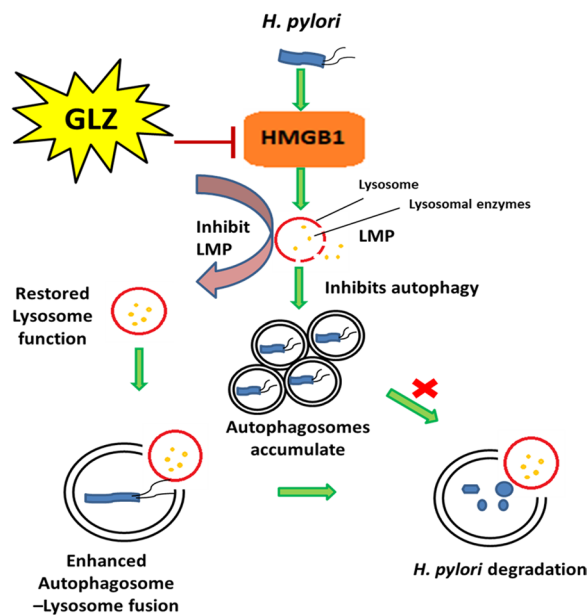


Fig. 8 Schematic diagram represents the mechanism that inhibiting HMGB1 induces autophagy through lysosomal membrane permeabilization (LMP). Glycyrrhizin inhibiting the HMGB1 expression induces autophagy by restoration of lysosomal membrane integrity. Recovered lysosomal membrane reduces LMP along with enhanced autolysosome formation which ultimately degrades the intracellular *H. pylori* from its gastric niche

dextran activity to inhibition of LMP by glycyrrhizin. Here, also we found that glycyrrhizin exposure reduced LMP by inducing consistent puncta formation of dextran granules indicating intact lysosomes whereas in infected cells diffuse staining is observed due to lysosomal efflux. Additionally, both HMGB1 and *H. pylori* infection are responsible for LMP (Bravo et al. 2019; Feng et al. 2022). Thus it has been proved that glycyrrhizin induces autophagy and lysosomal degradation by reducing LMP. Moreover, LMP is linked to the activation of ROS and inflammation (Kavčič et al. 2017). We evaluated the effect on ROS generation and cytokine expression. ROS level and inflammatory cytokine expression are commonly enhanced during infection (Hardbower et al. 2013). Consistently, the results showed that glycyrrhizin inhibited ROS production and inflammatory cytokine level in AGS cells. Therefore, our findings confirmed that inhibiting HMGB1 by glycyrrhizin induced autophagosomal maturation and lysosomal degradation in *H. pylori*-infected gastric cells by rescuing them from LMP.

Further, we verified our findings in *in vivo* mice model. In line, our results showed inhibition of HMGB1 expression and induction of autophagy by glycyrrhizin in gastric tissues. Inflammation is a major problem during *H. pylori* infection. Inflammation induces gastric damage and

causes further complications. Here, glycyrrhizin induces autophagy accompanied by a reduction in inflammation. Furthermore, glycyrrhizin is able to repair gastric tissue damages.

Conclusion

Our results demonstrated for the first time that induction of autophagy by inhibiting HMGB1 can reduce *H. pylori* infection in both *in vitro* and *in vivo* conditions. In addition, our data revealed that restoring the degradative capacity of autophagy by inhibiting HMGB1-induced LMP resulted in the inhibition of *H. pylori* pathogenesis (Fig. 8). As both the host and pathogen play critical roles in disease progression, induction of autophagy and lysosomal degradation further affects downstream responses like inflammation and ROS generation. Hence, in the future glycyrrhizin might be used as a potent inducer of autophagy that reduces *H. pylori* infection to inhibit the progression of gastric disorders. The mechanism of antibacterial action of glycyrrhizin would provide novel strategies and targets to address the problem of antimicrobial resistance. Glycyrrhizin could also be used in synergistic composition with other drugs for *H. pylori* infection as standard *H. pylori* treatment requires triple therapy.

Supplementary Information

The online version contains supplementary material available at <https://doi.org/10.1186/s10020-023-00641-6>.

Additional file 1: Figure S1. MTT assay of glycyrrhizin for different doses. (a) AGS cells were treated with glycyrrhizin (50–200 μM) or DMSO for 24 h. MTT assay was performed to measure the % viability level. Densitometric analyses are graphically represented. Graphs generated using GraphPad Prism 5 were represented as mean ± SEM (n=3); One-way ANOVA was performed and significance was calculated. ns=non-significant. **Figure S2.** Standard agar dilution method for determination of *Helicobacter pylori* viability. Briefly, serially diluted bacterial suspension of OD at 600nm 0.1 were spotted on BHIA medium containing glycyrrhizin of 200 μM concentration along with control where no glycyrrhizin was added and incubated them in the microaerophilic condition for 3–4 days. *H. pylori* viability was determined by counting the number of bacterial colonies (CFU/mL) in the BHIA medium. Graphs generated using GraphPad Prism 5 were represented as mean ± SEM (n=3); One-way ANOVA was performed and significance was calculated. ns=non-significant. **Figure S3.** Transfection of siHMGB1, siATG5 and nonspecific siRNA in AGS cells. (a) Cells were transfected with non-specific siRNA (siNS) and HMGB1 siRNA for 48 h. Immunoblotting was performed for quantification of HMGB1 inhibition. (b) Cells were transfected with non-specific siRNA (siNS) and ATG5 siRNA (siATG5) for 48 h. Immunoblotting was performed for quantification of ATG5 inhibition. Beta-actin was used as a loading control. **Figure S4.** Glycyrrhizin treatment in *H. pylori*-infected mice. C57BL/6 mice (n = 5 per group) were treated with antibiotics every 7 days. Then after 7 days incubation period, mice were infected with the *H. pylori* SS1 strain thrice a week on alternate days. Mice were incubated for 14 days and then administered with or without GLZ (10 mg /kg body weight), every day for 4 weeks. At the end of treatment, mice were sacrificed and gastric tissues and serum were collected. (b) Immunoblot showing the expression of autophagy proteins LC3B-II of mouse gastric tissues. α-tubulin was used as a protein loading control.

Acknowledgements

The authors thank the Indian Council of Medical Research (ICMR), Council for Scientific and Industrial Research (CSIR), Department of Biotechnology (DBT), and University Grants Commission (UGC) for fellowship assistance.

Author contributions

Conceptualization and design: SB and UK. Analysis and interpretation: SB, AKM, SD, UK, BCK and PB. Data collection: SB, UK, BCK, DS, SP, PB, AG. Writing the article: SB and UK. Final approval of the article: UK, BCK, SP, PB, DS, AG, SB, AKM and SD. All authors read and approved the final manuscript.

Funding

This research was funded by a grant from the Department of Biotechnology (DBT), Government of India, and Project (BT/PR3093/BIC/101/1076/2018).

Availability of data and materials

All required data included in text and supplementary. Any further any formation required is available with the corresponding author.

Declarations

Ethics approval and consent to participate

Experiments were conducted under the guidelines of the Institutional Animal Ethical Committee, NICED, Kolkata (PRO/157/- 260 July 2022).

Consent for publication

Not applicable.

Competing interests

Authors declare no Competing interests.

Received: 30 December 2022 Accepted: 21 March 2023

Published online: 10 April 2023

References

- Basak P, Maitra P, Khan U, Saha K, Bhattacharya SS, Dutta M, Bhattacharya S. Capsaicin inhibits *Shigella flexneri* intracellular growth by inducing autophagy. *Front Pharmacol* 2022;13.
- Bravo J, Díaz P, Corvalán AH, Quest AF. A novel role for *Helicobacter pylori* gamma-glutamyltranspeptidase in regulating autophagy and bacterial internalization in human gastric cells. *Cancers*. 2019;11:801.
- Chmiela M, Karwowska Z, Gonciarz W, Allushi B, Stączek P. Host pathogen interactions in *Helicobacter pylori* related gastric cancer. *World J Gastroenterol*. 2017;23:1521.
- Feng L, Liang L, Zhang S, Yang J, Yue Y, Zhang X. HMGB1 downregulation in retinal pigment epithelial cells protects against diabetic retinopathy through the autophagy-lysosome pathway. *Autophagy*. 2022;18:320–39.
- Fu Y, Zhou E, Wei Z, Liang D, Wang W, Wang T, Guo M, Zhang N, Yang Z. Glycyrhizin inhibits the inflammatory response in mouse mammary epithelial cells and a mouse mastitis model. *FEBS J*. 2014;281:2543–57.
- Gene E, Calvet X, Azagra R, Gisbert J. Triple vs. quadruple therapy for treating *Helicobacter pylori* infection: a meta-analysis. *Aliment Pharmacol Ther*. 2003;17:1137–43.
- Giraud-Gatineau A, Coya JM, Maure A, Biton A, Thomson M, Bernard EM, Marrec J, Gutierrez MG, Larrouy-Maumus G, Brosch R. The antibiotic bedaquiline activates host macrophage innate immune resistance to bacterial infection. *Elife*. 2020;9: e55692.
- González MF, Díaz P, Sandoval-Bórquez A, Herrera D, Quest AF. *Helicobacter pylori* outer membrane vesicles and extracellular vesicles from *Helicobacter pylori*-infected cells in gastric disease development. *Int J Mol*. 2021;22:4823.
- Hardbower DM, de Sablet T, Chaturvedi R, Wilson KT. Chronic inflammation and oxidative stress: the smoking gun for *Helicobacter pylori*-induced gastric cancer? *Gut Microbes*. 2013;4:475–81.
- Hu W, Zhang L, Li MX, Shen J, Liu XD, Xiao ZG, Wu DL, Ho IH, Wu JC, Cheung CK. Vitamin D3 activates the autolysosomal degradation function against *Helicobacter pylori* through the PDIA3 receptor in gastric epithelial cells. *Autophagy*. 2019;15:707–25.
- Huang C-C, Tsai K-W, Tsai T-J, Hsu P-I. Update on the first-line treatment for *Helicobacter pylori* infection—a continuing challenge from an old enemy. *Biomarker Res*. 2017;5:1–6.
- Jung DE, Yu SS, Lee YS, Choi BK, Lee YC. Regulation of SIRT3 signal related metabolic reprogramming in gastric cancer by *Helicobacter pylori* oncoprotein CagA. *Oncotarget*. 2017;8:78365.
- Kavčič N, Pegan K, Turk B. Lysosomes in programmed cell death pathways: from initiators to amplifiers. *Bio Chem*. 2017;398:289–301.
- Khatoun J, Rai RP, Prasad KN. Role of *Helicobacter pylori* in gastric cancer: updates. *World J Gastrointest Oncol*. 2016;8:147.
- Kim J-J, Lee H-M, Shin D-M, Kim W, Yuk J-M, Jin HS, Lee S-H, Cha G-H, Kim J-M, Lee Z-W. Host cell autophagy activated by antibiotics is required for their effective antimycobacterial drug action. *Cell Host Microbe*. 2012;11:457–68.
- Kim I-J, Lee J, Oh SJ, Yoon M-S, Jang S-S, Holland RL, Reno ML, Hamad MN, Maeda T, Chung HJ. *Helicobacter pylori* infection modulates host cell metabolism through VacA-dependent inhibition of mTORC1. *Cell Host Microbe*. 2018;23(583–593): e588.
- Kralik P, Ricchi M. A basic guide to real time PCR in microbial diagnostics: definitions, parameters and everything. *Front Microbiol*. 2017;8:108.
- Levine B, Mizushima N, Virgin HW. Autophagy in immunity and inflammation. *Nature*. 2011;469(7330):323–35.
- Li N, Tang B, Jia Y-P, Zhu P, Zhuang Y, Fang Y, Li Q, Wang K, Zhang W-J, Guo G. *Helicobacter pylori* CagA protein negatively regulates autophagy and promotes inflammatory response via c-Met-PI3K/Akt-mTOR signaling pathway. *Front Cell Infect Microbiol*. 2017;7:417.
- Liao W-C, Huang M-Z, Wang ML, Lin C-J, Lu T-L, Lo H-R, Pan Y-J, Sun Y-C, Kao M-C, Lim H-J. Statin decreases *Helicobacter pylori* burden in macrophages by promoting autophagy. *Front Cell Infect Microbiol*. 2017;6:203.
- Libânio D, Dinis-Ribeiro M, Pimentel-Nunes P. *Helicobacter pylori* and micro-RNAs: Relation with innate immunity and progression of preneoplastic conditions. *World J Clin Oncol*. 2015;6:111.
- Lin H-J, Hsu F-Y, Chen W-W, Lee C-H, Lin Y-J, Chen Y-M, Chen C-J, Huang M-Z, Kao M-C, Chen Y-A. *Helicobacter pylori* activates HMGB1 expression and recruits RAGE into lipid rafts to promote inflammation in gastric epithelial cells. *Front Immunol*. 2016;7:341.
- Lv X, Zhu Y, Deng Y, Zhang S, Zhang Q, Zhao B, Li G. Glycyrrhizin improved autophagy flux via HMGB1-dependent Akt/mTOR signaling pathway to prevent Doxorubicin-induced cardiotoxicity. *Toxicology*. 2020;441: 152508.
- Mollica L, De Marchis F, Spitaleri A, Dallacosta C, Pennacchini D, Zamai M, Agresti A, Trisciuglio L, Musco G, Bianchi ME. Glycyrrhizin binds to high-mobility group box 1 protein and inhibits its cytokine activities. *Chem Bio*. 2007;14:431–41.
- Ogawa M, Yoshimori T, Suzuki T, Sagara H, Mizushima N, Sasakawa C. Escape of intracellular *Shigella* from autophagy. *Science*. 2005;307:727–31.
- Padhi A, Pattnaik K, Biswas M, Jagadeb M, Behera A, Sonawane A. Mycobacterium tuberculosis LprE suppresses TLR2-dependent cathelicidin and autophagy expression to enhance bacterial survival in macrophages. *J Immunol*. 2019;203:2665–78.
- Raju D, Hussey S, Ang M, Terebiznik MR, Sibony M, Galindo-Mata E, Gupta V, Blanke SR, Delgado A, Romero-Gallo J. Vacuolating cytotoxin and variants in Atg16L1 that disrupt autophagy promote *Helicobacter pylori* infection in humans. *Gastroenterol*. 2012;142:1160–71.
- Saha K, Sarkar D, Khan U, Karmakar BC, Paul S, Mukhopadhyay AK, Dutta S, Bhattacharya S. Capsaicin inhibits inflammation and gastric damage during *H. pylori* infection by targeting NF- κ B-miRNA axis. *Pathogens*. 2022;11:641.
- Shrivastava SR, Shrivastava PS, Ramasamy J. World health organization releases global priority list of antibiotic-resistant bacteria to guide research, discovery, and development of new antibiotics. *J Med Soc*. 2018;32:76.
- Sierra JC, Piazzuelo MB, Luis PB, Barry DP, Allaman MM, Asim M, Sebrell TA, Finley JL, Rose KL, Hill S. Spermine oxidase mediates *Helicobacter pylori*-induced gastric inflammation, DNA damage, and carcinogenic signaling. *Oncogene*. 2020;39:4465–74.
- Tang D, Kang R, Livesey KM, Cheh C-W, Farkas A, Loughran P, Hoppe G, Bianchi ME, Tracey KJ, Zeh HJ III. Endogenous HMGB1 regulates autophagy. *J Cell Bio*. 2010;190:881–92.

- Tang B, Li N, Gu J, Zhuang Y, Li Q, Wang H-G, Fang Y, Yu B, Zhang J-Y, Xie Q-H. Compromised autophagy by MIR30B benefits the intracellular survival of *Helicobacter pylori*. *Autophagy*. 2012;8:1045–57.
- Terebiznik MR, Raju D, Vázquez CL, Torbricki K, Kulkarni R, Blanke SR, Yoshimori T, Colombo MI, Jones NL. Effect of *Helicobacter pylori*'s vacuolating cytotoxin on the autophagy pathway in gastric epithelial cells. *Autophagy*. 2009;5:370–9.
- Thung I, Aramin H, Vavinskaya V, Gupta S, Park J, Crowe S, Valasek M. the global emergence of *Helicobacter pylori* antibiotic resistance. *Aliment Pharmacol Ther*. 2016;43:514–33.
- Tshibangu-Kabamba E, Yamaoka Y. *Helicobacter pylori* infection and antibiotic resistance—from biology to clinical implications. *Nat Rev Gastroenterol & Hepatol*. 2021;18:613–29.
- Tsugawa H, Mori H, Matsuzaki J, Sato A, Saito Y, Imoto M, Suematsu M, Suzuki H. CAPZA1 determines the risk of gastric carcinogenesis by inhibiting *Helicobacter pylori* CagA-degraded autophagy. *Autophagy*. 2019;15(2):242–58.
- Xie Z, Zhang Y, Huang X. Evidence and speculation: the response of *Salmonella* confronted by autophagy in macrophages. *Future Microbiol*. 2020;15:1277–86.
- Yang X-J, Si R-H, Liang Y-H, Ma B-Q, Jiang Z-B, Wang B, Gao P. Mir-30d increases intracellular survival of *Helicobacter pylori* through inhibition of autophagy pathway. *World J Gastroenterol*. 2016;22:3978.
- Yang L, Li C, Jia Y. MicroRNA-99b promotes *Helicobacter pylori*-induced autophagy and suppresses carcinogenesis by targeting mTOR. *Oncol Lett*. 2018;16:5355–60.
- Yang Y, Shu X, Xie C. An overview of autophagy in *Helicobacter pylori* infection and related gastric cancer. *Front Cell Infect Mi*. 2022;12:410.
- Yin H, Yang X, Gu W, Liu Y, Li X, Huang X, Zhu X, Tao Y, Gou X, He W. HMGB1-mediated autophagy attenuates gemcitabine-induced apoptosis in bladder cancer cells involving JNK and ERK activation. *Oncotarget*. 2017;8:71642.

Publisher's Note

Springer Nature remains neutral with regard to jurisdictional claims in published maps and institutional affiliations.

Ready to submit your research? Choose BMC and benefit from:

- fast, convenient online submission
- thorough peer review by experienced researchers in your field
- rapid publication on acceptance
- support for research data, including large and complex data types
- gold Open Access which fosters wider collaboration and increased citations
- maximum visibility for your research: over 100M website views per year

At BMC, research is always in progress.

Learn more biomedcentral.com/submissions



Article

Capsaicin Inhibits Inflammation and Gastric Damage during *H. pylori* Infection by Targeting NF- κ B–miRNA Axis

Kalyani Saha ^{1,†}, Deotima Sarkar ^{1,†} , Uzma Khan ¹, Bipul Chandra Karmakar ², Sangita Paul ², Asish K. Mukhopadhyay ², Shanta Dutta ³ and Sushmita Bhattacharya ^{1,*}

- ¹ Department of Biochemistry, National Institute of Cholera and Enteric Diseases, Indian Council of Medical Research (ICMR-NICED), P-33, CIT Rd, Subhas Sarobar Park, Phool Bagan, Belegghata, Kolkata 700010, India; kalyan.saha86@gmail.com (K.S.); deotima_s@yahoo.com (D.S.); uzma.khan1493@gmail.com (U.K.)
 - ² Department of Microbiology, National Institute of Cholera and Enteric Diseases (ICMR-NICED), Indian Council of Medical Research, P-33, CIT Rd, Subhas Sarobar Park, Phool Bagan, Belegghata, Kolkata 700010, India; bkniced032@gmail.com (B.C.K.); sangitapaul13292@gmail.com (S.P.); mukhopadhyay.niced@gov.in (A.K.M.)
 - ³ Department of Bacteriology, National Institute of Cholera and Enteric Diseases, Indian Council of Medical Research (ICMR-NICED), P-33, CIT Rd, Subhas Sarobar Park, Phool Bagan, Belegghata, Kolkata 700010, India; shanta.niced@icmr.gov.in
- * Correspondence: sushmita.bh@icmr.gov.in; Tel.: +91-97179-96740
† These authors contributed equally to this work.



Citation: Saha, K.; Sarkar, D.; Khan, U.; Karmakar, B.C.; Paul, S.; Mukhopadhyay, A.K.; Dutta, S.; Bhattacharya, S. Capsaicin Inhibits Inflammation and Gastric Damage during *H. pylori* Infection by Targeting NF- κ B–miRNA Axis. *Pathogens* **2022**, *11*, 641. <https://doi.org/10.3390/pathogens11060641>

Academic Editors: Francesca Sisto and Rossella Grande

Received: 7 April 2022

Accepted: 10 May 2022

Published: 1 June 2022

Publisher's Note: MDPI stays neutral with regard to jurisdictional claims in published maps and institutional affiliations.



Copyright: © 2022 by the authors. Licensee MDPI, Basel, Switzerland. This article is an open access article distributed under the terms and conditions of the Creative Commons Attribution (CC BY) license (<https://creativecommons.org/licenses/by/4.0/>).

Abstract: *Helicobacter pylori* (*H. pylori*) infection is considered as one of the strongest risk factors for gastric disorders. Infection triggers several host pathways to elicit inflammation, which further proceeds towards gastric complications. The NF- κ B pathway plays a central role in the upregulation of the pro-inflammatory cytokines during infection. It also regulates the transcriptional network of several inflammatory cytokine genes. Hence, targeting NF- κ B could be an important strategy to reduce pathogenesis. Moreover, treatment of *H. pylori* needs attention as current therapeutics lack efficacy due to antibiotic resistance, highlighting the need for alternative therapeutic approaches. In this study, we investigated the effects of capsaicin, a known NF- κ B inhibitor in reducing inflammation and gastric complications during *H. pylori* infection. We observed that capsaicin reduced NF- κ B activation and upregulation of cytokine genes in an in vivo mice model. Moreover, it affected NF- κ B–miRNA interplay to repress inflammation and gastric damages. Capsaicin reduced the expression level of mir21 and mir223 along with the pro-inflammatory cytokines. The repression of miRNA further affected downstream targets such as e-cadherin and Akt. Our data represent the first evidence that treatment with capsaicin inhibits inflammation and induces antimicrobial activity during *H. pylori* infection. This alternative approach might open a new avenue in treating *H. pylori* infection, thus reducing gastric problems.

Keywords: *H. pylori*; capsaicin; miRNA; NF- κ B; cytokines; inflammation

1. Introduction

Gastric cancer is one of the leading causes of mortality worldwide. *H. pylori*, a common gastric pathogen, is considered to be one of the most important carcinogens involved in gastric cancer [1–6]. Although only 2% of infected individuals develop cancer, it also causes other gastric complications such as ulcer and gastritis. In the beginning, infection leads towards inflammation and gastric damage, but in later stages, tumor development occurs [6]. The important paradigm is about the progression of the disease—how *H. pylori* infection gradually migrates towards gastric complications. There are several factors involved during *H. pylori* pathogenesis—genetics, host environment, and virulence factors [7–9]. During the infection process, the pro-inflammatory cytokine levels rise. This cytokine upregulation is triggered by virulence factors secreted by *H. pylori* [7,8,10,11]. One of the factors, CagA,



Capsaicin Inhibits *Shigella flexneri* Intracellular Growth by Inducing Autophagy

Priyanka Basak¹, Priyanka Maitra¹, Uzma Khan¹, Kalyani Saha¹,
Satya Sundar Bhattacharya², Moumita Dutta³ and Sushmita Bhattacharya^{1*}

¹Division of Biochemistry, National Institute of Cholera and Enteric Diseases, Kolkata, India, ²Department of Environmental Science, Tezpur University, Tezpur, India, ³Division of Electron Microscopy, National Institute of Cholera and Enteric Diseases, Kolkata, India

OPEN ACCESS

Edited by:

Dongsheng Zhou,
Beijing Institute of Microbiology and
Epidemiology, China

Reviewed by:

Sue Twine,
National Research Council Canada
(NRC-CNRC), Canada
Mingkai Li,
Fourth Military Medical University,
China

*Correspondence:

Sushmita Bhattacharya
durgasushmita@gmail.com

Specialty section:

This article was submitted to
Pharmacology of Infectious Diseases,
a section of the journal
Frontiers in Pharmacology

Received: 24 March 2022

Accepted: 16 May 2022

Published: 06 July 2022

Citation:

Basak P, Maitra P, Khan U, Saha K,
Bhattacharya SS, Dutta M and
Bhattacharya S (2022) Capsaicin
Inhibits *Shigella flexneri* Intracellular
Growth by Inducing Autophagy.
Front. Pharmacol. 13:903438.
doi: 10.3389/fphar.2022.903438

Antibiotic treatment plays an essential role in preventing *Shigella* infection. However, incidences of global rise in antibiotic resistance create a major challenge to treat bacterial infection. In this context, there is an urgent need for newer approaches to reduce *S. flexneri* burden. This study largely focuses on the role of the herbal compound capsaicin (Caps) in inhibiting *S. flexneri* growth and evaluating the molecular mechanism behind bacterial clearance. Here, we show for the first time that Caps inhibits intracellular *S. flexneri* growth by inducing autophagy. Activation of autophagy by Caps is mediated through transcription factor TFEB, a master regulator of autophagosome biogenesis. Caps induced the nuclear localization of TFEB. Activation of TFEB further induces the gene transcription of autophagosomal genes. Our findings revealed that the inhibition of autophagy by silencing TFEB and Atg5 induces bacterial growth. Hence, Caps-induced autophagy is one of the key factors responsible for bacterial clearance. Moreover, Caps restricted the intracellular proliferation of *S. flexneri*-resistant strain. The efficacy of Caps in reducing *S. flexneri* growth was confirmed by an animal model. This study showed for the first time that *S. flexneri* infection can be inhibited by inducing autophagy. Overall observations suggest that Caps activates TFEB to induce autophagy and thereby combat *S. flexneri* infection.

Keywords: *Shigella flexneri*, autophagy, TFEB, capsaicin, gene transcription

1 INTRODUCTION

Shigella flexneri, a common gastrointestinal pathogen, causes bacillary dysentery that affects millions every year worldwide (Nandy et al., 2011; Taneja and Mewara, 2016; Williams and Berkley, 2018; McQuade et al., 2020). According to the available information, *S. flexneri* infection is highly predominant in developing nations. Children below 5 years of age are affected with severe morbidity and mortality (Chang et al., 2016; Baker and The, 2018; Khalil et al., 2018; Chanin et al., 2019; Chen et al., 2020). The pathogen invades the intestinal epithelial and immune cells, causing ulcerative lesions in the gut under severe conditions (Killackey et al., 2016). To date, the only treatment option is antibiotics as no licensed vaccine has been developed (Hosangadi et al., 2019). Recently, the reverse vaccinology approach has been considered to improve vaccine research against *Shigella* (Hajjalibeigi et al., 2021). Excessive use of antibiotics has led to a significant rise in antibiotic-resistant bacteria (Puzari et al., 2018; Ranjbar and Farahani, 2019). Hence, in the current scenario, there is an imperative need to search for alternative approaches in treating *S. flexneri* infection.